



Fakultät für Medizin

Institut für Virologie

Preclinical improvement of a therapeutic vaccine for chronic hepatitis B (*TherVacB*)

Jinpeng Su

Vollständiger Abdruck der von der Fakultät für Medizin der Technischen Universität München zur Erlangung des akademischen Grades eines

Doctor of Philosophy (Ph.D.)

genehmigten Dissertation.

Vorsitzender: Priv.-Doz. Dr. Maximilian Reichert

Betreuerin: Prof. Dr. Ulrike Protzer

Prüfer der Dissertation:

1. Prof. Dr. Percy Knolle
2. Prof. Dr. Markus Gerhard

Die Dissertation wurde am 09.09.2020 bei der Fakultät für Medizin der Technischen Universität München eingereicht und durch die Fakultät für Medizin am 26.11.2020 angenommen.

Table of contents

Abstract	5
Zusammenfassung	7
Abbreviations	11
1. Introduction	17
1.1 Hepatitis B virus infection	17
1.1.1 Hepatitis B virus	17
1.1.2 Courses of HBV infection	19
1.1.3 Immunopathogenesis of HBV infection.....	20
1.2 Current prevention and treatment for HBV infection	22
1.2.1 Prophylactic HBV vaccines.....	22
1.2.2 Current treatments for HBV infection.....	23
1.3 Antiviral immunity to HBV infection	24
1.3.1 The role of CD4 T cells in HBV infection.....	24
1.3.2 Antiviral immunity of HBV-specific CD8 T cells	25
1.3.3 Antiviral immunity of B cells and antibodies in HBV infection	26
1.4 Therapeutic vaccination against chronic hepatitis B	28
1.4.1 Therapeutic hepatitis B vaccines in clinical trials	28
1.4.2 Adjuvants	30
1.4.3 Viral vectors	34
1.5 Mouse models to study the therapy of chronic hepatitis B	36
1.6 Aims of the study.....	39
2. Results	41
2.1 Optimization of the <i>TherVacB</i> immunization protocol.....	41
2.1.1 Selection of the adjuvants for protein priming	41
2.1.2 Estimation of the optimal MVA dose for boost.....	44
2.1.3 Estimation of the optimal protein dose for priming	48
2.1.4 Comparison of different delivery routes for various adjuvants.....	50
2.2 Investigation of novel adjuvants to improve protein priming in <i>TherVacB</i>	59

Table of contents

2.2.1	Physiochemical characterization of antigen/adjuvant formulations ...	59
2.2.2	Antigen integrity in the adjuvant formulations.....	63
2.2.3	Activation of dendritic cells by novel combination adjuvants in vitro..	66
2.2.4	Immunogenicity evaluation of the novel adjuvant formulations in wild-type C57BL/6 mice.....	69
2.2.5	Short-term immunogenicity evaluation of the novel adjuvant formulations in AAV-HBV mice	75
2.2.6	Long-term analysis of the novel adjuvant formulations in AAV-HBV mice	81
2.3	Exploration of critical factors for efficient protein priming in <i>TherVacB</i>	93
2.3.1	Importance of administering recombinant antigens during the priming phase of <i>TherVacB</i>	93
2.3.2	Criteria of adjuvant selection for the priming in <i>TherVacB</i>	96
2.3.3	Contribution of different T-cell subsets during the priming phase of <i>TherVacB</i>	102
2.4	Investigation of novel viral vector to improve the boost of <i>TherVacB</i>	111
2.4.1	Construction of VSV-GP vector encoding HBsAg and HBcAg	111
2.4.2	Confirmation of HBsAg and HBcAg expression in the recombinant VSV-GP-HBs/c.....	113
2.4.3	First immunogenicity trial of VSV-GP-HBs/c vector in wild-type C57BL/6 mice	116
2.4.4	Evaluation of different heterologous prime-boost strategies with VSV-GP-HBs/c in wild-type C57BL/6 mice	117
2.4.5	Evaluation of different heterologous prime-boost strategies with VSV-GP-HBs/c in AAV-HBV mice	123
3.	Discussion	129
3.1	Determining the optimal immunization protocol of <i>TherVacB</i>	129
3.2	Employing novel adjuvants to improve the protein priming of <i>TherVacB</i> ...	131
3.2.1.	Lipo- and SWE-based antigen/adjuvant formulations remain stable and intact for long time <i>in vitro</i>	132

3.2.2 Immunization with novel adjuvant formulations increases the magnitude of HBV-specific humoral responses.....	133
3.2.3 Immunization with novel adjuvant formulations elicits balanced HBV-specific helper T-cell responses	135
3.2.4 Immunization with novel adjuvant formulations induces strong HBV-specific CD8 T-cell responses	137
3.2.5 Immunization with novel adjuvant formulations leads to long-term control of persistent HBV replication in AAV-HBV mice.....	138
3.2.6 General remarks and future directions of adjuvant development	139
3.3 Exploring critical factors for efficient protein priming of <i>TherVacB</i>	141
3.3.1 Administering recombinant HBsAg/HBcAg is critical for potent priming of <i>TherVacB</i>	141
3.3.2 Incorporating Th1/Th2-balanced adjuvant is essential for potent protein priming of <i>TherVacB</i>	142
3.3.3 CD4 T cells are the key T-cell subset contributing to <i>TherVacB</i> -mediated immune responses during the priming phase	143
3.4 Developing novel VSV-GP-HBs/c vector to improve the <i>TherVacB</i> regimen	145
3.4.1 Heterologous prime-boost strategies with VSV-GP-HBs/c induce strong HBV-specific immune responses in wild-type mice.....	146
3.4.2 Protein prime – VSV-GP boost vaccination breaks the immune tolerance against HBV in AAV-HBV mice	147
3.4.3 General remarks and potential applications of VSV-GP-HBs/c vector	148
3.5 Conclusion	150
4. Materials and methods.....	151
4.1 Materials	151
4.1.1 Vaccine components	151
4.1.2 Mouse models.....	152
4.1.3 Cell lines	153

Table of contents

4.1.4 Cell culture media.....	153
4.1.5 Antibodies	154
4.1.6 Peptides	156
4.1.7 Plasmids	157
4.1.8 Oligonucleotides.....	157
4.1.9 Enzymes	158
4.1.10 Commercial kits.....	158
4.1.11 Buffers and solutions	159
4.1.12 Chemicals and reagents.....	161
4.1.13 Laboratory devices and equipment.....	162
4.1.14 Consumables	164
4.1.15 Software.....	165
4.2 Methods	166
4.2.1 General cell culture	166
4.2.2 Recombinant MVA amplification	167
4.2.3 Characterization of the stability and integrity of novel adjuvant formulations <i>in vitro</i>	169
4.2.4 Generation and stimulation of human monocyte-derived dendritic cells <i>in vitro</i>	172
4.2.5 Generation and characterization of VSV-GP-HBs/c vector	173
4.2.6 Mouse experiments	176
4.2.7 Isolation of lymphocytes from different murine organs.....	178
4.2.8 Detection of T-cell responses in murine primary lymphocytes.....	180
4.2.9 Analyses of HBV parameters in murine serum and liver tissue.....	182
4.2.10 Statistical analysis	184
5. List of figures	185
6. References.....	189
Publications and meetings	203
Acknowledgments.....	205

Abstract

Although safe and effective prophylactic vaccines against hepatitis B virus (HBV) infection are available, chronic hepatitis B (CHB) still represents a major global health problem, with nearly 900,000 deaths per year due to HBV-related liver cirrhosis and hepatocellular carcinoma. The currently available antiviral treatment suppresses HBV replication, but cannot completely eradicate the virus. Therefore, new therapeutic strategies against CHB are highly desired.

It is well-documented that adaptive immunity against the virus is essential for efficient HBV control. Consequently, therapeutic vaccination that can induce strong anti-HBV immunity represents a promising strategy to treat CHB. However, to date, therapeutic hepatitis B vaccines have demonstrated only limited success in clinical trials, implying that these strategies need further improvement. To this end, our laboratory has developed the heterologous prime-boost vaccine *TherVacB*, employing a protein prime with particulate hepatitis B S (HBsAg) and core antigen (HBcAg) and a modified vaccinia virus Ankara (MVA) boost regimen. The aim of this work was to improve the *TherVacB* regimen for clinical development.

In the first part of the study, the optimal *TherVacB* immunization protocols were established. Through titrating the vaccine components, 10 µg for each protein and 3×10^7 infectious units for recombinant MVA were selected as the optimal immunization doses. Administration of the vaccine via various routes determined intramuscular injection as the most efficient delivery route for *TherVacB*. Hereby, the data indicated that the adjuvant selection for protein priming significantly influences the overall efficacy of the *TherVacB* regimen.

In the second part of the study, novel adjuvants were therefore investigated to improve the protein prime of *TherVacB*. We investigated liposome (Lipo)- and squalene-in-water emulsion (SWE)-based antigen/adjuvant formulations. Both types of formulations proved stable and intact for at least 12 weeks *in vitro*. The selected Lipo- and SWE-based adjuvants exhibited strong immunostimulatory properties *in vitro* and elicited very high levels of HBV-specific antibodies, as well as robust CD4 and CD8 T-

Abstract

cell responses, outcompeting previously tested adjuvants in wild-type mice. In adeno associated virus (AAV)-HBV transduced mice, in which persistent HBV replication was established, immunization with Lipo-based formulation LMQ not only induced strong anti-HBV immunity, but also led to long-term immune control of HBV infection. Therefore, LMQ formulation represents a promising candidate to improve the efficacy of the *TherVacB* regimen. In addition, by comparing the efficacy of *TherVacB* immunization with different adjuvant formulations, it was emphasized that efficient protein priming is the key to *TherVacB* success.

In the third part of the study, consequently, the critical factors for efficient protein priming in *TherVacB* were explored. The results demonstrated that recombinant HBsAg and HBeAg, as well as a balanced T helper (Th) 1 and Th2 directing adjuvant determine the potency of *TherVacB*. Moreover, CD4 T cells induced during the priming phase of *TherVacB* were verified as the key T-cell subset contributing to vaccine-mediated antiviral efficacy against persistent HBV replication.

In the fourth part of the study, a novel nontoxic vesicular stomatitis virus (VSV) vector was developed to further improve the immune responses induced by *TherVacB*. First, a chimeric VSV variant VSV-GP encoding HBsAg and HBeAg (VSV-GP-HB/c) was successfully generated. Evaluation of the immunogenicity in wild-type and AAV-HBV mice revealed only a weak anti-HBV immunity upon multiple administrations with viral vector vaccines. However, VSV-GP-HBs/c functioned as well as did the according MVA-HBs/c as a boost vector after protein priming. Thus, the VSV-GP-HBs/c vector may be employed as a substitute or additional viral vector to boost the immune responses in the *TherVacB* regimen.

Taken together, the present study shows that the improved *TherVacB* immunization induces robust HBV-specific immune responses and leads to the long-term control of persistent HBV infection. Moreover, this work reveals that potent protein priming with a Th1/Th2-balanced adjuvant, and CD4 T cells induced during the priming phase of *TherVacB*, are crucial for the overall efficacy of therapeutic vaccination. These findings will be important for clinical development of *TherVacB* and may provide implications for rationally designing and optimizing other therapeutic vaccines.

Zusammenfassung

Obwohl sichere und effektive prophylaktische Impfungen gegen das Hepatitis B Virus (HBV) verfügbar sind, stellt die chronische Hepatitis B mit nahezu 900.000 Toten pro Jahr aufgrund von Leberzirrhose und hepatozellulärem Karzinom eine globale Gesundheitsbedrohung dar. Die verfügbaren antivirale Medikamente unterdrücken die HBV Replikation, können das Virus jedoch nicht vollständig auslöschen. Daher werden neue Behandlungsstrategien für die chronische Hepatitis B benötigt.

Es wurde hinreichend belegt, dass das adaptive Immunsystem essentiell für die Kontrolle von HBV Infektionen ist. Daher stellt eine therapeutische Impfung, die eine starke anti-HBV Immunantwort hervorrufen kann, eine vielversprechende Strategie zur Behandlung von der chronischen Hepatitis B dar. Dennoch haben therapeutische Impfungen gegen HBV und andere Infektionen bisher nur einen begrenzten Erfolg in klinischen Studien gezeigt, weshalb die Impfstrategien verbessert werden müssen. Unser Labor hat dafür einen heterologen therapeutischen Hepatitis B Impfstoff namens *TherVacB* entwickelt. *TherVacB* basiert auf einem proteinbasierten *priming* mit partikulären Hepatitis B S- (HBsAg) und Core-Antigen (HBcAg) und einem vektorbasierten *boost* mit Modified-Vaccinia-Virus-Ankara (MVA). Das Ziel dieser Arbeit war es, *TherVacB* für die klinische Entwicklung zu verbessern.

Im ersten Abschnitt wurden optimale *TherVacB* Impfschemata etabliert. Nach Titration der Impfkomponten wurden 10 µg pro Protein und 3×10^7 infektiöse Einheiten MVA als optimale Dosen ausgewählt. Die intramuskuläre Injektion war die effektivste Verabreichung. Interessanterweise fand sich, dass die Adjuvantierung des proteinbasierten *priming* die Effektivität von *TherVacB* in signifikantem Maße beeinflusst.

Im zweiten Teil wurden deshalb neuartigen Adjuvanzen untersucht um das proteinbasierte *priming* von *TherVacB* zu verbessern. Zuerst wurde gezeigt, dass Liposomen und Squalene-in-Wasser Emulsion (SWE)-basierte Adjuvans-Formulierungen von HBsAg und HBcAg für 12 Wochen *in vitro* stabil und intakt sind. Ausgewählte Liposom- und SWE-basierte Adjuvanzen zeigten starke

Zusammenfassung

immunstimulatorische Eigenschaften *in vitro* und induzierten sehr hohe Niveaus an HBV spezifischen Antikörpern sowie robuste CD4- und CD8-T-Zellantworten in Wildtypmäusen. In Adeno-assoziierte Virus (AAV)-HBV transduzierten Mäusen, die ein Modell für die persistierende HBV Infektion darstellen, führte die Immunisierung mit der Liposom-basierte Formulierung LMQ nicht nur zu starken anti-HBV Immunantworten, sondern auch zu Langzeitkontrolle der HBV Infektion. Daher stellt die LMQ Formulierung einen vielversprechenden Kandidaten dar um die Effizienz von *TherVacB* zu verbessern. Hierbei wurde noch einmal untermauert, dass effizientes, proteinbasiertes *priming* kritisch für den Erfolg von *TherVacB* ist.

Im dritten Abschnitt der Studie wurden die essentiellen Faktoren für ein effizientes proteinbasierte *priming* von *TherVacB* identifiziert. Die Ergebnisse zeigten, dass sowohl die Qualität des rekombinante HBsAg und HBcAg, als auch eine balancierte Th1/Th2 (T Helferzell Typ 1 und 2) Immunantwort die Effektivität von *TherVacB* bestimmt. Hierbei wurden CD4 T Zellen als kritische T Zellpopulation für das *priming* und einen potenten antiviralen Effekt von *TherVacB* gegen HBV identifiziert.

Im vierten Teil wurde ein nicht pathogenes Vesicular Stomatitis Virus (VSV) als neuartiger Vektor entwickelt um die *TherVacB*-induzierte Immunantwort zu verbessern. Ein bicistronischer, rekombinanter Vektor VSV-Vektor, der für HBsAg und HBcAg kodiert (VSV-GP-HBs/c) wurde erfolgreich produziert. Obwohl die Immunogenität des Vektors alleine limitiert war, stellte sich VSV-GP-HBs/c nach einem proteinbasierten *priming* als vergleichbar effektiver *boost* Vektor zu MVA-HBs/c in Wildtyp und AAV-HBV Mausmodellen heraus. Daher könnte der VSV-GP-HBs/c Vektor als alternativer oder zusätzlicher viraler Vektor zum *boost* der Immunantwort in der *TherVacB* Strategie Einsatz finden.

Zusammenfassend zeigt diese Arbeit, dass die verbesserte *TherVacB* Impfung robuste HBV spezifische Immunantworten induziert und eine Langzeitkontrolle von persistierenden HBV Infektionen erlaubt. Des Weiteren zeigen die hier präsentierten Daten, dass ein funktionales proteinbasiertes *priming* mit einem Adjuvans, das eine balancierte Th1/Th2-Antwort induziert, genauso wie die Induktion einer potenten CD4 T Zell-Antwort eine Schlüsselrolle in der Effizienz der Impfung einnehmen. Diese

Erkenntnisse sind essentiell für die weitere klinische Entwicklung von *TherVacB* und bieten möglicherweise Hinweise für das Design und die Optimierung anderer therapeutischer Vakzine-Schemata.

Abbreviations

α	anti
$^{\circ}\text{C}$	degree Celsius
AAV	adeno associated virus
AAV-HBV	adeno-associated virus carrying a replication-competent HBV genome
ACK	ammonium-chloride-potassium
Ad5	adenovirus serotype 5
ADCC	antibody-dependent cell-mediated cytotoxicity
ADCP	antibody-dependent cellular phagocytosis
Ad-HBV	adenoviral vectors containing a replication-competent HBV genome
ALT	alanine aminotransferase
Alum	aluminum salts
anti-HBc	antibodies against HBV core antigen
anti-HBs	antibodies against HBV surface antigen
APCs	antigen presenting cells
BFA	brefeldin A
BR	Braunschweig
cccDNA	covalently closed circular DNA
c-di-AMP	cyclic-di-AMP
CHB	chronic hepatitis B
CMV	cytomegalovirus
CTLs	CD8 cytotoxic T lymphocytes
DCs	dendritic cells
DMEM	Dulbecco's Modified Eagle's Medium
DMSO	dimethyl sulfoxide
EDTA	Ethylenediaminetetraacetic acid

Abbreviations

ELISA	enzyme-linked immunosorbent assay
EMA	European Medicines Agency
FACS	Fluorescence-activated cell sorting
FCS	fetal calf serum
FDA	Food and Drug Administration
GE	genome equivalents
GM-CSF	granulocyte-macrophage colony-stimulating factor
GP	glycoprotein
GSK	GlaxoSmithKline
h	hour
HBcAg	HBV core antigen
HBcrAg	Hepatitis B core-related antigen
HBeAg	HBV e antigen
HBs/c	HBsAg-P2A-HBcAg
HBsAg	HBV surface antigen
HBV	hepatitis B virus
HBVtg mice	HBV transgenic mice
HBx	HBV x protein
HCC	hepatocellular carcinoma
HDI	hydrodynamic injection
HE	hematoxylin/eosin
HMGU	Helmholtz center Munich
hMoDCs	human monocytes derived dendritic cells
i.m.	intramuscular injection
i.p.	intraperitoneal injection
IC	immune complex
IFN γ	Interferon γ

Abbreviations

IFU	infectious units
IG	InvivoGen company
IgG	Immunoglobulin G
IHC	immunohistochemistry
IL-4	interleukin-4
IL-5	interleukin-5
IL-6	interleukin-6
iTreg	induced regulatory T cells
IU/ml	international units per milliliter
LALs	liver associated lymphocytes
LCMV	lymphocytic choriomeningitis virus
Lipo	liposome
LPS	lipopolysaccharide
M	matrix protein
mAb	monoclonal antibody
MACS	magnetic-activated cell sorting
MHC	major histocompatibility complex
min	minute
ml	milliliter
mM	millimolar
MOI	multiplicity of infection
MPL	Monophosphoryl lipid A
mV	millivolt
MVA	modified vaccinia virus Ankara
N	nucleoprotein
n.a.	not applicable
n.d.	not detectable

Abbreviations

n.s.	not significant
NAGE	native agarose gel electrophoresis
NAs	nucleoside analogues
ng	nanogram
NLRs	NOD-like receptors
nm	nanometer
nM	nanomolar
no adj	no adjuvant
no vac	non-vaccinated
NTCP	sodium taurocholate cotransporting polypeptide
OD	optical density
ODN	oligodeoxynucleotide
ORF	open reading frame
OVA	ovalbumin
P	phosphoprotein
PAGE	polyacrylamide gel electrophoresis
PBMCs	peripheral blood mononuclear cells
PBS	phosphate-buffered saline
PBST	PBS containing 0.05% Tween 20
PCEP	polyphosphates
PD1	programmed cell death protein 1
PDI	poly-dispersity index
PEG-IFN α	pegylated Interferon alpha
PEIU/ml	Paul Ehrlich Institute Units/milliliter
PFA	paraformaldehyde
PRRs	pattern recognition receptors
PTA	phosphotungstic acid

PVDF	polyvinylidene difluoride
pVSV-GP	VSV-GP genomic plasmid
qPCR	quantitative polymerase chain reaction
rcDNA	relaxed circular DNA
RPMI	Roswell Park Memorial Institute
RT	room temperature
s.c.	subcutaneous injection
S/CO	signal to cut off
SDS	Sodium Dodecyl Sulfate
sec	second
SEM	standard error of the mean
SWE	squalene-in-water emulsion
TBS	Tris-buffered saline
TBST	Tris-buffered saline (TBS) containing 1% Tween-20
TCID ₅₀	Median Tissue Culture Infectious Dose
TEM	transmission electron microscopy
TEMED	Tetramethylethylenediamine
Tfh	follicular helper T cells
TGF- β	transforming growth factor- β
Th1	T helper 1
Th2	T helper 2
<i>TherVacB</i>	Therapeutic hepatitis B vaccine
TIM-3	T-cell immunoglobulin mucin-3
TLRs	Toll-like receptors
TNF	tumor necrosis factor
TP	terminal protein
Treg	regulatory T cells

Abbreviations

TRIS	Tris(hydroxymethyl)-aminomethane
TUM	Technical University of Munich
U/L	units per liter
µg	microgram
µl	microliter
µM	micromolar
VFI	Vaccine Formulation Institute
VSV	vesicular stomatitis virus
WHO	World Health Organization

1. Introduction

1.1 Hepatitis B virus infection

Hepatitis B virus (HBV) infection is a serious global health problem. There are approximately 260 million people worldwide living with chronic hepatitis B. In 2015, an estimated 887 000 deaths resulted from the HBV-related cirrhosis and hepatocellular carcinoma (HCC) (WHO report, 2017).

1.1.1 Hepatitis B virus

The hepatitis B virus is a small enveloped DNA virus, which belongs to the *Hepadnaviridae* family. The viruses from this family show a narrow host range and hepatic tropism in their respective hosts (Lamontagne, 2016). According to the genome sequence divergence, the human HBV has been classified into ten genotypes (A-J), showing a distinct geographical distribution (Velkov, 2018). In addition, infection with various HBV genotypes may result in different disease severity and the clinical outcomes (Sunbul, 2014).

The mature HBV virion (Dane particle) has a spherical lipid-containing structure of 42-47 nm in diameter. It consists of an outer lipid membrane derived from plasma membranes and an inner icosahedral capsid. The outer membrane is embedded with three forms of viral envelope proteins (HBs): small (S-HBs), middle (M-HBs), and large (L-HBs). The icosahedral inner capsid is assembled from 120 dimers of HBV core protein, harboring a partially double-stranded relaxed circular DNA (rcDNA) of approximately 3.2 kb in size. The rcDNA is composed of a complete negative DNA strand and a partial positive strand. The 5' end of the negative strand is covalently linked to viral polymerase, which provides the reverse transcriptase and RNase H activity (Fig.1.1 A) (Dane,1970; Knipe and Howley, 2007). In addition to the mature virion (Dane particle), there is an excessive amount of non-infectious subviral particles detected in the blood of HBV infected patients. The subviral particles, which do not contain either HBV capsid or genome inside, exist in two main forms: filaments and

Introduction

spheres. Filaments display a width of 22 nm in variable lengths, whereas smaller spheres are usually 17-25 nm in diameter (Fig.1.1 B). The biological function of the subviral particles is unclear. One of their possible functions is to serve as an immunological decoy to adsorb virus-neutralizing antibodies. In addition, it has been reported that the subviral particles contribute to the HBV-specific immune tolerance, which is a precondition of persistent HBV infection (Chai, 2008; Hu, 2017).

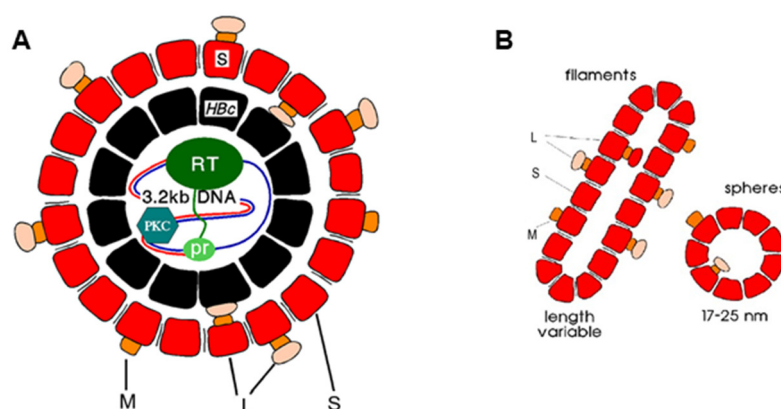


Fig.1.1 The structure of HBV virions and subviral particles.

- (A) The structure of mature HBV virion (Dane particle). It consists of an outer lipid membrane embedded with viral surface proteins, and an inner icosahedral nucleocapsid harboring a partially double-stranded relaxed circular DNA (rcDNA) (Modified from Gerlich, 2013).
- (B) The structure of non-infectious HBV subviral particles. There are two forms of subviral particles: filaments and spheres (Gerlich, 2013).

The HBV genome has a very small size (~3.2 kb) and a compact organization, which comprises four overlapping but frame-shifted open reading frames (ORF) (Fig.1.2; Locarnini, 2013). The largest ORF P encodes the viral polymerase, which consists of four domains: terminal protein (TP), spacer, reverse transcriptase, and RNase (Seeger and Mason, 2015). The ORF preS/S encodes the large (L-), middle (M-), and small (S-) envelope proteins. While all three HBV envelope proteins share the same S domain, L and M proteins have the additional domain: preS1/preS2 and preS2, respectively. Another ORF preC/C encodes for hepatitis B e antigen (HBeAg) and core antigen (HBcAg), which builds the icosahedral viral capsid. Besides the common domain of core, HBeAg has an additional N-terminal part (PreC) that determines the secretory property of HBeAg. It has been commonly considered that there is a significant

correlation between the levels of serum HBeAg and HBV viral titer (Lamontagne, 2016). The smallest ORF X encodes the HBV x protein (HBx), which is a transcriptional transactivator protein with the function of initiating and maintaining viral transcription. Moreover, it has been reported that HBx has a crucial impact on the development of hepatocellular carcinoma (Geng, 2015).

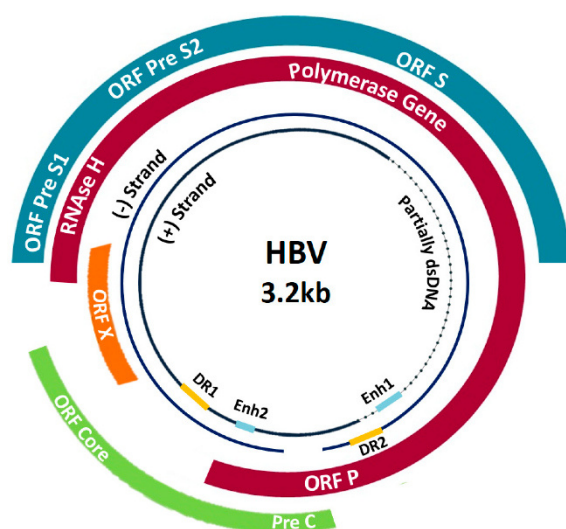


Fig.1.2 The genome organization of HBV. HBV has a partially double-stranded circular DNA genome of approximately 3.2kb in size. The genome includes four overlapping open reading frames (ORF), four promoters, and two enhancer elements to regulate the transcription of viral RNA. The ORF P encodes for polymerase, ORF S encodes for three forms of surface proteins (S, M, L), ORF preC/C encodes for HBeAg and HBcAg, ORF X encodes for regulatory protein HBx (Al-Sadeq, 2019).

A crucial step during the HBV life cycle is the formation of covalently closed circular DNA (cccDNA). HBV enters into the hepatocytes by interacting with sodium taurocholate cotransporting polypeptide (NTCP), which was identified as a functional receptor of HBV (Yan and Zhong, 2012). Afterwards, the uncoated capsid is transported to the cell nucleus, where the viral genome rcDNA is released and converted to cccDNA. The cccDNA resides within the nucleus and functions as the template for the virus transcription (Hu, 2017). Once cccDNA is formed, it is extraordinarily stable and establishes a lifelong HBV reservoir (Ko, 2017). None of the currently available treatments is able to target cccDNA, albeit a cure for chronic hepatitis B requires the elimination of cccDNA (Nassal, 2015).

1.1.2 Courses of HBV infection

HBV can be transmitted very efficiently with the blood from infected individuals. There are two common routes of transmission: 1) perinatal transmission (from the infected mother to child at birth), which is the major transmission route in high endemic areas;

Introduction

and 2) horizontal transmission (exposure to the infected body fluids), which is the main transmission route in low endemic areas (Lamontagne, 2016).

The outcome of HBV infection is complex and variable. It can cause acute and self-limiting disease, as well as persistent infection resulting in chronic hepatitis, liver cirrhosis and HCC (Locarnini, 2015).

The symptoms of HBV infection include liver inflammation, associated with fever, abdominal pain, vomiting, and jaundice. Nevertheless, there are also many cases of asymptomatic HBV infection. Generally, 95% of the HBV-infected healthy adults can resolve an acute infection within six months, at which time point viral DNA is undetectable and the antibodies against hepatitis B surface antigen (HBsAg) are generated (Lamontagne, 2016). However, the likelihood of progressing to chronicity highly depends on the age when a person gets infected. While less than 5% of HBV infections in adults result in chronic infection, 80–90% of infected infants and 30–50% of children infected before six years old will develop a chronic infection (WHO guideline, 2015). The chronic infection is indicated by sustained, detectable expression of HBsAg for at least six months after the initial infection (Lamontagne, 2016).

1.1.3 Immunopathogenesis of HBV infection

During acute resolving infection, the host immune system functions efficiently and timely against HBV. Especially, the vigorous and multi-specific CD8 T cells play a critical role in HBV clearance (Maini, 1999; Thimme, 2003). In addition, the neutralizing antibodies generated by B cells can prevent sufficiently the spread of the virus to non-infected hepatocytes (Bertoletti and Ferrari, 2016).

During the development of chronic HBV infection, a progressive loss of functionality of HBV-specific T cells is observed (EASL guideline, 2017). These dysfunctional T cells during chronic hepatitis B are characterized by low antigen-specific cell numbers, poor proliferation, limited production of antiviral cytokines, high expression of inhibitory receptors, such as PD1 (programmed cell death protein 1) and TIM-3 (T-cell immunoglobulin mucin-3), as well as increased apoptosis (Maini and Pallett, 2018;

Pardoll, 2012).

Several mechanisms may contribute to the dysfunction of HBV-specific T cells. It has been reported that high viral load and continuous antigen stimulation can impair the virus-specific T-cell responses (Wherry, 2003). As the HBV antigen load is high in CHB, the expression of co-inhibitory molecules, such as PD-1, are significantly upregulated on the surface of the exhausted T cells, which is closely related to their unresponsiveness (Gehring and Protzer, 2019). Moreover, the extrinsic secretion of suppressive cytokines including interleukin-10 (IL-10) and transforming growth factor- β (TGF- β), as well as the induction of regulatory T (Treg) cells also result in a progressive loss of T-cell functions (Fig.1.3; Stoop, 2005). Lastly, the liver is an organ with intrinsic immunotolerant features, which may also contribute to the immunological tolerance during CHB (Protzer, 2012).

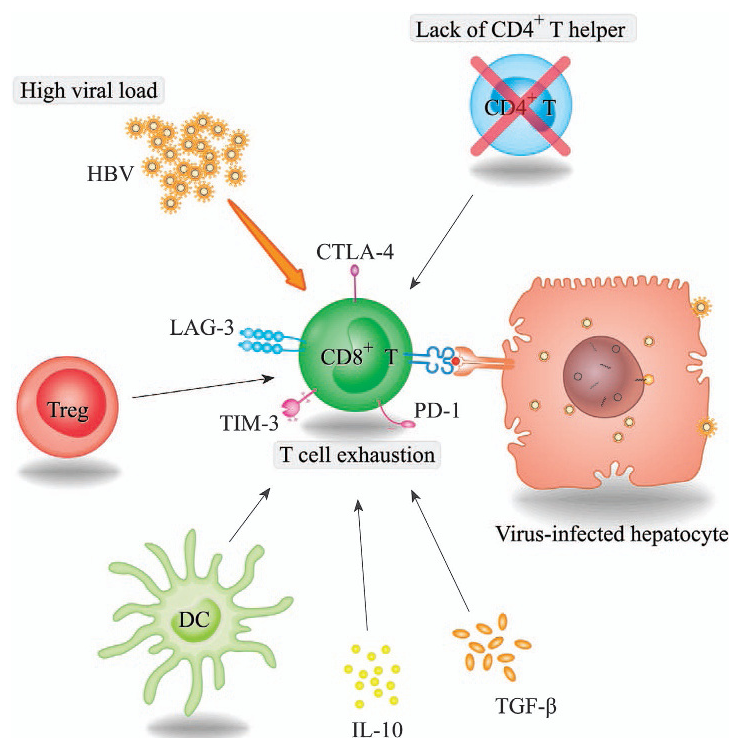


Fig.1.3 The mechanisms involved in T-cell exhaustion during chronic HBV infection.

The exhaustion of CD8 T cell results from high viral (or antigen) load, loss of CD4 T cell help, upregulation of co-inhibitory molecules such as PD1, extrinsic secretion of suppressive cytokines IL-10 and TGF- β , and the induction of Treg cells (Ye, 2015).

1.2 Current prevention and treatment for HBV infection

1.2.1 Prophylactic HBV vaccines

Currently, vaccination is the most effective way of hepatitis B prevention (Chen, 2009). Moreover, preventing HBV infection by administration of a prophylactic vaccine can in the long run decrease the incidence of chronic hepatitis B and HCC. Since it is difficult to target the populations at risk of HBV infection and the rate of mother-to-child transmission is high, the approach of universal vaccination of the newborns is a more feasible and cost-effective strategy (Alter, 1990; Arevalo and Washington, 1988). It is recommended by WHO that all newborns should receive the prophylactic hepatitis B vaccine, preferably within 24 hours after birth. The prevalence of chronic HBV infection in children under 5 years of age had dropped to 1.3% in 2015, which can be attributed to the worldwide HBV immunization program (WHO guideline, 2015).

The currently available prophylactic HBV vaccines are recombinant subunit vaccines containing HBsAg produced in yeast cells as the antigen. One of the most commonly used prophylactic vaccines is Engerix-B, which was developed by Glaxo-Smith-Kline (GSK) and licensed in 1989 (Baschieri, 2012). In Engerix-B formulation, HBsAg is adsorbed onto the adjuvant aluminum hydroxide, which can enhance the antibody responses against HBsAg *in vivo*. Immunization regimen of Engerix-B consists of a series of three doses given on a zero-, one- and six-month schedule via intramuscular route (Velu, 2007). In 2017, the American Food and Drug Administration approved one new HBV prophylactic vaccine HEPLISAV-B, in which HBsAg is combined with immunostimulatory CpG-1018 adjuvant. The CpG-1018 adjuvant binds to Toll-like receptor (TLR)-9 to stimulate a directed immune response to HBsAg (Halperin, 2013). The immunization of HEPLISAV-B is recommended to be given with only two doses on a zero- and one-month schedule. The benefits of protection with two doses administered over one month make HEPLISAV-B an important alternative for the prevention of hepatitis B (Schillie, 2018).

After a complete vaccination series, protective anti-HBs antibodies can be induced in about 95% of the vaccinees. Protection lasts at least 20 years and probably even

lifelong (Van Damme and Van Herck, 2007). However, when the chronic infection is already established, the administration of the prophylactic HBV vaccine cannot help to control the disease (Dikici, 2003).

1.2.2 Current treatments for HBV infection

There is no specific treatment for acute hepatitis B. Therefore, patients' care is more focused on maintaining comfort and adequate nutritional balance (WHO guideline, 2015).

Current treatments for chronic hepatitis B include two general categories: immunomodulatory drugs like conventional pegylated interferon alpha (PEG-IFN α), and antiviral drugs such as lamivudine, telbivudine, entecavir, adefovir, and tenofovir (Nash 2009; Lok, 2005).

Treatment with interferons aims to boost the immune system to help eliminate hepatitis B virus. They are administered by subcutaneous injections over 6 months up to 1 year. The benefits of interferon treatment include: the finite treatment duration, a higher rate of HBeAg and HBsAg seroconversion and no drug resistance (Rijckborst, 2011). However, interferon therapy is not well tolerated, which is demonstrated by its common and severe side effects (Nguyen, 2020; Ganem, 2004). The treatment with antiviral nucleos(t)ide analogues (NAs) can significantly reduce the HBV replication, which leads to reduced hepatic inflammation and damage (Woo, 2017). However, the NAs do not directly target the HBV persistent form cccDNA, thus cannot completely eradicate the virus (Revill, 2016). Long-term and often lifelong treatments are needed by most patients, which suffer from the treatment-associated risks of side effects, poor patient compliance and drug resistance, as well as high economic burdens (Locarnini, 2015). Therefore, developing new therapeutic strategies to achieve complete viral elimination during CHB is highly demanded.

1.3 Antiviral immunity to HBV infection

It is generally accepted that HBV behaves as a stealth virus, which does not trigger an innate immune response *in vivo* (Chisari, 1995; Maini and Gehring, 2016) and thus does not support adaptive immune responses. The adaptive immunity against HBV plays a crucial role in the resolution of HBV infection.

1.3.1 The role of CD4 T cells in HBV infection

Efficient host defense against foreign pathogens is achieved through the coordination of complex signaling networks that link both innate and adaptive immune systems (Zhou, 2009). Through the production of cytokines and chemokines, CD4 T cells, also referred to as T helper cells, orchestrate the full network of immune responses. Specifically, CD4 T cells exert multiple critical functions in host immunity, ranging from recruitment of innate immune cells to site of infection, promotion of B cells for antibody production, activation of cytotoxic T cells, as well as non-immune cells (Luckheeram, 2012). Additionally, a specific CD4 T-cell subset, known as regulatory T cell (Treg), also plays a critical role in the suppression of immune reactions (Sakaguchi, 2009).

Upon interaction with the antigen presented by antigen presenting cells (APCs), such as dendritic cells (DCs), CD4 T cells can differentiate into two major effector subsets, T helper 1 (Th1) cells and T helper 2 (Th2) cells (Murphy and Weaver, 2016). Th1 cells lead to increased cellular immunity against intracellular microorganisms. They are triggered by the polarizing cytokine IL-12 and their effector cytokines are IFN γ and IL-2. Th2 cells are required for efficient humoral immunity against extracellular pathogens including helminths. They are triggered by polarizing cytokines IL-4 and IL-2, and their effector cytokines are IL-4, IL-5, and IL-13 (Luckheeram, 2012; Zhou, 2009). In addition to the classical Th1 and Th2 cells, there are also some newly defined CD4 T-cell subsets, including Th17 cells, follicular helper T (Tfh) cells, and Tregs (Zhu and Paul, 2008).

While CD8 T cells are the major immune cells contributing to the clearance of HBV infection, it has been shown that CD4 T cells are crucial in regulating CD8 T cell-

mediated responses (Yang, 2010). In addition, CD4 T cells have an essential role in the formation of memory CD8 T-cell responses (Penna, 1996; Trautmann, 2014). During chronic HBV infection, a lack of virus-specific CD4 T cells is also recognized as one major cause resulting in the exhaustion of CD8 T cells, which require the continuous supply of cytokines to maintain their effector functions (Saeidi, 2018).

During HBV infection, the cooperation of CD4 T cells and B cells is very important for the generation of high-affinity antibodies. Anti-HBs production is thought to be T cell-dependent (Milich, 1987), whereas antibody responses to HBcAg can be generated through both the T cell-dependent and T cell-independent pathway (Milich and McLachlan, 1986). Production of anti-HBs may be impaired by the low frequency of functional HBV-specific CD4 T cells during CHB (Raziorrouh, 2014).

1.3.2 Antiviral immunity of HBV-specific CD8 T cells

As one major component of cellular adaptive immunity, CD8 T cells generally mediate the protection against intracellular pathogens (Murphy and Weaver, 2016). In HBV infection, it has been shown that strong HBV-specific CD8 T-cell responses closely correlate with viral clearance during acute infection (Maini, 1999). Moreover, the antiviral role of CD8 T cells has also been confirmed by depletion studies in experimentally HBV-infected chimpanzees, in which the virus titer remained at high levels after CD8 T-cell depletion (Thimme, 2003).

Immune control of HBV infection by CD8 T cells is mediated in both a cytolytic and a non-cytolytic manner (Guidotti, 1999; Thimme, 2003; Phillips, 2010). Cytolytic effector functions of CD8 T cells involve the production of the cytolytic molecules, including perforin and granzyme B, to directly eliminate the infected hepatocytes. This results in the elimination of all viral forms, including cccDNA and integrated HBV DNA (Ando, 1994, Maini and Burton, 2019) (Fig.1.4 B). Non-cytolytic control of HBV is achieved through the release of antiviral cytokines, such as IFN γ and tumor necrosis factor (TNF). Secretion of antiviral cytokines by CD8 T cells has the potential to inhibit HBV replication in multiple hepatocytes with minimal cell lysis, which can avoid extensive

Introduction

liver damage. $\text{IFN}\gamma$ and TNF mediate cccDNA degradation by upregulating the expression of APOBEC deaminases in hepatocytes (Fig.1.4 A) (Lucifora and Xia, 2014; Xia and Stadler, 2016).

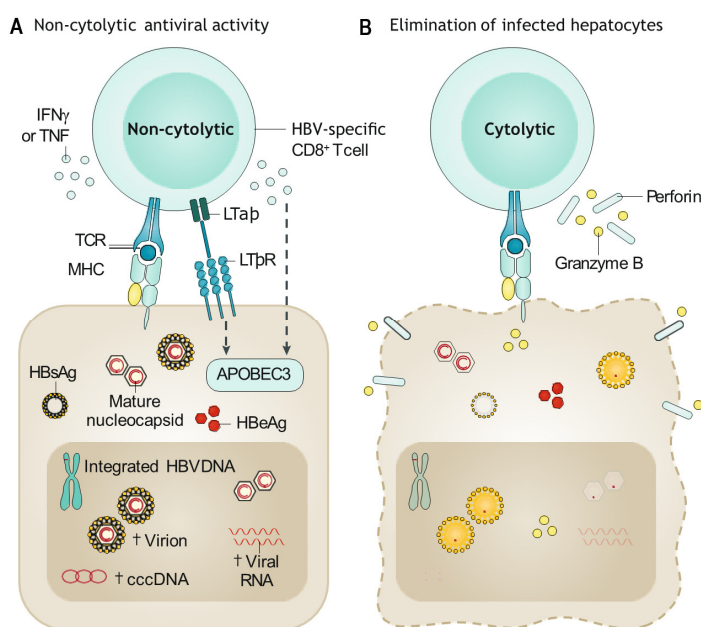


Fig.1.4 Antiviral functions of HBV-specific CD8 T cells.

(A) Non-cytolytic control of HBV by the release of antiviral cytokines $\text{IFN}\gamma$ and TNF, which can degrade the cccDNA by the induction of APOBEC3.

(B) Elimination of the HBV-infected hepatocytes is through producing the cytolytic molecules such as perforin and Granzyme B, which can remove all viral forms including cccDNA and integrated HBV DNA (Maini and Burton, 2019).

1.3.3 Antiviral immunity of B cells and antibodies in HBV infection

B cells are the major component of humoral adaptive immunity, which mainly target extracellular pathogens. The well-known effector function of B cells is to produce neutralizing antibodies, which can prevent the entry of pathogens into their target cells (Corti and Lanzavecchia, 2013; Murphy and Weaver, 2016).

During HBV infection, only antibodies against the surface protein (anti-HBs) have the neutralizing activity. They can recognize and bind to key viral epitopes required for the HBV infectivity (Cerino, 2015). Anti-HBs also plays an important role in limiting the viral spread by preventing the HBV binding to its receptor NTCP on non-infected hepatocytes (Yan and Zhong, 2012; Bertoletti and Ferrari, 2016). In addition to that, anti-HBs may form antigen-antibody immune complexes with the circulating subviral particles, especially during chronic HBV infection (Gerlich, 2007). It has been reported that HBsAg/anti-HBs immune complexes can bind Fc receptors on dendritic cells to promote T-cell priming (Bournazos and Ravetch, 2017). This mechanism has been

exploited in the development of an HBsAg – anti-HBs immune complex-based therapeutic vaccination strategy for CHB (Liu, 2016). Furthermore, the anti-HBs can also exert Fc-dependent effector functions of antibody-dependent cellular phagocytosis (ADCP) and antibody-dependent cell-mediated cytotoxicity (ADCC) to eliminate virus-infected cells (Lu, 2018) (Fig.1.5).

The main feature of HBV-specific B cells is to differentiate into plasma cells and to secrete high-affinity antibodies directed against the virus. However, B cells can also secrete some antiviral cytokines, such as $IFN\gamma$, TNF, and IL-6 (Karnowski, 2012), which can eliminate the virus through noncytolytic mechanisms during HBV infection (Hösel, 2009; Palumbo, 2015) (Fig.1.5).

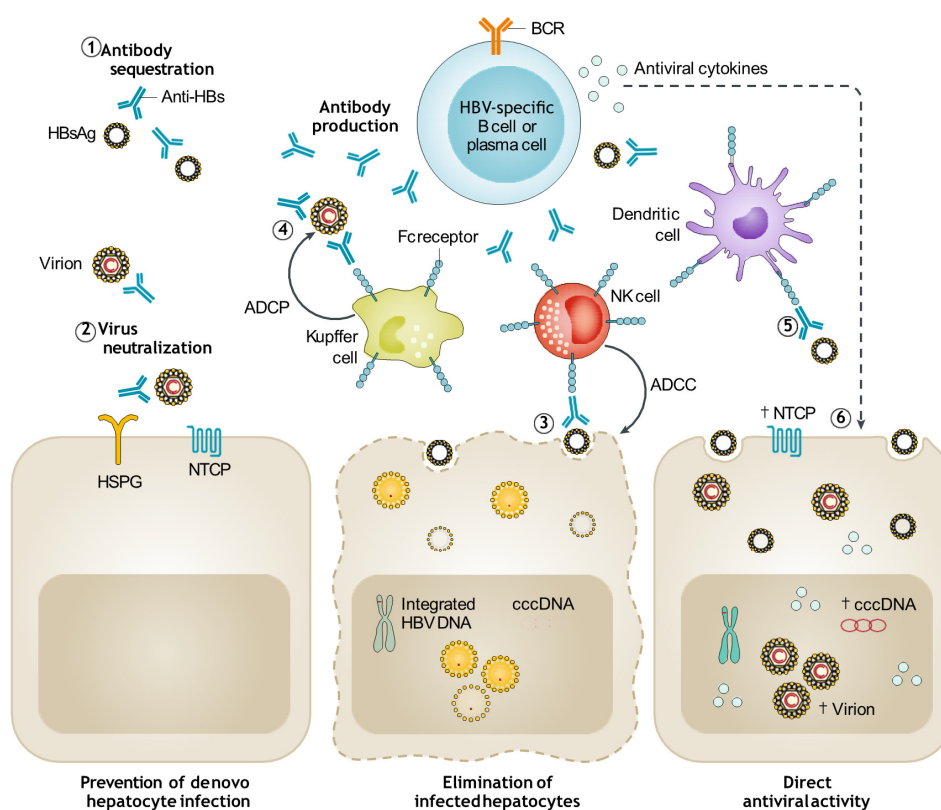


Fig.1.5 Antiviral functions of B cells and antibodies in HBV infection.

These antiviral functions include the production of anti-HBs antibodies that: are sequestered by circulating HBsAg (step 1); bind HBsAg on virions to block virus attachment (Step 2); bind HBsAg on the surface HBV infected cells to induce ADCC by NK cells and ADCP by Kupffer cells (Step 3 and 4); form HBsAg - anti-HBs immune complexes binding dendritic cells (step 5). In addition, B cells also involves the production of antiviral cytokines (for example, IL-6) (Step 6) (Maini and Burton, 2019).

1.4 Therapeutic vaccination against chronic hepatitis B

A fundamental goal of CHB therapy is the restoration of robust HBV-specific adaptive immune responses, which is necessary for the virus clearance (Maini and Pallett, 2018). Through inducing *de novo* or boosting the existing HBV-specific T-cell and B-cell responses, therapeutic vaccination is a promising strategy to restore the endogenous adaptive immunity and achieve the 'cure' of the disease (Gehring and Protzer, 2019).

1.4.1 Therapeutic hepatitis B vaccines in clinical trials

Currently, there are multiple therapeutic vaccines against CHB in clinical trials (Kosinska, 2017; Lobaina and Michel, 2017).

The first therapeutic vaccination trials were based on prophylactic vaccines containing HBsAg. In these studies, prophylactic vaccine led to a significant increase in HBeAg seroconversion, induction of HBV-specific T cells, and reduction in HBV levels in some of the patients. However, the antiviral effects were not sustained and did not achieve any control of the virus (Pol and Michel, 2006). In addition, several clinical trials were combining a prophylactic vaccine with conventional antiviral therapies. They also did not show noticeable improvements in the disease control (Vandepapelière, 2007; Aguilar and Lobaina, 2014).

While numerous therapeutic HBV vaccines have used surface proteins as the target antigen, HBcAg is also an important target of the immune response during self-limiting hepatitis B (Ferrari, 1991; Tsai, 1992). A vaccination approach based on the combination of recombinant HBsAg and HBcAg, called HeberNasvac, is currently developed as a therapeutic vaccine for CHB. In a recently completed phase III clinical trial, HeberNasvac immunization was compared with PEG-IFN in treatment-naïve chronic hepatitis B patients. With respect to the PEG-IFN treated group, a superior sustained reduction of serum HBV DNA and a higher rate of HBeAg seroconversion were observed in the HeberNasvac treated patients. In addition, unlike the PEG-IFN treatment, HeberNasvac vaccination was safe and well-tolerated in the patients

(Al Mahtab and Akbar, 2018). However, the immunologic responses accounting for the therapeutic effects were not analyzed in the clinical trials. In a recently published preclinical study, it has been shown that the immunization with HeberNasvac favored the induction of CD4, but not CD8 T-cell responses that are essential for virus clearance (Bourgine, 2018). Currently, an ongoing study with HeberNasvac as adjunct therapy to antivirals has entered phase IIb/III of clinical trials. The aim of this trial is to assess the efficacy of the HeberNasvac vaccination on the control of HBV replication after finishing the treatment with antivirals (Lobaina and Michel, 2017).

The DV-601 candidate is another vaccine that employs a combination of HBsAg and HBcAg (Marshall, 2007). DV-601 vaccine also contains ISCOMATRIX adjuvant to enhance the immune responses towards HBV antigens. The preliminary results demonstrated that immunization with DV-601 elicited HBV-specific immune responses and resulted in significant HBV DNA reduction in all dosage groups (Spellman and Martin, 2011). Moreover, the vaccine was well-tolerated and safe. Despite phase I trials were terminated several years ago, no relevant results have been published and no further studies are ongoing.

An antigen-antibody immune complex therapeutic vaccine candidate was developed by the team of Prof. Yumei Wen (Wen, 1995). This strategy is based on the formation of HBsAg / anti-HBs immune complexes (IC), which can then bind the Fc receptors of DCs to promote T-cell proliferation (Xu, 2005). A significant virological effect was observed in a Phase IIb clinical trial, in which HBsAg IC mixed with alum adjuvant was used in CHB patients. It was demonstrated that the HBeAg seroconversion rate was 21.8% in the group immunized with 60 µg HBsAg IC, and only 9% in the control group immunized with alum alone (Xu, 2008). However, the results of a phase III clinical trials were disappointing. A decrease in serum HBV DNA and normalization of liver function were comparable in the HBsAg IC and alum only immunized groups (Xu, 2013). This can be because HBsAg IC with alum adjuvant preferentially induce antibody but not cytotoxic T-cell responses that would be necessary for therapeutic efficacy (Kosinska, 2017).

Introduction

DNA-based vaccines have also been assessed as therapeutic vaccines for CHB in several clinical trials. Despite the encouraging preclinical results, the DNA-based vaccines only led to minor clinical improvements in chronic hepatitis B patients (Mancini-Bourgine, 2004; Yang, 2006; Fontaine, 2015). A novel DNA vaccine candidate INO-1800 has recently been evaluated in phase I clinical trial. INO-1800 is a mixture of recombinant DNA vaccines, which contains the plasmids encoding the HBsAg and the consensus sequence of the HBcAg (Obeng-Adjei, 2012). The Inovio Pharmaceuticals announced INO-1800 was safe, well-tolerated, and generated HBV-specific T cells, especially cytotoxic CD8 T cells in the phase I clinical trials. Nevertheless, the efficacy of INO-1800 vaccine on the larger cohorts of chronic hepatitis B patients has to be further evaluated.

To induce strong T-cell responses, employing immunogenic recombinant viral vectors could be a good choice. TG1050 is an adenovirus serotype 5 (Ad5)-based vaccine, which expresses HBV polymerase and domains of core and S proteins. During the preclinical evaluations, TG1050 induced potent, multi-specific, and long-lasting T-cell response. In addition, a decrease in levels of circulating HBV DNA and HBsAg was observed (Martin, 2015). The recently completed phase Ib trials were assessed in CHB patients under the antiviral treatment. TG1050 displayed a good safety profile and was able to induce HBV-specific cellular immune responses. As the virological response is concerned, only minor decreases in serum HBsAg levels were observed, while many vaccine recipients reached unquantifiable hepatitis B core-related antigen (HBcrAg) levels by the end of the study (Zoulim, 2020). However, due to the natural infections, sustained Ad5-specific neutralizing antibody titers in human population result in pre-existing immunity against Ad5-based vaccine vectors (Tatsis, 2004). This could be a major handicap for further development of TG1050.

1.4.2 Adjuvants

Adjuvants are defined as substances used to boost and/or shape the immune responses to a vaccine (EMA adjuvant guideline, 2005). The benefits of using

adjuvants include: sparing of vaccine dose, enabling a more rapid immune response, broadening the magnitude and functionality of antibody responses, and inducing the effective T-cell responses (Reed, 2013). In numerous preclinical and clinical studies, it has been proven that adjuvants are the key components in vaccines, especially subunit vaccines. The currently approved adjuvants for human use are summarized in Table 1.1.

Table 1.1 The summary of adjuvants approved for human use

Adjuvant	Description	Approved vaccine products
Aluminum-based mineral salts (Alum)	E.g. Aluminum phosphate, Calcium phosphate, Aluminum hydroxide	Eg. Anthrax (BioThrax [®] , Emergent Biosolutions) Hepatitis A (Vaqta [®] , Merck) DTP (Triple Antigen [™] , CSL limited)
MF59	Submicron oil-in-water emulsion	Influenza (FLUAD [®] , Novartis)
Monophosphoryl lipid A (MPL)	Bacteria-derived immunostimulant	Hepatitis B (Fendrix [®] , GlaxoSmithKline)
Virosomes	Spherical vesicles containing viral membrane proteins in the lipid membrane	Hepatitis A (Epaxal [®] , Berna Biotech) Influenza (Inflexal [®] , Berna Biotech)
CpG-1018	CpG, a synthetic form of DNA that mimics bacterial oligodeoxynucleotide and viral genetic material	Hepatitis B (Heplisav-B [®] , Dynavax)
AS01B	Liposome combines with MPL and QS-21, a natural compound extracted from the Chilean soapbark tree	RZV (Shingrix [®] , GlaxoSmithKline)
AS03	Emulsion-based, containing α -Tocopherol, squalene, and polysorbate 80	Influenza (Pandemrix [®] , GlaxoSmithKline)
AS04	VLPs and MPL adsorbed onto Alum	HPV (Cervarix [®] , GlaxoSmithKline)

Collected the information from the website of British society for immunology; Nanishi, 2020.

Introduction

The classical adjuvants are divided into two main categories: particulate vaccine-delivery systems and immunostimulatory adjuvants (Cooper, 2018). The delivery system adjuvants promote a more effective presentation of vaccine antigens to the APCs. They include alum, emulsions, liposomes, virosomes, microparticles, etc. Aluminum salts are the most widely used adjuvants in the history of vaccinology (Table 1.1). They primarily enhance Th2-biased antibody responses and have little effect on Th1-type responses (Leroux-Roels, 2010). Emulsions, such as oil-in-water and water-in-oil emulsions, consist of combinations of various oils and surfactants. So far one emulsion adjuvant: MF59, which consists of squalene, Tween 80, and Span 85 detergents, has been approved for human use (Table 1.1; Kalvodova, 2010). Liposomes are synthetic nanospheres, comprised of various phospholipid bilayers (Aguilar and Rodriguez, 2007). Antigens can be encapsulated or associated with the liposomes' surface for effective delivery to APCs.

The immunostimulatory adjuvants directly activate the innate immune system. Most of them are targeting the innate pattern recognition receptors (PRRs), such as Toll-like receptors (TLRs), NOD-like receptors (NLRs), C-type lectins, and RIG-I-like receptors (Reed, 2013). TLR4 ligand Monophosphoryl lipid A (MPL), a less toxic derivative of lipopolysaccharide (LPS), is approved for use in HBV vaccine Fendrix from GSK (Table 1.1). MPL mediates its adjuvant effects on Th1 cells, and further enhances the induction of antigen-specific CD8 cytotoxic T cells (CTLs) (Mbawuike, 1996). TLR-9 ligand: CpG oligodeoxynucleotide (ODN) is another advanced developed adjuvant, which is used in the HBV HEPLISAV-B vaccine from Dynavax (Table 1.1) (Eng, 2013). Several immunostimulatory adjuvants are derived from plants. QS-21 is a purified fraction of natural saponin QuilA, which is extracted from the soap bark tree (*Quillaja Saponaria*) (Kensil, 1998). QS21 has shown potent adjuvant abilities by enhancing antigen presentation to APCs, inducing the CTLs production, eliciting both Th1 and Th2 cytokine secretion (Newman, 1997).

Over the past decade, a new generation of adjuvants has been emerging, which are combination adjuvants. These adjuvants typically contain one delivery system component, and one to two immunostimulatory substances (Garçon and Di Pasquale,

2017). The combination of the individual adjuvants allows the vaccine to benefit from a synergistic effect, thereby resulting in improved antigen-specific immune responses (Gerdt, 2015). Moreover, by selection of appropriate components for combination adjuvants, a complementary effect on the induction of both, Th1- and Th2-type immune responses, could be observed. As an example, the adjuvant AS04 in the human papilloma virus (HPV) vaccine – Cervarix, is a combination adjuvant based on MPL and aluminum salts (Table 1.1). Aluminum salts provoke Th2-biased responses and thereby humoral responses, whereas MPL stimulates Th1-type responses and facilitates the induction of CTLs. Therefore, Cervarix vaccine supplemented with AS04, is able to induce not only a robust humoral response, but also strong cellular responses against L1 protein of HPV types 16 and 18 (Einstein, 2009).

Adjuvants execute their functions by a variety of mechanisms. Some adjuvants, such as emulsions, can act through the formation of a depot at the injection site resulting in slow and sustained release of the antigen (Shah, 2015). Moreover, some adjuvants can also induce a local immunocompetent environment at the injection site, which can result in the recruitment of immune cells, such as APCs.

The recruited APCs express a repertoire of PRRs both on the cell surface (TLRs, CLRs) and intracellularly (NLRs and RLRs). These PRRs can be recognized and activated by various classes of immunostimulatory adjuvants that represent their ligands. This leads to the maturation and activation of the recruited APCs. Mature APCs upregulate the expression of MHC and co-stimulatory molecules, which help to increase the capacity of antigen presentation. In the further step, the mature APCs migrate to the draining lymph nodes to interact with antigen-specific B or T cells to activate the potent antibody-secreting B cells and/or effector CTLs (Fig. 1.6) (Awate, 2013).

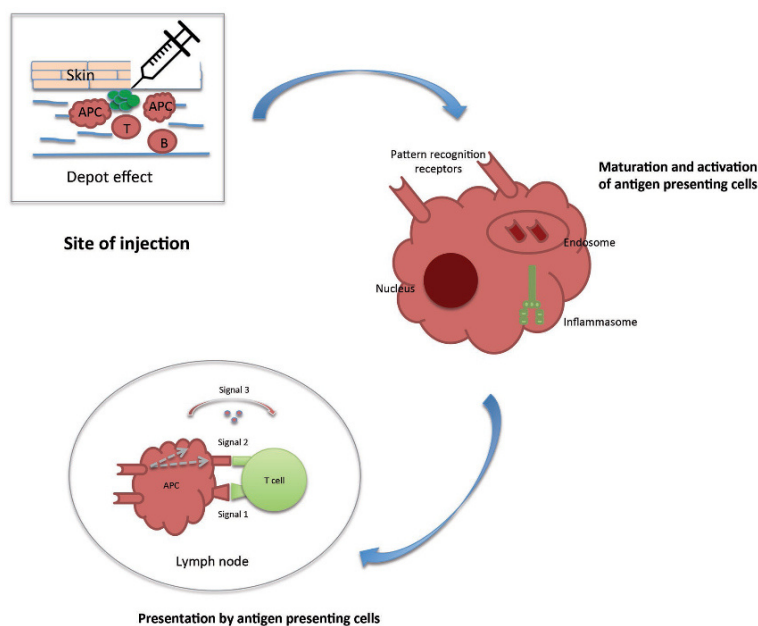


Fig.1.6 The potential mechanisms of action of adjuvants.

Adjuvants may act by a combination of a variety of mechanisms, including the formation of depot site, induction of cytokines and chemokines, recruitment of immune cells (such as APCs), maturation and activation of APCs, as well as enhancement of antigen presentation in the lymph nodes (Gerdt, 2015).

1.4.3 Viral vectors

Recombinant viral vectors represent promising vaccine platforms for therapeutic vaccines, due to their ability to induce antigen-specific cellular immune responses. Since the development of vaccinia virus as a vaccine vector in 1984, there are numerous viruses explored as vaccine vectors, such as adenovirus (Ad), Modified Vaccinia Virus Ankara (MVA), and vesicular stomatitis virus (VSV).

Recombinant adenoviruses, especially human Ad5, have been one of the most intensively investigated viral vectors for vaccine development. The benefits of using adenoviruses include eliciting robust CD8 T cells and strong antibody responses. Moreover, adenoviruses are known to allow for high titer of virus during manufacturing (Shiver, 2002). However, pre-existing immunity against this vector was shown to correlate with the reduction in antigen-specific immunogenicity in clinical trials (Buchbinder, 2008). The utility of the adenoviruses from non-human origins has been tested to circumvent the pre-existing immunity problem (Colloca, 2012). An outstanding example is ChAd3-EBOZ, a simian adenoviral vector encoding the Ebola Zaire glycoprotein, which was evaluated in phase I and II clinical trials in response to the Ebola epidemic (Ledgerwood, 2017). Currently, there is an adenovirus-based

therapeutic vaccine candidate against chronic hepatitis B, TG1050, which successfully completed phase I clinical trials (Zoulim, 2020).

Recombinant MVA is a safe and well-tolerated attenuated vector that has consistently displayed excellent immunogenicity profiles (Sebastian and Gilbert, 2015). Antigens expressed from the MVA vectors are able to induce strong CTLs responses. Moreover, as a virus, MVA can stimulate both, innate and adaptive immune responses, which contribute to MVA-mediated protective immune responses. The MVA genome can be readily modified and tolerates the insertion of foreign genes, with a packaging capacity of at least 25 kb. Due to its strengths, MVA has been widely used as a clinical candidate vaccine against various infectious diseases such as HBV, HIV, malaria (Cavanaugh, 2011; Afolabi, 2013; Sebastian and Gilbert, 2015), and also in cancer (Acres and Bonnefoy, 2008; Ramlau, 2008).

However, an induction of immunity against the MVA vector itself, may be a drawback, as it may become dominant upon repetitive application (Kastenmuller, 2007). The dominant MVA-specific immune responses can significantly decrease the efficacy of the vaccination with MVA. Therefore, MVA is often used in heterologous prime-boost vaccination schemes to overcome the problem of anti-vector immunity when repetitive immunizations are required.

Recombinant vesicular stomatitis virus (VSV) is a new emerging vaccine vector that has been recently investigated in clinical trials (Coller, 2017; Suder, 2018). The benefits of using VSV include inducing robust cellular and humoral immunity against encoded antigens. Moreover, the VSV-based vectors can be easily produced as they maintain sustained high titer growth in cell culture. In addition, as a negative-strand RNA virus, VSV does not generate DNA intermediates during viral replication, which circumvents the potential of virus integration into the host genome (Humphreys and Sebastian, 2018). Lastly, the antibodies against VSV in the human population are extremely rare, which can avoid the problems associated with pre-existing immunity against the vector in patients (Lichty, 2004).

Unlike other replication-deficient vectors, most VSV-based vaccine vectors are replication-competent, though attenuated. As wild-type VSV has been reported to

Introduction

show neurovirulence, safety is still a main concern of VSV application. Attenuation of VSV may be achieved in several manners. The distinguished example combines down-regulation of N protein expression with truncation of the VSV-G, resulting in the attenuated vector rVSVN4CT1, which has been approved for clinical studies (Cooper, 2008; Humphreys and Sebastian, 2018). Furthermore, a chimeric VSV variant, called VSV-GP, has also been proved to successfully abrogate the VSV's neurotoxicity without losing its efficacy in a variety of preclinical models (Schreiber, 2019). VSV-GP is a VSV variant with its G protein replaced by the lymphocytic choriomeningitis virus (LCMV)-derived glycoprotein (GP) (Muik, 2014). Of note, it has been reported that VSV-GP does not induce vector-specific humoral immunity *in vivo*, therefore it can be used repetitively without a loss of immunogenicity towards the encoded antigens (Tober, 2014). This unique feature makes VSV-GP a useful platform for the development of various vaccines against a broad spectrum of diseases.

1.5 Mouse models to study the therapy of chronic hepatitis B

Animal models are crucial for understanding the pathogenesis of chronic hepatitis B and developing new therapeutic strategies against CHB. Although mouse is the best characterized and most convenient laboratory animal, it cannot be infected with HBV (Guo, 2018). This is due to the fact that HBV has a very limited host range with strict hepatic tropism. Except humans, it was experimentally shown that HBV can only infect chimpanzees and macaques, as well as tree shrews (*Tupaia belangeri*) (Dupinay, 2013). After numerous efforts over many decades, several mouse models that can support persistent HBV replication have been successfully established (Dembek and Protzer, 2015; Guo, 2018).

In the last 20 years, the most commonly used HBV mouse model has been HBV transgenic (HBVtg) mouse. It was generated through introducing a 1.3-fold HBV genome into the mouse genome (Guidotti, 1995). HBVtg mice replicate HBV in hepatocytes, produce all HBV antigens and release infectious virus into the blood. The model has been utilized to explore the pathogenesises of HBV infection, and evaluate

many antivirals against CHB, such as lamivudine and entecavir (Julander, 2003; Weber 2002). Moreover, HBVtg mice show immunotolerance to HBV antigens, but this tolerance can be broken, which makes the model suitable for the evaluation of therapeutic vaccination against CHB (Shimizu, 1998). A major limitation of HBVtg mice is that HBV genome is integrated in the mouse genome, thereby the virus cannot be fully eliminated. Additionally, the mouse hepatocytes do not support cccDNA formation, which is the natural template for HBV transcription. Consequently, the effects of new HBV therapeutics on the viral clearance and eradication of HBV cccDNA cannot be investigated in this mouse model.

Hydrodynamic injection (HDI), a tail vein injection of a replication-competent HBV plasmid, has been found to successfully deliver HBV DNA into the livers of immunocompetent mice (Yang, 2002). However, not all of the injected mice develop persistent HBV infection. In many cases, HBV antigen expression and replication after HDI are only transient. It has been reported that plasmid backbone, mouse strain, and sex can greatly affect HBV replication duration in mice (Huang, 2006; Kosinska 2017b). Moreover, the HDI procedure, a rapid delivery of considerable amount of liquid into the hepatocytes, causes an immense burden to the mice, with significant hepatocytes damage and ALT elevation directly after injection (Kosinska 2017b; Dembek and Protzer, 2015).

To increase the *in vivo* transfer efficiency, viral vectors, specifically adenovirus (Ad) and adeno-associated virus (AAV), were employed to deliver HBV genome into the mouse hepatocytes (Tang, 2019). Infection of mice with high doses of Ad-HBV (adenoviral vectors containing a replication-competent HBV genome) leads to self-limiting HBV infection (John von Freyend, 2011). In contrast, by injecting relatively low doses of Ad-HBV, persistent HBV infection could be established in the immunocompetent mice (Huang, 2012). Nevertheless, the adenovirus infection elicits a strong vector-specific immune response, which may make it difficult to interpret the HBV-related immune responses (Tang, 2019).

Transduction of mouse hepatocytes with recombinant AAV carrying HBV genome (AAV-HBV) proved to be very efficient in various immunocompetent mouse strains

Introduction

(Dion, 2013; Kosinska, 2019). AAV-HBV mice show persistence of HBsAg, HBeAg, and HBV DNA in serum, as well as viral replicative intermediates and transcripts in the liver, for at least one year upon AAV-HBV transduction (Dion, 2013). Unlike adenovirus, infection of AAV-HBV vector does not stimulate vector-specific immune responses. Moreover, AAV-HBV infection also induces the immune tolerance to HBV antigens that mimics chronic infection in humans (Hwang and Park, 2018). Interestingly, the formation of HBV cccDNA was recently observed in hepatocytes of AAV-HBV transduced mice (Lucifora, 2017). All these advantages make the AAV-HBV mouse model especially suitable to explore the efficacy of novel therapeutic strategies on elimination of persistent HBV infection.

Even though the mouse models mentioned above are very valuable and allow studying many aspects of HBV pathogenesis, they are not suited to study the entire HBV life cycle (Hwang and Park, 2018). Therefore, several human liver chimeric mouse models have been investigated to overcome this problem (Allweiss and Dandri, 2016). Two requirements need to be achieved to partially reconstitute human hepatocytes in mouse liver: First, liver damage must be induced in mouse hepatocytes, which permits repopulation of the mouse liver with human hepatocytes (Dandri, 2001). Next, the adaptive immune system of mice must be abolished to allow the survival of transplanted human hepatocytes (Allweiss and Dandri, 2016). With transplanted human hepatocytes in the liver, these chimeric mouse models can fully support HBV infection, thereby are an excellent model to study the all steps of HBV infection, virus spread, and the nature of cccDNA (Hwang and Park, 2018). However, the immunodeficiency of these mice makes them unsuitable to investigate endogenous HBV-specific B- and T-cell responses induced by immunotherapeutic strategies such as therapeutic vaccination.

1.6 Aims of the study

Chronic HBV infection is still a major global health problem. It can rarely be cured by the currently available treatments. Therefore, developing new therapeutic strategies to treat CHB is highly demanded. Since the induction of robust HBV-specific adaptive immune responses is necessary to clear the virus, therapeutic vaccination represents a promising new strategy to treat CHB and achieve a 'cure' of the disease.

Our laboratory has developed a heterologous prime-boost therapeutic hepatitis B vaccine, termed *TherVacB*, which is based on two protein immunizations using particulate, recombinant HBsAg and HBcAg followed by a boost using MVA vectors expressing HBV antigens (Backes and Jäger, 2016). To improve the *TherVacB*, making it suitable for clinical use, the studies conducted for this thesis focus on the optimization of the *TherVacB* regimen.

An optimal immunization protocol is essential to further improve the *TherVacB* regimen. To this end, the first part of the thesis aimed to establish the optimal *TherVacB* immunization protocol, by titration of vaccine component doses and comparison of delivery routes in HBV-transgenic (HBVtg) mice.

In both HBVtg and AAV-HBV mice, we found that the success of *TherVacB* largely depends on an appropriate adjuvant for the protein priming, which simultaneously generates neutralizing antibody responses and elicits potent CD4 and CD8 T-cell responses (Kosinska, 2019; Michler and Kosinska, 2020). Therefore, the second part of this thesis aimed to investigate novel adjuvants to improve protein priming in the *TherVacB* regimen. To achieve this goal, first, the stability and integrity of antigen/adjuvant formulations over prolonged storage time were to be characterized *in vitro*. Next, the effects of various adjuvants on the activations of dendritic cells needed to be investigated *in vitro*. Finally, the immunogenicity of the most promising antigens/adjuvant formulations was evaluated in wild-type mice and persistent HBV replication mouse models.

Since proper protein priming is the key to *TherVacB* success, the third part of this thesis aimed to explore the critical factors that contribute to a satisfactory outcome of

Introduction

TherVacB during the priming phase. To this purpose, the importance of individual vaccine components, antigens and adjuvant, for priming was determined. In addition, the roles of different T-cell subsets in the *TherVacB*-mediated immune responses during the priming phase were explored by antibody-mediated T-cell subset depletion *in vivo*.

For *TherVacB*, the boosting immunization with the recombinant MVA is one of the steps critical to activate strong HBV-specific T-cell responses and break HBV-specific immune tolerance. Despite many benefits from employing MVA vectors, the dominant MVA-specific immune responses can significantly decrease the efficacy of MVA vaccination. Therefore, the aim of the fourth part of this thesis was to develop the novel VSV-GP vector (a VSV variant with its G protein replaced by LCMV-derived glycoprotein) to improve the *TherVacB* regimen. In the first step, a bicistronic recombinant VSV-GP encoding HBsAg and HBcAg (VSV-GP-HBs/c) should be generated. Next, the immunogenicity of VSV-GP-HBs/c had to be proven in wild-type mice. Finally, various prime-boost immunization regimens using VSV-GP-HBs/c needed to be evaluated in AAV-HBV mice and compared to MVA-based *TherVacB* protocols.

2. Results

2.1 Optimization of the *TherVacB* immunization protocol

To improve the efficacy of *TherVacB* regimen and optimize it for clinical development in the near future, an optimal immunization protocol is indispensable. The following experiments aimed at optimizing the *TherVacB* immunization protocol by adjuvants selection, vaccine component dose titrations, and vaccine delivery route comparison in HBV transgenic (HBVtg) mice.

2.1.1 Selection of the adjuvants for protein priming

When the *TherVacB* strategy was initialized, the vaccination delivery route was subcutaneous injection (s.c.) for protein priming and intraperitoneal injection (i.p.) for MVA vector boost. Since intramuscular injection (i.m.) is the most common route of vaccine administration in clinics, it was decided to change all *TherVacB* delivery routes to intramuscular injections. Therefore, it was necessary to select a suitable adjuvant for the *TherVacB* scheme via the i.m. route.

Cyclic di-AMP (c-di-AMP) is a STING agonist that has been proven to exert superior adjuvant properties in the influenza vaccine and other vaccine studies (Ebensen, 2017; Volckmar, 2019). Moreover, it was found to be well-tolerated *in vivo*. Thereby, it was of interest to test this new STING agonist c-di-AMP as an adjuvant in the *TherVacB* scheme. In this section, c-di-AMP from two sources was explored as an adjuvant in *TherVacB* schemes and compared with previously used combination of CpG and PCEP (polyphosphates) (Backes and Jäger, 2016).

HBVtg mice were immunized with 15 µg of HBcAg adjuvanted with c-di-AMP intramuscularly from either our collaboration partner in Braunschweig (BR) or the InvivoGen company (IG) at week 0 and week 2. A group of mice immunized with HBcAg adjuvanted with CpG + PCEP was used as the control. At week 4, mice received 3×10^7 infectious units (IFU) of MVA-core vector intramuscularly to boost the immune response. At week 5, mice were sacrificed to analyze the HBV-specific

Results

antibody responses and HBV-related parameters in the murine serum and to detect T-cell responses in the livers and spleens of the mice (Fig.2.1).

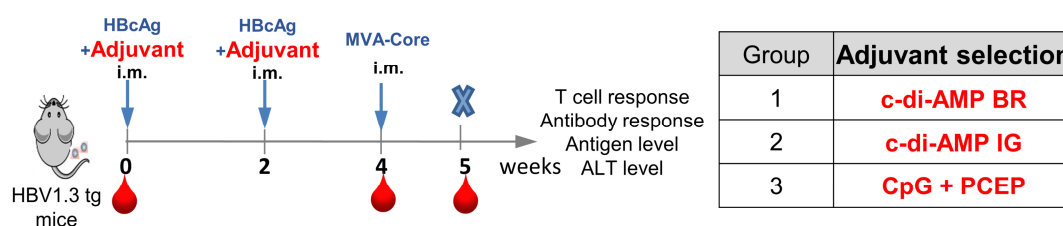


Fig.2.1 Immunization scheme of adjuvant selection.

HBV1.3tg mice received two protein vaccinations formulated with the adjuvants listed in the table on the right at week 0 and week 2, followed by an MVA-boost immunization at week 4. The mice were sacrificed at week 5 for the final analysis in the serum, liver, and spleen.

The vaccine-induced antibody response was determined by the detection of HBcAg-specific antibodies (anti-HBc) in the serum of mice one week after MVA boost. Immunization of mice with all three formulations induced remarkably high anti-HBc titers compared to the unvaccinated controls. Moreover, the anti-HBc levels in mice immunized with both c-di-AMP formulations were significantly higher than those in mice immunized with the CpG + PECP formulation ($p < 0.05$) (Fig.2.2 A).

Immunizations with c-di-AMP formulations, but not the CpG + PECP formulation, resulted in an overall 25–45% decrease in serum HBeAg at week 5 compared to the baseline at week 0 (Fig.2.2 B). Although HBsAg was not included for priming in this experiment, the serum HBsAg in the mice that received all three formulations was reduced to almost undetectable levels at week 5 (Fig.2.2 C). There was no significant serum alanine aminotransferase (ALT) elevation observed for any of the groups at the analyzed time point of week 5 (Fig.2.2 D).

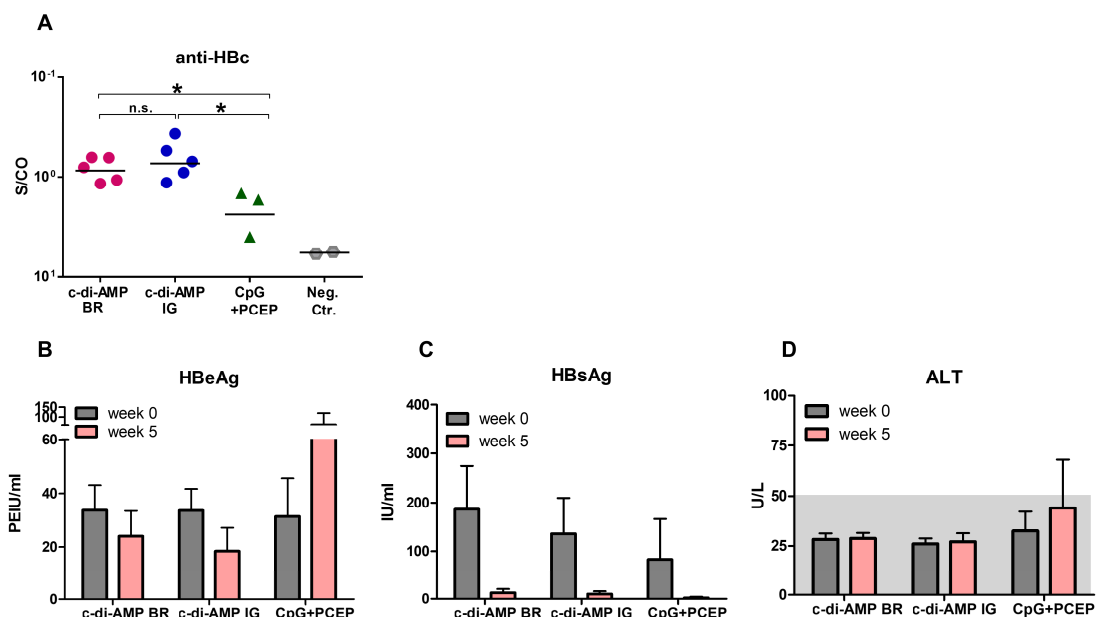


Fig.2.2 Antibody responses and HBV serological analyses of adjuvant selection.

(A) The levels of anti-HBc were detected in the serum of immunized mice at the endpoint.

(B, C, D) The levels of HBeAg (B), HBsAg (C), and ALT (D) were detected in the serum of immunized mice at the start point and endpoint.

Statistical analysis was performed using Mann-Whitney test. Asterisks (*) mark statistically significant differences: * $p < 0.05$; *ns*—not significant.

In the next step, the induction of cellular immune responses after immunization with the tested formulations was evaluated by the intracellular IFN γ staining of peptide-stimulated liver-associated lymphocytes (LALs) and splenocytes one week after MVA boost.

Vaccination of mice with two c-di-AMP formulations led to strong core-specific CD8 T-cell responses in both liver and spleen, whereas the CpG + PECP formulation displayed a trend of weaker induction of core-specific responses (Fig.2.1 A and C). In addition, MVA vector B8R-specific CD8 T-cell responses in mice immunized with all three formulations were similar in spleen and liver (Fig.2.3 B and D)

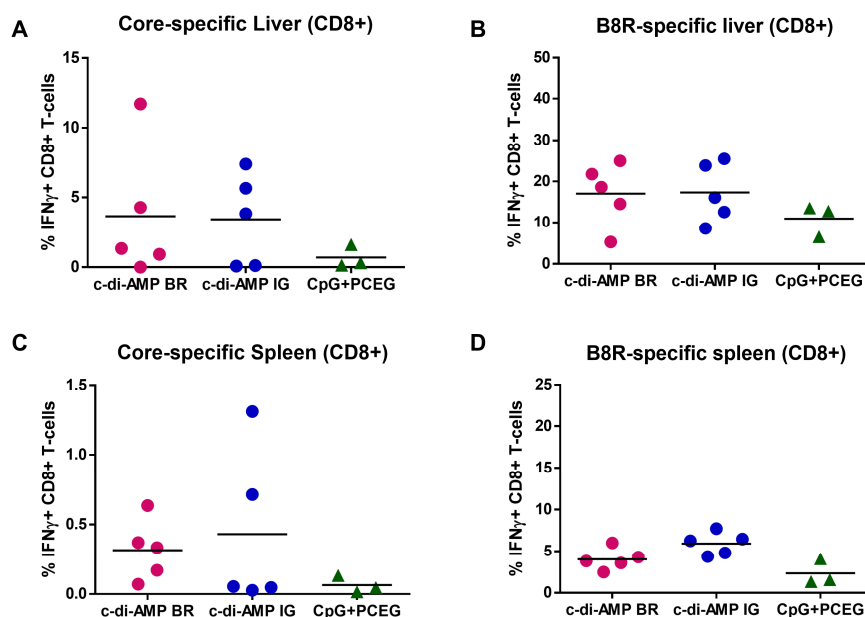


Fig.2.3 T-cell response analysis of adjuvant selection.

(A, B) Percentages of intrahepatic core- (A) and B8R-specific (B) IFN γ + CD8 T cells determined by intracellular cytokine staining after core-specific overlapping peptide pool and MVA-specific peptide B8R *ex vivo* stimulation.

(C, D) Percentages of splenic core- (C) and B8R-specific (D) IFN γ + CD8 T cells determined by intracellular cytokine staining after core-specific overlapping peptide pool and MVA-specific peptide B8R *ex vivo* stimulation.

Taken together, these findings indicate that immunization with both c-di-AMP formulations stimulated strong and comparable antibody and T-cell responses, which were superior to those in the mice that received the CpG+ PCEP formulation. Thus, the immunogenicity of c-di-AMP was similar, independently which source of the adjuvant was used. Considering the accessibility, the c-di-AMP from InvivoGen was selected as the adjuvant for the further studies.

2.1.2 Estimation of the optimal MVA dose for boost

Since the vaccine administration was changed to the i.m. route, it was necessary to determine the optimal doses of protein and MVA via the new delivery route. The experiments in this section aimed to determine the appropriate dose of MVA for intramuscular immunization in HBVtg mice.

HBVtg mice were immunized with 15 μ g of HBcAg adjuvanted with c-di-AMP at week 0 and week 2. At week 4, different doses of MVA vector— 3×10^6 infectious units (IFU),

1×10^7 IFU, 3×10^7 IFU, and 1×10^8 IFU—were administered to boost the immune response. At week 5, the mice were sacrificed to analyze the antibody responses and HBV-related parameters in the serum and detect T-cell responses in the livers and spleens of the mice (Fig.2.4).

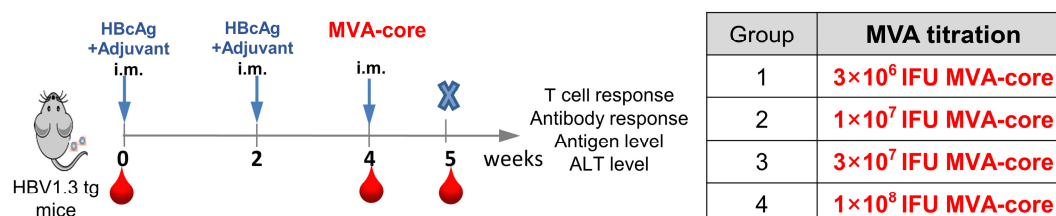


Fig.2.4 Immunization scheme of MVA dose titration.

HBV1.3tg mice received c-di-AMP adjuvanted HBcAg twice at week 0 and week 2, followed by a different dose of MVA-core boost immunization at week 4. The four different MVA doses are listed in the right table. The mice were sacrificed at week 5 for the final analysis in the serum, liver, and spleen.

The humoral immune responses induced by the immunization were analyzed by the detection of anti-HBc in the serum of mice one week after MVA boost. The levels of anti-HBc in the serum of mice boosted with all four doses of MVA were significantly increased compared to the baseline of negative controls at week 5. Moreover, boosting with 3×10^7 IFU MVA induced significantly higher levels of anti-HBc than those in mice immunized with 1×10^7 IFU MVA, which indicated that the boosting with a higher dose of MVA could further enhance antibody responses ($p < 0.05$) (Fig.2.5 A). Since HBsAg was not included for priming in this study, only weak anti-HBs responses were detected in the serum of mice that received all doses of MVA (Fig.2.5 B).

Immunization of mice with high-doses of MVA, 3×10^7 IFU and 1×10^8 IFU, led overall to a more than 50% decrease in serum HBeAg at week 5 compared to the baseline at week 0. In contrast, there was no noticeable reduction in serum HBeAg in the mice that received two lower-doses of MVA, 3×10^6 IFU and 1×10^7 IFU. This indicated the better antiviral effects in the higher-dose MVA groups (Fig.2.5 C). Despite the weak anti-HBs responses, all mice showed more than 90% reduction of HBsAg levels compared to the baseline at week 0, which might be induced by HBV-specific T-cell

Results

responses (Fig.2.5 D). In addition, a mild ALT elevation was observed in the mice boosted with all doses of MVA, especially with the higher 3×10^7 IFU and 1×10^8 IFU ones (Fig.2.5 E).

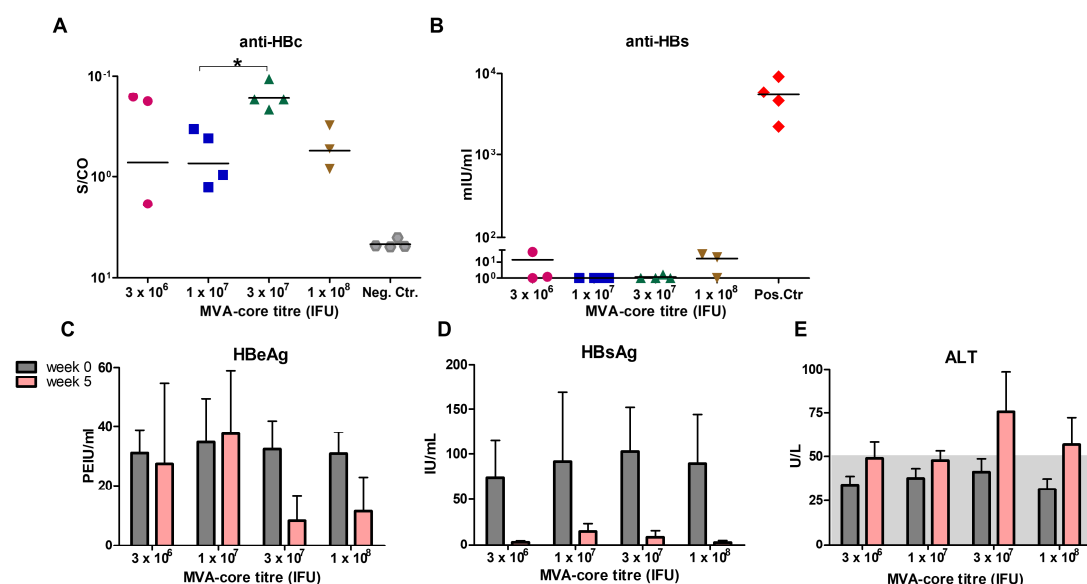


Fig.2.5 Antibody responses and HBV serological analyses of MVA dose titration.

(A, B) The levels of anti-HBc (A) and anti-HBs (B) antibodies were detected in the serum of mice at the endpoint.

(C, D, E) The levels of HBeAg (C), HBsAg (D), and ALT (E) were detected in the serum of mice at start point and endpoint.

Statistical analysis was performed using Mann-Whitney test. Asterisks (*) mark statistically significant differences: * $p < 0.05$.

Next, the effects of boost immunization with different doses of MVA on the induction of T-cell responses were evaluated by the intracellular IFN γ staining of LALs and splenocytes upon *ex vivo* peptide stimulation.

Comparable overall core-specific CD8 T-cell responses were detected in spleen and liver of all mice (Fig.2.6 A). However, when the mice were divided into two groups: mice with high antigenemia (HBeAg > 20 PEIU/ml) and low antigenemia (HBeAg < 20 PEIU/ml), there were certain differences detected among mice boosted with different doses of MVA. In the low-antigenemia group, the core-specific responses could be detected even in the mice boosted with the lowest MVA dose of 3×10^6 IFU (Fig.2.6 B). In the high-antigenemia group, the core-specific responses were only detected in the

mice boosted with the higher doses of MVA 3×10^7 IFU and 1×10^8 IFU (red symbols indicate positive responses; grey symbols indicate nonresponsive) (Fig.2.6 C). Moreover, no clear differences were detected in the B8R-specific CD8 T-cell responses in the mice boosted with all four doses of MVA (Fig.2.6 D).

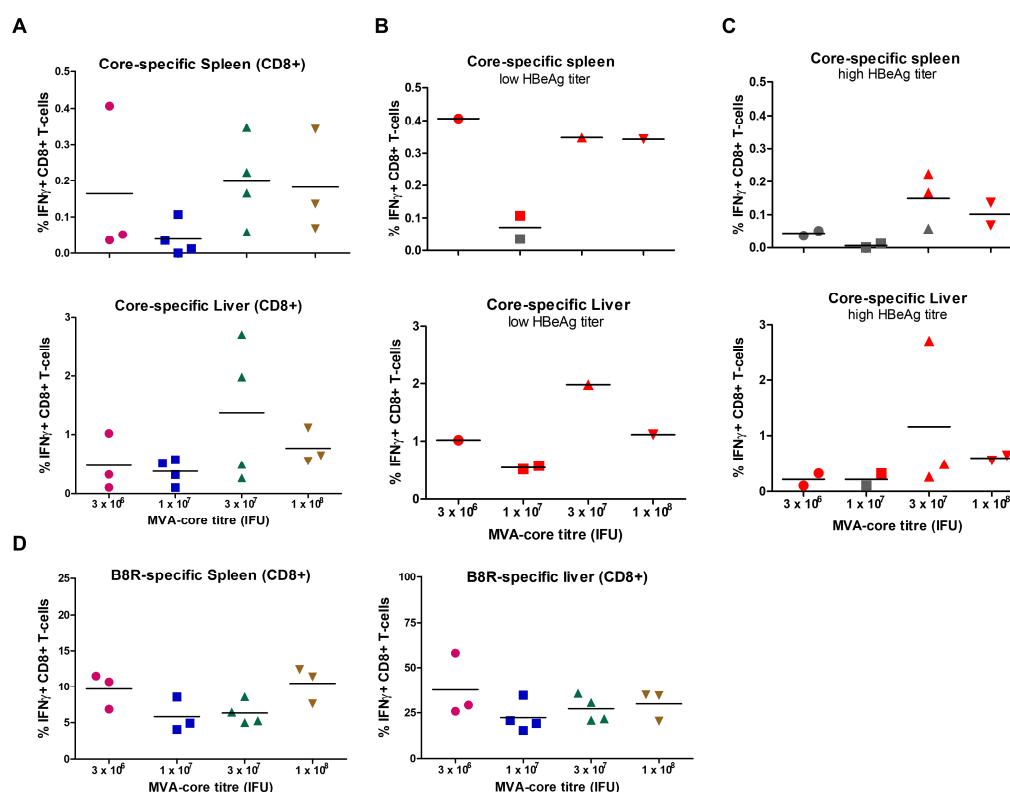


Fig.2.6 T-cell response analysis of MVA dose titration.

- (A) Percentages of splenic and intrahepatic core-specific IFN γ + CD8 T cells determined by intracellular cytokine staining after core-specific peptide pool *ex vivo* stimulation.
 (B, C) Splenic and intrahepatic core-specific CD8 T-cell responses in low-(B) and high-antigenemic mice (C). Red symbols show positive responses; grey symbols show nonresponsive.
 (D) Percentages of splenic and intrahepatic B8R-specific IFN γ + CD8 T cells determined by intracellular cytokine staining after MVA-specific peptide B8R *ex vivo* stimulation.

In HBVtg mice, which have strong HBV-specific tolerance, boost with high doses of MVA of 3×10^7 IFU and 1×10^8 IFU induced higher antibody responses, noticeable antigen decreases, mild ALT elevation, and better T-cell responses for the high-antigenemic mice. To ensure sufficient efficacy of *TherVacB*, nevertheless reduce the vaccination dose, 3×10^7 IFU was considered the optimal MVA dose for further studies.

Results

2.1.3 Estimation of the optimal protein dose for priming

After obtaining the optimal MVA dose for boost, the optimal doses of HBV antigens (HBsAg, HBcAg) for priming were determined *in vivo*.

HBVtg mice were immunized with escalating doses of 5 µg, 10 µg, or 15 µg of each HBsAg and HBcAg intramuscularly at week 0 and week 2. As adjuvant c-di-AMP was used. At week 4, 3×10^7 IFU MVA-S and 3×10^7 IFU MVA-core vectors were administered intramuscularly to boost the immune response. At week 5, the mice were sacrificed to analyze the antibody responses and HBV-related parameters in the murine serum and to detect T-cell responses in the livers and spleens of the mice (Fig.2.7).

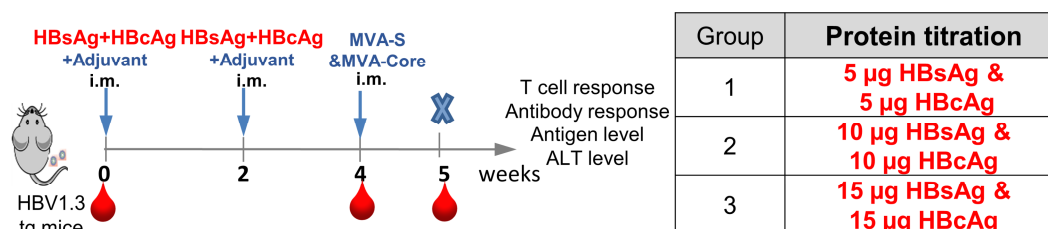


Fig.2.7 Immunization scheme of protein dose titration.

HBV1.3tg mice received different doses of HBsAg and HBcAg adjuvanted with c-di-AMP twice at week 0 and week 2, followed by the MVA-S and MVA-core boost immunization at week 4. The three different protein doses used for priming are listed in the right table. The mice were sacrificed at week 5 for the final analysis in the serum, liver, and spleen.

Evaluation of humoral immune responses was performed by the detection of anti-HBs and anti-HBc in the serum of mice one week after MVA boost. Since both HBsAg and HBcAg were introduced in the vaccination, there were strong inductions of both anti-HBc and anti-HBs detected in the mice primed with all three doses of protein compared to the baseline of non-vaccinated controls at week 5. In addition, despite using different doses of HBsAg and HBcAg for priming, the levels of antibodies in all three groups of mice were comparable, which suggested that the lowest protein dose was sufficient to induce adequate antibody responses (Fig.2.8 A and B).

Compared to the baseline at week 0, there was a dramatic HBsAg decrease in the serum of mice that received all three doses of protein for priming (Fig.2.8 C). No prominent HBeAg reduction was observed in the serum of mice that received 5 µg and

10 μ g of protein for priming. Immunization of mice with 15 μ g of protein induced only a slight HBeAg decrease (Fig.2.3 D). In addition, ALT levels remained stable before and after in the mice that received all three doses of protein for priming (Fig.2.8 E).

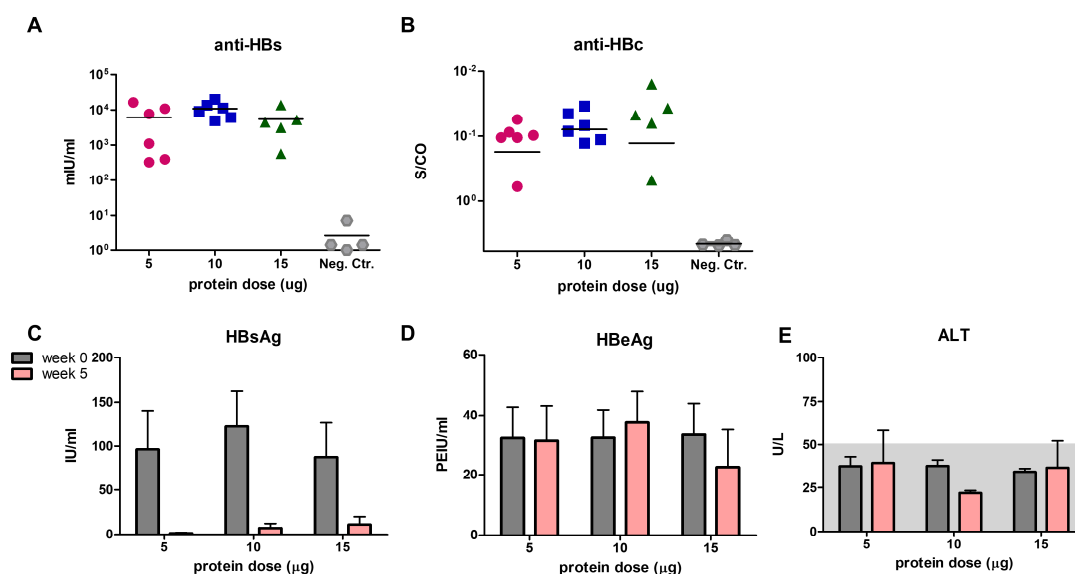


Fig.2.8 Antibody responses and HBV serological analyses of protein dose titration.

(A, B) The levels of anti-HBs (A) and anti-HBc (B) antibodies were detected in the serum of mice at the endpoint.

(C, D, E) The levels of HBsAg (C), HBeAg (D), and ALT (E) were detected in the serum of mice at the start point and endpoint.

In the next step, HBV-specific T-cell responses induced by different doses of protein were analyzed by intracellular IFN γ staining in peptide-stimulated LALs and splenocytes of mice one week after MVA boost.

The magnitudes of intrahepatic S-specific CD8 T-cell responses were comparable in that of mice primed with 10 μ g and 15 μ g of protein. Furthermore, the intrahepatic S-specific CD8 T-cell responses in mice primed with 10 μ g and 15 μ g of protein were significantly stronger compared to those in the mice primed with 5 μ g of protein ($p < 0.05$) (Fig.2.9 A, upper panel). Consistent with the responses detected in the liver, immunization of mice with 10 μ g of protein elicited significantly higher S-specific CD8 T-cell responses in the spleen compared to those in the mice primed with 5 μ g of protein ($p < 0.05$) (Fig.2.9 A, lower panel). Core-specific CD8 T-cell responses displayed similar trends as the S-specific ones, with inferior efficacy detected in the

Results

mice primed with 5 μg of protein (Fig.2.9 B). As expected, comparable B8R-specific responses were observed in both the liver and the spleen of mice primed with all three doses of protein (Fig.2.9 C).

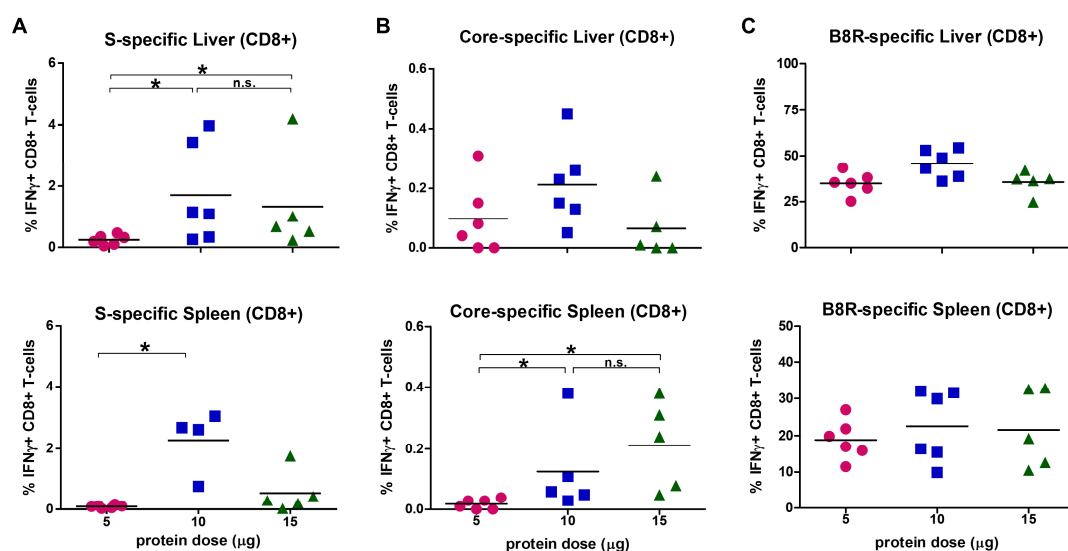


Fig.2.9 T-cell response analysis of protein dose titration.

(A) Percentages of S-specific IFN γ + CD8 T cells after *ex vivo* stimulation with S-specific peptide pool in liver (upper panel) and spleen (lower panel).

(B) Percentages of core-specific IFN γ + CD8 T cells after *ex vivo* stimulation with core-specific peptide pool in liver (upper panel) and spleen (lower panel).

(C) Percentages of MVA-specific IFN γ + CD8 T cells after *ex vivo* stimulation with MVA-specific B8R peptide in liver (upper panel) and spleen (lower panel).

Statistical analysis was performed using Mann-Whitney test. Asterisks (*) mark statistically significant differences: * $p < 0.05$; n.s.—not significant.

Taken together, these findings indicate that while the production of antibodies in mice immunized with three different doses of protein was comparable, the HBV-specific T-cell responses in the mice primed with 10 μg and 15 μg of protein were stronger than those in the mice primed with 5 μg of protein. As there was no significant improvement of *TherVacB* efficacy using 15 μg of protein for priming, 10 μg of HBsAg and 10 μg of HBcAg were selected as the optimal protein doses for the further studies.

2.1.4 Comparison of different delivery routes for various adjuvants

As discussed previously, in consideration of a clinical application, the delivery routes for *TherVacB* were altered from the initial ones (s.c. for protein priming, i.p. for MVA

boost) to the current ones (i.m. for both priming and boost). To ensure that the delivery route alteration does not compromise the efficacy of *TherVacB*, a comparison of the current and the initial delivery routes was required. To obtain more objective results and avoid the individual adjuvant bias, apart from the current adjuvant c-di-AMP, one TLR3 ligand poly-ICLC and the RIG-I Ligand were included as adjuvants for protein priming. The immunogenicity of three adjuvanted formulations was evaluated and compared in two different delivery routes.

HBVtg mice were intramuscularly or subcutaneously immunized with HBsAg and HBcAg adjuvanted with c-di-AMP or poly-ICLC or the RIG-I Ligand at week 0 and week 2. At week 4, mice received MVA-S and MVA-core vectors intramuscularly or intraperitoneally. At week 5, the mice were sacrificed to analyze the antibody responses and HBV antigen levels in the murine serum and to detect T-cell responses in the livers and spleens of the mice (Fig.2.10).

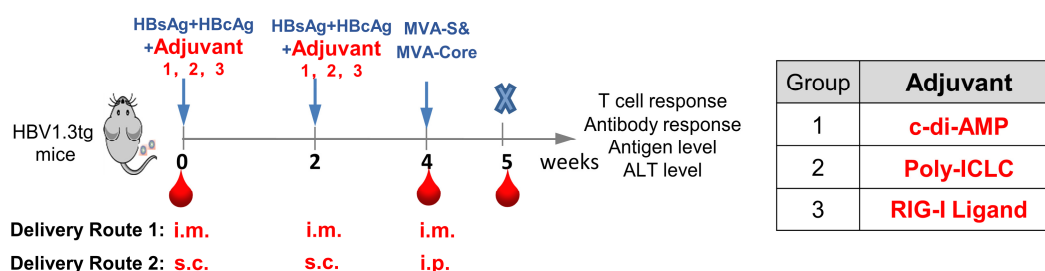


Fig.2.10 Immunization scheme of different delivery routes for various adjuvants.

Mice were immunized with HBsAg and HBcAg with the adjuvants listed in the right table via i.m. or s.c. at week 0 and week 2. At week 4, mice received MVA-S and MVA-core vectors via i.m. or i.p. to boost the immune responses. The mice were sacrificed at week 5 for the final analysis in the serum, liver, and spleen.

The levels of anti-HBs and anti-HBc were determined by the Architect™ and BEP III immunoassays in the murine serum at week 5, respectively. As shown in Fig.2.11 A, comparably high levels of anti-HBs were generated in all immunized mice, independent of the delivery route. Nevertheless, the antibodies titers in mice immunized with the poly-ICLC formulation via s.c./i.p. varied markedly (Fig.2.11 A). The poly-ICLC adjuvant used in this study was formulated into an emulsion, which was

Results

difficult to retain in a homogenous state for the duration of the immunization procedure. Thus, it cannot be guaranteed that all mice in the group received the identical doses. Consistent with robust anti-HBs responses, the serum HBsAg levels decreased to undetectable levels in all immunized mice, independent of the delivery route (Fig.2.11 C and E).

In mice immunized with c-di-AMP formulations, the levels of anti-HBc induced by i.m./i.m. route were significantly higher compared to those induced by s.c./i.p. route ($p < 0.05$). Additionally, immunization with c-di-AMP formulation via i.m./i.m. route elicited significantly higher levels of anti-HBc in comparison to immunization with the RIG-I Ligand formulations via both i.m./i.m. and s.c./i.p. routes ($p < 0.05$). In mice immunized with poly-ICLC and the RIG-I Ligand formulations, immunization by both delivery routes induced comparably high levels of anti-HBc with respect to the baseline of negative controls (Fig.2.11 B).

Compared to the baseline at week 0, there was a visible serum HBeAg decrease in all immunized mice, except the ones immunized with the RIG-I Ligand formulation via i.m./i.m. route (Fig.2.11 D). Looking more closely at individual mice, a remarkable HBeAg decrease was observed in at least six out of eight mice immunized with c-di-AMP formulations via both routes and with poly-ICLC via i.m./i.m. route. The levels of serum HBeAg at week 5 in these groups were significantly lower compared to the baseline at week 0 ($p < 0.05$) (Fig.2.11 F).

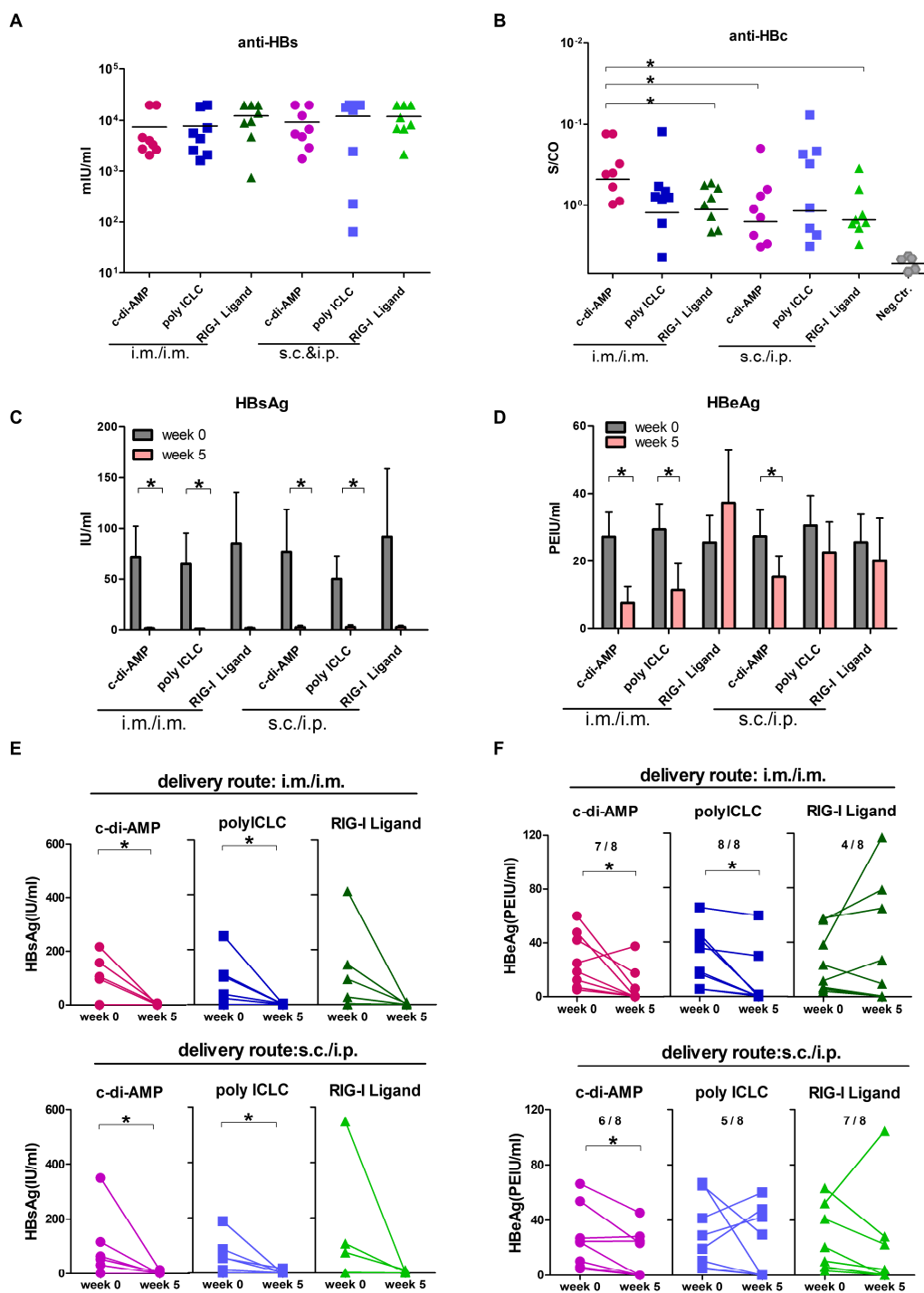


Fig.2.11 Antibody response and antigen level analyses of different delivery routes for various adjuvants.

(A, B) The levels of anti-HBs (A) and anti-HBc (B) antibodies were detected in the serum of experimental mice at the endpoint.

(C, D) The levels of HBsAg (C) and HBeAg (D) were detected in the serum of immunized mice at the start point and endpoint. The fraction number in (D) indicates how many mice out of the eight mice in total showed a serum HBeAg decrease.

Statistical analysis was performed using Mann-Whitney test. Asterisks (*) mark statistically significant differences: * $p < 0.05$.

Results

The magnitude of the S- and core-specific CD8 T-cell responses elicited by the immunization of various groups was compared by the intracellular IFN γ and TNF α staining of peptide-stimulated LALs and splenocytes one week after MVA boost. In mice immunized with c-di-AMP formulations, the frequencies of intrahepatic S-specific IFN γ + CD8 T cells were comparably high when induced via either delivery route (Fig.2.12 A, upper panel). Nevertheless, the S-specific IFN γ + TNF α + CD8 T-cell responses induced via i.m./i.m. route were stronger in comparison to those induced via s.c./i.p. route (Fig.2.12 A, lower panel). Similar to this trend, comparable core-specific IFN γ + CD8 T-cell responses were observed in the livers of mice immunized via both delivery routes. However, the frequencies of core-specific IFN γ + TNF α + CD8 T cells in mice immunized via i.m./i.m. route appeared slightly higher than those in the livers of mice immunized via s.c./i.p. route (Fig.2.12 B).

The i.m./i.m. delivery route displayed much clearer advantages, in comparison to the s.c./i.p. delivery route in the spleen. The frequencies of both IFN γ + and IFN γ + TNF α + S-specific CD8 T cells were significantly higher in mice immunized via i.m./i.m. route compared to those in mice immunized via s.c./i.p. route ($p < 0.05$) (Fig.2.12 C). The profiles of core-specific responses displayed a similar tendency (Fig.2.12 D). These findings suggest the i.m./i.m. delivery route was more likely to recruit multifunctional T-cell responses to the liver and spleen.

In mice immunized with poly-ICLC formulations, in general, the T-cell responses were weaker than in mice immunized with c-di-AMP formulations, especially when c-di-AMP formulation was delivered via i.m./i.m. route. The magnitude of intrahepatic S-specific CD8 T-cell responses was comparable between the two delivery routes, whereas vaccination elicited stronger intrahepatic core-specific CD8 T-cell responses via the i.m./i.m. route compared to the s.c./i.p. route (Fig.2.12 A and B). In the spleen, immunization with polyICLC-formulation via the i.m./i.m. route induced better CD8 T-cell responses, especially S-specific ones, compared to the s.c./i.p. route (Fig.2.12 C and D). However, the mice immunized with poly-ICLC formulations via i.m./i.m. route experienced a mild bodyweight loss, especially after the first injection of poly-ICLC formulation at week 0 (Fig.2.13 A and B). The reason for the weight loss could be that

the poly-ICLC emulsion was not well tolerated in these mice. Further optimization of the adjuvant components would be required to reduce the toxicity of this formulation. By contrast, the mice in other groups maintained or even gained bodyweight (Fig.2.13 A and B).

Concerning the RIG-I Ligand, its efficacy was also inferior to that of c-di-AMP. Particularly, S-specific CD8 T-cell responses were notably weaker in both, livers and spleens, of mice immunized via both delivery routes (Fig.2.12 A and C). The magnitude of core-specific CD8 T-cell responses was slightly higher in mice immunized via s.c./i.p. route compared to those immunized via i.m./i.m. route (Fig.2.12 B and D). Nevertheless, the overall efficacy of the RIG-I Ligand formulation was lower than the c-di-AMP formulation. Thus, with regard to practicability and effectivity, the RIG-I Ligand triphosphate 3pRNA was not an ideal candidate in this study, as it needed to be mixed with transfection reagent Jet PEI *in vitro* in a complicated and long process.

Results

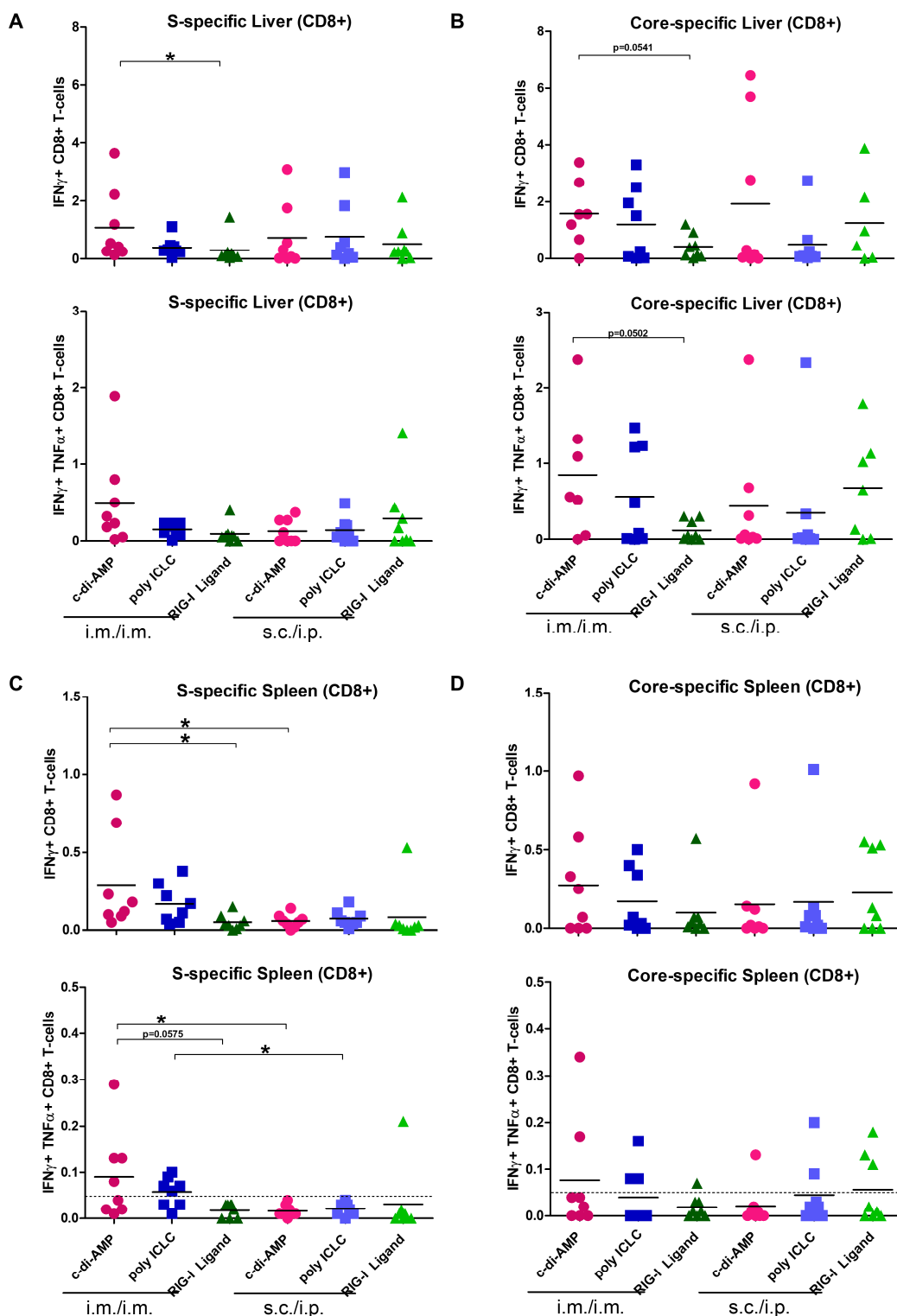


Fig.2.12 T-cell response analysis of different delivery routes for various adjuvants.

(A-D) Percentages of intrahepatic and splenic S- and core-specific IFN γ + and IFN γ + TNF α + CD8 T cells after *ex vivo* stimulation with S-specific peptide pool (A, C) and core-specific peptide pool (B, D).

Statistical analysis was performed using Mann-Whitney test. Asterisks (*) mark statistically significant differences: * $p < 0.05$.

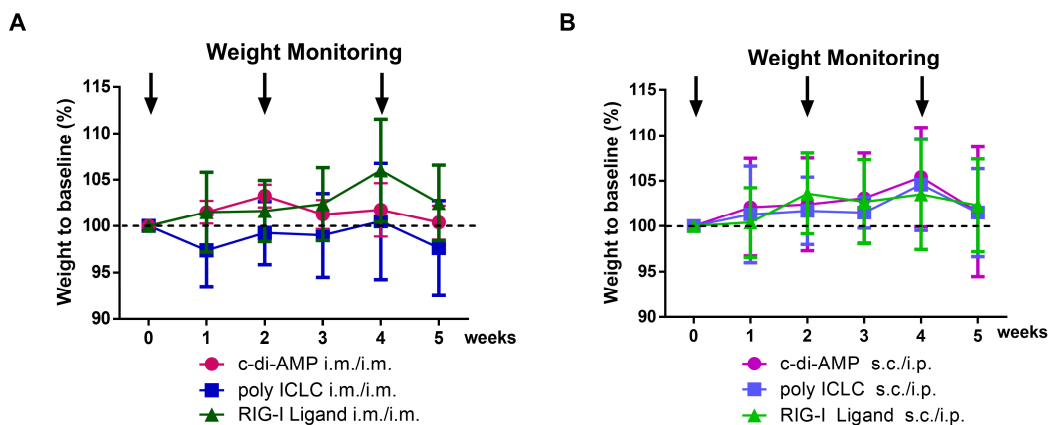


Fig.2.13 Weight monitoring of different delivery routes for various adjuvants.

Weight of the mice immunized via both i.m./i.m. (A) and s.c./i.p. (B) delivery routes was monitored every week and compared to the baseline at the start point of the experiment. Arrows show the time points of vaccination.

Concerning the various adjuvants, c-di-AMP proved to be a superior adjuvant for antibody generation and the induction of cellular immune responses, especially via i.m./i.m. route. Concerning the delivery routes, the i.m./i.m. delivery route worked better for both c-di-AMP and poly-ICLC, displaying higher anti-HBc induction, significant HBeAg reduction, and stronger T-cell responses. In contrast, the s.c./i.p. route exceeded i.m. route for the delivery of the RIG-I Ligand formulation. This result might be related to the distinct transfection efficiency in different tissues of the RNA transfection reagents that were used for the RIG-I Ligand *in vivo* transfection. Considering the above results and clinical practices, it was concluded that intramuscular injection was sufficiently effective to be the optimal delivery route for the further *TherVacB* studies.

To summarize the studies in this chapter, 10 µg for protein, 3×10^7 IFU for MVA, and intramuscular injection were estimated as the optimal doses and delivery route of *TherVacB* in HBVtg mice. Moreover, it was shown that the selection of appropriate adjuvant is essential, as it greatly shaped the overall efficacy of the *TherVacB* regimen.

2.2 Investigation of novel adjuvants to improve protein priming in *TherVacB*

Results of the studies described in the previous chapter clearly demonstrated that, apart from the optimal vaccine dose and delivery route, the success of *TherVacB* largely depends on an appropriate adjuvant for protein priming. To gain deeper insights into the role of the priming immunization and to improve the efficacy of the *TherVacB* regimen, it was necessary to explore novel adjuvants for protein priming, which can simultaneously generate neutralizing antibody responses and elicit potent CD4 and CD8 T-cell responses. Thus, a collaboration with the Vaccine Formulation Institute was initiated to select a series of novel adjuvants and study their ability to improve the protein priming of the *TherVacB* regimen. The experiments described in this chapter aimed to characterize the stability and integrity of the antigen/adjuvant formulations by various physiochemical assays *in vitro*, and to evaluate the immunogenicity of antigen/adjuvant formulations in wild-type and persistent HBV replication mouse models.

2.2.1 Physiochemical characterization of antigen/adjuvant formulations

In this study, three different types of adjuvant formulations—liposome (Lipo), squalene-in-water emulsion (SWE), and water-in-oil emulsion Montanide ISA720—were investigated to improve *TherVacB* efficacy. In addition, the liposome and SWE delivery systems were combined with immunostimulants TLR4 ligand monophosphoryl lipid A (MPL) and QS21 saponin as combination adjuvants. According to the doses of MPL and QS21 mixed with these two delivery systems, these combination adjuvants were designated as Lipo 1-7 and SWE 1-7. Detailed information on MPL and QS21 doses in each combination adjuvant is shown in table 2.1.

Results

Table2.1 Description of the novel adjuvants

Group	Numbering	MPL ($\mu\text{g}/100\mu\text{l}$)	QS21 ($\mu\text{g}/100\mu\text{l}$)
No adjuvant	-	0	0
Liposome based formulations (Lipo)	1	0	5
	2	1	5
	3	2	5
	4	4	5
	5	1	2.5
	6	2	2.5
	7	4	2.5
Squalene-in-Water Emulsion based formulations (SWE)	1	0	5
	2	1	5
	3	2	5
	4	4	5
	5	1	2.5
	6	2	2.5
	7	4	2.5
Montanide ISA720	-	0	0

No adj: no adjuvant; MPL, synthetic Monophosphoryl lipid A; QS21, fraction 21 from QuilA, extracted by the bark of *Quillaja saponaria*; Lipo, Liposome-based formulations; SWE, Squalene-in-Water Emulsion-based formulations; ISA720, Montanide ISA720.

The antigens, HBsAg and HBcAg, were formulated with individual combination adjuvants. These antigen/adjuvant formulations are now referred to as adjuvant formulations and are listed in table2.1. To analyze the stability of these adjuvant formulations, they were incubated at 4 °C and the vaccine stability was monitored at the time points of week 0, week 1, and week 2 by the physicochemical assays of particle size, poly-dispersity index, zeta potential and pH.

Detailed physicochemical characterizations of every antigen/adjuvant formulation were performed from week 0 to week 2. The results demonstrated that all adjuvant formulations showed comparable particle size, poly-dispersity index, and zeta potential at all examined time points (Fig.2.14 A-C). In addition, the pH was maintained at similar

levels over time (Fig.2.14 D), which revealed that the antigens and adjuvants were compatible and stable in the analyzed formulations for at least two weeks.

The overall particle size distribution analysis of all formulations after two weeks of storage indicated that the average particle diameters of the Lipo- and SWE-based adjuvant formulations were approximately 120 nm and 140 nm, respectively. Moreover, there was one single peak observed in the particle size distribution curve, implying antigens did not form any irregular aggregates in the adjuvant formulations (Fig.2.14 E).

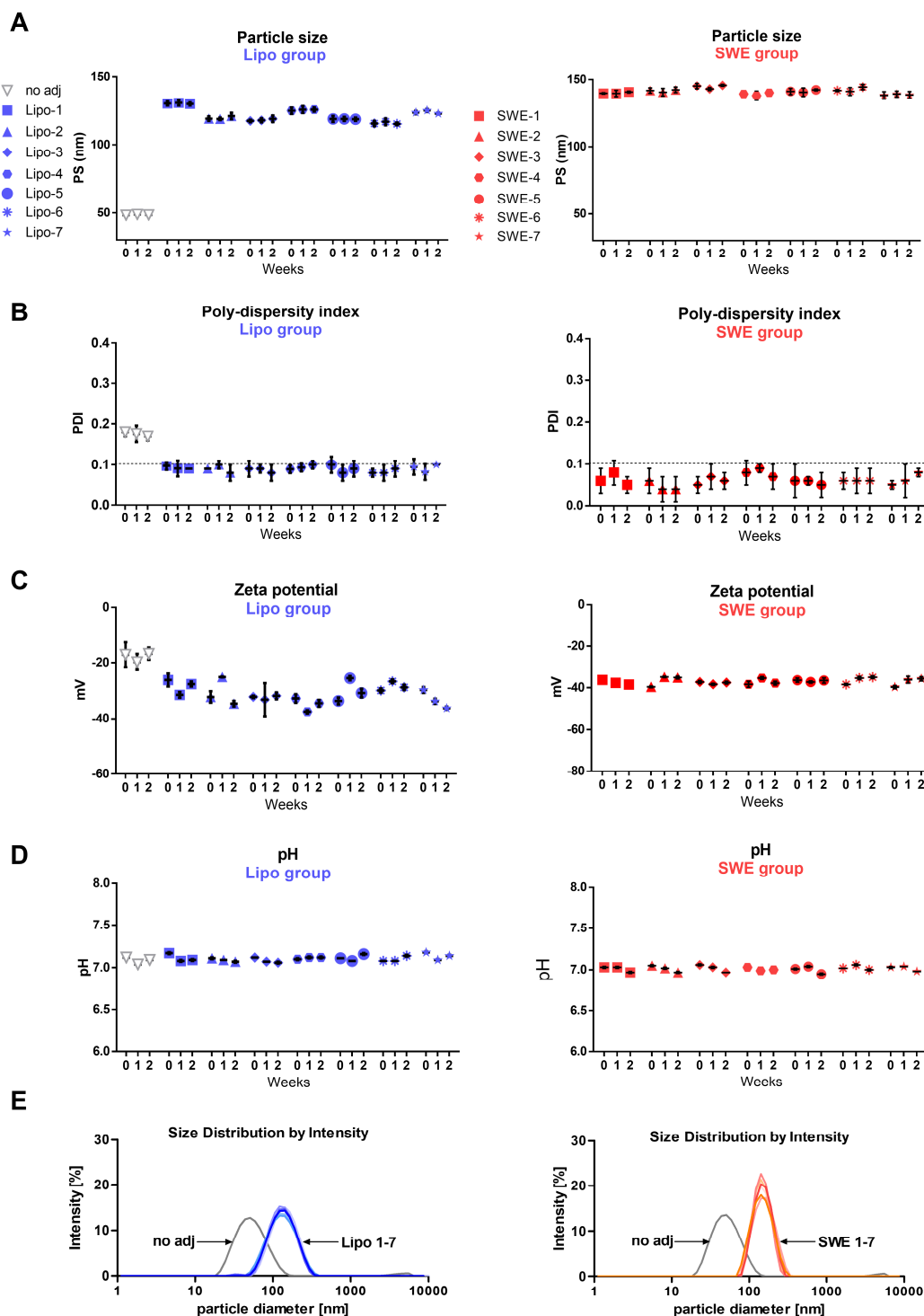


Fig.2.14 Physicochemical characterization of the Lipo- and SWE-based formulations.

(A-D) HBsAg and HBcAg were formulated with Lipo- and SWE-based adjuvants as adjuvant formulations. The formulations were characterized at week 0 and after incubation at 4 °C for one week and two weeks. Graphs show particle size (A), polydispersity index (B), zeta potential (C), and pH (D) of these formulations at different time points.

(E) The particle size distribution analysis of the Lipo- and SWE-based formulations after two weeks of storage at 4 °C by dynamic light scattering. No-adjuvant proteins (no adj) were used as control.

2.2.2 Antigen integrity in the adjuvant formulations

The integrity of antigens in the vaccines was crucial for the vaccine to stimulate proper antigen-specific immune responses *in vivo*. After identifying the stability of the adjuvant formulations, the integrity of HBsAg and HBcAg in the formulations was characterized at different time points by antigen-specific ELISA, Western blot, native agarose gel electrophoresis (NAGE), and transmission electron microscopy (TEM).

In the first step, the antigen integrity was analyzed at week 0 directly after the formulation of antigens/adjuvants. In the ELISA and Western blot analysis of HBsAg, the adjuvanted HBsAg from all formulations showed comparable signals to the no-adjuvant (no adj) and freshly prepared original HBsAg (Fig.2.15 A and C). Similarly, Lipo- and SWE-adjuvanted HBcAg demonstrated comparable signals to the no adj and original HBcAg in ELISA analysis. By contrast, the Montanide ISA720-formulated HBcAg presented lower signals in the analysis (Fig.2.15 B). The results were confirmed by HBcAg capsid NAGE and Western blot analysis. While all the Lipo- and SWE-based formulations exhibited bands resembling the original HBcAg in these two analyses, neither nucleic acid nor capsid bands were detected with the Montanide ISA720-formulated HBcAg (Fig.2.15 D and E). When the antigen integrity in these formulations was analyzed after two weeks of storage, similar results as at week 0 were observed. Thus, it was concluded that water-in-oil emulsion Montanide ISA720 interfered with the integrity of the HBcAg, and this adjuvant was excluded from further studies.

Results

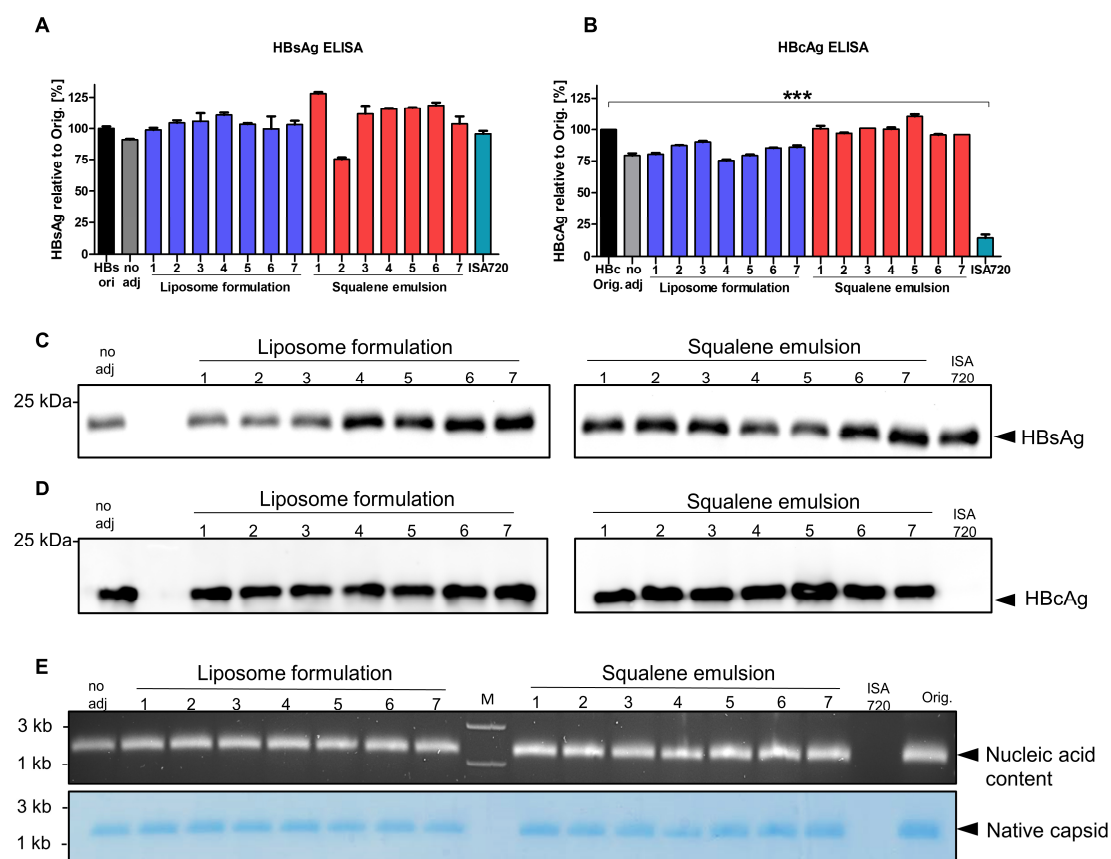


Fig.2.15 Antigen integrity analysis of the adjuvant formulations at week 0 *in vitro*.

(A, B) Direct ELISA of HBsAg (A) and HBcAg (B) in the adjuvant formulations at week 0.

No adj represents the antigens that were formulated with buffer instead of adjuvants; Orig. represents freshly prepared original antigens. The values are depicted as the percentages of individual OD₄₅₀ value relative to the mean OD₄₅₀ value in the original antigen group.

(C, D) Western blot analysis of HBsAg (C) and HBcAg (D) in the formulations.

(E) Native agarose gel electrophoresis of adjuvanted HBcAg particles. Nucleic acids were stained with Roti®-GelStain (top), and the protein was subsequently stained with Coomassie blue with the same gel (bottom). M: marker.

Statistical analyses were performed using Mann-Whitney test. Asterisks (*) mark statistically significant differences, *** $p < 0.001$.

To examine the antigen integrity after long-term storage, these formulations were stored for 12 weeks at 4 °C and compared with freshly prepared original antigens by HBsAg- and HBcAg-specific ELISA. Consistent with the previous results, all adjuvant formulations and the no adj control group displayed at least 100% signal relative to original antigens in both HBsAg and HBcAg ELISA, suggesting that the HBsAg and HBcAg in these formulations remained intact even after 12 weeks of storage (Fig.2.16 A and B).

Transmission electron microscopy (TEM) analysis of the representative Lipo-3 adjuvanted formulation was performed at week 12. Not only intact HBsAg and HBcAg particles but also intact Lipo-3 adjuvant were clearly visible, which indicated the adjuvant formulation remained stable, even after 12 weeks of storage (Fig.2.16 C).

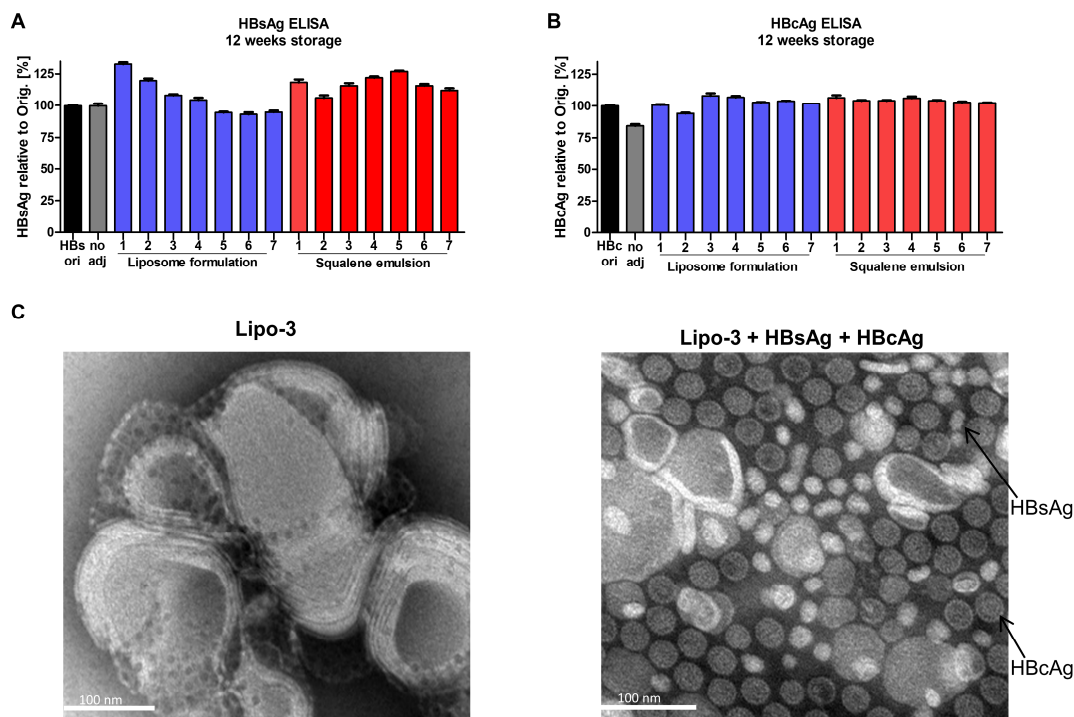


Fig.2.16 Antigen integrity analyses of the adjuvant formulations after 12 weeks of storage *in vitro*.

(A, B) ELISA of HBsAg (A) and HBcAg (B) in the adjuvant formulations at week 12.

The values are depicted as the percentages of individual OD₄₅₀ value relative to the mean OD₄₅₀ value in the original antigen group.

(C) Transmission electron microscopy analysis of Lipo-3 adjuvanted HBsAg/HBcAg after 12 weeks of storage at 4 °C. The Lipo-3 adjuvant only was used as a control. The arrows show the exemplary HBsAg and HBcAg particles in the EM image. Scale bars indicate 100nm.

Taken together, the findings suggest that Lipo- and SWE-based adjuvant formulations can remain stable and intact for at least 12 weeks *in vitro*.

Results

2.2.3 Activation of dendritic cells by novel combination adjuvants in vitro

To further analyze the immunostimulatory properties of the novel combination adjuvants, six representative candidates were selected based on the doses of MPL and QS21. Lipo/SWE-QS21 combinations, referred to as LQ and SQ, respectively, were included based on previous encouraging results from other vaccines (Younis, 2018). Following these two groups, the combinations of LQ/SQ with low-toxicity moderate-dose MPL, referred to as LMQ and SMQ, respectively, were selected. Moreover, to explore the QS21 dose effects on immune response stimulation, combination adjuvants containing lower QS21 dose as in LMQ and SMQ were selected and are referred to as LMQ^{low} and SMQ^{low} (Table2.2).

Table2.2 Description of the selected combination adjuvants.

Group	Numbering	Nomenclature	MPL (µg/100µl)	QS21 (µg/100µl)
no adjuvant	-	no adj	0	0
Lipo	1	LQ	0	5
	3	LMQ	2	5
	6	LMQ^{low}	2	2.5
SWE	1	SQ	0	5
	3	SMQ	2	5
	6	SMQ^{low}	2	2.5

The numbering follows the order in table2.1.

In the first step, the immunostimulatory properties of these combination adjuvants were analyzed by *in vitro* activation assay. In this study, human monocyte-derived dendritic cells (hMoDCs) were used as antigen-presenting cells (APCs). After differentiating the human monocytes into immature hMoDCs, they were stimulated with these six novel combination adjuvants listed in table2.2 (Fig.2.17). The LPS and no adj medium served as the positive and negative controls, respectively. In addition, to explore whether the delivery systems affected the activation of APCs, the delivery systems (Lipo, SWE) only were included as stimulants. After 6 or 48 hours of stimulation, the cell culture

supernatant was collected to determine the concentration of proinflammatory cytokines by ELISA. The expression of costimulatory molecules CD86 and CD80 on the hMoDCs was analyzed by flow cytometry after 48 hours of culture.

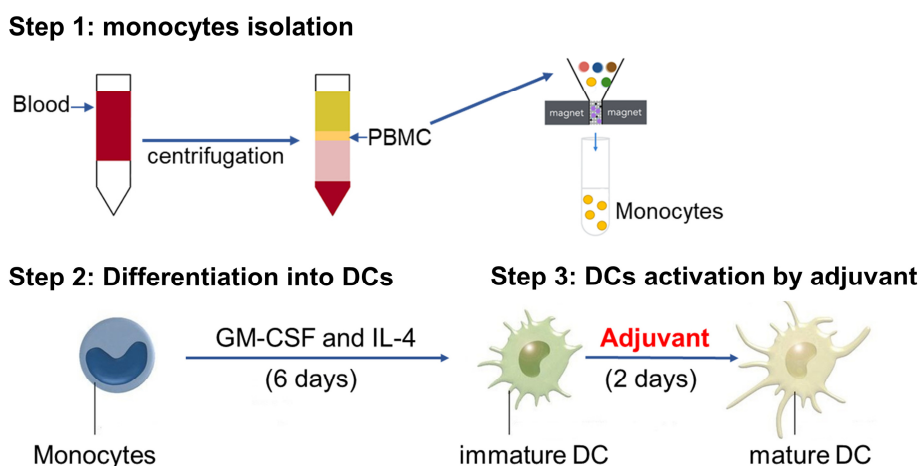


Fig.2.17 The scheme of human-derived dendritic cell generation and stimulation.

In the first step, human monocytes were isolated from peripheral blood mononuclear cells (PBMCs) with a negative selection of magnetic-activated cell sorting (MACS). In the second step, the monocytes were cultivated with GM-CSF and IL-4 cytokines to differentiate into immature hMoDCs. At day 6, cells were harvested as immature hMoDCs. In the third step, the immature hMoDCs were stimulated with 1/40 immunization doses of Lipo- or SWE-based combination adjuvants (listed in table2.2), or delivery systems only, or 1 μ g/ml LPS or no adj medium. Lastly, the activation of hMoDCs was characterized by proinflammatory cytokine secretion and costimulatory molecule expression after 6 or 48 hours of stimulation.

Stimulation of hMoDCs with six novel combination adjuvants and LPS, but not with no adj or Lipo/SWE delivery systems only, induced significant secretion of tumor necrosis factor alpha (TNF α). In particular, hMoDCs stimulation with the combination adjuvants that contained MPL induced significantly higher TNF α secretion compared to the no adj stimulated DCs ($p < 0.05$) (Fig.2.18 A). In addition, the secretion of proinflammatory cytokine interleukin-6 (IL-6) was associated with a profound increase in hMoDCs stimulated with all adjuvants compared to the no adj stimulated hMoDCs (Fig.2.18 B). In agreement with inducing the production of TNF α and IL-6, hMoDC stimulation with these six novel combination adjuvants remarkably increased the surface expression of CD86 and CD80. By contrast, the expression of CD86 and CD80 in the hMoDCs stimulated with Lipo or SWE only remained at background levels similar to no adj

Results

control (Fig.2.18 C and D), indicating that the six novel combination adjuvants were able to promote DCs activation, but the delivery systems on their own were not.

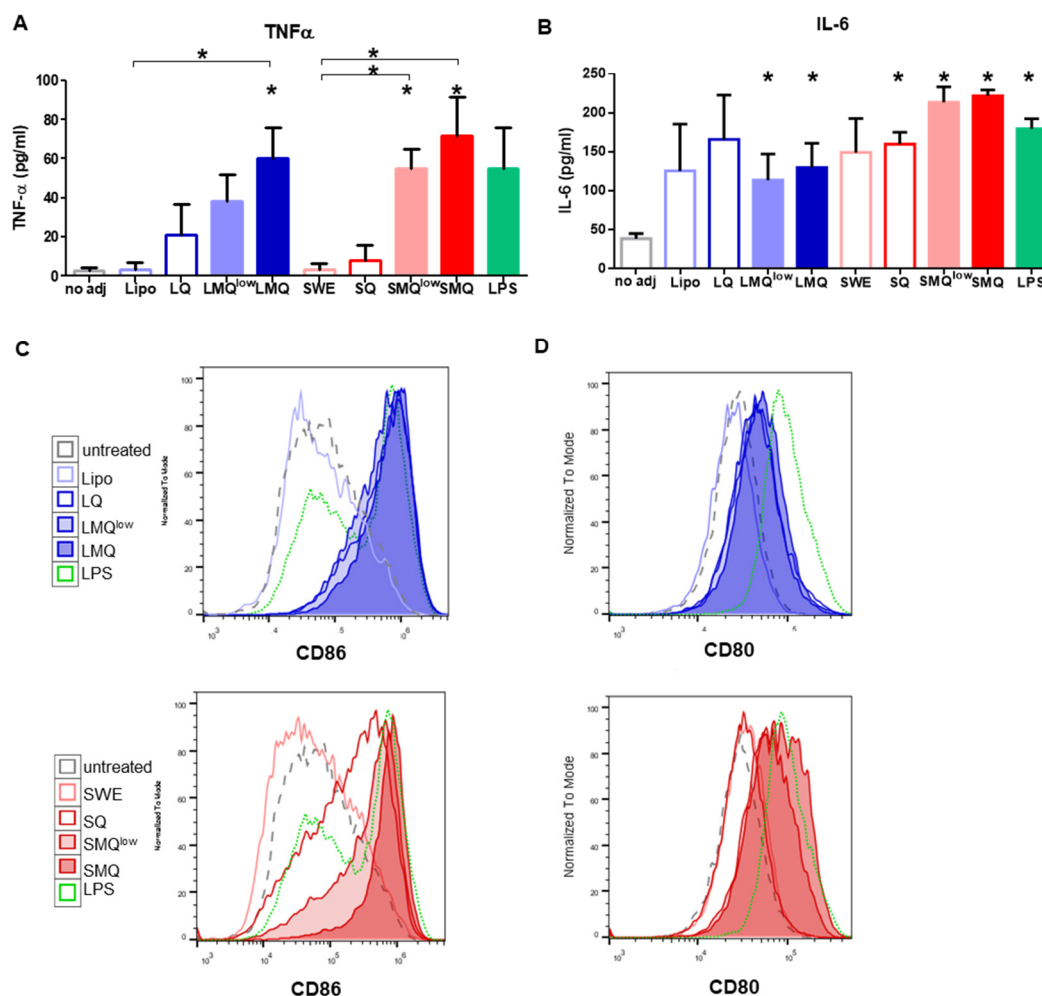


Fig.2.18 Activation of hMoDCs by Lipo- and SWE-based combination adjuvants.

(A, B) The secretions of cytokines TNF α (A) and IL6 (B) were analyzed after adjuvants stimulated DCs for 6 hours and 48 hours, respectively.

(C, D) The flow cytometry analysis of the expressions of surface markers CD86 (C) and CD80 (D) on hMoDCs after 48 hours of stimulation. The hMoDCs were either non-stimulated (no adj) (grey, dashed line), or stimulated by the Lipo delivery system alone (light blue, solid line), the Lipo-based combination adjuvants (light to dark blue shaded areas), the SWE delivery system alone (light red, solid line), the SWE-based combination adjuvants (light to dark red shaded areas), or LPS (green, dotted line).

Statistical analyses were performed using unpaired t-test. Asterisks (*) mark statistically significant differences compared to no adj group, * $p < 0.05$.

In summary, Lipo- and SWE-based novel combination adjuvants exhibited strong immunostimulatory effects resulting in enhanced activation and maturation of hMoDCs *in vitro*.

2.2.4 Immunogenicity evaluation of the novel adjuvant formulations in wild-type C57BL/6 mice

Since all six combination adjuvants exhibited strong immunostimulatory properties *in vitro*, they were formulated with HBsAg/HBcAg and used in *TherVacB* regimens to investigate their effects on the vaccine efficacy *in vivo*.

Wild-type C57BL/6 mice were immunized with HBsAg/HBcAg formulated with the novel combination adjuvants intramuscularly twice at week 0 and week 2. As compared in the previous chapter, c-di-AMP was selected as a positive control adjuvant. Mice immunized with HBV antigens without adjuvant (no adj) served as negative controls. At week 4, mice received 3×10^7 IFU of MVA-core and MVA-S intramuscularly to boost the immune response. Mice were sacrificed at week 5 to analyze the HBV-specific antibody responses in the serum and to detect T-cell responses in the spleens of the mice (Fig.2.19).

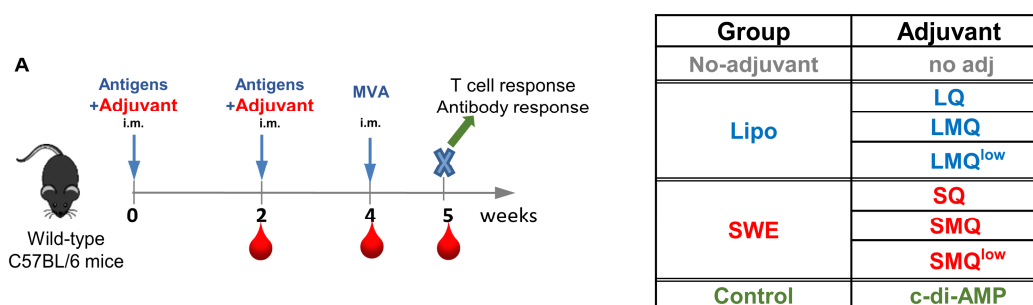


Fig.2.19 Immunization scheme of novel adjuvant formulations in wild-type C57BL/6 mice. Mice were immunized with adjuvanted formulations listed in the table at week 0 and week 2. At week 4, mice received MVA-S and MVA-core to boost the immune response. At week 5, the mice were sacrificed for antibody and T-cell response analyses in the serum and spleen.

Results

The humoral immune response induced by the vaccination with novel adjuvant formulations was evaluated by the detection of anti-HBs and anti-HBc in the serum of mice one week after MVA boost. Immunization of mice with the novel adjuvant formulations elicited comparable levels of anti-HBs, which were all significantly higher than those in no adj immunized mice ($p < 0.05$). The average values of anti-HBs in the serum of mice immunized with the novel adjuvant formulations were as high as 10^6 mIU/ml, which was 1 log higher than those in mice immunized with the c-di-AMP formulation (Fig.2.20 A). All vaccine formulations, even the no adj group, induced profound anti-HBc responses compared to the baseline of the control group. The levels of anti-HBc in the no adj group were comparable to those detected in mice immunized with the novel adjuvant formulations. Only LMQ formulation induced significantly higher anti-HBc titers as compared to no adj group ($p < 0.05$) (Fig.2.20 B).

The subclass of IgG antibodies secreted by antigen-specific B cells is regulated by different subsets of CD4 helper T cells (Stevens, 1988). While Th1 cells enhance the secretion of IgG₂ subclass, Th2 cells induce B cells to secrete IgG₁ subclass. The IgG₁ and IgG_{2b} subclasses of anti-HBs and anti-HBc were analyzed in murine serum by ELISA to assess the impact of novel adjuvant formulations on helper T-cell responses. Detection of HBsAg-specific IgG subclasses demonstrated that immunization of mice with all six novel adjuvant formulations generated not only Th2 response-associated IgG₁ subclass, but also high levels of Th1 response-associated IgG_{2b} subclass (Fig.2.20 C). By contrast, immunization of mice with all vaccine formulations, even the one without adjuvant, induced predominantly HBcAg-specific IgG_{2b} subclass (Fig.2.20 D). This finding combined with the strong anti-HBc induction in the no adj group confirmed that HBcAg itself is a powerful immunogen and induces Th1-biased responses (Billaud, 2005).

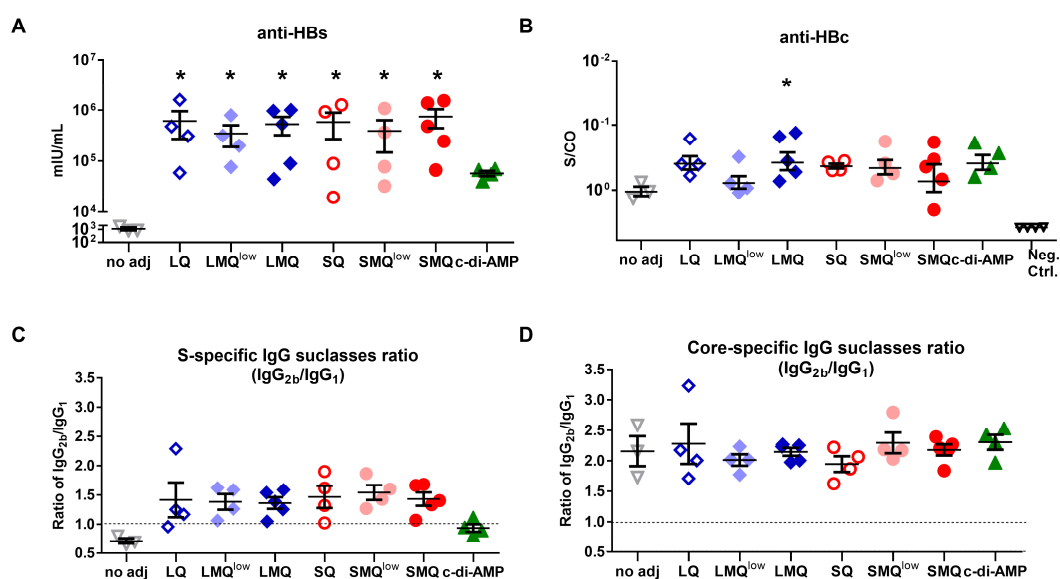


Fig.2.20 Humoral responses induced by immunization with novel adjuvant formulations in wild-type C57BL/6 mice.

(A, B) The levels of anti-HBs (A) and anti-HBc (B) were detected in the serum of immunized mice at the endpoint of week 5. The negative control of the anti-HBc immunoassay setting was included as a reference (B).

(C, D) The IgG₁ and IgG_{2b} ratio of HBsAg- (C) and HBcAg-specific (D) IgG subclasses. The OD₄₅₀ values of IgG₁ and IgG_{2b} values were detected with the serum of immunized C57BL/6 mice at the endpoint by ELISA. The ratio of IgG_{2b}: IgG₁ was calculated based on the respective OD₄₅₀ values.

Asterisks (*) mark statistically significant differences compared to no adj group. Statistical analysis was performed by Kruskal-Wallis test with Dunn's multiple comparison correction or Mann-Whitney test: * $p < 0.05$.

To evaluate the impact of the novel adjuvant formulations on the magnitude of the S- and core-specific CD4 T-cell responses, intracellular IFN γ and TNF α staining of peptide-stimulated splenocytes from immunized mice was performed. Immunization of mice with all novel adjuvant formulations stimulated robust S-specific IFN γ +, as well as multifunctional IFN γ + TNF α + CD4 T-cell responses, which were significantly higher compared to those in mice immunized with no adj or c-di-AMP formulation ($p < 0.05$, or $p < 0.0001$) (Fig.2.21 A and C). Overall, core-specific CD4 T-cell responses were not as strong as the S-specific ones. Despite this, core-specific IFN γ + CD4 T cells in mice immunized with novel adjuvant formulations were at least comparable to those in the c-di-AMP formulation immunized mice (Fig.2.21 B and D).

Results

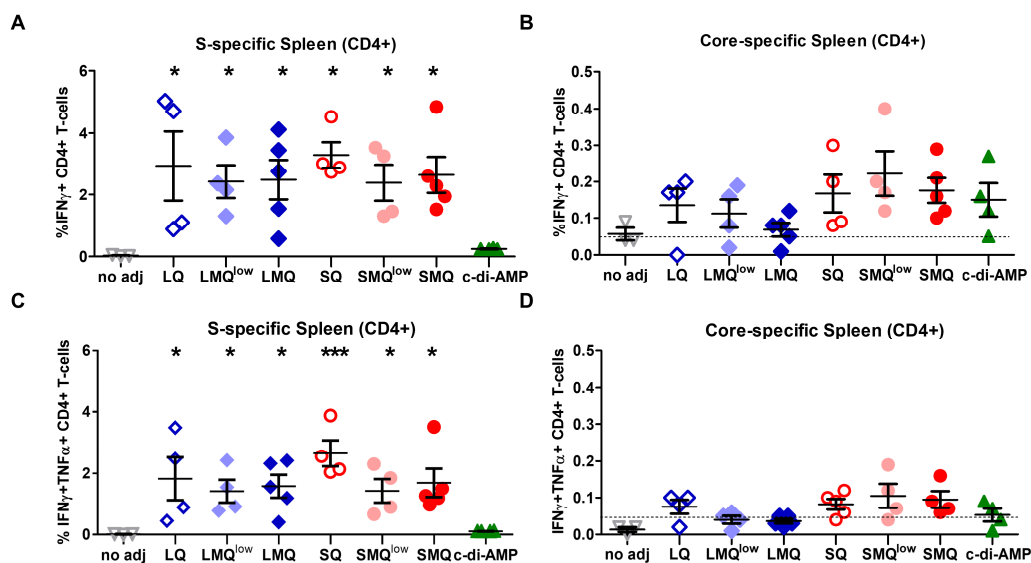


Fig.2.21 CD4 T-cell responses induced by the immunization with novel adjuvant formulations in wild-type C57BL/6 mice.

(A, B) Percentages of splenic S- and core-specific IFN γ + CD4 T cells determined by intracellular cytokine staining after S- and core-specific overlapping peptide pool *ex vivo* stimulation.

(D, E) Percentages of splenic S- and core-specific IFN γ + TNF α + CD4 T cells determined by intracellular cytokine staining after S- and core-specific overlapping peptide pool *ex vivo* stimulation.

Asterisks (*) mark statistically significant differences compared to no adj group. Statistical analysis was performed by Kruskal-Wallis test with Dunn's multiple comparison correction or Mann-Whitney test: * $p < 0.05$, *** $p < 0.001$.

In the next step, the induction of CD8 T-cell responses after immunization with the novel adjuvant formulations was determined by the intracellular IFN γ and TNF α staining of peptide-stimulated splenocytes from immunized mice.

Immunization of mice with all novel adjuvant formulations induced on average 10% S-specific IFN γ + CD8 T-cell responses, which were around 20 times higher than those in mice immunized with the c-di-AMP formulation (Fig.2.22 A). Of note, the magnitude of S-specific IFN γ + TNF α + CD8 T-cell responses in the mice vaccinated with the high QS21 dose formulations was significantly higher than in the no adj and c-di-AMP formulation immunized mice ($p < 0.05$ or 0.01) (Fig.2.22 C), which confirmed the function of QS21 in enhancing cellular immune responses (Newman, 1997). In this experiment, no core-specific CD8 T cells were detected in any immunized mice (Fig.2.22 B and D). The reason was that the mice were immunized with genotype A HBcAg, whereas the splenocytes from the immunized mice were stimulated with a

genotype D core-specific peptide pool to detect the CD8 T-cell responses. As there is a mismatch of the core-specific CTL epitope between the two genotypes, the HBcAg genotype for immunization and *ex vivo* stimulation should be kept consistent in future experiments. In addition, immunization with all formulations resulted in comparable B8R-specific CD8 T-cell responses after the MVA boost, demonstrating the equal immunization efficiency for all groups (Fig.2.22 E).

No obvious weight loss was observed for any individual mouse during the immunization process, indicating that the novel adjuvant formulations were well tolerated and had no obvious side effects *in vivo* (Fig.2.22 F).

Results

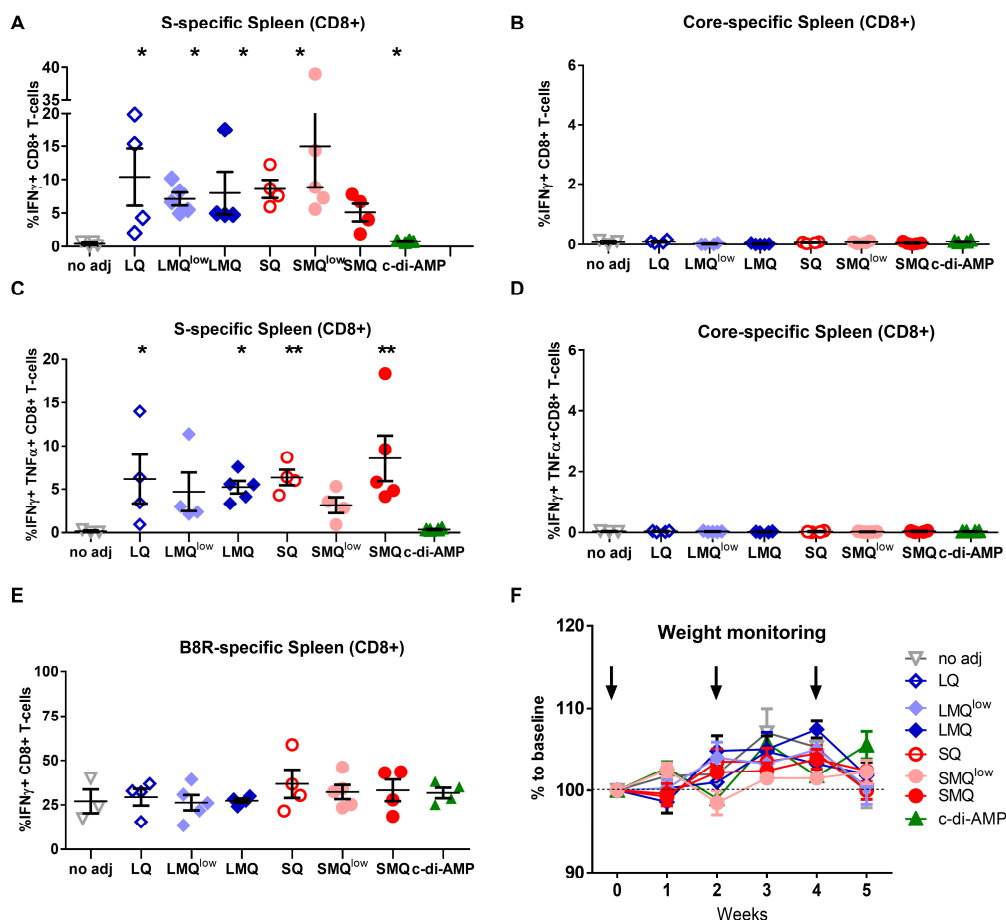


Fig.2.22 CD8 T-cell responses induced by immunization with novel adjuvant formulations in wild-type C57BL/6 mice.

(A, B, E) Percentages of splenic S- and core-specific $\text{IFN}\gamma^+$ CD8 T cells determined by intracellular cytokine staining after S-specific peptide pool (A), core-specific peptide pool (B), and MVA B8R epitope (E) *ex vivo* stimulation.

(C, D) Percentages of splenic S- and core-specific $\text{IFN}\gamma^+$ $\text{TNF}\alpha^+$ CD8 T cells determined by intracellular cytokine staining after S-specific peptide pool (C) and core-specific peptide pool (D) *ex vivo* stimulation.

(F) Weight of the mice in every group was monitored weekly and compared to the baseline at the start point of the experiment. Arrows show the time points of vaccination.

Asterisks (*) mark statistically significant differences compared to no adj group. Statistical analysis was performed by Kruskal-Wallis test with Dunn's multiple comparison correction or Mann-Whitney test: * $p < 0.05$, ** $p < 0.01$.

Immunization with all novel adjuvant formulations was well tolerated and stimulated strong humoral and cellular immune responses in C57BL/6 wild-type mice, and these formulations were superior to the previously tested adjuvant c-di-AMP. Moreover, the formulations containing high QS21 dose resulted in more robust and multifunctional $\text{IFN}\gamma^+$ $\text{TNF}\alpha^+$ S-specific CD8 T-cell responses. Therefore, the adjuvant formulation

candidates LQ, LMQ, SQ, and SMQ were selected for further evaluation in the AAV-HBV mouse model.

2.2.5 Short-term immunogenicity evaluation of the novel adjuvant formulations in AAV-HBV mice

To evaluate the potency of *TherVacB* with selected novel adjuvant formulations to break HBV-specific immune tolerance and reduce the persistent HBV replication, an AAV-HBV (adeno-associated virus carrying a replication-competent HBV genome) mouse model was employed in this study. In the AAV-HBV mice, the HBV antigenemia and DNA remain stable in serum for at least one year, and the replication of HBV persists in hepatocytes (Dion, 2013). Moreover, the transduction of the HBV genome by AAV vector in this mouse model induces HBV-specific immune tolerance, which resembles chronic HBV infection in patients (Lan, 2017).

In the first step, wild-type C57BL/6 mice were intravenously infected with AAV-HBV six weeks prior to vaccination to establish the persistent HBV replication. Mice were bled shortly before immunization and allocated into groups with comparable serum HBsAg and HBeAg levels. Afterwards, the AAV-HBV mice were immunized with the selected antigen/adjuvant formulations intramuscularly twice in a two-week interval and boosted with MVA-S/MVA-core intramuscularly at week 4. Non-vaccinated (no vac) and no-adjuvant (no adj) groups served as negative controls. To be able to study the impact of immunization with novel adjuvant formulation on long-term immune control of persistent HBV replication, the mice were sacrificed at week 10, instead of at week 5 as before, to perform the final immunological and virological analyses in serum, liver, and spleen. At week 5, the mice were only bled to pre-characterize the antibody and T-cell responses in blood. In this section, the study focuses on the short-term analysis at week 5 in blood (Fig.2.23).

Results

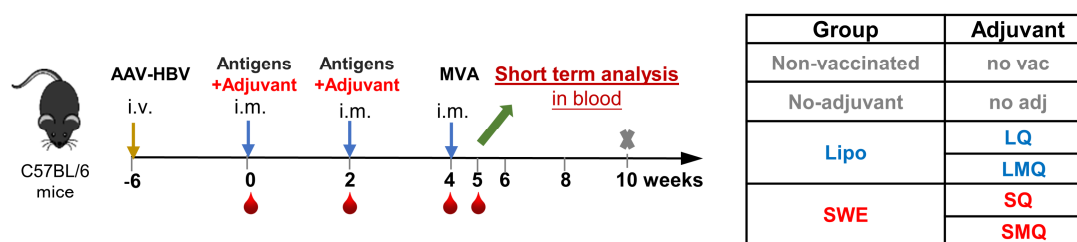


Fig.2.23 Immunization scheme of novel adjuvant formulations in short-term analysis of AAV-HBV mice.

Mice were intravenously infected with AAV-HBV six weeks prior to vaccination to establish the persistent HBV replication. Afterwards, the mice were immunized with the antigen/adjuvant formulations listed in the table at week 0 and week 2. At week 4, mice received MVA-S and MVA-core to boost the immune response. At week 5, as short-term analysis, the mice were bled for antibody and T-cell response analyses in blood. Afterwards, the mice were monitored until week 10 to perform the final analysis.

In the first step, the detection of anti-HBs and anti-HBc was performed in the serum of mice by the Architect™ and BEP III immunoassays at week 5, respectively. Consistent with the strong humoral immune responses in wild-type mice, immunization of AAV-HBV mice with four selected novel adjuvant formulations induced significantly higher levels of both anti-HBs and anti-HBc compared to no vac controls ($p < 0.05$). The levels of anti-HBs in the no adj group were almost undetectable and were significantly lower than those in mice immunized with four novel adjuvant formulations ($p < 0.05$). Unexpectedly, the anti-HBc responses in the no adj group were comparably high as those detected in mice immunized with the adjuvanted formulations (Fig.2.24 A and B). Correlating with the strong antibody responses, there was a more than 3-log decrease of serum HBsAg in mice immunized with all adjuvant formulations at week 5, resulting in a level that was significantly lower compared to the baseline at week 0 ($p < 0.05$). In addition, no adj immunization only resulted in 1-log HBsAg reduction compared to the baseline at week 0 (Fig.2.24 C). A pronounced 50%–80% decrease from the baseline in serum HBeAg levels was detected in the mice vaccinated with LQ, LMQ, and SQ formulations, but not with SMQ formulation (Fig.2.24 D).

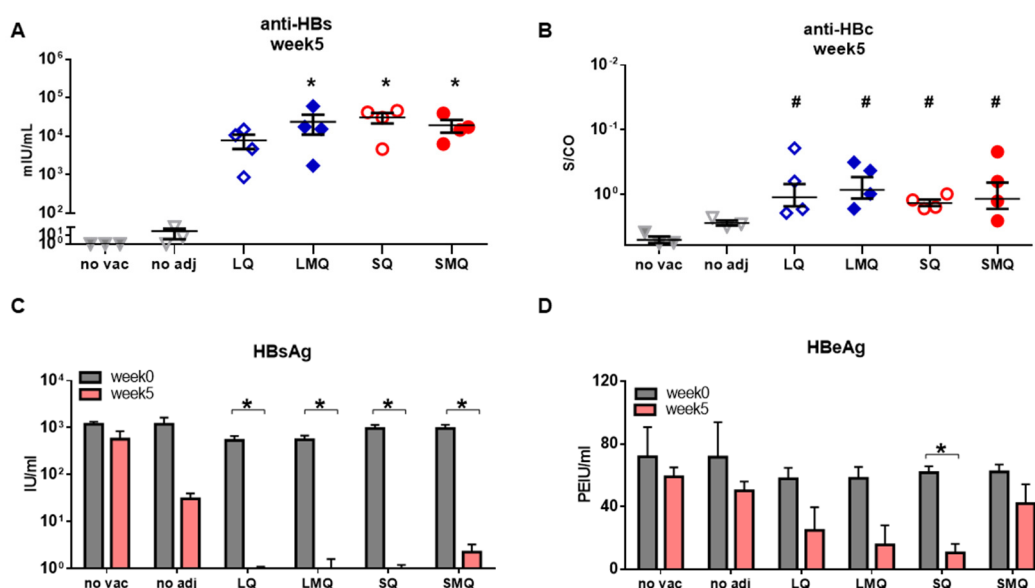


Fig.2.24 Antibody response and antigen decrease induced by immunization with novel adjuvant formulations in short-term analysis of AAV-HBV mice.

(A, B) The levels of anti-HBs (A) and anti-HBc (B) were detected in the serum of mice at week 5. (C, D) The levels of HBeAg (C) and HBsAg (D) were detected in the serum of mice at week 0 and week 5.

Hash (#) symbols mark statistically significant differences compared to no vac group; Asterisks (*) mark statistically significant differences compared to no adj group. Statistical analysis was performed by Kruskal-Wallis test with Dunn's multiple comparison correction or Mann-Whitney test or Wilcoxon test: * $p < 0.05$, ** $p < 0.01$.

Before evaluating the T-cell responses induced by vaccination with novel adjuvant formulations in murine blood at week 5, the assay of the T-cell response analysis in blood was established. For the assay validation, one group of naïve mice was immunized with wild-type MVA vector. One week later, the lymphocytes were isolated from blood and spleen and stimulated with MVA-specific B8R peptide or irrelevant negative control peptide OVA_{S8L} overnight. On the second day, the magnitude of T-cell responses was analyzed and compared in the blood and the spleen by intracellular IFN γ staining (Fig.2.25 A).

As shown in the dot plots of one representative mouse in Fig. 2.25 B, strong B8R-specific CD8 T-cell responses were detected in the blood of all mice tested. Moreover, the frequencies of IFN γ + CD8 T cells in the blood were comparable to those in the

Results

spleen of the same mouse. In addition, no OVA_{S8L}-specific responses were detected in either the blood or the spleen of tested mice (Fig.2.25 B).

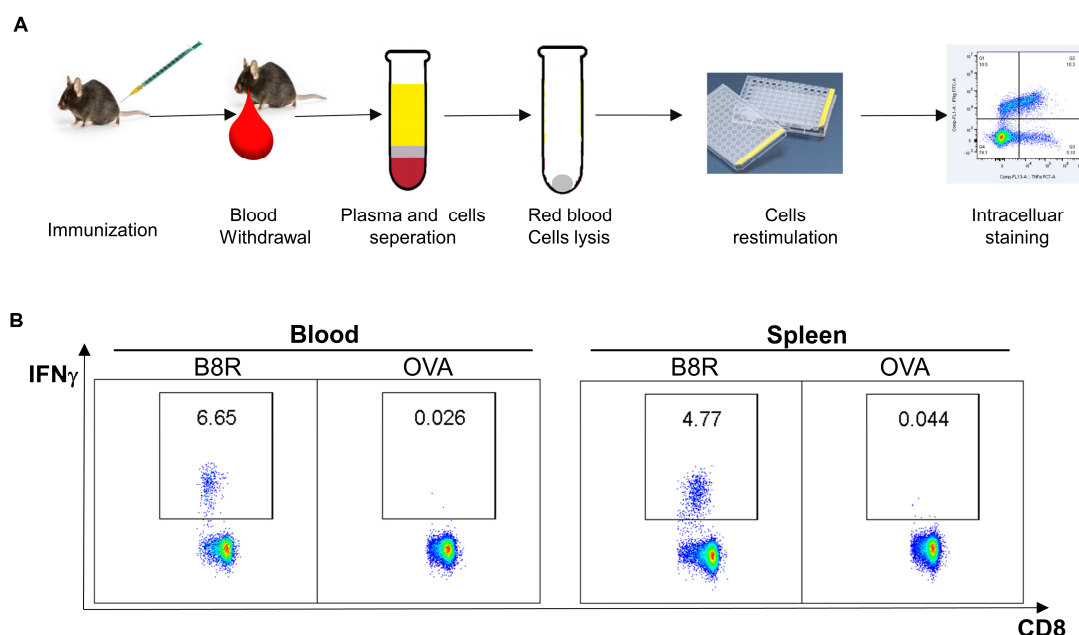


Fig.2.25 Validation of T-cell response analysis in murine blood.

- (A) The methodical scheme of T-cell response analysis in mice blood. One week after MVA immunization, blood was drawn from mice and centrifuged to separate the plasma and cells. The red blood cells were lysed by ACK buffer and the lymphocytes were stimulated with MVA-specific B8R peptide or negative control peptide OVA_{S8L} overnight. On the second day, the magnitude of T-cell responses was analyzed by intracellular IFN γ staining.
- (B) Dot plots of the B8R- and OVA_{S8L}-specific CD8 T-cell responses of a representative mouse in blood and spleen. Presented values indicate the percentage of IFN γ + CD8 T cells in the CD8 T-cell population.

After the successful validation of T-cell response analysis in murine blood, the assay was used to assess HBV-specific CD4 and CD8 T-cell responses at week 5 in the blood of AAV-HBV mice that were immunized with different adjuvant formulations.

Immunization of mice with all novel adjuvant formulations induced significantly higher percentages of S-specific IFN γ + CD4 T cells compared to the no vac controls ($p < 0.05$). Moreover, immunization with LMQ and SMQ formulations, in which MPL was included, exhibited enhanced S-specific CD4 T-cell responses, which were significantly higher than those in the mice vaccinated without adjuvant ($p < 0.01$). The results demonstrate the superior efficacy of LMQ and SMQ formulations on the induction of S-specific CD4 T-cell responses (Fig.2.26 A). No core-specific CD4 T-cell

responses were detectable in the blood of mice immunized with any vaccine formulations at the time point analyzed (Fig.2.26 B).

Immunization of mice with all novel adjuvant formulations elicited vigorous S-specific CD8 T-cell responses, which were significantly higher than those in the no vac and no adj groups of mice ($p < 0.05$) (Fig.2.26 C). The overall core-specific CD8 T-cell responses in blood were not as strong as the S-specific ones. The reason could be that HBcAg is not secreted and exists primarily in the HBV-infected hepatocytes (Pondé, 2012). Thus, core-specific T cells may predominantly remain in the liver where they could encounter the antigen, but may not circulate in the blood. Despite this, the magnitude of core-specific CD8 T-cell responses was significantly higher in mice immunized with LQ, LMQ, and SQ formulations compared to those in no vac mice ($p < 0.05$). In contrast, and very unexpected, nearly no core-specific CD8 T-cell responses were detected in the blood of mice vaccinated with SMQ formulation, with values significantly lower than those in the SQ formulation vaccinated mice ($p < 0.05$) (Fig.2.26 D).

Results

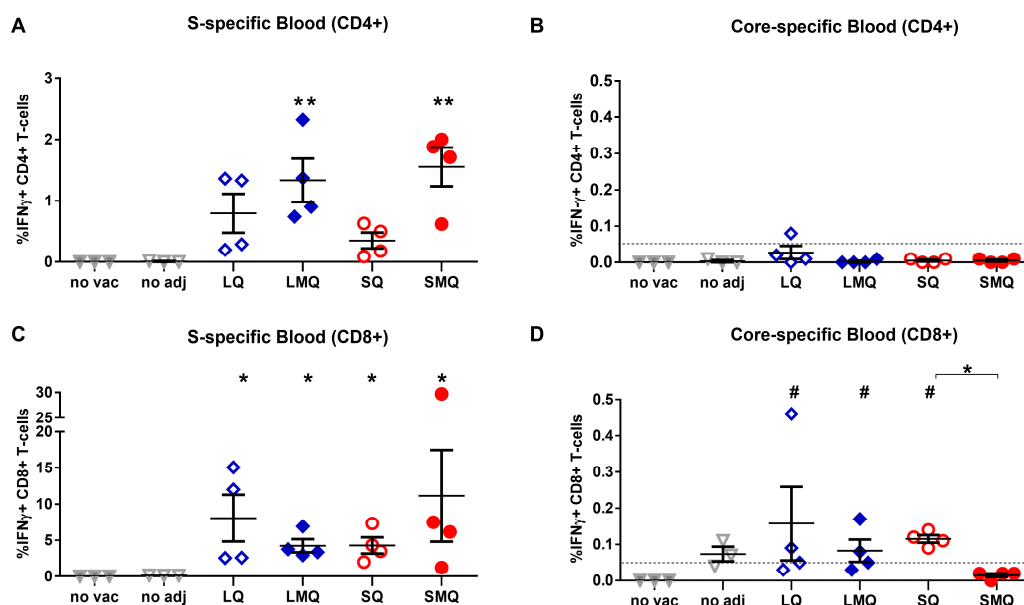


Fig.2.26 T-cell responses in blood induced by immunization with novel adjuvant formulations in the short-term analysis of AAV-HBV mice.

(A, B) Percentages of S- and core-specific IFN γ + CD4 T cells in blood determined by intracellular cytokine staining after S- and core-specific overlapping peptide pools *ex vivo* stimulation.

(C, D) Percentages of S- and core-specific IFN γ + CD8 T cells in blood determined by intracellular cytokine staining after S- and core-specific overlapping peptide pools *ex vivo* stimulation.

Hash (#) symbols mark statistically significant differences compared to no vac group; Asterisks (*) mark statistically significant differences compared to no adj group. Statistical analysis was performed by Kruskal-Wallis test with Dunn's multiple comparison correction or Mann-Whitney test: * $p < 0.05$, ** $p < 0.01$.

In the short-term analysis of AAV-HBV mice, vaccination with novel adjuvant formulations stimulated strong HBsAg- and HBcAg-specific antibody responses, accompanied by a marked HBsAg and HBeAg decrease in the serum. Moreover, immunization with all novel adjuvant formulations, especially LMQ and SMQ, induced strong S-specific CD4 and CD8 T-cell responses in blood. Compared with the other formulations, immunization with SMQ was less effective in inducing core-specific CD8 T-cell responses in the blood.

2.2.6 Long-term analysis of the novel adjuvant formulations in AAV-HBV mice

After the preliminary characterization of antibody and T-cell responses in blood at week 5, the mice were monitored until week 10 to investigate the impact of *TherVacB* immunization with novel adjuvant formulations on long-term immune control of persistent HBV replication. During the immunization and monitoring stages (from week 0 to week 10), the mice were bled every two weeks to check serum HBsAg and HBeAg levels (Fig.2.27 A). Moreover, the weight of the mice was monitored regularly. Similar to wild-type mice, no weight loss was observed in any individual mouse of any group during the entire experimental process (Fig.2.27 B), indicating all vaccine formulations were well tolerated and had no obvious side effects in AAV-HBV mice with long-term analysis. At week 10, mice were sacrificed to perform the final immunological and virological analyses in serum, liver, and spleen (Fig.2.27 A).

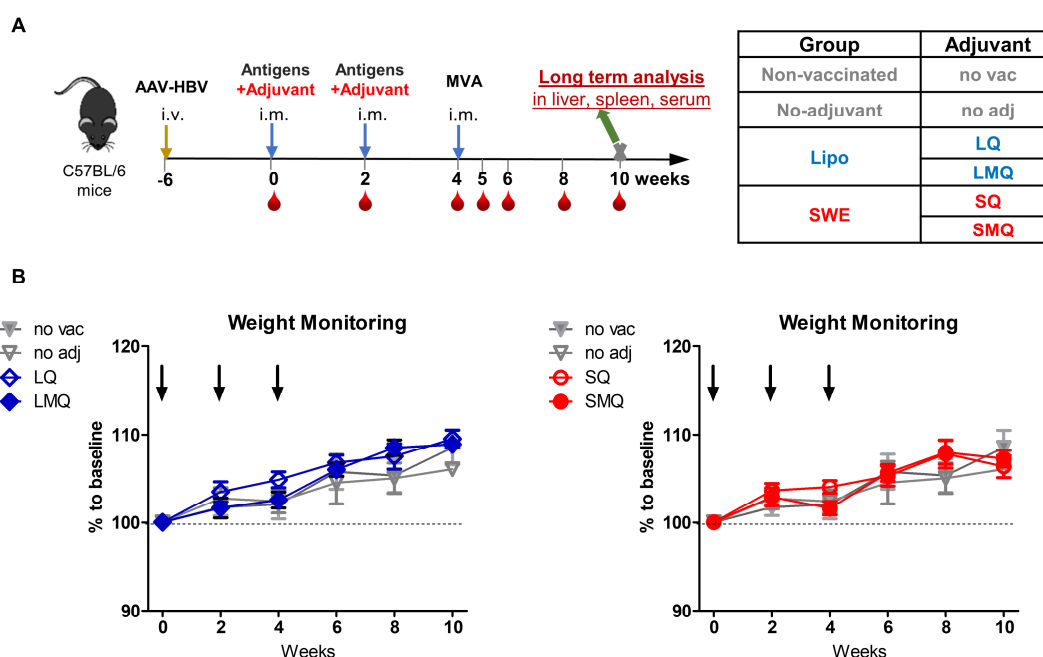


Fig.2.27 Experimental scheme and weight monitoring of AAV-HBV mice immunized with novel adjuvant formulations in long-term analysis.

(A) AAV-HBV mice were immunized with the antigen/adjuvant formulations listed in the right table at week 0 and week 2. At week 4, mice received MVA-S and MVA-core to boost the immune response. From week 0 to week 10, mice were bled every two weeks to check serum HBsAg and HBeAg levels. At week 10, mice were sacrificed to perform the final analysis in the liver, spleen, and serum.

(B) Weight of the mice in every group was monitored every two weeks and compared to the baseline at the start point of the experiment. Arrows show the time points of vaccination.

Results

In the first step, the induction of humoral immune responses after the immunization with novel adjuvant formulations was assessed by the detection of anti-HBs and anti-HBc in the serum of mice at week 10. As shown at week 5, immunization of mice with the four novel adjuvant formulations induced very high anti-HBs titers, which were significantly higher compared to those in both no vac and no adj treated mice ($p < 0.05$) (Fig.2.28 A). Moreover, the levels of anti-HBc in the mice vaccinated with all novel adjuvant formulations were significantly higher than those in no vac controls ($p < 0.05$) and were also considerably higher than those in the no adj group (Fig.2.28 B).

To evaluate the breadth of the immune responses resulting from vaccination with novel adjuvant formulations, the IgG₁ and IgG_{2b} subclasses of anti-HBs and anti-HBc were analyzed in mice serum by ELISA. Vaccination with all novel adjuvant formulations induced comparable levels of S-specific IgG₁ and IgG_{2b} subclasses (Fig.2.28 C), which implied that the novel adjuvant formulations induced Th1/Th2-balanced S-specific responses. As was observed in the wild-type mice, immunization with all vaccine formulations, including the no adj group, generated predominantly IgG_{2b} subclass of anti-HBc antibodies, which correlated with the fact that HBcAg preferentially activates Th1-biased responses (Fig.2.28 D).

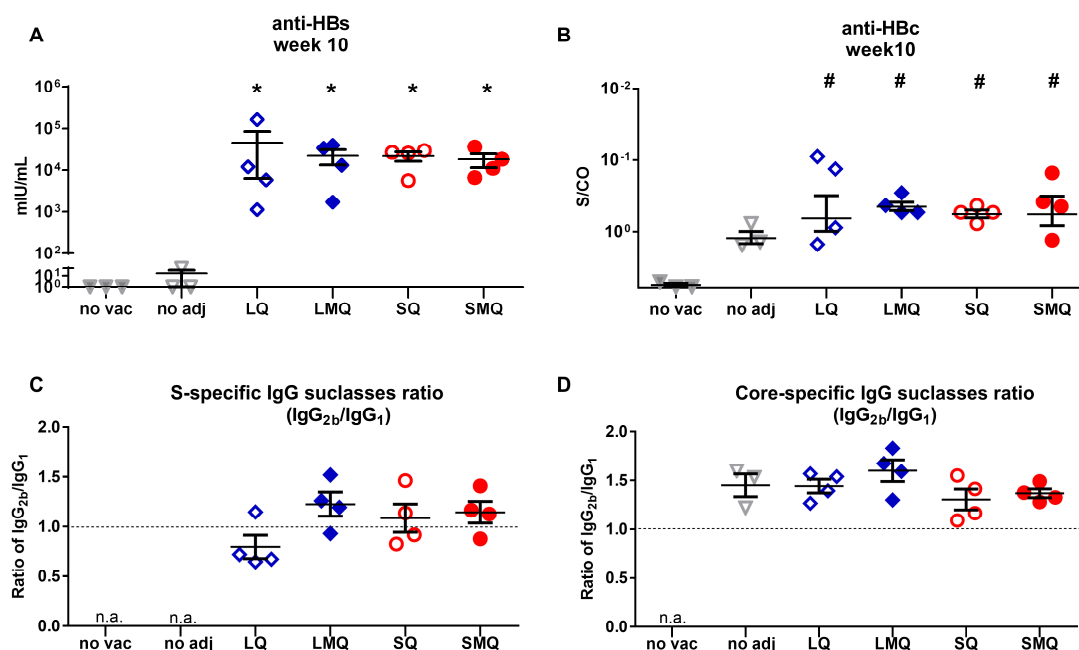


Fig.2.28 Antibody responses induced by immunization with novel adjuvant formulations in long-term analysis of AAV-HBV mice.

(A, B) The levels of anti-HBs (A) and anti-HBc (B) were detected in the serum of experimental mice at the endpoint.

(C, D) The IgG₁ and IgG_{2b} ratio of anti-HBs (C) and anti-HBc (D). The OD₄₅₀ values of IgG₁ and IgG_{2b} values were detected with the serum of immunized C57BL/6 mice at the endpoint by ELISA. Then, the ratio of IgG_{2b}: IgG₁ was calculated based on the respective OD₄₅₀ values. n.a. means not applicable.

Hash (#) symbols mark statistically significant differences compared to no vac group; Asterisks (*) mark statistically significant differences compared to no adj group. Statistical analysis was performed by Kruskal-Wallis test with Dunn's multiple comparison correction or Mann-Whitney test: * $p < 0.05$.

To further verify the induction of helper T-cell responses after the immunization with adjuvant formulations, the production of both Th2 cytokine interleukin-5 (IL-5) and Th1 cytokine IFN γ was evaluated in the splenocytes, which were *ex vivo* stimulated with HBsAg or HBcAg. A robust secretion of S-specific IL-5 as well as IFN γ was observed in splenocytes of mice immunized with novel adjuvant formulations as compared to those in splenocytes of no vac or no adj treated mice. Of note, splenocytes from the mice immunized with LMQ and SMQ formulations, in which MPL was included, secreted about two-fold higher levels of Th1 cytokine IFN γ compared to those from the mice immunized with LQ and SQ formulations (Fig.2.29 A). Conversely, immunization with LMQ and SMQ formulations induced lower Th2 cytokine IL-5 secretion than

Results

immunization with LQ and SQ formulations, a finding that indicates the remarkable effects of MPL on inducing Th1-biased responses (Wheeler, 2001) (Fig.2.29 C).

The amount of IFN γ secreted by core-specific splenocytes from mice immunized with novel adjuvant formulations was significantly higher than those secreted by the cells of no vac mice ($p < 0.05$). In addition, there was no significant difference in IFN γ induction from core-specific cells between the groups with or without the addition of MPL, pointing to the role of HBcAg itself on the induction of Th1-biased responses (Fig.2.29 B). Furthermore, stimulation of splenocytes from the mice immunized with novel adjuvant formulations with HBcAg also resulted in the detection of IL-5 (Fig.2.29 D). The simultaneous production of IFN γ and IL-5 confirmed that immunization with novel adjuvant formulations was able to induce Th1/Th2-balanced responses.

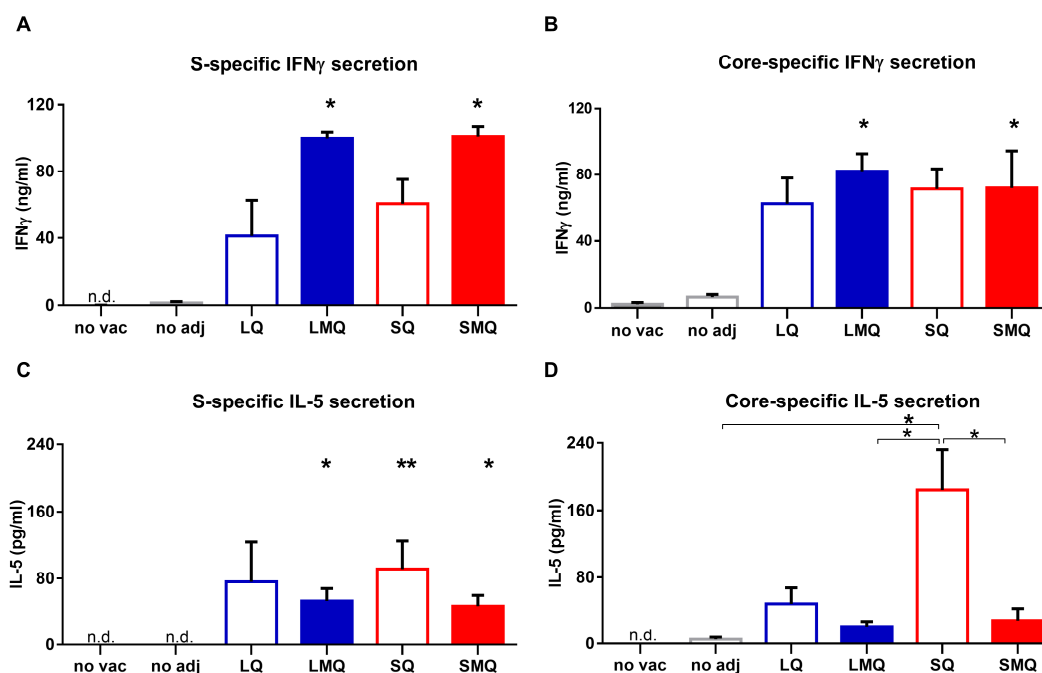


Fig.2.29 Helper T-cell responses induced by immunization with novel adjuvant formulations in long-term analysis of AAV-HBV mice.

Splenocytes from the mice immunized with different formulations were stimulated with 20 μ g/ml HBsAg or HBcAg for 48 hours. The cytokine levels in the supernatant were quantified by ELISA. (A, B) Analysis of IFN γ secretion by HBsAg- (A) or HBcAg- (B) stimulated splenocytes from the vaccinated mice. Results are depicted in ng/ml.

(C, D) Analysis of IL5 secretion by HBsAg- (C) or HBcAg- (D) stimulated splenocytes from the vaccinated mice. Results are depicted in pg/ml.

Asterisks (*) mark statistically significant differences compared to no adj group. Statistical analysis was performed by Kruskal-Wallis test with Dunn's multiple comparison correction or Mann-Whitney test: * $p < 0.05$, ** $p < 0.01$. n.d.—not detectable.

It has been shown that CD8 T cells are the main effector cells to determine whether acute HBV infection will progress to resolution or chronicity (Thimme, 2003). The impact of the vaccination with novel adjuvant formulations on the induction of CD8 T-cell responses was assessed in the final analysis of week 10.

To detect S- and core-specific CD8 T cells induced by the vaccination with novel adjuvant formulations, the LALs and splenocytes were *ex vivo* stained with S₁₉₀- and C₉₃-specific multimers, respectively. Considerably high levels of S- and core-specific CD8 T cells were detected in the livers of mice immunized with novel adjuvant formulations, especially LMQ and SQ formulations. The average percentages of S-specific CD8 T cells in the liver of mice immunized with these two formulations were

Results

around 3.5%, which were significantly higher than those in the livers of no vac and no adj treated mice ($p < 0.05$) (Fig.2.30 A). The frequencies of intrahepatic core-specific CD8 T cells were much higher than the S-specific ones. Approximately 20% of core-specific CD8 T cells were detected in the livers of mice immunized with LQ, LMQ, and SQ formulations. In contrast, less than 10% of core-specific CD8 T cells were detected in the livers of mice immunized with SMQ formulation, a similar profile as in no adj group of mice (Fig.2.30 B). In contrast to the high levels of HBV-specific CD8 T cells in the liver, low amounts of S- and core-specific CD8 T cells were observed in the lymphatic organ spleen (Fig.2.30 C and D). This finding implies that the antigen-specific CD8 T cells induced by vaccination mainly remained in the liver to control HBV-infection.

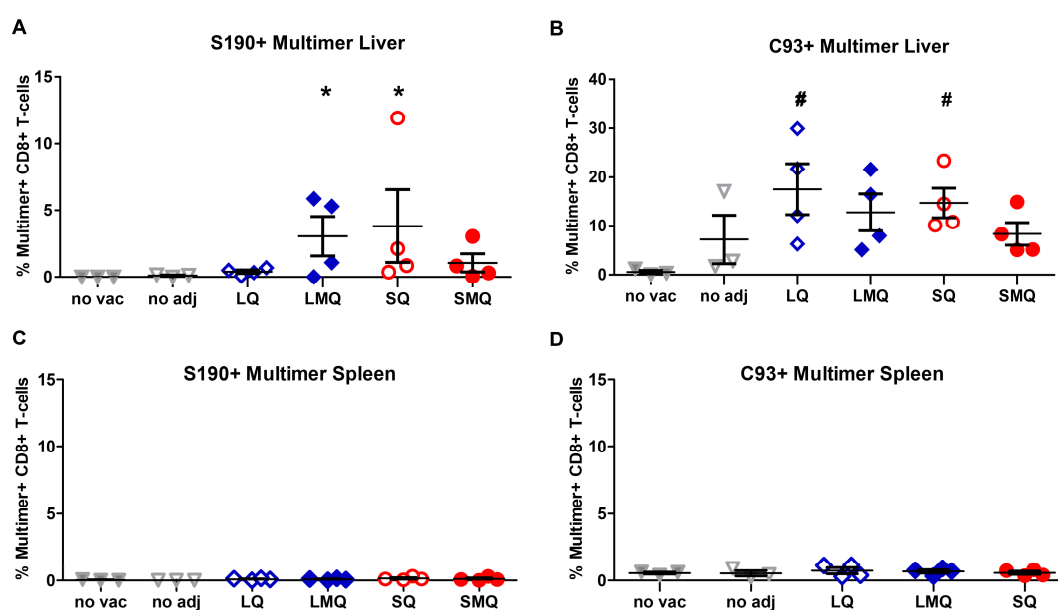


Fig.2.30 Antigen-specific CD8 T cells induced by immunization with novel adjuvant formulations in the liver and spleen of AAV-HBV mice in long-term analysis.

(A, B) Percentages of liver-associated S- and core-specific CD8 T cells determined by S₁₉₀- (A) and C₉₃-specific (B) multimers staining *ex vivo*.

(C, D) Percentages of splenic S- and core-specific CD8 T cells determined by S₁₉₀- (C) and C₉₃-specific (D) multimers staining *ex vivo*.

Hash (#) symbols mark statistically significant differences compared to no vac group; Asterisks (*) mark statistically significant differences compared to no adj group. Statistical analysis was performed by Kruskal-Wallis test with Dunn's multiple comparison correction or Mann-Whitney test: * $p < 0.05$, ** $p < 0.01$.

In the next step, the functionality of S- and core-specific CD8 T cells was analyzed by intracellular IFN γ and TNF α staining of LALs and splenocytes upon *ex vivo* peptide stimulation.

Neither intrahepatic nor splenic S-specific IFN γ + CD8 T cells were detectable in the mice immunized without adjuvant, implying S-specific CD8 T-cell responses greatly needed the assistance of a proper adjuvant. Immunization of mice with LMQ, SQ, and SMQ formulations stimulated strong S-specific IFN γ + CD8 T-cell responses in both liver and spleen, and these responses were significantly higher than those in the no vac and no adj treated mice ($p < 0.05$, or $p < 0.01$) (Fig.2.31 A and B). Furthermore, more than 90% S-specific IFN γ + CD8 T-cells induced by the immunization with novel adjuvant formulations in both spleen and liver were also multifunctional IFN γ + TNF α + double-positive (Fig.2.31 C and D).

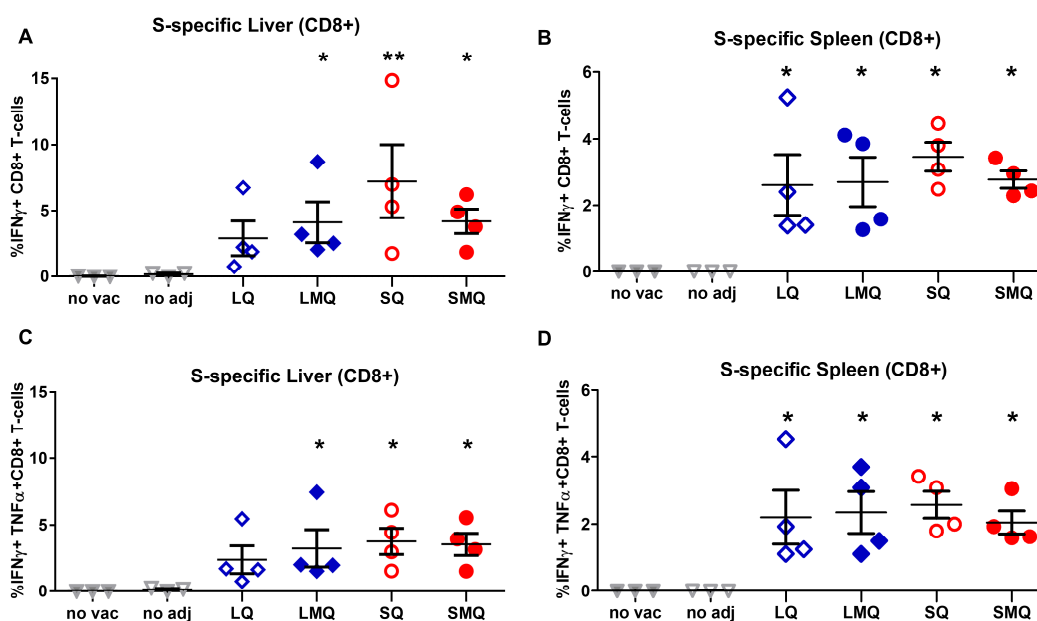


Fig.2.31 The functionality of S-specific CD8 T cells induced by immunization with novel adjuvant formulations in the liver and spleen of AAV-HBV mice in long-term analysis.

(A-D) Percentages of S-specific IFN γ + and IFN γ + TNF α + CD8 T cells determined by intracellular cytokine staining of LALs (A, C) and splenocytes (B, D) after S-specific peptide pool *ex vivo* stimulation.

Asterisks (*) mark statistically significant differences compared to no adj group. Statistical analysis was performed by Kruskal-Wallis test with Dunn's multiple comparison correction or Mann-Whitney test: * $p < 0.05$, ** $p < 0.01$.

Results

The average frequencies of core-specific IFN γ ⁺ CD8 T cells in the livers of mice immunized with LQ, LMQ, and SQ formulations were around 5%, which was significantly higher than those in the no vac group ($p < 0.05$). Additionally, approximately 2% core-specific IFN γ ⁺ CD8 T cells were detected in the livers of the mice in the no adj group, which confirmed that HBcAg is a potent immunogen for activating Th1-biased immune responses. Consistent with the low levels of core-specific CD8 T cells, almost no core-specific IFN γ ⁺ CD8 T cells were detectable in the livers of mice immunized with SMQ formulation, with values significantly lower than those in mice immunized with LMQ and SQ formulations ($p < 0.05$) (Fig.2.32 A). From these contrasting results, one can conclude that different approaches for priming resulted in distinct T-cell functions. Unlike the S-specific responses detected in both liver and spleen, core-specific IFN γ ⁺ CD8 T-cell responses were mainly localized in the liver but not in the spleen (Fig.2.32 B). This could be because HBcAg is not a secreted viral protein, which is principally expressed in the infected hepatocytes. Core-specific IFN γ ⁺ TNF α ⁺ double-positive CD8 T cells were undetectable in either the liver or the spleen, demonstrating that these T cells displayed a different profile from the multifunctional S-specific CD8 T cells (Fig.2.32 C and D).

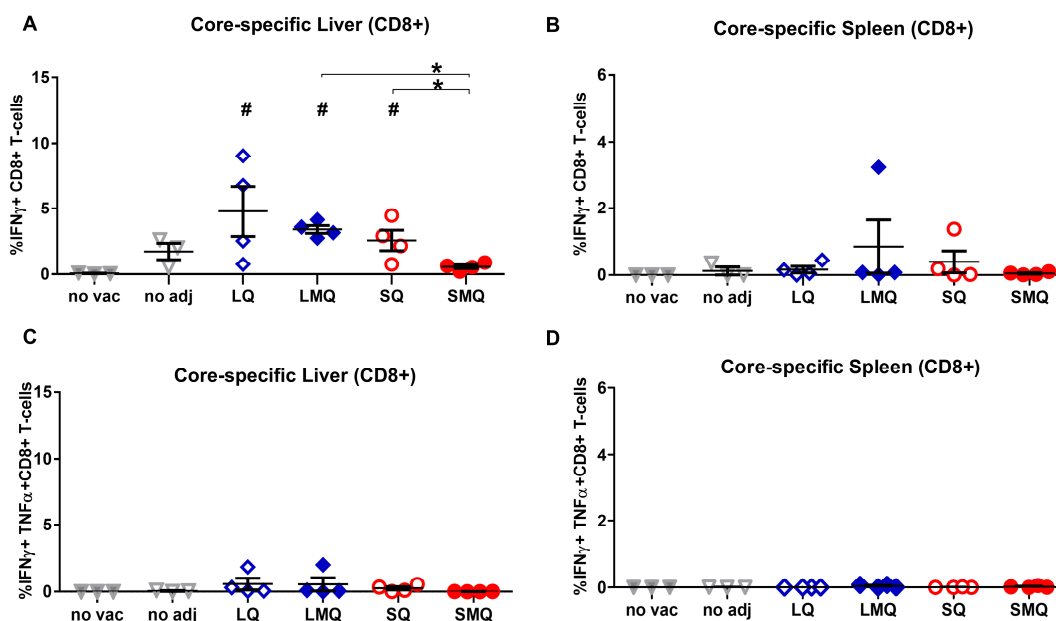


Fig.2.32 The functionality of core-specific CD8 T cells induced by immunization with novel adjuvant formulations in the liver and spleen of AAV-HBV mice in long-term analysis.

(A-D) Percentages of S-specific IFN γ + and IFN γ + TNF α + CD8 T cells determined by intracellular cytokine staining of LALs (A, C) and splenocytes (B, D) after core-specific peptide pool *ex vivo* stimulation.

Hash (#) symbols mark statistically significant differences compared to no vac group. Statistical analysis was performed by Kruskal-Wallis test with Dunn's multiple comparison correction or Mann-Whitney test: * $p < 0.05$.

To assess the impact of immunization with different adjuvant formulations on long-term control of persistent HBV replication, the HBsAg and HBeAg levels in murine serum were monitored for 10 weeks from the starting point of *TherVacB* vaccination.

While there was a 1-log HBsAg decrease in the serum of mice in the no adj group, immunization with all adjuvanted formulations resulted in a 3-log decrease in serum HBsAg compared to the baseline at week 0. Of note, the most dramatic HBsAg decrease occurred after the first and second protein priming and correlated with the high levels of anti-HBs in the serum after protein priming (Fig.2.33 A).

Compared to the baseline at week 0, a slight HBeAg decrease was observed in the serum of mice immunized without adjuvant. Immunization with Lipo-based formulations, especially LMQ, induced a more than 50% serum HBeAg decrease (Fig.2.33 B, left). With respect to the SWE-based formulations, immunization with the

Results

SQ formulation displayed a similar HBeAg decrease as those in mice immunized with Lipo-based formulations. By contrast, consistent with the poor core-specific CD8 T-cell responses, immunization with SMQ formulation resulted in minor effects on the reduction of serum HBeAg levels (Fig.2.33 B, right).

To further evaluate the long-term antiviral effects of the immunization with novel adjuvant formulations, core-specific immunohistochemistry (IHC) staining and intrahepatic HBV DNA were analyzed using the liver tissues of all mice at the endpoint. In agreement with the enhanced antigen decreasing effects, liver IHC staining revealed that immunization with LQ, LMQ, and SQ formulations, but not with no adj, led to a four-fold reduction in numbers of core-positive hepatocytes (Fig.2.33 C and D). In addition, immunization with these formulations led to a 50% suppression of intrahepatic HBV DNA (Fig.2.33 E). In contrast, immunization with SMQ formulation exhibited only minor effects on the reduction of core-positive hepatocytes and suppression of intrahepatic HBV DNA. These striking differences in antiviral effects resulting from different priming approaches again demonstrates how important proper priming for the overall efficacy of a therapeutic vaccine.

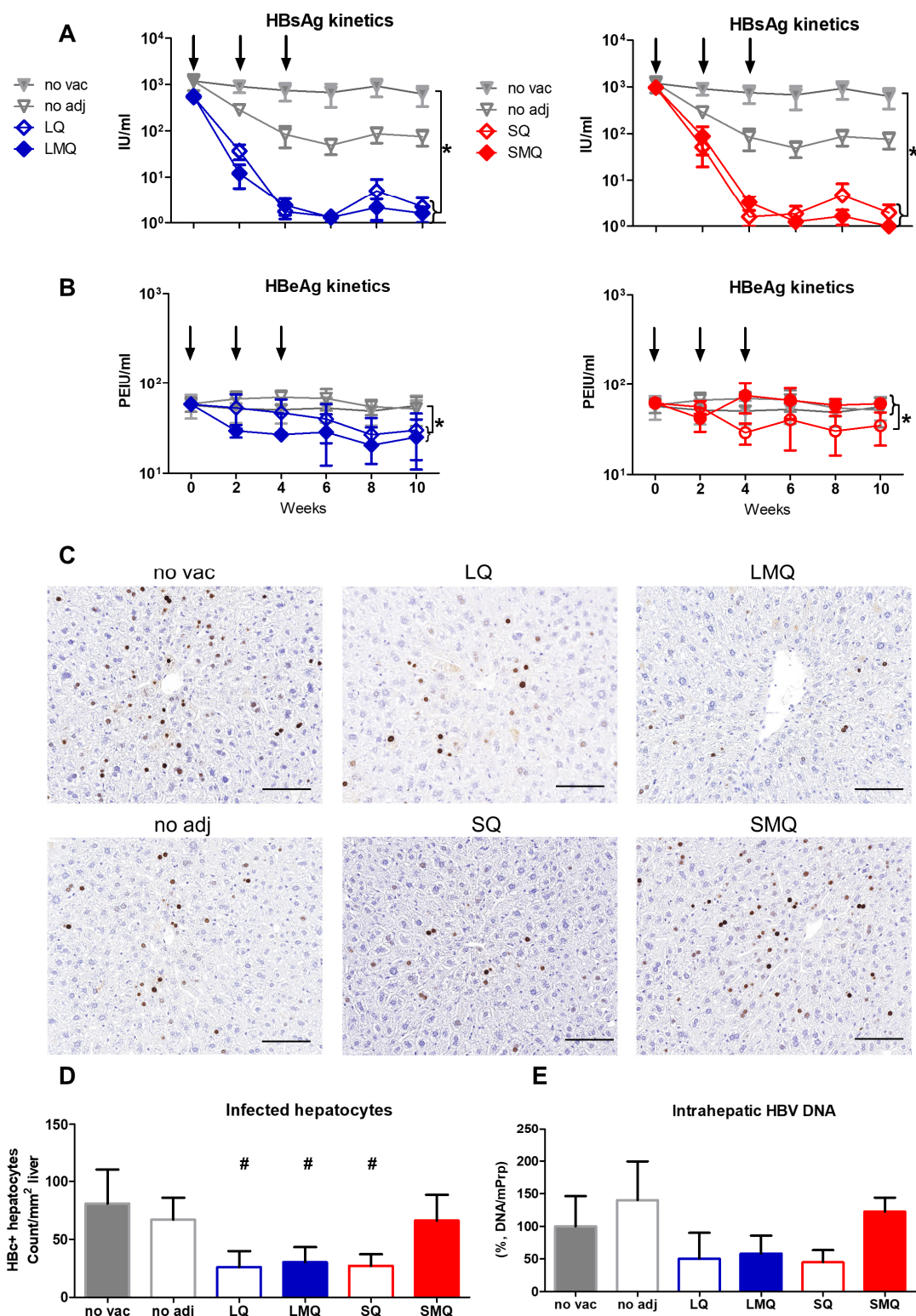


Fig.2.33 Long-term antiviral effects induced by immunization with novel adjuvant formulations in AAV-HBV mice.

(A, B) Time kinetics of serum HBsAg (A) and HBeAg (B) levels in the whole experimental stage.

Arrows show the time points of vaccination.

(C, D) Representative images (C) and quantification (D) of liver IHC staining for core-positive hepatocytes (brown dots) at endpoint. Scale bars indicate 100µm.

Results

(E) Intrahepatic HBV-DNA was determined in liver tissue lysates. The HBV-DNA copies were determined by qPCR and normalized to cell numbers using the single-copy gene mPrp. The HBV-DNA copies in individual mice were indicated relative to the mean value determined in no vac group (set to 100%).

Hash (#) symbols mark statistically significant differences compared to no vac group. Statistical analysis was performed by Kruskal-Wallis test with Dunn's multiple comparison correction or Mann-Whitney test: * $p < 0.05$.

In the long-term analysis of AAV-HBV mice, immunization of all Lipo- and SWE-based adjuvant formulations elicited very high levels of anti-HBs and anti-HBc. Compared to immunization with LQ and SQ formulations, immunization with LMQ and SMQ induced remarkably stronger intrahepatic and splenic S-specific CD4 T-cell responses. Moreover, immunization with LMQ formulation not only elicited strong S- and core-specific CD8 T-cell responses, but also led to profound long-term immune control of persistent HBV replication in AAV-HBV mice. In contrast, immunization with SMQ failed to elicit core-specific CD8 T-cell responses and thus had minor antiviral effects.

To summarize the studies in this chapter, all Lipo- and SWE-based antigen/adjuvant formulations could remain stable and intact for at least 12 weeks *in vitro*. The selected Lipo- and SWE-based novel combination adjuvants displayed strong immunostimulatory activities by the activation of hMoDCs *in vitro*. Immunization of wild-type and AAV-HBV infected mice with LMQ formulation not only elicited very strong HBV-specific humoral and cellular immune responses, but also led to long-term immune control of persistent HBV replication in AAV-HBV mice. Therefore, LMQ formulation is a promising candidate to improve the efficacy of the *TherVacB* regimen.

2.3 Exploration of critical factors for efficient protein priming in *TherVacB*

The studies in last chapter demonstrate that proper protein priming with an appropriate adjuvant is the key factor determining the success of *TherVacB*. On one hand, immunization with the adjuvanted antigens can induce CD4 helper T cells and high levels of neutralizing antibodies that in turn decrease antigen levels in the periphery; on the other hand, the immunization can prime virus-specific effector T cells, which can be expanded by the MVA vectors during the boost.

To further improve the *TherVacB* strategy, it would be necessary to explore the critical factors during the priming phase determining the efficacy of *TherVacB*. In the studies described in this chapter, the impact of individual vaccine components (antigens, adjuvant) for priming was determined and the role of different T-cell subsets mediating the immune responses during the priming phase of *TherVacB* was explored.

2.3.1 Importance of administering recombinant antigens during the priming phase of *TherVacB*

Since there are high loads of circulating HBsAg and HBeAg antigens in the periphery of chronic hepatitis B-infected patients or mice, it would be interesting to explore whether external adjuvant administration can assist the endogenous HBV antigens to efficiently induce HBV-specific responses. To address this question, four different types of adjuvants—LMQ, SMQ, STING agonist c-di-AMP, and TLR9 agonist CpG 1018—were employed in this study (Fig.2.34).

In a first step, persistent HBV replication in the C57BL/6 mice was established by infection with AAV-HBV six weeks prior to the vaccination. Afterwards, the AAV-HBV mice received the adjuvant LMQ, SMQ, c-di-AMP, or CpG-1018 intramuscularly twice at week 0 and week 2, and boosted with recombinant MVA expressing HBsAg and HBcAg intramuscularly at week 4. The LMQ adjuvanted HBsAg/HBcAg (S+C+LMQ) for priming served as a positive control. During the experiments, mice were bled every two weeks to monitor serum HBsAg and HBeAg levels. At week 10, the mice were sacrificed to perform the final analysis in serum, liver, and spleen (Fig.2.34).

Results

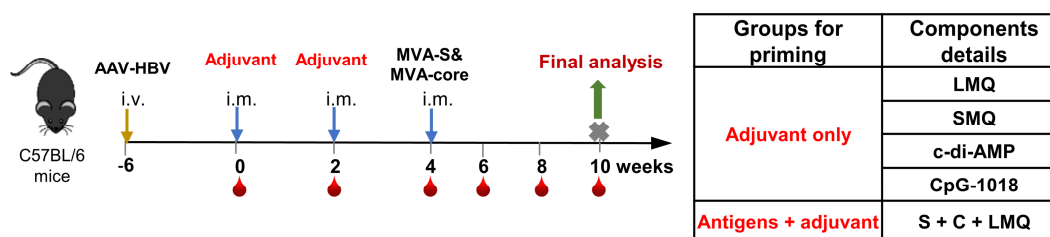


Fig.2.34 Experimental scheme of adjuvant only for priming in AAV-HBV mice.

Mice were infected with AAV-HBV six weeks prior to the vaccination to establish the persistent HBV replication. Afterwards, the mice were immunized with the adjuvants listed in the right table at week 0 and week 2. At week 4, mice received MVA-S and MVA-core vectors to boost the immune response. At week 10, the mice were sacrificed to perform the final analysis in the liver, spleen, and serum.

The effects of priming with adjuvant only on antibody generation were evaluated by the detection of anti-HBs and anti-HBc in the serum of mice at week 10. As shown in Fig.2.35 A and B, neither anti-HBs nor anti-HBc were generated in any mouse primed with adjuvant only. In contrast, very high levels of both anti-HBs and anti-HBc were detected in the mice primed with LMQ adjuvanted HBsAg/HBcAg (Fig.2.35 A and B).

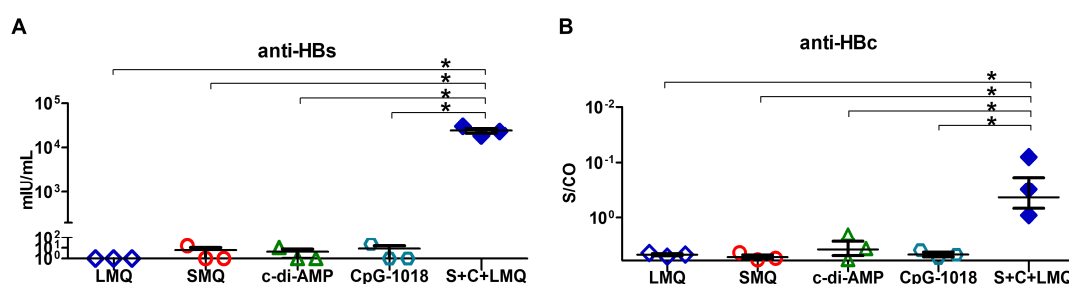


Fig.2.35 Antibody responses induced by priming with adjuvant only in AAV-HBV mice.

(A, B) The levels of anti-HBs (A) and anti-HBc (B) detected in the serum of immunized mice at study endpoint are depicted.

Statistical analysis was performed by Kruskal-Wallis test with Dunn's multiple comparison correction: * $p < 0.05$.

In the next step, CD4 and CD8 T-cell responses induced by priming only with adjuvant were analyzed by intracellular IFN γ staining of peptide-stimulated LALs at week 10.

No matter which type of adjuvant was used, employing adjuvant only for priming and MVA vector expressing HBV antigens for boost did not stimulate any HBV-specific CD4 or CD8 T-cell responses (Fig.2.36 A-D). By contrast, immunization with LMQ adjuvanted HBsAg/HBcAg induced not only very strong S-specific CD4 T-cell

responses but also very strong S- and core-specific CD8 T-cell responses (Fig.2.36 A, C, D). There were also no core-specific CD4 T-cell responses detected in the mice primed with adjuvanted antigens at the analyzed time points (Fig.2.36 B).

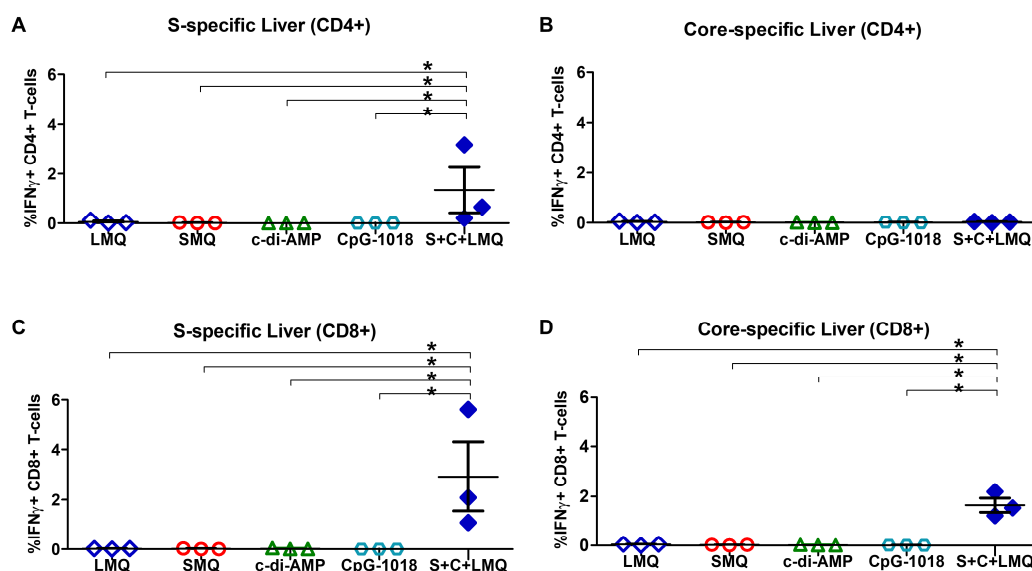


Fig.2.36 T-cell responses induced by priming with adjuvant only in AAV-HBV mice.

(A, B) Percentages of S- (A) and core-specific(B) IFN γ + CD4 T cells in the liver determined by intracellular cytokine staining after S- and core-specific overlapping peptide pool *ex vivo* stimulation.

(C, D) Percentages of S- (C) and core-specific (D) IFN γ + CD8 T cells in liver determined by intracellular cytokine staining after S- and core-specific overlapping peptide pool *ex vivo* stimulation.

Statistical analysis was performed by Kruskal-Wallis test with Dunn's multiple comparison correction: * $p < 0.05$.

Consistent with the lack of anti-HBs generation, the serum HBsAg levels in the mice only primed with all different types of adjuvants remained as stable as the baseline at week 0, whereas the levels of HBsAg in the mice primed with LMQ adjuvanted HBsAg/HBcAg decreased dramatically after the protein priming (Fig.2.37 A). Similarly, the levels of HBeAg in the mice only primed with adjuvant remained comparable before and after immunization, which correlated with a lack of HBV-specific T-cell responses detectable in these mice (Fig.2.37 B). Hence, it was shown that immunization only with adjuvant was not able to induce neutralizing antibodies or T-cell responses to decrease the levels of circulating antigens.

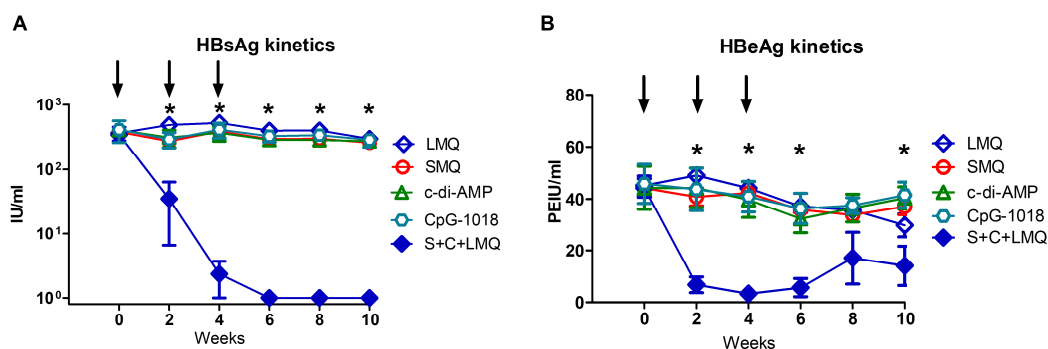


Fig.2.37 Antigen decreases induced by priming with adjuvant only in AAV-HBV mice.

(A, B) Time kinetics of serum HBsAg (A) and HBeAg (B) levels from the initiation of *TherVacB* at week 0 to the endpoint of analysis at week 10. Arrows show the time points of vaccination. Statistical analyses were performed using 2-way analysis of variance (ANOVA): * $p < 0.05$.

Even with high loads of endogenous antigens *in vivo*, priming only with adjuvant was not sufficient to induce any HBV-specific antibody or T-cell responses. It is critical to include recombinant HBsAg/HBcAg during the priming phase of *TherVacB*.

2.3.2 Criteria of adjuvant selection for the priming in *TherVacB*

After confirming the importance of HBsAg/HBcAg priming in the vaccination, the adjuvant selection criteria for *TherVacB* was explored in the studies described in this section. Two different types of adjuvants were included and compared in the *TherVacB* setting: the model Th2-biased adjuvant aluminum salts (Alum) and Th1/Th2-balanced combination adjuvants LMQ and SMQ.

The AAV-HBV mice were immunized with HBsAg/HBcAg (S+C) only or HBsAg/HBcAg adjuvanted with Alum, LMQ, or SMQ twice at week 0 and week 2, and boosted with MVA-S and MVA-core at week 4. Non-vaccinated (no vac) mice served as a negative control. At week 10, the mice were sacrificed to perform the final analysis in serum, liver, and spleen (Fig.2.38).

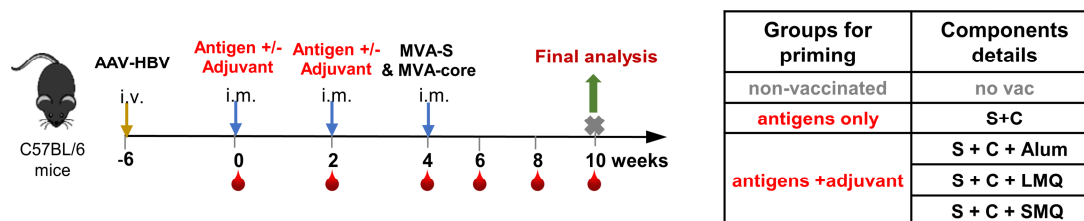


Fig.2.38 Experimental scheme of different types of adjuvants for priming in AAV-HBV mice.

Mice were infected with AAV-HBV six weeks prior to the vaccination to establish the persistent HBV replication. Afterwards, the mice were immunized with the vaccines listed in the right table at week 0 and week 2. At week 4, mice received MVA-S and MVA-core vectors to boost the immune responses. At week 10, the mice were sacrificed to perform the final analysis in the liver, spleen, and serum.

The humoral immune responses induced by immunization with various formulations were evaluated by the detection of anti-HBs and anti-HBc in the murine serum at week 10. Immunization only with antigens (S+C) induced moderate amounts of anti-HBs that were not significantly different from those in the no vac mice. Of note, immunization with Alum, LMQ, or SMQ formulations generated significantly higher levels of anti-HBs compared to immunization only with antigens ($p < 0.05$) (Fig.2.39 A). Vaccination with all formulations, including the antigens-only group, induced significantly higher levels of anti-HBc than the no vac group ($p < 0.05$) (Fig.2.39 B).

To address the differences in antibodies induced by the Alum, LMQ and SMQ formulations, the IgG₁ and IgG_{2b} subclasses of anti-HBs and anti-HBc were analyzed in murine serum by ELISA. In accordance with the previous results, immunization with LMQ and SMQ formulations induced comparable S-specific IgG₁ and IgG_{2b} subclasses. In contrast, immunization with the Alum formulation induced predominantly the Th2-associated IgG₁ subclass of anti-HBs (Fig.2.39 C). Th1-associated IgG_{2b} was the dominant IgG subclass of anti-HBc in all vaccinated mice, even in mice immunized with Th2-biased adjuvant Alum formulations (Fig.2.39 D).

Results

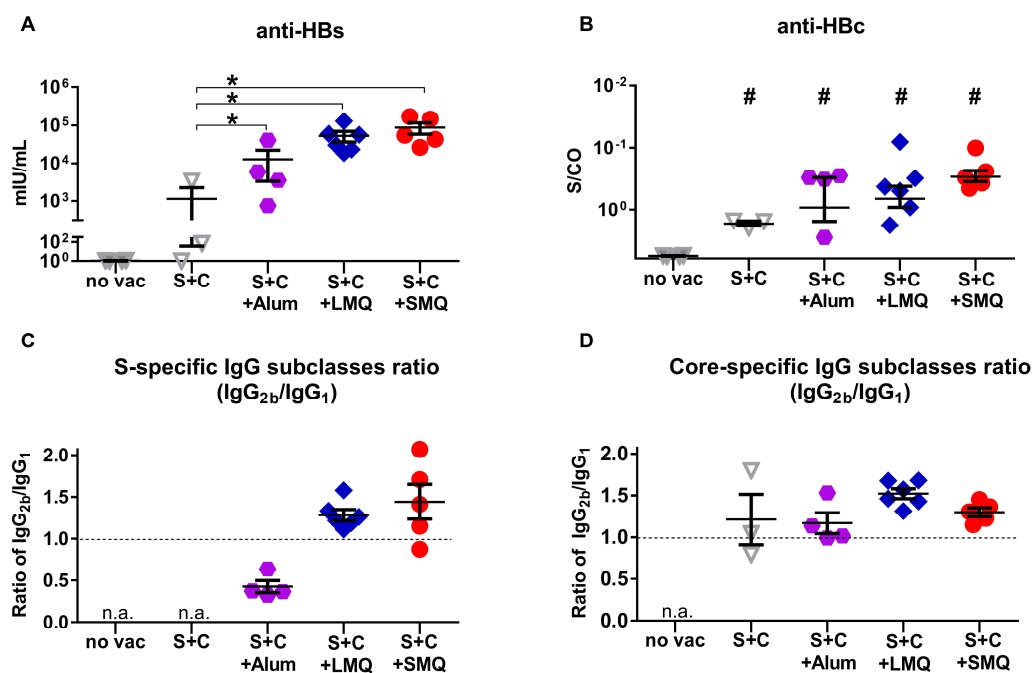


Fig.2.39 The humoral immune responses of different types of adjuvants for priming in AAV-HBV mice.

(A, B) The levels of anti-HBs (A) and anti-HBc (B) antibodies were detected in the serum of immunized mice at the endpoint.

(C, D) The IgG_{2b}/IgG₁ ratio of S- (C) and core-specific (D) IgG subclasses. The levels of IgG_{2b} and IgG₁ were detected in the serum of mice at the endpoint by ELISA. Then, the ratio of IgG_{2b}: IgG₁ was calculated based on the respective OD₄₅₀ values. n.a.—not applicable.

Hash (#) symbols mark statistically significant differences compared to no vac group. Statistical analysis was performed by Kruskal-Wallis test with Dunn's multiple comparison correction or Mann-Whitney test: * $p < 0.05$.

To compare the impact of immunization with Alum, LMQ and SMQ formulations on the induction of helper T-cell responses, splenocytes from immunized mice were isolated and *ex vivo* stimulated with particulate HBsAg or HBcAg for 48 hours. Afterwards, the secretion of Th1 cytokine IFN γ and Th2 cytokine interleukin 5 (IL-5) by splenocytes was detected in the supernatants by ELISA.

IFN γ levels in splenocyte cultures from the mice immunized with LMQ or SMQ formulations were around 50 ng/ml IFN γ upon stimulation with HBsAg. By contrast, very small amounts of S-specific IFN γ were secreted by splenocytes from the mice immunized with the Alum formulation, and these amounts were significantly lower than those from the mice immunized with LMQ or SMQ formulations ($p < 0.05$) (Fig.2.40 A). With HBcAg stimulation, around 25 ng/ml IFN γ was secreted by the splenocytes from

the mice immunized with the Alum formulation, which was comparable to those in the antigen-only immunized mice. Considering the HBcAg features of activation of Th1-biased immune responses, the core-specific IFN γ secretion in these two groups may be mainly mediated by HBcAg itself, but not the adjuvant. Nevertheless, the splenocytes from the mice immunized with LMQ or SMQ formulations secreted approximately 50 ng/ml core-specific IFN γ , displaying that immunization with these formulations had an enhancement effect on the core-specific IFN γ secretion compared to immunization without adjuvant and with Alum formulation (Fig.2.40 B).

With either HBsAg or HBcAg stimulation, the production of Th2 cytokines IL-5 in mice immunized with Alum formulation was not elevated compared to the mice immunized with LMQ and SMQ formulations. The reason for this might be that the Th1-biased boost with viral vector MVA in the *TherVacB* strategy interfered with Th2-biased immune responses elicited by priming with Alum formulation (Fig.2.40 C and D).

Results

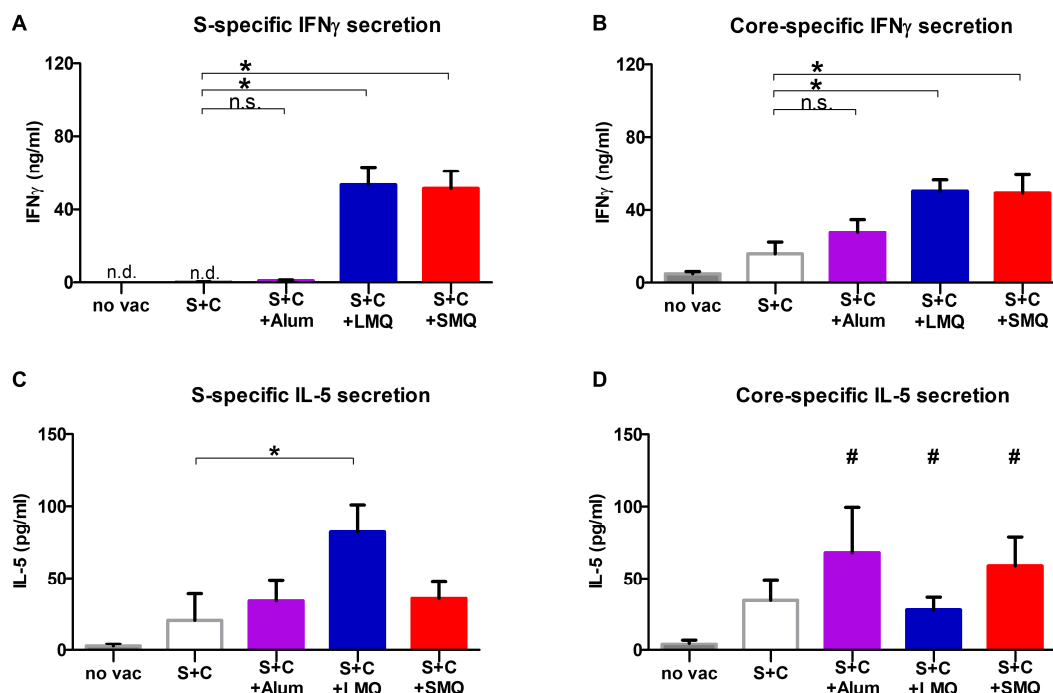


Fig.2.40 Helper T-cell responses of different types of adjuvants for priming in AAV-HBV mice.

(A-D) Analysis of IFN γ and IL-5 secreted by HBsAg- (A, C) or HBcAg (B, D)-stimulated splenocytes from the mice vaccinated with different formulations. The cytokine levels in the supernatant were quantified by ELISA. Results of IFN γ are depicted in ng/ml. Results of IL-5 are depicted in pg/ml. n.d.—not detectable.

Hash (#) symbols mark statistically significant differences compared to no vac group. Statistical analysis was performed by Kruskal-Wallis test with Dunn's multiple comparison correction or Mann-Whitney test: * $p < 0.05$; n.s.—not significant.

In the next step, the impact of vaccination with various priming formulations on the induction of CD4 and CD8 T-cell responses was analyzed by intracellular IFN γ staining of LALs. Immunization with Alum formulation elicited moderate S-specific CD4 T-cell responses. Of note, immunization with LMQ or SMQ formulations stimulated enhanced S-specific CD4 T-cell responses, which were significantly higher than those in mice immunized with the antigen-only formulation ($p < 0.05$) (Fig.2.41 A).

Following the distinct difference in CD4 T-cell responses, no S-specific CD8 T-cell responses were detected in mice immunized with Alum formulation. By contrast, immunization of mice with LMQ or SMQ formulations stimulated robust S-specific CD8 T-cell responses that were significantly higher than those in mice immunized with Alum formulation ($p < 0.05$) (Fig.2.41 C). Therefore, it can be concluded that HBsAg required assistance from a Th1/Th2-balanced adjuvant to stimulate not only humoral but also

cellular immune responses.

Immunization only with antigens induced similar core-specific CD8 T-cell responses compared to immunization with the adjuvanted formulations (Fig.2.41 D), confirming that HBcAg is a potent immunogen, which can induce strong core-specific CD8 T-cell responses without co-administration of adjuvant.

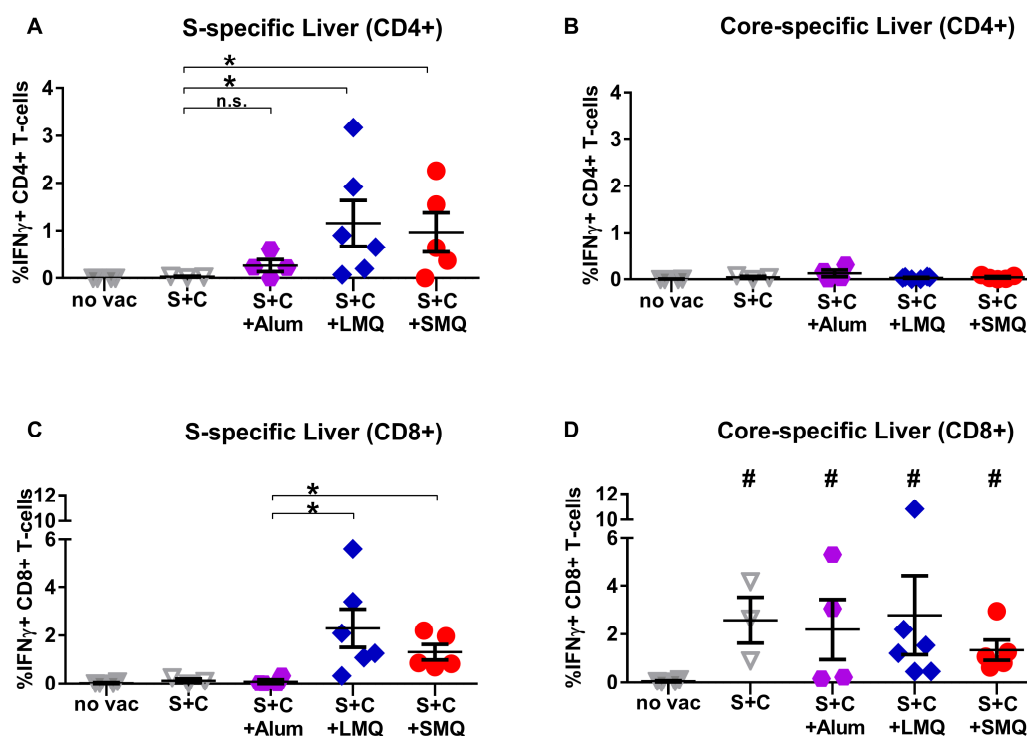


Fig.2.41 The CD4 and CD8 T-cell responses of different types of adjuvants for priming in AAV-HBV mice.

(A, B) Percentages of S- (A) and core-specific (B) IFN γ + CD4 T cells in the liver determined by intracellular cytokine staining after S- and core-specific overlapping peptide pool *ex vivo* stimulation.

(C, D) Percentages of S- (C) and core-specific (D) IFN γ + CD8 T cells in the liver determined by intracellular cytokine staining after S- and core-specific overlapping peptide pool *ex vivo* stimulation.

Hash (#) symbols mark statistically significant differences compared to no vac group. Statistical analysis was performed by Kruskal-Wallis test with Dunn's multiple comparison correction or Mann-Whitney test: * $p < 0.05$; n.s.—not significant.

To summarize the studies, it was revealed that the induction of S-specific immune responses highly needs the assistance of a Th1/Th2-balanced adjuvant, whereas HBcAg is a potent immunogen that can induce immune responses without adjuvant.

TherVacB primed with Alum formulation induced high levels of anti-HBs and anti-HBc, and moderate S-specific CD4 T-cell responses. But it failed to elicit any S-specific CD8 T-cell responses that are the main effectors to clear the HBV-infected hepatocytes. By contrast, *TherVacB* primed with Th1/Th2-balanced LMQ or SMQ formulations stimulated vigorous HBV-specific CD4 and CD8 T-cell responses, apart from the generation of high levels of antibodies. Therefore, enabling induction of Th1-type immune responses should be included as a common criterium of adjuvant selection for therapeutic vaccines. Referring specifically to *TherVacB*, to generate neutralizing antibodies as well as T-cell responses simultaneously, external administration of HBsAg and HBcAg together with a Th1/Th2-balanced novel adjuvant is required.

2.3.3 Contribution of different T-cell subsets during the priming phase of *TherVacB*

In the studies described in section 2.3.1 and 2.3.2, it was presented that priming with HBsAg/HBcAg together with a Th1/Th2 adjuvant determines the efficacy of *TherVacB*. In this study, the role of different T-cell subsets in mediating the immune responses during the priming phase of *TherVacB* was explored. To address this question, antibody-mediated CD4 and CD8 T-cell depletion were employed *in vivo*.

In the first step, the depletion efficiency of anti-mouse CD4 (α CD4) GK1.5 and anti-mouse CD8 (α CD8) RmCD8.2 monoclonal antibodies (mAb) was assessed in naïve mice. For depletion of CD4 T cells, mice were injected intraperitoneally (i.p.) with 300 μ g and 150 μ g of GK1.5 mAb or relevant isotype IgG_{2b} mAb control two days and one day prior to the final analysis (Fig.2.42 A). For depletion of CD8 T cells, mice received a single dose of 50 μ g of RmCD8.2 mAb or relevant isotype control IgG_{2b} mAb i.p. one day prior to the final analysis (Fig.2.42 B).

One day after administration of depleting antibodies, the mice were sacrificed to analyze the depletion efficiency in blood, spleen, lymph nodes, and liver by flow cytometry. To avoid any antibody binding competition, the anti-CD4 mAb RM 4-5 and

anti-CD8 mAb 53-6.7 were used for the flow cytometry analysis, which recognize a different epitope on CD4 and CD8 than GK1.5 and RmCD8.2.

As the dot plots of the representative mice shown in Fig.2.42 C demonstrate, the efficiency of CD4 T-cell depletion was more than 99% in the blood, spleen, lymph nodes, and liver upon administration of α CD4 mAb. In contrast, the mice receiving the rat IgG_{2b} isotype control mAb displayed normal levels of CD4 expression in all tested organs, within the range of 25%–50% of CD45+ CD3+ positive population (Fig.2.42 C). Unlike the efficient CD4 T-cell depletion by the depleting mAb, CD8 T cells were somehow more resistant to mAb-mediated depletion, which was also found in other groups (Cross, 2019; Snook, 2014). As shown in Fig.2.42 D, more than 95% depletion of CD8 T cells was observed in the blood and liver of α CD8 mAb injected mice. However, in lymphoid organs spleen and lymph nodes, average CD8 T-cell depletion efficiency was around 95% and 80%, respectively (Fig.2.42 D). Therefore, it was not clear whether the CD8 T-cell depletion efficiency was sufficient to infer the role of CD8 T cells in the antiviral effects of *TherVacB*. When interpreting the results described below, overall low CD8 T-cell depletion efficiency in lymphoid organs should be considered. In addition, the mice receiving rat IgG_{2b} isotype control mAb displayed normal-range levels of CD8 expression in all tested organs.

Results

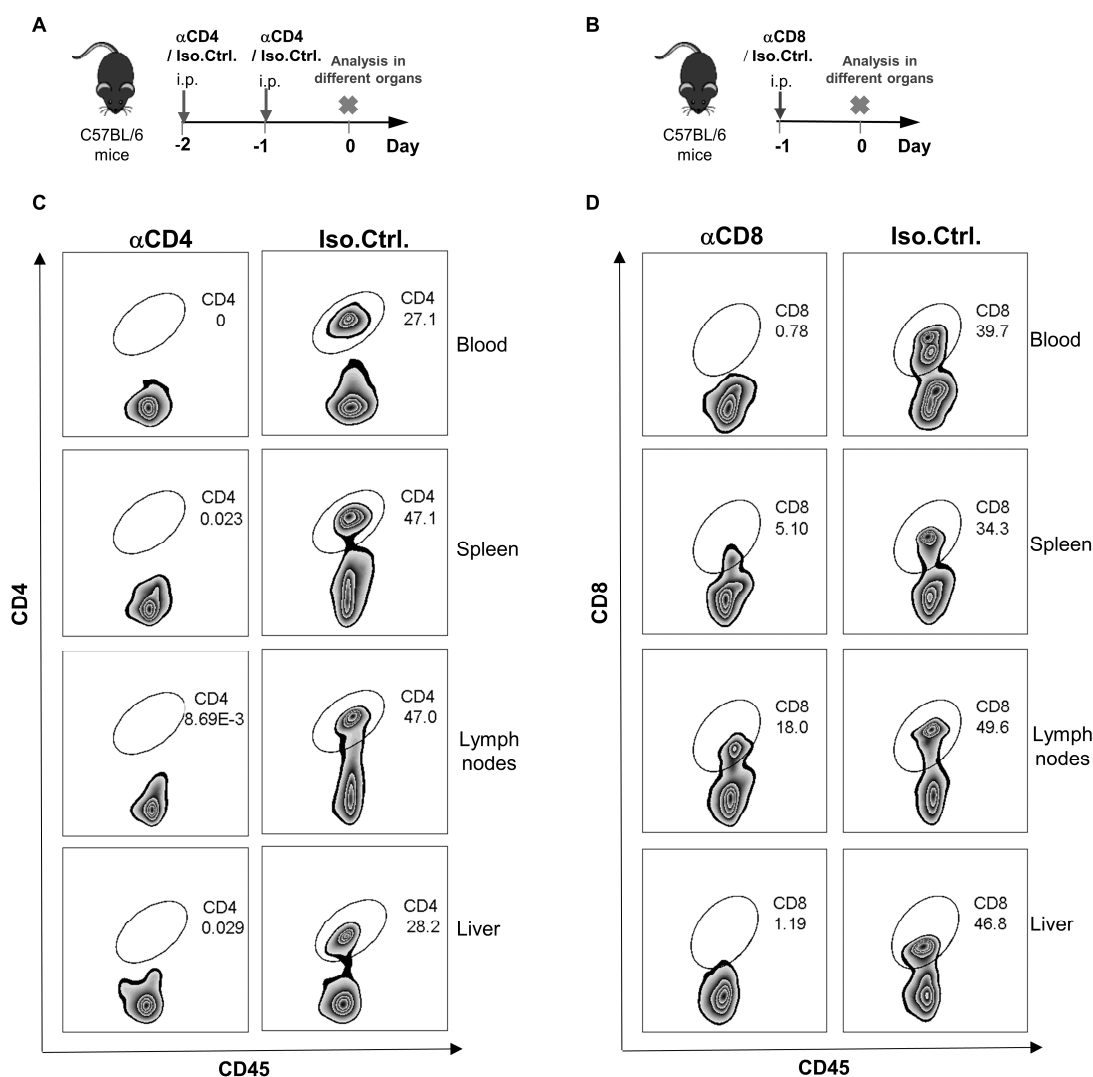


Fig.2.42 CD4 and CD8 T-cell depletion in different organs of naïve mice.

- (A) The experimental scheme of CD4 T-cell depletion. Mice were treated with 300 μ g and 150 μ g of anti-CD4 (α CD4) GK1.5 mAb or isotype rat IgG_{2b} control i.p. two days and one day prior to the analysis. One day after the mAb injection, the efficiency of T-cell depletion was assessed by flow cytometry with the lymphocytes from blood, spleen, lymph nodes, and liver.
- (B) The experimental scheme of CD8 T-cell depletion. Mice were treated with 50 μ g of anti-CD8 (α CD8) RmCD8.2 mAb or isotype rat IgG_{2b} control i.p. one day prior to the analysis. One day after the mAb injection, the efficiency of T-cell depletion was assessed by flow cytometry with the lymphocytes from blood, spleen, lymph nodes, and liver.
- (C) Exemplary dot plots of CD4 expression in the blood, spleen, lymph nodes, and liver of α CD4 injected and isotype control mAb treated mice. The cells were gated on CD45 and CD3. Presented values show the percentage of CD4 T cells in the CD45+ T-cell population.
- (D) Exemplary dot plots of CD8 expression in the blood, spleen, lymph nodes, and liver of α CD8 injected and isotype control mAb treated mice. The cells were gated on CD45 and CD3. Presented values show the percentage of CD8 T cells in the CD45+ T-cell population.

To demonstrate the role of different T-cell subsets during the priming phase of *TherVacB*, the T-cell subset depletion and *TherVacB* were applied in AAV-HBV mice. CD4 and CD8 T-cell depletion was conducted one day prior and during the protein prime immunizations at week 0 and week 2. The protein vaccine consisted of HBsAg/HBcAg adjuvanted with LMQ (Fig.2.43 A).

To ensure CD4 and CD8 T cells were only specifically depleted during the priming phase of *TherVacB*, the levels of CD4 and CD8 T cells in the blood of the mice were monitored during the experiment and compared to the levels in the isotype IgG treated mice. After the treatment with depleting mAbs, the CD4 and CD8 T-cell numbers rapidly decreased in the blood of the mice. Even two weeks after the initial depletion, the levels of CD4 and CD8 T cells only recovered to around 25% compared to the values detected in the isotype IgG treated mice at week 2. Over time, the recovery rate of peripheral CD4 and CD8 T cells displayed an increasing trend. At week 6, CD4 and CD8 T-cell numbers in the depleted mice were replenished to more than 75% of the levels in isotype IgG treated mice, which was considered as the functional recovery of CD4 and CD8 T cells *in vivo* (Fig.2.43 B and C). The mice were then boosted with MVA-core and MVA-S at week 6. Afterwards, the mice were monitored for six more weeks to study the long-term effects of T-cell subset depletion on the priming phase of *TherVacB*. At week 12, the mice were sacrificed to perform the final analysis in the liver, spleen, and serum (Fig.2.43 A).

Results

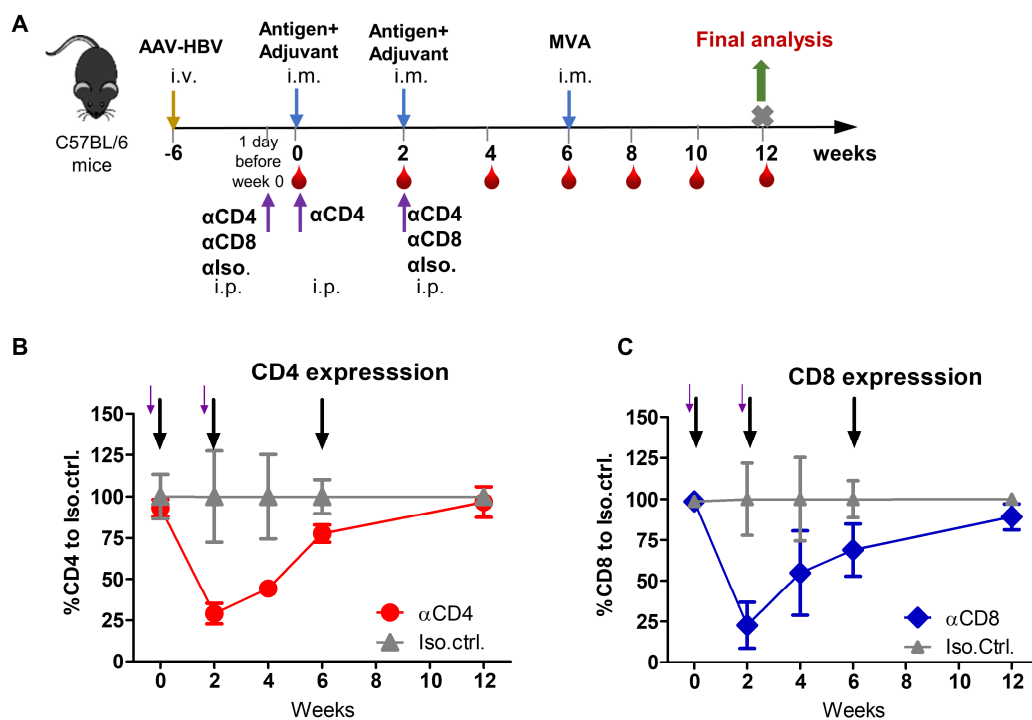


Fig.2.43 Experimental scheme and monitoring of CD4 and CD8 T-cell counts after depletion during *TherVacB* in AAV-HBV mice.

(A) Experimental scheme of the study. After the establishment of persistent HBV replication, mice were i.p. injected with depleting mAbs before the first and second immunization. On the first day of week 0 and week 2, the mice were immunized with LMQ adjuvanted antigens. The mice were boosted with MVA-core/MVA-S immunization at week 6. At week 12, the mice were sacrificed to perform the final analysis in the liver, spleen, and serum. During the entire experimental process, the levels of CD4 and CD8 T cells in the blood were monitored by flow cytometry analysis; the levels of HBsAg and HBeAg in the serum were also checked every two weeks.

(B, C) Levels of CD4 (B) and CD8 (C) T cells during the experimental process in murine blood. The levels of CD4 and CD8 T cells in blood were normalized to the levels in the isotype IgG treated mice. Black arrows show the time points of vaccination. Purple arrows show the time points of depleting antibody injections.

In the first step, the impact of CD4 and CD8 T-cell depletion on the *TherVacB*-mediated antigen decrease and antibody generation was assessed in the serum of mice at week 12.

In the isotype IgG control as well as α CD8 mAb treatment groups, both serum HBsAg and HBeAg exhibited significant decreases after *TherVacB* immunization with LMQ formulation. By contrast, when CD4 T cells were depleted before the first and second protein priming of *TherVacB*, the levels of HBsAg and HBeAg remained stable compared to the baseline at week 0. This implied that *TherVacB*-mediated antigen

decrease during the priming phase was impaired by CD4 T-cell depletion but not by CD8 T cell depletion (Fig.2.44 A and B). Consistent with the impaired antigen decrease, *TherVacB* immunization of the CD4-depleted mice resulted in a significant reduction of anti-HBs and anti-HBc in comparison to immunization of the control mice ($p < 0.05$). In contrast, the levels of anti-HBs and anti-HBc in the CD8-depleted mice immunized with *TherVacB* were comparable to the isotype IgG controls. This demonstrated the important role of CD4 T cells in antibody production during the priming phase of *TherVacB* (Fig.2.44 C and D), but also in overall antiviral efficacy of *TherVacB*.

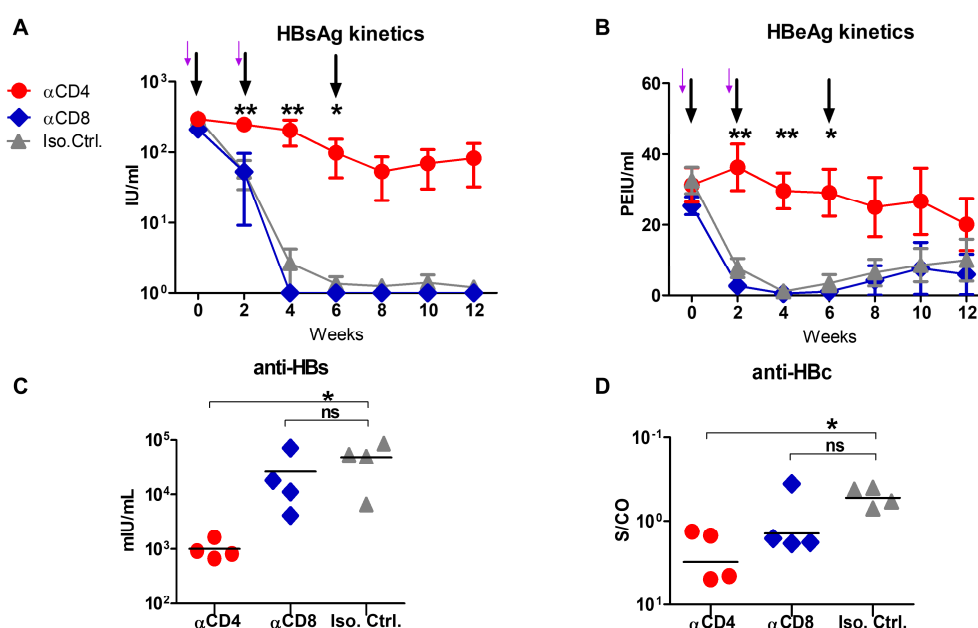


Fig.2.44 Antigen kinetics and antibody responses after depletion of CD4 or CD8 T cells during the priming phase of *TherVacB* in AAV-HBV mice.

(A, B) Time kinetics of serum HBsAg (A) and HBeAg (B) levels throughout the experiment.

Black arrows show the time points of vaccination. Purple arrows show the time points of depleting antibody injections.

(C, D) The levels of anti-HBs (C) and anti-HBc (D) antibodies were detected in the serum of immunized mice at the endpoint.

Statistical analysis was performed by 2-way ENOVA or Kruskal-Wallis test with Dunn's multiple comparison correction or Mann-Whitney test: * $p < 0.05$. n.s.—not significant.

At week 12, the impact of CD4 and CD8 T-cell depletion during the priming phase of *TherVacB* on vaccine-induced T-cell responses was analyzed by intracellular IFN γ staining of LALs with S- and core-specific peptide pools overnight stimulation.

Results

With CD4 T-cell depletion during the priming phase of *TherVacB*, immunization with *TherVacB* did not elicit any S-specific CD4 T-cell responses at week 12, when the depleted T cells fully recovered to similar levels as the isotype control group. *TherVacB* immunization of CD8-depleted mice also showed impaired S-specific CD4 T-cell responses, in which the mean percentage of IFN γ + S-specific CD4 T cells was only 0.75%. Concerning the isotype IgG treatment group, the magnitude of S-specific CD4 T-cell responses induced by *TherVacB* was much stronger than that in the CD4 and CD8 T-cell depletion groups. However, the response was not as high as previously demonstrated for standard *TherVacB* immunization, which could be related to the isotype IgG injection (Fig.2.45 A). As shown previously, core-specific CD4 T-cell responses were not detectable in any group at the analyzed time point (Fig.2.45 B). Regarding *TherVacB*-induced CD8 T-cell responses, *TherVacB* immunization of CD4-depleted mice stimulated significantly lower levels of IFN γ + S-specific CD8 T cells compared to those in the CD8-depleted mice ($p < 0.05$) (Fig.2.45 C). Core-specific CD8 T-cell responses showed a similar trend, with lower responses observed in the mice with CD4 T-cell depletion (Fig.2.45 D). This implied an important role of efficient CD4 T cell priming in the induction of HBV-specific CD8 T-cell responses. Concerning the isotype IgG treatment group, very weak S- and core-specific CD8 T-cell responses were detected. The reason could be that the repeated application of isotype rat IgG leads to a mouse anti-rat IgG response (Arora, 2006).

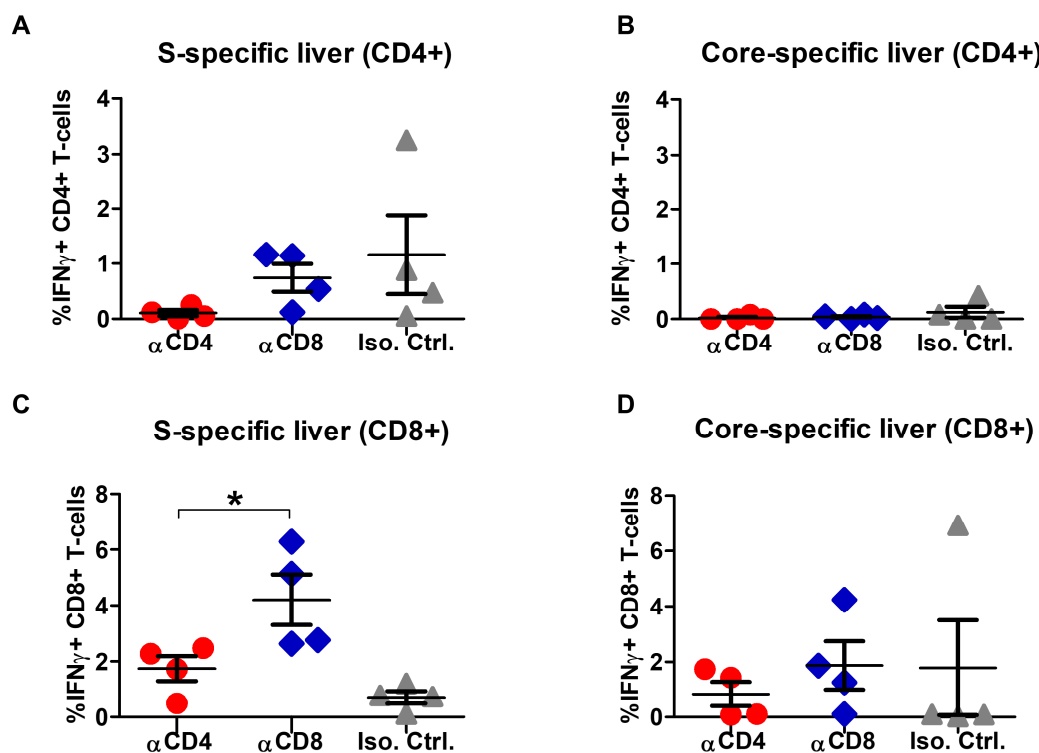


Fig.2.45 T-cell responses after CD4 and CD8 T-cell depletion during the priming of *TherVacB* in AAV-HBV mice.

(A, B) Percentages of intrahepatic S- (A) and core-specific (B) IFN γ + CD4 T cells were determined by intracellular cytokine staining after S- and core-specific peptide pool *ex vivo* stimulation.

(C, D) Percentages of intrahepatic S- (C) and core-specific (D) IFN γ + CD8 T cells were determined by intracellular cytokine staining after S- and core-specific peptide pool *ex vivo* stimulation.

Statistical analysis was performed by Kruskal-Wallis test with Dunn's multiple comparison correction or Mann-Whitney test: * $p < 0.05$.

Taken together, the findings suggest that *TherVacB*-mediated antibody and T-cell response induction, as well as HBV antigen decrease, could be impaired by the CD4 T-cell depletion during the priming phase of *TherVacB*.

To summarize the studies in this chapter, external administration of recombinant HBsAg and HBcAg, together with a Th1/Th2-balanced adjuvant is critical to induce both neutralizing antibodies and T-cell responses against HBV, which also strongly determines the overall efficacy of *TherVacB* regimen. Moreover, CD4 T cells induced during the priming phase of *TherVacB* are the key T-cell subset that contributes to

Results

TherVacB-mediated immune responses and antiviral efficacy against persistent HBV replication.

2.4 Investigation of novel viral vector to improve the boost of *TherVacB*

In the *TherVacB* strategy, the boost immunization with the recombinant MVA expressing HBV antigens is one of the critical steps to activate strong HBV-specific T-cell responses and break HBV-specific immune tolerance in persistent HBV replication mouse models. While MVA has been proven safe and displayed excellent immunogenicity profiles in numerous vaccine studies (Volz and Sutter, 2017; Acres and Bonnefoy, 2008), induction of immunity against the MVA vector itself can be a drawback. The dominant MVA-specific immune responses can significantly decrease the efficacy of additional MVA vaccination. Therefore, it is necessary to explore novel viral vectors, which can be applied repetitively, to further boost the immune responses elicited by the *TherVacB* strategy.

In previous work of Prof. von Laer's lab, it has been reported that replication-competent VSV pseudotyped with the glycoprotein of LCMV, termed VSV-GP, can be repetitively applied without losing vaccine efficacy (Tober, 2014). As an innovative platform, VSV-GP has the potential to be used for priming as the substitute of protein, or for boosting as the substitute of MVA. To investigate this novel VSV-GP for the *TherVacB* regimen, the following experiments aimed at the construction of novel recombinant VSV-GP-HBs/c expressing simultaneously HBsAg and HBcAg, and the immunogenicity evaluation of VSV-GP-HBs/c in wild-type and AAV-HBV mice.

2.4.1 Construction of VSV-GP vector encoding HBsAg and HBcAg

Since both S- and core-specific immune responses, correlated with profound antiviral effects of *TherVacB*, the sequences of both antigens were simultaneously inserted into a single VSV-GP vector. A P2A sequence was inserted between HBsAg and HBcAg sequences to allow the equimolar expression of both proteins.

The first step was to clone the genes of interest into VSV-GP genomic plasmid (pVSV-GP). The HBsAg-P2A-HBcAg (HBs/c) cassette was inserted into position 5 in the pVSV-GP between the GP and L genes. To this purpose, the luciferase gene on position 5 of pVSV-GP variant T436 was removed by the XhoI and NheI restriction

Results

enzyme digestion. Subsequently, the HBs/c insert was cleaved out of the pVAX1 plasmid by using the same restriction enzymes and then ligated into the XhoI/NheI site of pVSV-GP vector to obtain pVSV-GP-HBs/c (Fig.2.46 A).

The successful insertion of HBs/c into pVSV-GP was proven by XhoI/NheI digestion. The characteristic band of 1354 bp, corresponding to HBs/c cassette, was visualized on the agarose gel (Fig.2.46 B). Additionally, the nucleic acid sequence of pVSV-GP-HBs/c was verified by DNA sequencing.

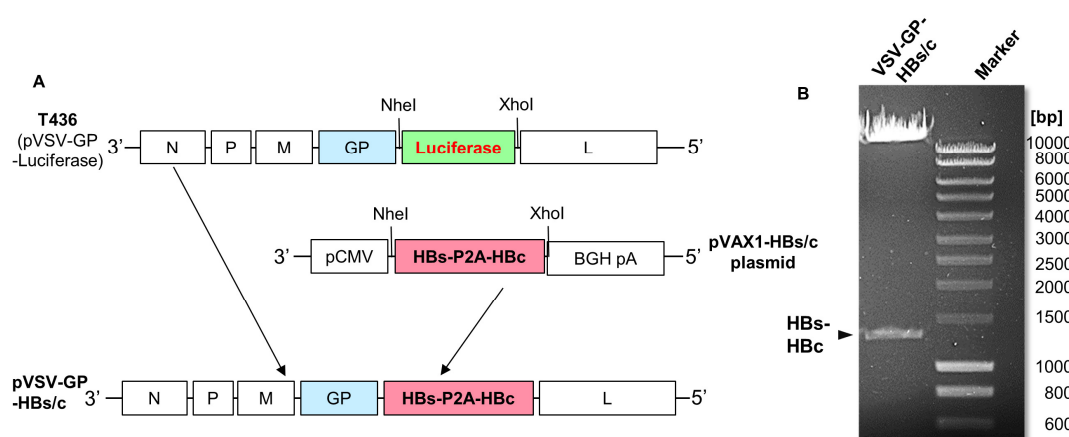


Fig.2.46 Cloning strategy and control digestion of pVSV-GP encoding HBsAg and HBcAg.

(A) Scheme of pVSV-GP cloning strategy. The HBs/c cassette was inserted into position 5 in the VSV-GP genomic plasmid between GP and L genes. The luciferase gene on position 5 of pVSV-GP variant T436 was removed by XhoI/NheI digestion and HBs/c insert was cleaved out of the pVAX1 plasmid by the identical enzymes following insertion into the pVSV-GP vector.

(B) Control digestion of pVSV-GP-HBs/c DNA. 1 μ g of DNA was digested with XhoI and NheI restriction enzymes for 1h at 37 °C and visualized on 1% agarose gel containing Roti-GelStain. The arrow shows the HBs/c corresponding band.

In the next step, the recombinant negative-strand RNA VSV-GP virus was rescued based on the reverse genetics system (Marzi, 2011). Briefly, 293T cells were simultaneously transfected with the following plasmids: full-length genome plasmid pVSV-GP-HBs/c; plasmids expressing the proteins needed for VSV replication, nucleoprotein (N), phosphoprotein (P), matrix protein (M), and original VSV G protein; and the plasmid expressing the bacteriophage T7 polymerase. The co-transfection resulted in viral transcription, protein expression, genome replication, and production

of recombinant VSV-GP particles that encoded for HBsAg and HBcAg. Afterwards, the newly rescued virus was passaged and plaque-purified for large-scale production.

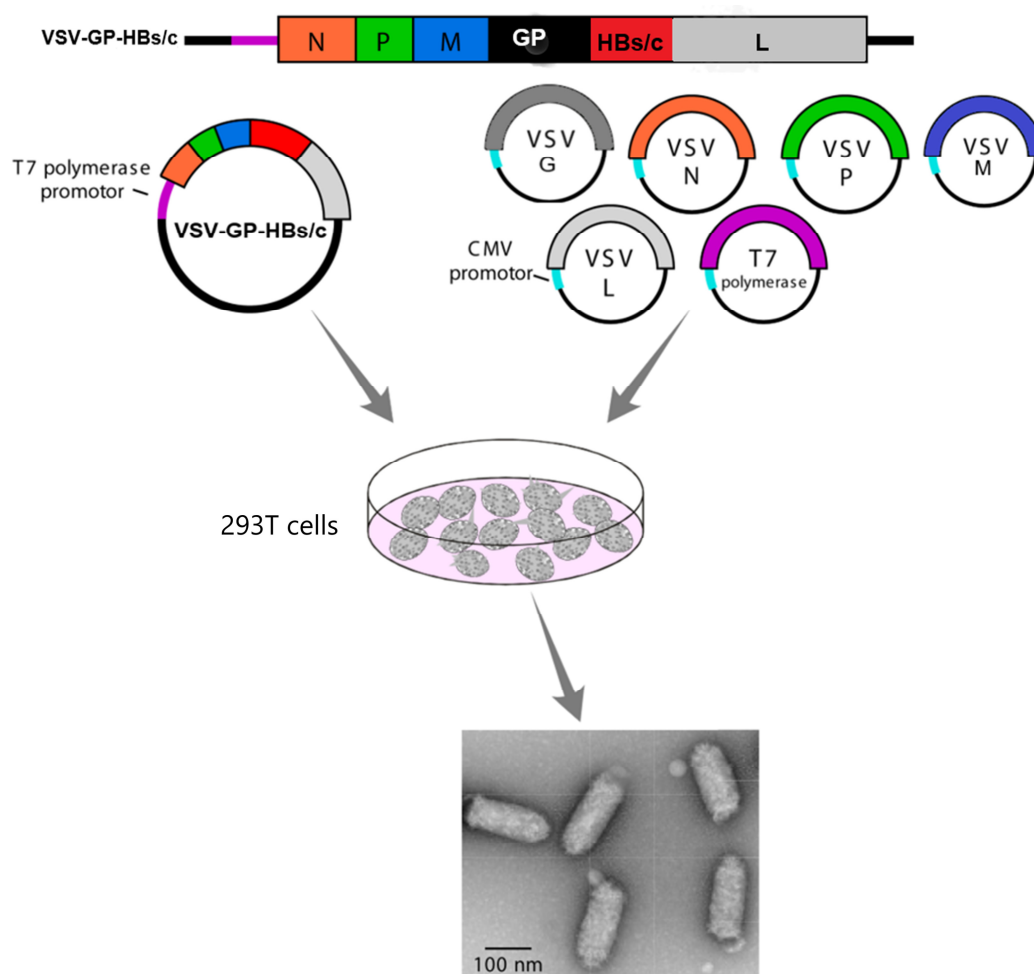


Fig.2.47 Scheme of recombinant VSV-GP virus generation.

The VSV genomic plasmid pVSV-GP-HBs/c together with expression plasmids for VSV replication (N, P, M, G, T7 polymerase) were transfected into 293T cells. Following the incubation of 48 – 72 hours, VSV-GP-HBs/c particles were harvested and purified. Electron microscopy shows the morphology of the rVSV/EBOV-GP virus as an example. The scheme was adapted based on Marzi, 2011.

2.4.2 Confirmation of HBsAg and HBcAg expression in the recombinant VSV-GP-HBs/c

After the successful construction of the recombinant VSV-GP-HBs/c, the proper expression of HBsAg and HBcAg from the vector was verified by Western blot analysis, immunofluorescence staining, and the immunoassays.

Results

In the first step, BHK-21 cells were infected with 0.1 MOI VSV-GP-HBs/c or 'empty' VSV-GP vector for 40 hours, when the infected cells were not yet lysed by the VSV-GP virus. Then, the cell lysates were harvested for Western blot analysis. The BHK-21 cells under the same culture conditions but without virus infection served as a mock control. The expression of both HBsAg and HBcAg was specifically detected in the lysates of VSV-GP-HBs/c infected BHK-21 cells. By contrast, neither HBsAg nor HBcAg were detected in the lysates of mock and 'empty' VSV-GP infected cells. In addition, the expression of the 'housekeeping' protein tubulin was comparable in the cell lysates of all three groups, indicating the comparable protein content in each lane of the gel (Fig.2.48 A).

Furthermore, the expression of HBsAg and HBcAg in the virus-infected cells was also confirmed by immunofluorescence staining of 'empty' VSV-GP and VSV-GP-HBs/c infected BHK-21 cells. Both HBsAg and HBcAg were visualized by the immunofluorescence staining of VSV-GP-HBs/c infected BHK-21 cells (Fig.2.48 B, upper panels). In the cells infected with 'empty' VSV-GP, neither HBsAg nor HBcAg was detectable (Fig.2.48 B, lower panels).

To explore whether the HBsAg and HBcAg encoded by VSV-GP-HBs/c were secreted from the infected cells, the expression of HBsAg and HBcAg was analyzed in both cell lysate and supernatant of BHK-21 cells 40 hours post-infection. Cell lysate and supernatant of 'empty' VSV-GP infected cells served as controls. Since HBeAg is encoded by the same open reading frame as HBcAg (Lamontagne, 2016), the detection of HBcAg expression was performed by the diagnostic detection of HBeAg, which correlates with the level of HBcAg expression. HBsAg or HBcAg expression was detected neither in cell lysates nor in the supernatant of 'empty' VSV-GP infected cells (Fig.2.48 C). In the VSV-GP-HBs/c infected cells, the expression of HBsAg was mostly detected in the cell lysates, but not in the supernatant, suggesting that HBsAg remained in the virus-infected cells (Fig.2.48 C, left). The detection of HBeAg, as an indirect method to confirm HBcAg expression, displayed positive signals in both cell lysates and supernatant of VSV-GP-HBs/c infected cells, indicating that the cleavage of P2A linker between two antigens could perform properly (Fig.2.48 C, right).

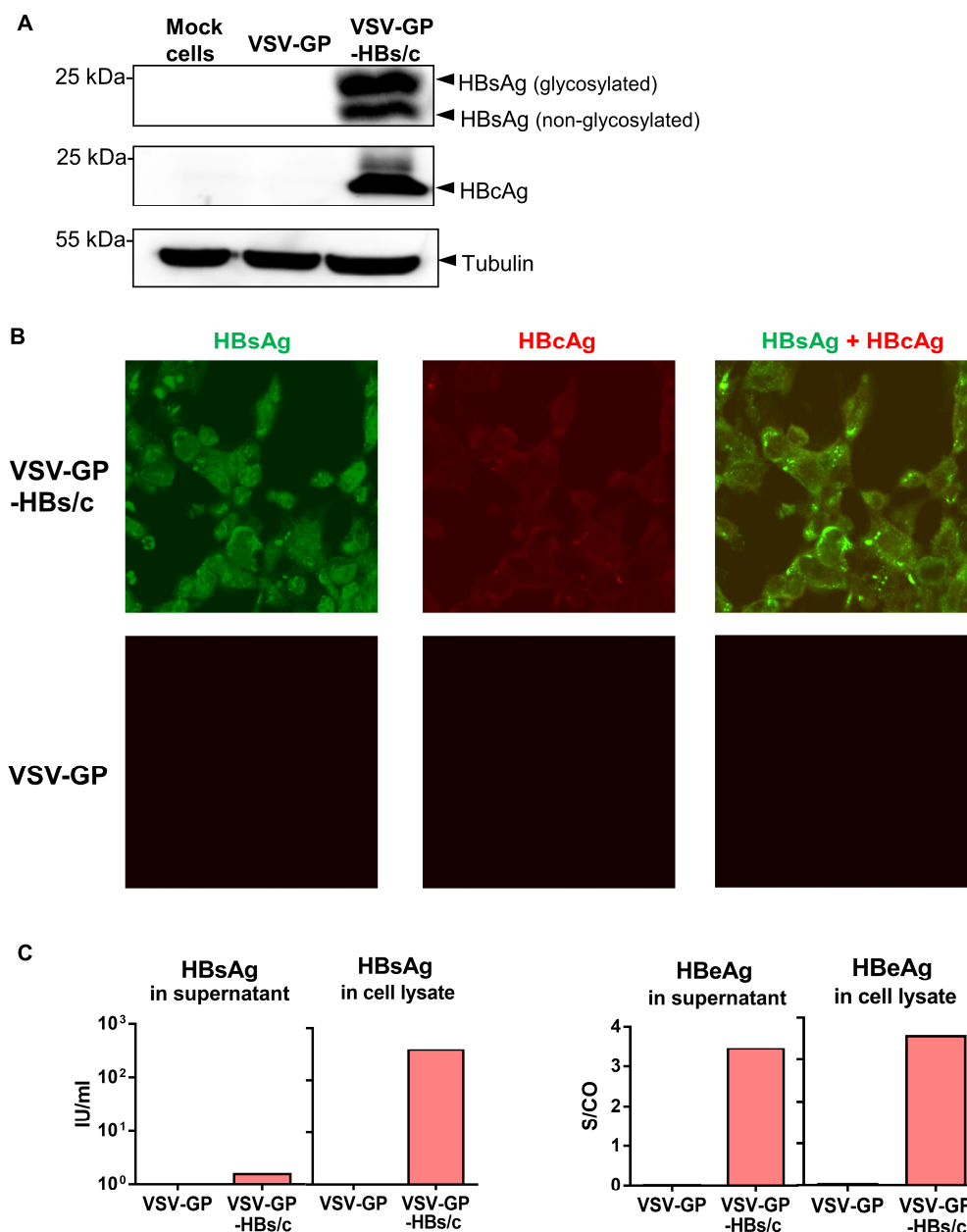


Fig.2.48 HBsAg and HBeAg expression in BHK-21 cells after VSV-GP-HBs/c infection.

After BHK-21 cells were infected with 0.1 MOI VSV-GP-HBs/c or 'empty' VSV-GP vector and cultured for 40 hours, the cell lysates and supernatant were harvested.

(A) Western blot analysis of HBsAg, HBeAg, and tubulin with the lysates of mock cells, VSV-GP and VSV-GP-HBs/c infected cells. Detection was performed by HBsAg-specific monoclonal antibody (mAb) HB1, HBeAg-specific mAb 8C9, and commercial Tubulin mAb, and then peroxidase-coupled secondary antibodies.

(B) Immunofluorescence staining of HBsAg and HBeAg in VSV-GP and VSV-GP-HBs/c infected cells. Cells were stained with HB1 mAb and DAKO polyclonal Ab, and then Alexa Fluor 647- and Alexa Fluor 594-coupled secondary antibodies for HBsAg (green) and HBeAg (red), respectively.

(C) The levels of HBsAg and HBeAg (HBeAg) were detected with the lysates and supernatant of VSV-GP and VSV-GP-HBs/c infected cells

Results

The recombinant VSV-GP-HBs/c was successfully generated. Moreover, the proper expression of protein HBsAg and HBcAg from VSV-GP-HBs/c vector was confirmed by various assays.

2.4.3 First immunogenicity trial of VSV-GP-HBs/c vector in wild-type C57BL/6 mice

To initially explore the VSV-GP-HBs/c immunogenicity *in vivo*, wild-type C57BL/6 mice were immunized with 10^7 TCID₅₀ of either VSV-GP or VSV-GP-HBs/c intramuscularly at week 0. The mice were sacrificed to analyze the antibody and T-cell responses in murine serum and spleen at week 1 (Fig.2.49 A).

Detection of anti-HBs and anti-HBc in the serum of mice was performed employing the Architect™ and BEP III platforms, respectively. Neither anti-HBs nor anti-HBc were detectable in mice immunized with either VSV-GP or VSV-GP-HBs/c. This might be due to the fact that the viral vector vaccines are not as good as protein-based vaccines at inducing antibodies in a short period.

To compare the HBV- and VSV-specific CD8 T-cell responses induced by immunization with VSV-GP and VSV-GP-HBs/c, intracellular IFN γ staining of peptide-stimulated splenocytes of immunized mice was performed.

The frequencies of core-specific IFN γ + CD8 T cells determined in the spleens of mice vaccinated with VSV-GP-HBs/c were significantly higher compared to those in mice immunized with VSV-GP ($p < 0.05$) (Fig.2.49 D). The mean percentages of S- and core-specific IFN γ + CD8 T cells were around 0.1% for the VSV-GP-HBs/c vaccinated mice, which is considered rather low (Fig.2.49 C and D). Immunization with VSV-GP and VSV-GP-HBs/c induced comparable VSV-specific CD8 T-cell responses (Fig.2.49 B), indicating that the genetic modification of recombinant VSV-GP-HBs/c resulted in functional VSV particles.

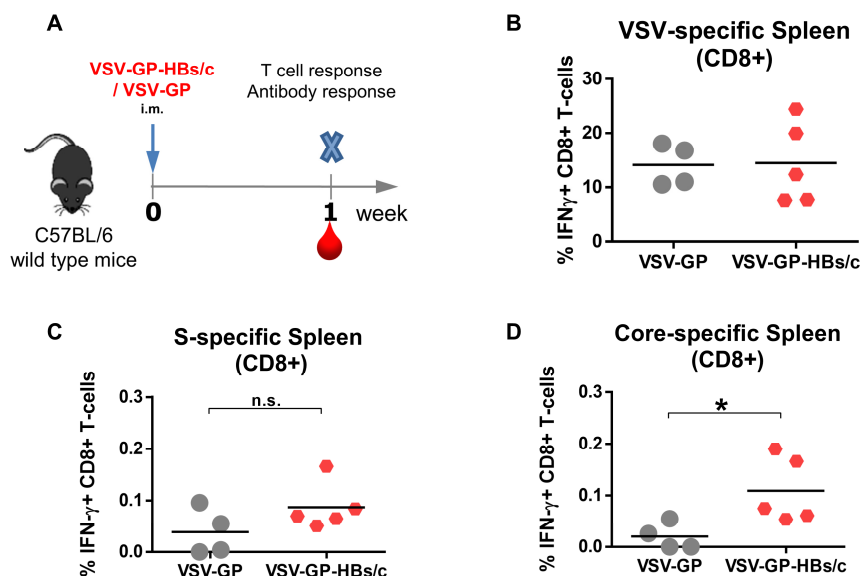


Fig.2.49 First immunogenicity trial of VSV-GP-HBs/c in wild-type C57BL/6 mice.

(A) Immunization scheme. At week 0, wild-type mice were immunized with either VSV-GP or the same amount of VSV-GP-HBs/c i.m. At week 1, the mice were sacrificed to analyze the antibody and T-cell responses in murine serum and spleen.

(B-D) Percentages of VSV- (B), S- (C), and core-specific (D) IFN γ + CD8 T cells in splenocytes determined by intracellular cytokine staining after VSV-specific NP52 epitope, S-, and core-specific overlapping peptide pools *ex vivo* stimulation.

Statistical analysis was performed by Mann-Whitney test: * $p < 0.05$; n.s.—not significant.

Taken together, the results indicate that a single immunization with the novel VSV-GP-HBs/c vector was able to induce HBV-specific immune responses. Since the observed responses after the single immunization were comparatively low, heterologous prime-boost strategies with VSV-GP-HBs/c were investigated in the next step.

2.4.4 Evaluation of different heterologous prime-boost strategies with VSV-GP-HBs/c in wild-type C57BL/6 mice

To investigate the potency of VSV-GP-HBs/c vaccines in eliciting strong HBV-specific immune responses, different VSV-GP-HBs/c-based heterologous prime-boost immunization regimens were evaluated in wild-type C57BL/c mice.

To begin with, the VSV-GP-HBs/c vector was explored as an alternative viral vector for boosting in *TherVacB* strategy. The mice were immunized twice with c-di-AMP adjuvanted HBsAg/HBcAg in a two-week interval and boosted with VSV-GP-HBs/c

Results

vector two weeks after the second protein priming (Fig.2.50, group 2). The classical protein prime–MVA vector boost *TherVacB* strategy with MVA, which harbored the same HBs/c insert as VSV-GP-HBs/c, was used as a reference. (Fig.2.50, group 1). In addition, to explore the possibilities of employing viral vectors for priming, heterologous viral vector prime–viral vector boost strategies with MVA and VSV-GP were examined. Mice were primed with MVA-HBs/c or VSV-GP-HBs/c at week 0 and boosted with either VSV-GP-HBs/c or MVA-HBs/c at week 4 (Fig.2.50, groups 3 and 4). One week after the last immunization, the mice were sacrificed to analyze the antibody responses in the murine serum and detect T-cell responses in the spleens of the mice (Fig.2.50).

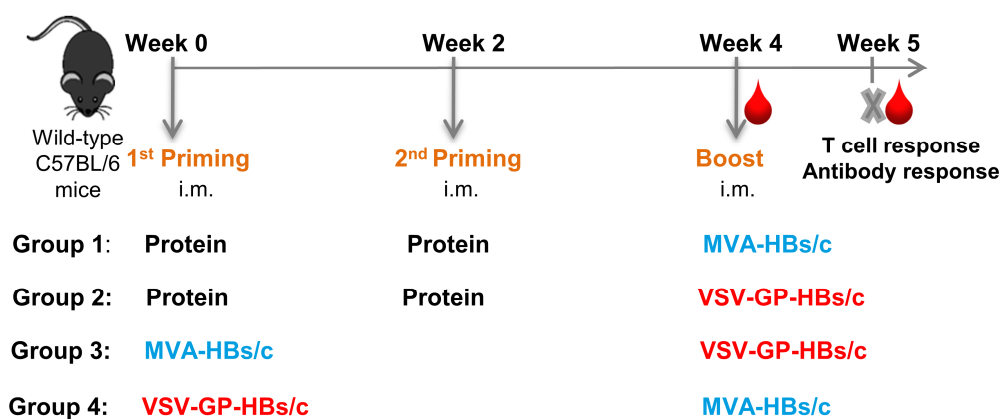


Fig.2.50 Immunization schemes of different heterologous prime-boost strategies with VSV-GP-HBs/c in wild-type C57BL/6 mice.

Mice in groups 1 and 2 were immunized with c-di-AMP adjuvanted HBsAg and HBcAg via i.m. at weeks 0 and 2. At week 4, intramuscular immunizations with MVA-HBs/c or VSV-GP-HBs/c, respectively, were used to boost the immune responses. Mice in groups 3 and 4 were immunized with MVA-HBs/c or VSV-GP-HBs/c at week 0 and boosted with VSV-GP-HBs/c or MVA-HBs/c at week 4. At week 5, the mice from all groups were sacrificed for antibody and T-cell response analysis.

The humoral immune response induced by the immunization with various regimens was evaluated by the detection of anti-HBs and anti-HBc in the murine serum one week after the last immunization.

Immunization of mice with all four regimens induced higher than 10^3 mIU/ml anti-HBs. Priming with protein tended to induce higher anti-HBs responses than priming with viral vectors. Moreover, the levels of anti-HBs in mice immunized with the protein/MVA regimen were significantly higher than those in mice immunized with the protein/VSV-

GP regimen ($p < 0.05$). This suggested that after protein priming, MVA-HBs/c could significantly boost antibody responses, whereas VSV-GP-HBs/c displayed only minor effects on anti-HBs levels. Concerning the regimens using viral vector for priming, the levels of anti-HBs in mice immunized with the MVA/VSV-GP regimen were comparable with those in mice immunized with the VSV-GP/MVA regimen (Fig.2.51 A). This implied that the immunization sequence of the viral vectors did not have an impact on antibody generation. In addition, immunization of mice with all four strategies elicited comparable anti-HBc responses that were markedly higher than the assay baseline of the negative control (Fig.2.51 B).

Comparison of S- and core-specific CD4 T-cell responses induced by the immunization with various regimens was performed by intracellular IFN γ staining of peptide-stimulated splenocytes isolated one week after the last immunization.

The magnitude of S-specific CD4 T-cell responses was comparable in the mice primed with either protein or MVA-HBs/c. By contrast, priming with VSV-GP-HBs/c elicited rather poor S-specific CD4 T-cell responses that were significantly lower than those in mice immunized with the protein/VSV-GP regimen ($p < 0.05$) (Fig.2.51 C).

The core-specific CD4 T-cell responses in mice primed with protein were significantly stronger than those in the mice primed with MVA-HBs/c or VSV-GP-HBs/c ($p < 0.05$) (Fig.2.51 D). This indicated that priming with protein is beneficial for the induction of core-specific CD4 T-cell responses.

Results

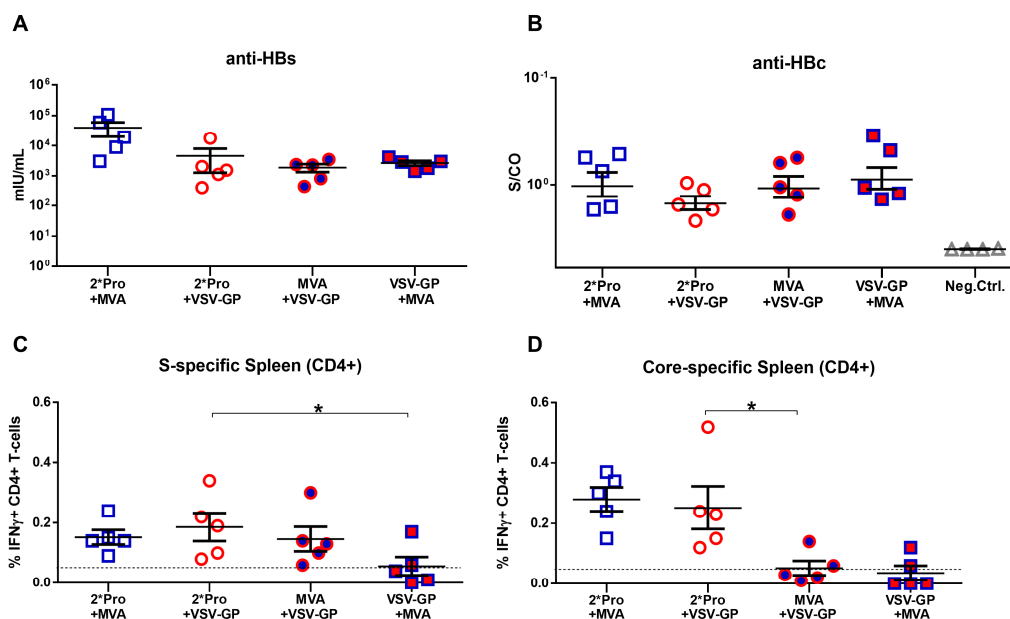


Fig.2.51 Antibody and CD4 T-cell responses induced by immunization with different heterologous prime-boost strategies with VSV-GP-HBs/c in wild-type C57BL/6 mice.

In the protein priming-based groups, mice were primed twice with adjuvanted HBsAg/HBcAg (2*Pro) and boosted with MVA-HBs/c (MVA) or VSV-GP-HBs/c (VSV-GP). In the viral vector-based groups, mice were both primed and boosted with MVA or VSV-GP.

(A, B) The levels of anti-HBs (A) and anti-HBc (B) were detected in the serum of immunized mice at the endpoint. The negative control of the anti-HBc immunoassay setting was included as a reference (B).

(C, D) Percentages of splenic S- and core-specific IFN γ + CD4 T cells determined by intracellular cytokine staining after S- and core-specific overlapping peptide pool *ex vivo* stimulation. Statistical analysis was performed by Kruskal-Wallis test with Dunn's multiple comparison correction or Mann-Whitney test: * $p < 0.05$.

The influence of the different vaccination regimes on the induction of CD8 T-cell responses was assessed by intracellular IFN γ and TNF α co-staining of splenocytes upon *ex vivo* peptide stimulation.

Immunization with protein priming-based regimens induced very strong S- and core-specific CD8 T-cell responses. There was no noticeable difference in the frequencies of S- and core-specific IFN γ + CD8 T cells between the protein/MVA and protein/VSV-GP groups. The magnitudes of S- and core-specific IFN γ + CD8 T-cell responses in the mice primed with viral vector were significantly lower compared to those in the mice primed with protein ($p < 0.05$) (Fig.2.52 A and B).

To explore the multifunctionality of S- and core-specific CD8 T-cell responses, HBV-specific IFN γ ⁺ TNF α ⁺ double-positive CD8 T cells were analyzed. Consistent with the IFN γ ⁺ CD8 T-cell responses, vaccination of mice with protein priming-based regimens elicited high levels of IFN γ ⁺ TNF α ⁺ double-positive S- and core-specific CD8 T cells, which were significantly higher than those in the viral vector primed mice. In the two groups of mice primed with protein, boost immunization with VSV-GP-HBs/c displayed the tendency to induce higher percentages of IFN γ ⁺ TNF α ⁺ double-positive S- and core-specific CD8 T cells than MVA-HBs/c (Fig.2.52 C and D). This implied that immunization with VSV-GP-HBs/c was particularly effective in inducing multifunctional HBV-specific CD8 T cells.

Boost immunization of mice with VSV-GP-HBs/c elicited strong VSV-specific CD8 T-cell responses, especially in the mice that received the protein/VSV-GP regimen. Of note, no VSV-specific CD8 T-cell responses were detected at the endpoint in the mice primed with VSV-GP-HBs/c. This suggested that the immunity against the VSV-GP-HBs/c vector could become undetectable in a short period of time (Fig.2.52 E). Comparable MVA-specific CD8 T-cell responses were detected in the groups of mice boosted with MVA-HBs/c. Unlike the VSV-GP-HBs/c for priming, the MVA-specific responses were still detected in the mice primed with MVA-HBs/c (Fig.2.52 F).

Results

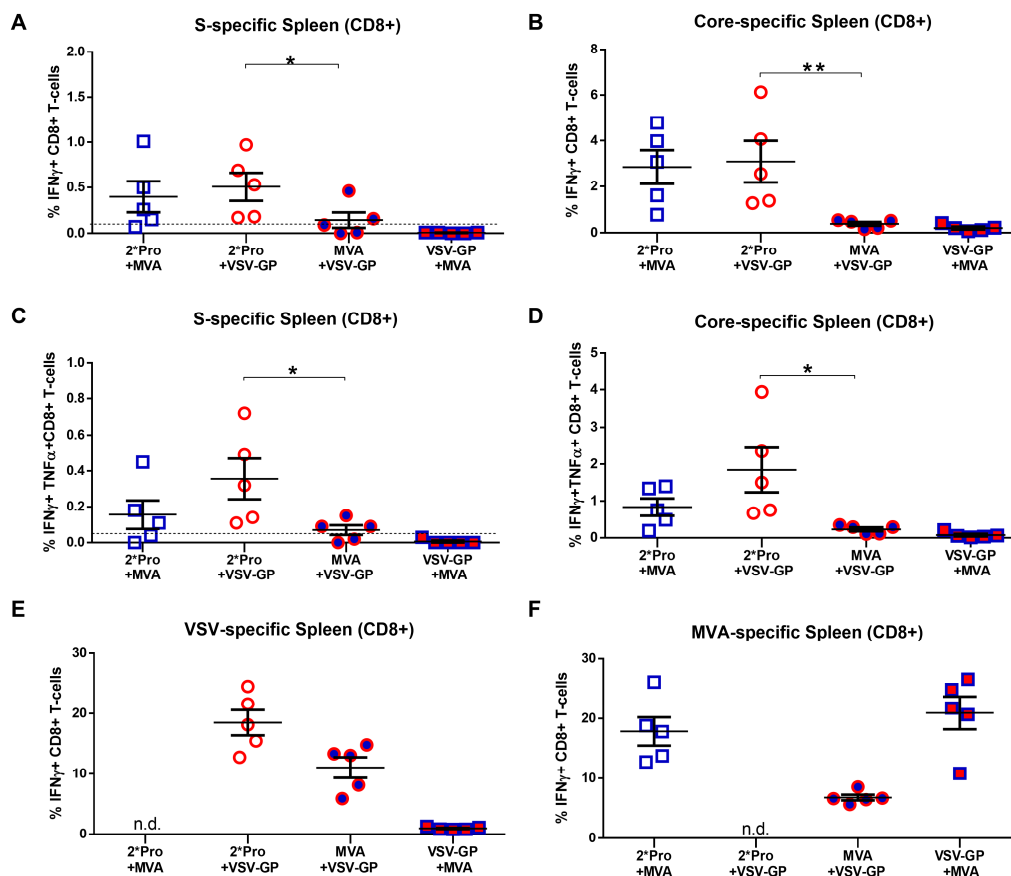


Fig.2.52 CD8 T-cell responses induced by immunization with different heterologous prime-boost strategies with VSV-GP-HBs/c in wild-type C57BL/6 mice.

(A, B) Percentages of MVA- (A) and VSV-specific (B) IFN γ + CD8 T cells in spleen determined by intracellular cytokine staining after MVA-specific B8R epitope peptide and VSV-specific NP52 epitope peptide *ex vivo* stimulation. n.d.—not detectable.

(C, D) Percentages of S- (C) and core-specific (D) IFN γ + CD8 T cells in spleen determined by intracellular cytokine staining after S-specific S208 epitope peptide and core-specific C93 epitope peptide *ex vivo* stimulation.

(E, F) Percentages of S- (E) and core-specific (F) IFN γ + TNF α + CD8 T cells in spleen determined by intracellular cytokine staining after S-specific S₂₀₈ epitope peptide and core-specific C₉₃ epitope peptide *ex vivo* stimulation.

Statistical analysis was performed by Kruskal-Wallis test with Dunn's multiple comparison correction or Mann-Whitney test: * $p < 0.05$, ** $p < 0.01$.

Since the neurotoxicity of the VSV vector is a safety concern during its application, the weight of the mice was monitored during the immunization process to determine the potential side effects of vaccination. Compared to the weight baseline at week 0, no obvious weight loss was observed in mice immunized with any of the four regimens (Fig.2.53). This gives evidence that the neurotoxicity of VSV could be abolished by pseudotyping the virus with the glycoprotein of LCMV (Miletic, 2004).

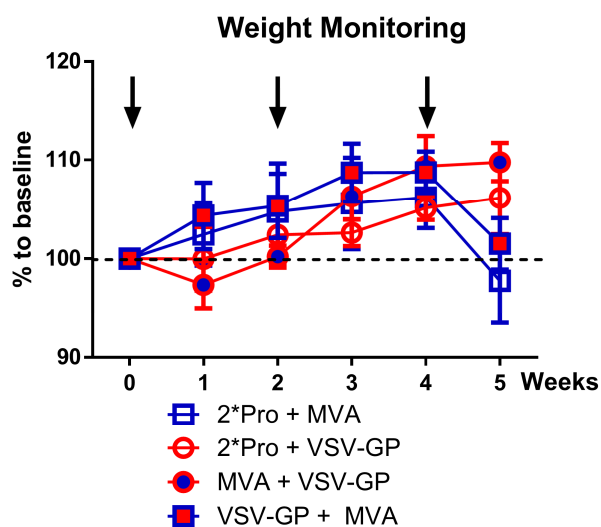


Fig.2.53 Weight monitoring of the wild-type C57BL/6 mice immunized with different heterologous prime-boost strategies.

Weight of the mice in every group was monitored every week and compared to the baseline at the start point of the experiment.

Arrows show the time points of vaccination.

Taken together, the results indicate that various heterologous prime-boost regimens with VSV-GP-HBs/c, especially the protein prime–VSV-GP-HBs/c boost regimen, were able to stimulate strong HBV-specific humoral and cellular immune responses in wild-type mice. Additionally, no obvious side effects were observed in mice immunized with VSV-GP-HBs/c-based regimens.

2.4.5 Evaluation of different heterologous prime-boost strategies with VSV-GP-HBs/c in AAV-HBV mice

To investigate the potency of VSV-GP-HBs/c vaccines to break HBV-specific immune tolerance, the immunogenicity of the most promising heterologous prime-boost strategies was evaluated in AAV-HBV mice in which persistent HBV replication was established.

Since the protein prime–VSV-GP vector boost regimen demonstrated encouraging results in wild-type mice, this regimen was further evaluated and compared with the classical *TherVacB* protein prime–MVA boost in AAV-HBV mice.

The AAV-HBV mice were immunized twice with c-di-AMP adjuvanted HBsAg/HBcAg in a two-week interval and boosted with MVA-HBs/c or VSV-GP-HBs/c two weeks after the second protein priming (Fig.2.54, groups 1 and 2). Additionally, to explore the possibility of replacing protein with the new VSV-GP vector for priming, one group of

Results

AAV-HBV mice was primed twice with VSV-GP-HBs/c vector in a two-week interval and boosted with MVA-HBs/c vector two weeks after the second priming (Fig.2.54, group 3). The non-vaccinated (no vac) AAV-HBV mice served as control (Fig.2.54, group 4). One week after the last immunization, the mice from all four groups were sacrificed to analyze the antibodies and antigen levels in the murine serum and detect T-cell responses in the livers and spleens of the mice (Fig.2.54).

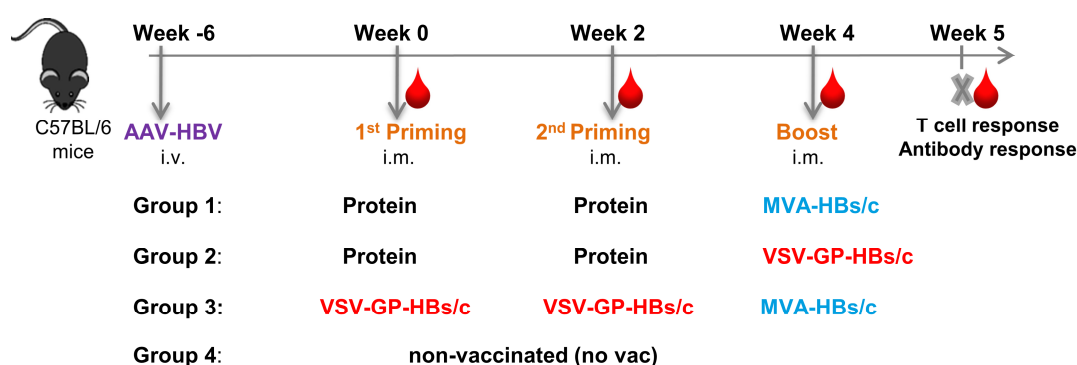


Fig.2.54 Immunization schemes of heterologous prime-boost strategies with VSV-GP-HBs/c in AAV-HBV mice.

C57BL/6 mice were infected with the AAV-HBV vector six weeks prior to the vaccination to establish the persistent HBV replication. Mice in groups 1 and 2 were immunized with c-di-AMP adjuvanted HBsAg and HBcAg via i.m. at weeks 0 and 2. At week 4, intramuscular immunizations of MVA-HBs/c for mice in group 1 and VSV-GP-HBs/c for mice in group 2 were used to boost the immune responses. Mice in group 3 were primed with VSV-GP-HBs/c at weeks 0 and 2 and boosted with MVA-HBs/c at week 4. At week 5, mice were sacrificed for the final analysis of the serum, liver, and spleen.

To investigate the effects of immunization with different regimens on antibody generation, the levels of anti-HBs and anti-HBc in the serum of AAV-HBV mice were determined one week after the last immunization.

Immunization of mice with protein priming-based regimens induced significantly higher levels of anti-HBs in comparison to immunization with the VSV-GP/MVA boost regimen ($p < 0.05$). In protein-primed mice, anti-HBs levels did not differ between MVA-HBs/c and VSV-GP-HBs/c boosted ones. As expected, the non-vaccinated control (no vac) mice did not generate any anti-HBs (Fig.2.55 A). The profile of anti-HBc revealed the same tendency as the anti-HBs profile. The levels of anti-HBc in the mice primed with

protein were remarkably higher than in the mice primed with VSV-GP-HBs/c vector (Fig.2.55 B).

Correlating with the strong antibody responses, the mice primed with protein displayed a profound reduction of serum HBsAg levels at week 5 ($p < 0.05$). The levels of serum HBsAg in the mice primed with VSV-GP-HBs/c vector only displayed a mild decrease compared to the baseline at week 0 (Fig.2.55 C).

A marked 50% decrease in serum HBeAg levels was detected in the mice immunized with protein/VSV-GP regimen at week 5. This implied increased efficacy of protein/VSV-GP regimen on the suppression of HBV replication. There was a moderate decrease of serum HBeAg in mice immunized with the other two regimens (Fig.2.55 D). In addition, in the serum of no vac mice, the levels of both HBsAg and HBeAg remained constant over the course of the experiment (Fig.2.55 C and D).

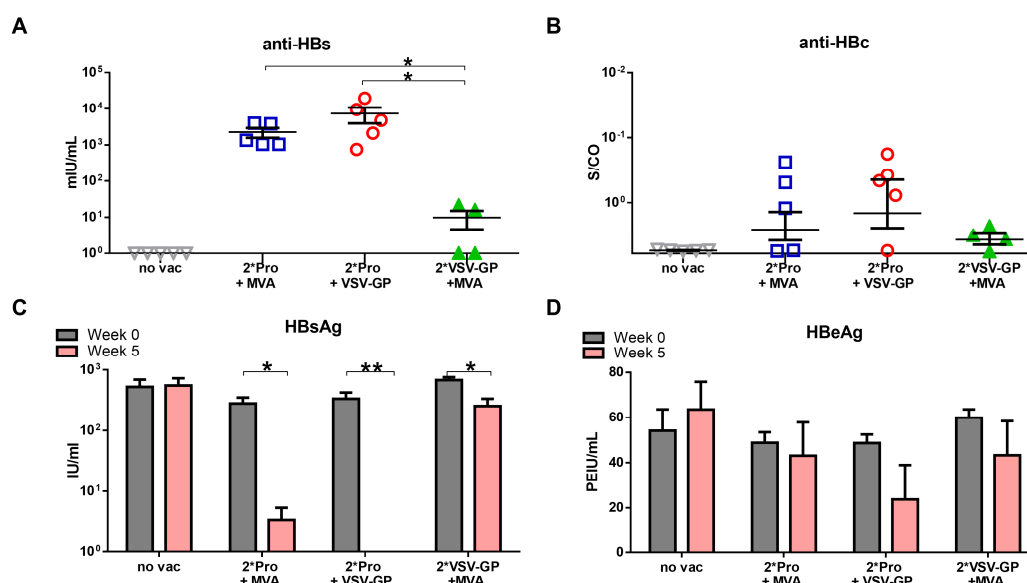


Fig.2.55 Antigen level alteration and antibody responses induced by heterologous prime-boost strategies with VSV-GP-HBs/c in AAV-HBV mice.

(A, B) The levels of anti-HBs (A) and anti-HBc (B) were detected in the serum of mice at week 5. (C, D) The levels of HBeAg (C) and HBsAg (D) were detected in the serum of mice at week 0 and week 5.

Statistical analysis was performed by Kruskal-Wallis test with Dunn's multiple comparison correction or Mann-Whitney test or Wilcoxon test: * $p < 0.05$, ** $p < 0.01$.

To assess whether these heterologous immunization strategies were able to break the immune tolerance against HBV, the evaluation of S- and core-specific CD4 and CD8

Results

T-cell responses was performed by intracellular IFN γ staining of peptide-stimulated LALs and splenocytes from immunized mice.

Immunization with protein prime-based regimens induced strong S-specific CD4 T-cell responses, especially immunization with the protein/MVA regimen. This confirmed the important role of protein priming in the induction of S-specific CD4 T-cell responses (Fig.2.56 A and C). In the two groups primed with protein, boost immunization with MVA-HBs/c induced higher percentages of S-specific IFN γ + CD4 T cells than boosting with VSV-GP-HBs/c. This implied that with protein priming, MVA-HBs/c had superior effects on the induction of S-specific CD4 T-cell responses than VSV-GP-HBs/c. S-specific IFN γ + CD4 T cells were undetectable in the liver and spleen of mice primed with VSV-GP-HBs/c. As shown previously, core-specific CD4 T-cell responses were not detectable in mice immunized with any regimen at the analyzed time point (Fig.2.56 B and D).

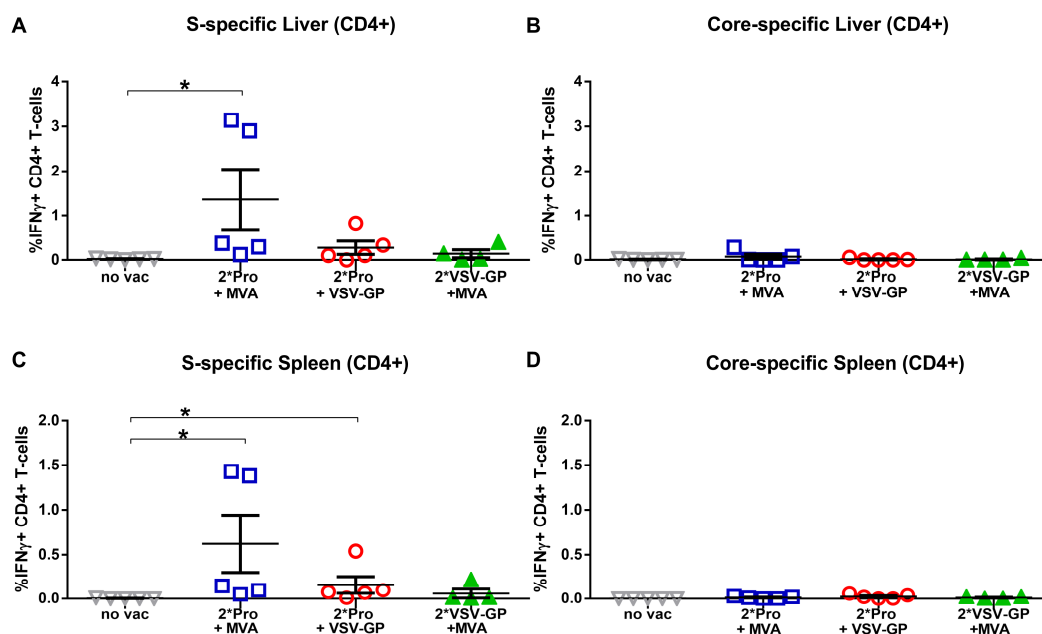


Fig.2.56 CD4 T-cell responses induced by heterologous prime-boost strategies with VSV-GP-HBs/c in AAV-HBV mice.

(A-D) Percentages of S- and core-specific IFN γ + CD4 T cells in the liver (A, B) and in the spleen (C, D) determined by intracellular cytokine staining after S- and core-specific overlapping peptide pools *ex vivo* re-stimulation.

Statistical analysis was performed by Kruskal-Wallis test with Dunn's multiple comparison correction or Mann-Whitney test: * $p < 0.05$.

Regarding the CD8 T-cell responses, the magnitudes of both intrahepatic and splenic S-specific IFN γ + CD8 T-cell responses in the mice primed with protein were very strong and were significantly higher than those in the no vac group ($p < 0.05$). In these two groups, boosting immunization with MVA-HBs/c exhibited the trend of inducing slightly stronger intrahepatic S-specific CD8 T-cell responses than boosting with VSV-GP-HBs/c. The frequencies of S-specific IFN γ + CD8 T cells in the mice primed with VSV-GP-HBs/c were rather low (Fig.2.57 A and B).

Consistent with S-specific CD8 T-cell responses, priming with protein stimulated high frequencies of intrahepatic core-specific IFN γ + CD8 T cells, and these frequencies were significantly higher than those in the no vac group ($p < 0.05$). In mice primed with protein, there was no obvious difference in intrahepatic core-specific CD8 T-cell responses between the MVA-HBs/c and the VSV-GP-HBs/c treated mice. However, the magnitude of splenic core-specific but not that of S-specific IFN γ + CD8 T-cell responses was noticeably higher in the mice boosted with VSV-GP-HBs/c. Priming with VSV-GP-HBs/c elicited moderate frequencies of core-specific IFN γ + CD8 T cells in the liver, but no responses in the spleen (Fig.2.57 C and D).

Results

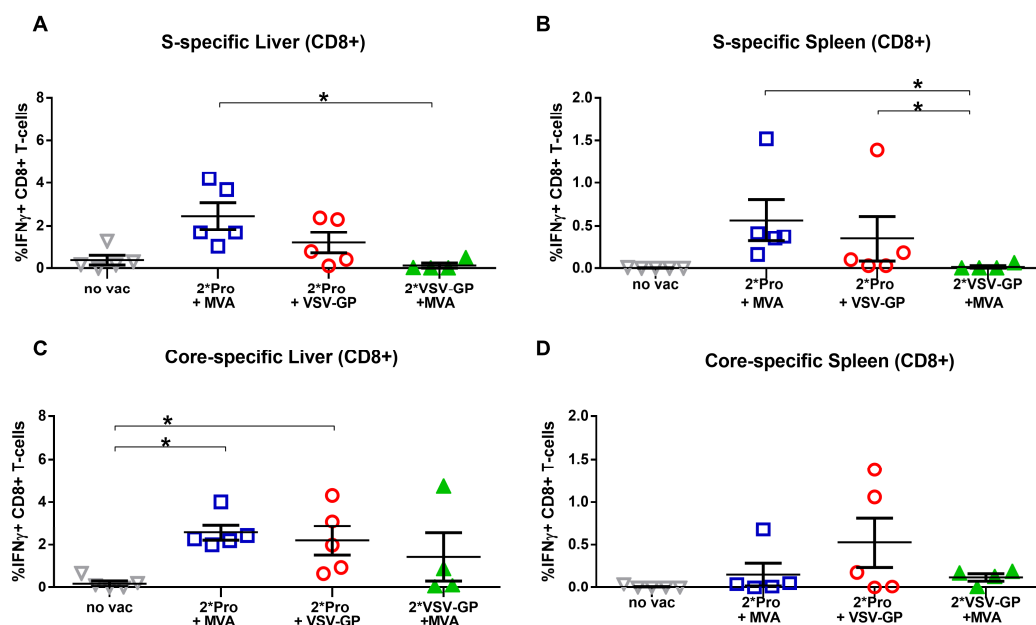


Fig.2.57 CD8 T-cell response analysis after heterologous prime-boost immunization with VSV-GP-HBs/c in AAV-HBV mice.

(A-D) Percentages of S- and core-specific IFN γ + CD8 T cells determined by intracellular cytokine staining of LALs (A, C) and splenocytes (B, D) after S-specific peptide pool *ex vivo* stimulation.

Statistical analysis was performed by Kruskal-Wallis test with Dunn's multiple comparison correction or Mann-Whitney test: * $p < 0.05$.

Immunization of mice using the VSV-GP-HBs/c prime–MVA-HBs/c boost regimen resulted in weak HBV-specific antibody and T-cell responses. Interestingly, the protein prime–VSV-GP vector boost immunization regimen induced strong HBV-specific humoral and cellular immune responses, which were comparable to the classical *TherVacB* strategy with protein prime–MVA vector boost.

To summarize the studies in this chapter, the VSV-GP-HB/c vector was successfully constructed, and the expression of HBsAg and HBcAg was confirmed. Evaluation of immunogenicity in wild-type and AAV-HBV mice indicated that VSV-GP-HBs/c functions well as boost vector in the *TherVacB* strategy. Moreover, it was demonstrated that employing adjuvanted protein for priming was crucial for the *TherVacB* to induce potent antibody and T-cell responses, while viral vectors failed to do so. Since it has been shown that VSV-GP can be used repetitively without losing vaccine efficacy, the potential advantages of multiple VSV-GP-HBs/c administrations in combination with protein priming will be explored in further steps.

3. Discussion

With the limitations of current antiviral therapies to cure chronic hepatitis B, therapeutic vaccination represents a promising new treatment strategy. In the recent work of our laboratory, the heterologous protein prime — modified vaccinia virus Ankara (MVA) boost therapeutic hepatitis B vaccine, termed *TherVacB*, has been developed. Previous studies have shown that *TherVacB* immunization elicits both anti-HBs seroconversion and strong HBV-specific T-cell responses (Backes and Jäger, 2016; Kosinska, 2019). *TherVacB* was able to break HBV-specific immune tolerance in low and intermediate antigenemic HBV transgenic (HBVtg) mice, but not in high antigenemic ones (Backes and Jäger, 2016; Kosinska, 2019). The limited efficacy of *TherVacB* in the presence of high antigenemia implies that further improvements are needed to make *TherVacB* suitable for clinical development. In this thesis, the *TherVacB* regimen was improved in different aspects to achieve a better immune control against HBV, as discussed below in the following individual chapters.

3.1 Determining the optimal immunization protocol of *TherVacB*

It was shown that vaccine immunogenicity and efficacy could be significantly affected by the choice of the immunization protocol (Schunk and Macallum, 2005). Therefore, the immunization protocol of *TherVacB* was optimized by determining the appropriate vaccine delivery routes and components doses, as well as selecting a proper adjuvant in HBVtg mice.

WHO recommends that vaccines containing adjuvants should be injected intramuscularly to reduce local adverse effects (WHO, 2020). Moreover, the vaccine administration via the intraperitoneal route is not feasible in humans. Thus, in this study, the delivery routes of *TherVacB*, were altered from the initial ones—s.c. for protein, i.p. for MVA—to the intramuscular immunization for both.

When the efficacy of *TherVacB* via i.m. was compared to that via s.c./i.p. routes, *TherVacB* immunization via the i.m. route elicited significantly stronger antibody and

Discussion

T-cell responses than the immunization via the initial s.c./i.p. routes (Fig.2.10 - 2.12). This observation suggests that the different delivery routes lead to the distinct vaccine localizations that could influence the priming of immune cells and, as a consequence, the vaccine-elicited immune responses (Zhang, 2015). The superior efficacy of intramuscular immunization for both protein and MVA suggests that the local immune cells primed by protein immunization via the i.m. route could be boosted more efficiently by the same placement of MVA injection. Nevertheless, the optimal delivery route for every vaccine needs to be empirically determined to achieve the best efficacy with the fewest side effects (Zhang, 2015).

Adjuvant, as an indispensable component in subunit vaccines, also remarkably influences the vaccine-induced immune responses (Coffman, 2010). The efficacy of *TherVacB* with three different types of adjuvants was compared in HBVtg mice.

It was shown in this study that *TherVacB* immunization with STING agonist c-di-AMP led not only to the production of high levels of anti-HBV antibodies, but also the strong induction of HBV-specific T-cell responses (Fig.2.11 – 2.12). These results support the previous findings that c-di-AMP contributes to the generation of both humoral and cellular immune responses required for efficacious vaccination against influenza (Ebensen, 2017). By contrast, immunization of mice with TLR3 ligand poly-ICLC and the RIG-I Ligand formulations induced high levels of anti-HBV antibodies, but moderate HBV-specific T-cell responses. These results reveal that different adjuvants can activate distinct profiles of innate immune response, consequently modulate the quality and quantity of adaptive immune responses (Await, 2013). Therefore, adjuvant development should be considered as one part of the entire vaccine development to achieve desirable immune responses (Zhang, 2015; EMA adjuvant guideline, 2005). Considering the cellular immune responses as the desired responses for the therapeutic vaccines, c-di-AMP could be a good adjuvant candidate for *TherVacB*.

Next, the optimal doses of *TherVacB* vaccine components (protein, MVA) via i.m. route were determined in HBVtg mice. It was shown previously that *TherVacB* immunization with 1×10^8 IFU recombinant MVA could induce HBV-specific T-cell responses in low and intermediate antigenemic HBVtg mice (Backes and Jäger, 2016). Interestingly, in

this study, immunization with 3×10^6 IFU MVA was found sufficient to induce strong HBV-specific immune responses in the HBVtg mice with low HBV antigen levels. Moreover, immunization with 1-log higher dose: 3×10^7 IFU of MVA was able to elicit strong HBV-specific immune responses even in the high antigenemic mice (Fig.2.4 – Fig.2.6), indicating that the selection of the potent adjuvant and optimization of the delivery route significantly improved the efficacy of *TherVacB*.

In the experiments determining the optimal dose of protein for priming, it was shown that immunization of mice with all three doses of protein induced comparably high levels of HBV-specific antibodies (Fig.2.8). This indicates that the lowest protein dose was sufficient to induce adequate antibody responses. Nevertheless, the T-cell responses in mice immunized with 10 μ g and 15 μ g of protein were significantly higher compared to those in mice immunized with 5 μ g of protein (Fig.2.9). These findings indicate that different doses of vaccination can result in distinct qualities of vaccine-induced immune responses. Therefore, the optimal vaccine doses should be decided based on the desired immune responses induced by vaccination (Zimmermann and Curtis, 2019).

Taken together, these results demonstrate that beyond the vaccination regimen, many immunization-related factors such as vaccine delivery route and dose, and adjuvant selection, could also influence the overall vaccine efficacy of *TherVacB*. Moreover, these findings obtained in preclinical hepatitis B models may pave the way for the clinical development of *TherVacB*.

3.2 Employing novel adjuvants to improve the protein priming of *TherVacB*

The results of the studies discussed in last chapter demonstrate that the success of *TherVacB* also largely depends on an appropriate adjuvant. To improve the efficacy of *TherVacB* regimen, three different categories of adjuvants: liposome (Lipo), squalene-in-water emulsion (SWE), and water-in-oil emulsion Montanide ISA720 were investigated for the protein priming of *TherVacB*. Moreover, the Lipo and SWE delivery

systems were combined with different doses of TLR4 ligand MPL and QS21 saponin as combination adjuvants. The antigens, HBsAg and HBcAg, were formulated with the investigated adjuvants. The results of *in vitro* characterization and *in vivo* immunogenicity evaluation of these novel antigen/adjuvant formulations (referred to as adjuvant formulations) are discussed below.

3.2.1. Lipo- and SWE-based antigen/adjuvant formulations remain stable and intact for long time *in vitro*

To assure vaccine quality, WHO has acknowledged the importance of clearly defining the stability characteristics of a vaccine (WHO guideline, 2006). Therefore, the stability of antigen/adjuvant formulation and the integrity of HBsAg/HBcAg were characterized by various assays at week 0, and after 2 weeks and 12 weeks of storage.

Transmission electron microscopy (TEM) analysis of the representative Lipo-based formulation (Lipo-3) was performed after the formulation had been stored at 4 °C for 12 weeks. The TEM imaging reveals that not only intact HBsAg and HBcAg particles but also intact Lipo-3 adjuvant were clearly visible in this long-term storage formulation (Fig.2.16). Furthermore, both HBsAg and HBcAg within all Lipo- and SWE-based formulations displayed the integrity profiles comparable to the original antigens at every time point analyzed, even after 12 weeks of storage (Fig.2.15 – Fig.2.16). These findings indicate that all Lipo- and SWE-based formulations could remain stable and intact for at least 12 weeks *in vitro*.

The long-term stability of Lipo- and SWE-based formulations could facilitate the vaccine preparation for immunization. After large-scale manufacturing, these formulations could be used for multiple immunizations, which can save the additional labor work and minimize the batch variation issues. Since the shelf-life for the licensed vaccines is at least 12 months (Kumru, 2014), it would be important to explore whether the investigated adjuvant formulations could remain stable after even much longer time of storage. In addition, most currently used vaccines require storage at a temperature of 2 – 8 °C or lower, which necessitates a cold-chain for long-term stability (Kumru,

2014). However, the cold-chain capacity around the world, especially in the developing regions, is quite limited (Yahia, 2009). Thus, it would also be interesting to investigate the temperature stability of these adjuvant formulations.

Montanide ISA720 is a novel water-in-oil emulsion adjuvant, which has been widely used in the development of both prophylactic and therapeutic vaccines against infectious diseases and cancers (Ascarateil, 2009). In addition, it has displayed excellent safety profiles and potent adjuvant abilities in various malaria and AIDS vaccine clinical trials (Toledo, 2001; Aucouturier, 2002). Therefore, Montanide ISA720 was also investigated as an adjuvant candidate for *TherVacB* regimen. It was shown in the present study that the antigen/Montanide formulation separated into two phases shortly after the manufacture procedure. Moreover, Montanide ISA720-formulated HBcAg displayed negative HBcAg-specific signals in all tested antigen integrity assays of HBcAg (Fig.2.15). These findings indicate that the Montanide ISA720 adjuvant may not be compatible with HBsAg/HBcAg and interfere with the integrity of HBcAg. Collectively, the difference in stability profiles between Lipo/SWE-based and Montanide ISA720 formulations reveals that distinct adjuvants interact with the specific antigens in various manners (Fox, 2013). Additionally, it may occur that certain adjuvants could not be compatible with particular antigens. Therefore, interactions between antigen and adjuvant should always be well-characterized to ensure optimal vaccine stability and efficacy (Fox, 2013).

3.2.2 Immunization with novel adjuvant formulations increases the magnitude of HBV-specific humoral responses

Numerous studies have shown that adjuvants enable inducing an enhanced magnitude of antibody responses to vaccine antigens (Reed, 2013). Thus, the question was raised as to whether immunization with these novel adjuvant formulations could increase the magnitude of HBV-specific humoral responses. To this end, the immunogenicity of the most promising adjuvant formulations was evaluated in both wild-type and AAV-HBV mice. AAV-HBV mouse model, in which HBV replication

Discussion

persists for at least 1 year and the HBV-specific immunotolerance can be observed, is a suitable model to mimic chronic HBV infection in humans (Dion, 2013; Lan, 2017).

The levels of anti-HBs were almost undetectable in both wild-type and AAV-HBV mice received the vaccines without adjuvant. By contrast, immunization with all Lipo- and SWE-based formulations elicited remarkably high levels of anti-HBs (Fig.2.20, Fig.2.24, Fig.2.28). These results prove the knowledge that adjuvants could potentiate the antibody responses to the vaccine antigens (Reed, 2013).

Previous studies have demonstrated that HBcAg has excellent immunogenic properties (Billaud, 2005; Aguilar, 2004; Riedl, 2002). On one hand, HBcAg is able to enhance priming of T cells by activating B cells to work efficiently as primary APCs (Milich and McLachlan, 1986; Kutscher and Bauer, 2012); on the other hand, the nucleic acids encapsulated into HBcAg capsid can activate TLR3 signaling and strongly facilitate HBcAg to prime Th1-type immunity (Riedl, 2002; Aguilar, 2004). The results obtained in this study also confirm that HBcAg could strongly stimulate immune responses. Immunization of both wild-type and AAV-HBV mice even without adjuvant induced profound anti-HBc responses. Nevertheless, the levels of anti-HBc in mice immunized with novel adjuvant formulations tended to be higher compared to those in mice immunized without adjuvant (Fig.2.20, Fig.2.24, Fig.2.28).

The average values of anti-HBs in mice immunized with all Lipo- and SWE-based formulations were even 1-log higher than those in mice immunized with c-di-AMP formulation (Fig.2.20). As the novel adjuvants investigated in this study are combination adjuvants, consisting of a delivery system and immunostimulants, the enhanced anti-HBs responses could be explained by the synergistic effects of the individual adjuvants. This concept is also reflected in the vaccine design of Fendrix, which is a recombinant HBV vaccine supplemented with combination adjuvant AS04 (Garçon and Di Pasquale, 2017). Fendrix was developed with the aim of improving the antibody responses in patients with renal insufficiency, who demonstrate the impaired immune responses to the classical Alum-adjuvanted HBV vaccines (Kundi, 2007). Both preclinical and clinical studies showed that HBV/AS04 induced higher antibody titers and seroconversion rates compared to the classical Alum formulation (Kundi,

2007; Hoebe, 2012). Similar to the patients with renal insufficiency, CHB patients display functionally impaired HBV-specific B-cells with defective antibody production ability (Burton, 2018). Hence, the application of the novel combination adjuvants in *TherVacB* might exhibit additional benefits for the CHB patients in the induction of anti-HBs, the hallmark of the functional cure of CHB (Lok, 2018; Revill, 2019).

3.2.3 Immunization with novel adjuvant formulations elicits balanced HBV-specific helper T-cell responses

It has been shown by many studies that the incorporation of an adjuvant into a vaccine could also shape the quality of the vaccine-induced immune response by influencing the effector functions of helper T cells (Coffman, 2010; Mescher, 2016). Hence, the study discussed here aimed at exploring the impact of the novel adjuvant formulations on the induction of HBV-specific helper T-cell responses in both wild-type and AAV-HBV mice.

It was formerly reported that the Th2-associated IgG₁ was the major subclass of anti-HBs in the vaccine recipients of Engerix-B, an Alum-adjuvanted HBV prophylactic vaccine (Honorati, 1997). The results of this study demonstrate that immunization with novel adjuvant formulations generated not only Th2-associated IgG₁ subclass, but also high levels of Th1-associated IgG_{2b} subclass of anti-HBs in both wild-type and AAV-HBV mice (Fig.2.20; Fig.2.28). Furthermore, a robust secretion of S-specific Th2 cytokine IL-5 and Th1 cytokine IFN γ was simultaneously observed in splenocytes of mice immunized with novel adjuvant formulations (Fig.2.29). These findings indicate that immunization with novel adjuvant formulations could elicit Th1/Th2-balanced S-specific responses.

As discussed above, HBcAg is a potent immunogen that preferentially activates Th1 cells (Billaud, 2005). Despite this, the Th2-associated IgG₁ subclass still represents one of the main IgG subclasses of anti-HBc detected in both wild-type and AAV-HBV mice immunized with novel adjuvant formulations (Fig.2.20; Fig.2.28). Moreover, stimulation of splenocytes with HBcAg also resulted in the detection of Th2 cytokine

Discussion

IL-5 (Fig.2.29). These results suggest that immunization with novel adjuvant formulations could induce mixed Th1/Th2 core-specific responses.

Immunization of both wild-type and AAV-HBV mice with novel adjuvant formulations induced significantly higher S-specific IFN γ + CD4 T-cell responses than immunization either without adjuvant or with c-di-AMP formulation (Fig.2.21, Fig.2.26). These results imply that immunization with novel adjuvant formulations could enhance the S-specific helper T-cell responses.

Core-specific IFN γ + CD4 T cells were barely detectable either in wild-type or AAV-HBV mice immunized with any vaccine formulations by intracellular staining at the analyzed time point (Fig.2.21, Fig.2.26). The potential explanation for this might be that the effector-phase core-specific CD4 T cells are very short-lived and might be eliminated via apoptosis at the analyzed time point (Wu, 2002; Dooms and Abbas, 2002). To confirm this hypothesis, it would be necessary to analyze the core-specific IFN γ + CD4 T-cell responses within a short period of time after the onset of immunization. Nevertheless, the induction of memory-phase core-specific helper T-cell responses could be speculated, as the cytokine secretion was observed from the splenocytes of immunized mice after *ex vivo* stimulation with intact HBcAg. The amount of core-specific IFN γ secreted by splenocytes from mice immunized with novel adjuvant formulations was significantly higher than those secreted by the splenocytes from the no adjuvant group (Fig.2.29). These results indicate that employing the novel adjuvants markedly enhances core-specific helper T-cell responses.

Since the combination adjuvants consist of different components, the roles of individual adjuvant components in HBV-specific CD4 T-cell responses were addressed. Immunization of wild-type mice with all novel adjuvant formulations induced comparably strong S-specific IFN γ + CD4 T-cell responses (Fig.2.21). Interestingly, in AAV-HBV mice, immunization with LMQ and SMQ formulations, in which MPL was included, exhibited remarkably stronger S-specific IFN γ + CD4 T-cell responses, compared to LQ and SQ formulations (Fig.2.26, Fig.2.29). These results prove that MPL could promote Th1-type antigen-specific responses, as it was previously shown for other vaccines (Wheeler, 2001; Meraz, 2014). This observation may also support

the hypothesis that including MPL in *TherVacB* could be beneficial to break the HBV-specific immune tolerance during the persistent HBV infection.

3.2.4 Immunization with novel adjuvant formulations induces strong HBV-specific CD8 T-cell responses

It is well-established that HBV-specific CD8 T cells are the major player for HBV clearance (Maini, 1999; Thimme, 2003). Thus, the question of whether immunization with novel adjuvant formulations could elicit robust HBV-specific CD8 T-cell responses was addressed below.

The results of the present study show that, indeed, immunization with the novel adjuvant formulations induced vigorous HBV-specific CD8 T-cell responses. The average frequencies of splenic S-specific IFN γ ⁺ CD8 T cells in the wild-type mice immunized with novel adjuvant formulations were 10%, which was around 20 times higher than those in mice immunized either without adjuvant or with c-di-AMP formulation (Fig.2.22). Moreover, it was observed that the frequencies of S-specific IFN γ ⁺ TNF α ⁺ CD8 T cells in the mice vaccinated with high QS21 dose formulations were considerably higher than in mice immunized with low QS21 dose formulations (Fig.2.22). These results support the previous finding that QS21 can enhance cellular immune responses (Newman, 1997).

Consistent with the observation in wild-type mice, there were neither S-specific CD8 T-cells nor IFN γ ⁺ CD8 T-cell responses detectable in AAV-HBV mice immunized without adjuvant. By contrast, immunization with LMQ, SQ, and SMQ formulations stimulated high levels of S-specific CD8 T cells and multifunctional IFN γ ⁺ TNF α ⁺ CD8 T-cell responses (Fig.2.26, Fig.2.30, Fig.2.31). These findings suggest that employing these novel adjuvant formulations could enhance *TherVacB* to induce S-specific CD8 T-cell responses. In addition, immunization with LQ formulation stimulated only a moderate S-specific CD8 T cell response, which might correlate with the poor helper T-cell responses in this group (Fig.2.26, Fig.2.30, Fig.2.31). The distinct outcome of

Discussion

LQ and LMQ immunization also suggests that the addition of MPL for the LMQ formulation promotes strong S-specific CD4 and CD8 T cell responses.

Apart from the prime immunization with adjuvanted antigens, boost immunization with recombinant MVA also greatly contributes to the induction of strong CD8 T-cell responses. In many studies, MVA has been proven to induce strong cytotoxic T lymphocyte (CTL) responses (Acres and Bonnefoy, 2008; Sebastian and Gilbert, 2015). Nevertheless, in this study, all vaccinated mice received the same MVA immunization. The S-specific CD8 T-cell responses in the mice vaccinated without adjuvant or with c-di-AMP formulation were still significantly lower than in the mice vaccinated with novel adjuvant formulations. These contrasting results lead to the assumption that different approaches for priming could result in distinct magnitudes of CD8 T-cell response. The detected core-specific CD8 T-cell responses also strengthen this hypothesis. Prime immunization of AAV-HBV mice with LQ, LMQ, SQ formulations induced strong intrahepatic core-specific CD8 T-cell responses. By contrast, almost no core-specific IFN γ + CD8 T cells were detected in the mice primed with SMQ formulation, with values even lower than those in the mice vaccinated without adjuvant. The failure of SMQ formulation might be explained by the fact that the SMQ adjuvant together with strongly immunogenic HBcAg overstimulated the immune system, which consequently triggered immunosuppressive mechanisms to inhibit the vaccine-induced CD8 T-cell responses. Since immunization with SQ formulation could stimulate strong core-specific T-cell responses, it would be interesting to explore whether reducing the dose of MPL in SMQ could help to enhance the immune responses.

3.2.5 Immunization with novel adjuvant formulations leads to long-term control of persistent HBV replication in AAV-HBV mice

The results obtained from both wild-type and AAV-HBV mice demonstrate that immunization with the novel adjuvant formulations resulted in the induction of strong HBV-specific antibody, CD4, and CD8 T-cell responses. Consequently, the question of

whether these potent immune responses contribute to the immune control of persistent HBV replication was raised.

It was demonstrated previously that chronic hepatitis B patients, who received the bone marrow transplantation from donors with natural immunity to HBV, can spontaneously resolve the HBV infection (Ilan, 1993). This clinical observation reflects the critical role of HBV-specific immunity in controlling HBV infection. Moreover, in the preclinical HBV mouse models, it has been observed that the potent HBV-specific immune responses induced by the therapeutic vaccination led to the control of persistent HBV replication, whereas the poor HBV-specific immune responses correlated with the persistence of HBV infection (Kosinska, 2019; Michler and Kosinska, 2020). The results of this study also confirm this finding. Immunization with SMQ formulation resulted in negligible effects on the HBeAg decrease, reduction of intrahepatic HBV DNA and numbers of core-positive hepatocytes. The minor antiviral effects of SMQ immunization correlated with poor T-cell responses observed in this group (Fig.2.30 – Fig.2.33). By contrast, consistent with the strong HBV-specific immune responses, immunization with LQ, LMQ, SQ formulations resulted in long-term reduction of HBV parameters in serum and liver, or even a complete loss of HBV in one or two mice of four in these groups (Fig. 2.33). These results suggest that *TherVacB*-induced HBV-specific immune responses, especially cytotoxic T cells could eliminate the HBV-infected hepatocytes (Ando, 1994) or degrade the HBV persistent form by cytokine secretion (Lucifora and Xia, 2014; Xia and Stadler, 2016). Collectively, the findings in the present study indicate that immunization with LQ, LMQ, SQ formulations could lead to elimination or long-term control of persistent HBV replication.

3.2.6 General remarks and future directions of adjuvant development

The results presented in this thesis demonstrate that employing the novel adjuvants markedly improved the efficacy of *TherVacB* in the preclinical evaluation. Despite this, many adjuvant-related concerns could be encountered during the clinical development of vaccines.

Discussion

The main issue of incorporating adjuvants into vaccines is the potential toxicity and adverse side effects of the adjuvants (Gupta, 1995). While numerous adjuvants have been developed in preclinical studies, only a few of these have been evaluated in clinical trials and approved for human use, because of the safety concerns (Morrow, 2012). The adjuvants investigated in this study were shown safe and well-tolerated in the preclinical mouse models (Fig.2.22, Fig.2.33). Moreover, these combination adjuvants share similar components with the approved adjuvants that have been well-documented to be safe in the clinical studies (Garçon and Di Pasquale, 2017). Nevertheless, further safety evaluations of these adjuvants need to be performed prior to clinical development.

The biological difference between animal models and humans, such as TLR expression, is another issue that needs to be considered during the adjuvant development. As an example, human and mouse TLR9s are expressed in different cell populations. While murine immune cells of the myeloid lineage express TLR9, these cell types in humans do not express TLR9 (Klinman, 2004; Bauer and Kirschning, 2001). The difference may lead to the failure of the promising adjuvants targeting TLR9 in the clinical trials. Thus, it is necessary to fully utilize information of adjuvants' modes of action and avoid using undefined components in adjuvant formulations (Reed, 2013). In the present study, while the Lipo-based adjuvants harbor comparable components with clinically used adjuvant AS01, the components of SWE-based adjuvants are similar to those in the advanced developed adjuvant AS02. That may accelerate the clinical development of the *TherVacB* regimen employing the novel adjuvants investigated in this study.

In the future, it would be of significant importance to explore the mechanisms behind the vaccine-induced immune responses, which could help rationally design and optimize the adjuvanted vaccines. Additionally, it would be interesting to understand why MPL and QS21 formulated in liposome as LMQ elicits strong T-cell responses, whereas the same molecules formulated in squalene-in-emulsion as SMQ fails to induce core-specific CD8 T-cell responses.

3.3 Exploring critical factors for efficient protein priming of *TherVacB*

The results discussed in last chapter reveal that efficient protein priming with an appropriate adjuvant is the key to *TherVacB* success. The finding raises the question – what are the critical factors contributing to efficient protein priming of *TherVacB*? As the priming is performed using the mixture of recombinant antigens and adjuvant, first, the impact of individual vaccine components was determined. Next, the role of CD4 and CD8 T cells in mediating the immune responses during the priming phase of *TherVacB* was explored.

3.3.1 Administering recombinant HBsAg/HBcAg is critical for potent priming of *TherVacB*

As chronic hepatitis B patients have high loads of circulating HBV antigens (Michler and Kosinska, 2020; Kim, 2020), it is meaningful to analyze whether administration of adjuvant alone can assist the endogenous HBV antigens to efficiently induce HBV-specific immune responses. To address this point, four different types of adjuvants were investigated.

Although followed by immunization with recombinant MVA expressing HBV antigens, none of the adjuvants administered alone were able to induce any HBV-specific neutralizing antibodies or T-cell responses, and thereby could not decrease the high levels of serum antigens. By contrast, priming with adjuvanted HBsAg/HBcAg elicited strong HBV-specific both humoral and cellular immune responses (Fig.2.34 – Fig.2.37). These findings indicate that high loads of endogenous HBV antigens could not trigger the induction of HBV-specific immune responses, even with the assistance of adjuvant. One possible explanation for this might be that there is strong immune tolerance to endogenous circulating HBV antigens (Mueller and Ahmed, 2009). To break this tolerance, it is necessary to administrate ‘fresh’ HBsAg/HBcAg together with a potent adjuvant to *de novo* prime HBV-specific immune cells. In addition, it has been observed in prior studies that physical co-delivery of antigen and adjuvant was crucial for certain adjuvants to exert their immune-enhancing effects (Davis, 2008). Thus, these results

may also be explained by the distinct distribution of endogenous HBV antigens and administered adjuvant *in vivo*.

3.3.2 Incorporating Th1/Th2-balanced adjuvant is essential for potent protein priming of *TherVacB*

Since the results of the novel adjuvant study clearly demonstrate that it is essential to include an adjuvant in the *TherVacB* regimen, the question was raised as to what are the selection criteria of an appropriate adjuvant for *TherVacB*. To this end, the outcomes of priming immunizations with: 1) antigens-only, 2) Th2-biased adjuvant Alum formulated antigens, and 3) Th1/Th2-balanced combination adjuvants LMQ and SMQ formulated antigens were compared.

Numerous therapeutic hepatitis B vaccine clinical trials were based on prophylactic HBV vaccines containing Alum-adjuvanted HBsAg (Aguilar and Lobaina, 2014). In addition, in some studies HBcAg was included in the vaccines to broaden the immune responses (Trujillo, 2014). Nevertheless, the antiviral effects of these vaccines were not sustained and did not achieve the control of HBV (Pol and Michel, 2006). It has been well-documented that Alum can initiate strong antigen-specific Th2-type responses (Brewer 1999), but is not able to augment cell-mediated immune responses (Kool, 2012). Thus, the discouraging outcomes of these clinical trials might be explained by insufficient induction of HBV-specific CD8 T-cell responses that predominantly contribute to the HBV clearance (Thimme, 2003).

In this study, immunization with Alum-adjuvanted antigens was followed by a boost immunization with recombinant MVA, which has been proven to induce strong CTL responses (Acres and Bonnefoy, 2008; Sebastian and Gilbert, 2015). It had been assumed that this combination could induce strong HBV-specific both humoral and cellular immune responses. The results of the present study demonstrate that *TherVacB* immunization with Alum formulation, indeed, induced high levels of HBV-specific antibodies, as well as moderate HBV-specific CD4 T-cell responses (Fig.2.39 and Fig.2.41). However, it failed to elicit any S-specific CD8 T-cell responses (Fig.2.41),

implying that *TherVacB* priming with Th2-biased adjuvant Alum is not sufficient to elicit HBV-specific CD8 T-cell responses that could be further boosted by the MVA immunization. Of note, *TherVacB* immunization with Th1/Th2-balanced LMQ or SMQ formulations not only generated very high levels of HBV-specific antibodies, but also induced vigorous HBV-specific CD4 and CD8 T-cell responses (Fig.2.39 – Fig.2.41). Collectively, these findings indicate that including a Th1/Th2-balanced adjuvant, but not a Th2-biased adjuvant in protein priming of *TherVacB* is the prerequisite of the overall efficacy of *TherVacB*.

3.3.3 CD4 T cells are the key T-cell subset contributing to *TherVacB*-mediated immune responses during the priming phase

In vivo antibody-mediated depletion of T cells makes it possible to study the role of specific T-cell populations during defined phases of *in vivo* immune responses (Laky and Kruisbeek, 2016). Hence, taking advantage of this method, the role of different T-cell subsets in mediating the immune responses during the priming phase of *TherVacB* was addressed.

First, the impact of CD4 T-cell depletion during the priming phase of *TherVacB* was explored. *TherVacB* immunization of the CD4-depleted mice induced significantly lower levels of anti-HBs and anti-HBc compared to immunization of the isotype IgG or α CD8 mAb-treated mice (Fig.2.44). These observations confirm that CD4 T cells play a vital part in promoting B cells to generate antibodies (den Haan and Bevan, 2000). Furthermore, HBV-specific CD4 and CD8 T-cell responses in the CD4-depleted mice were markedly lower than those in CD8-depleted mice (Fig.2.45). Consistent with the impaired antibody and T-cell responses, the levels of serum HBsAg and HBeAg remained stable after immunization in α CD4 mAb treatment group (Fig.2.44). Collectively, these results indicate the role of CD4 T cells in facilitating the induction of efficient *TherVacB*-mediated immune responses.

Next, the role of CD8 T cells in mediating the immune responses during the priming phase of *TherVacB* was investigated. The levels of HBV-specific antibodies and the

Discussion

trends of serum HBV antigens decrease in α CD8 mAb-treated mice were comparable with those in isotype IgG treated mice (Fig.2.44). Moreover, immunization of CD8-depleted mice stimulated much stronger HBV-specific T-cell responses than immunization of CD4-depleted mice (Fig.2.45). These observations indicate that CD8 T cells might not be essential in mediating immune responses during the priming phase of *TherVacB*. Nevertheless, this indication is not solid. The minor effects of CD8 T-cell depletion on the observed immune responses could also be explained by several reasons. First, CD8 T cells have been reported more resistant to mAb-mediated depletion (Cross, 2019). It was also shown in the present study that on average 20% of CD8 T cells were detected in the lymph nodes of mice after α CD8 mAb treatment during the T-cell depletion efficiency test (Fig.2.42). Even this low amount of CD8 T cells could be primed by *TherVacB* immunization with potent adjuvant LMQ and still exert their antiviral functions. Furthermore, accumulating evidence suggests that during viral infection CD4 T cells could develop into populations of effector T cells that have potent antiviral immunity, independent of CD4 T-cell helper activities (Snow, 1994; Swain, 2012). Hence, it is also likely that mice depleted of CD8 T-cell subset developed effector CD4 T-cell responses against HBV, which could compensate for the lack of CD8 T cells. Altogether, it seems difficult to conclude the role of CD8 T cells during the priming phase of *TherVacB* by antibody-mediated T-cell depletion method. Further studies with other methods such as adoptive T-cell transfer are needed to define the role of CD8 T cells induced during the priming phase of *TherVacB*.

Very weak HBV-specific T-cell responses were unexpectedly detected in the isotype IgG treatment group in this study (Fig.2.45). The reason for this might be that the repeated administrations of isotype rat IgG lead to a mouse anti-rat IgG response that may cause an unexpected immune deviation (Arora, 2006). Therefore, it would be necessary to include a group of mice only immunized with *TherVacB* as a positive control in further studies.

Previous studies in HBV-infected chimpanzees demonstrated that an early CD4 T-cell response to HBV infection is required to induce the CD8 T-cell response that leads to the clearance of the infection (Asabe, 2009; Chisari, 2010). In this study, it was shown

that during the therapeutic vaccination for CHB treatment, CD4 T-cells also play a critical role in initiating vaccine-mediated immune responses against persistent HBV infection. Moreover, the minor effects of CD8 T-cell depletion during the priming phase of *TherVacB* imply that in addition to assisting CD8 T cells, HBV-specific CD4 T cells might also make meaningful contributions in the anti-HBV immunity. The importance of vaccine-induced CD4 T-cell responses has also been verified in other vaccines. In a therapeutic cancer vaccination, it was shown that CD4 T cells but not CD8 T cells were essential in the antibody production and T-cell responses against tumor antigens (Kennedy, 2003). A similar finding was observed in a malaria vaccine candidate: depletion of CD4 T cells led to a loss of vaccine-induced protection (Biswas, 2012). Taken together, these findings clearly demonstrate that CD4 T cells are the key T-cell subset during the priming phase of *TherVacB*, contributing to the vaccine-induced HBV-specific antibody and T-cell responses and determining the success of the therapeutic vaccination.

3.4 Developing novel VSV-GP-HBs/c vector to improve the *TherVacB* regimen

Apart from the prime immunization with adjuvanted antigens, the boost immunization with recombinant MVA is the other critical step in *TherVacB* to break the immune tolerance against HBV and stimulate strong HBV-specific T-cell responses. To further improve the immune responses elicited by *TherVacB* and avoid the dominant MVA-specific responses to decrease the vaccine efficacy, the novel VSV-GP-HBs/c (VSV-GP encoding HBsAg and HBcAg) vector was developed. The results of the *in vivo* immunogenicity evaluation of the novel recombinant VSV-GP-HBs/c are discussed below.

3.4.1 Heterologous prime-boost strategies with VSV-GP-HBs/c induce strong HBV-specific immune responses in wild-type mice

The immunogenicity studies of VSV-GP-HBs/c vector in wild-type mice demonstrate that already a single immunization with this novel vector was able to induce HBV-specific T-cell responses, albeit very weak (Fig.2.49). This result supports the previous finding, showing that VSV-GP encoding ovalbumin (OVA) (VSV-GP-OVA) could induce OVA-specific immune responses upon a single immunization (Tober, 2014). Aiming to enhance rather low HBV-specific immune responses after the single immunization, heterologous prime-boost strategies with VSV-GP-HBs/c were subsequently applied. Immunization of mice in a protein prime – viral vector boost manner induced high levels of anti-HBs and anti-HBc, no matter which vector, MVA-HBs/c or VSV-GP-HBs/c, was employed (Fig.2.51). These results confirm that protein-based vaccine could induce strong antibody responses (Draper, 2015). Immunization with heterologous regimens based on two viral vectors: VSV-GP-HBs/c and MVA-HBs/c induced moderate levels of anti-HBs and anti-HBc, independent from the sequence of vaccination (Fig.2.51). The potential explanation for this might be that viral vector vaccines are not as potent as protein-based vaccines at inducing antibody response.

Recombinant viral vectors are well-known for inducing antigen-specific cellular immune responses (Truckenmiller, 2004). Unexpectedly, the HBV-specific CD8 T-cell responses were very weak in mice immunized with heterologous regimens based on two viral vectors: VSV-GP-HBs/c and MVA-HBs/c. By contrast, immunization with the protein prime – viral vector boost regimens elicited strong HBV-specific T-cell responses (Fig.2.52). These contrasting results might be explained by limited CD4 T-cell help in mice immunized with two viral vectors. Antigens formulated with a Th1/Th2 adjuvant could more efficiently activate CD4 T cells to promote the antiviral CD8 T-cell immunity than prime immunization with viral vector. In addition, in the two groups of mice primed with protein, no noticeable difference in HBV-specific T-cell responses was detected between the MVA-HBs/c and the VSV-GP-HBs/c boosted mice (Fig.2.52). These results demonstrate that with effective protein priming, the boosting

immunization with novel VSV-GP-HBs/c could induce comparably strong HBV-specific T-cell responses as boosting with MVA-HBs/c.

It was shown previously that vaccination with the VSV-GP vector does not induce self-specific neutralizing antibodies (Tober, 2014). The results of this study demonstrate that VSV-specific CD8 T-cell responses were already tested negative five weeks after VSV-GP-HBs/c immunization, indicating that the T-cell responses against VSV-GP vector could also become undetectable in a short period of time (Fig.2.52). These observations support the assumption that VSV-GP can be repetitively applied without losing the vaccine efficacy (Tober, 2014).

3.4.2 Protein prime – VSV-GP boost vaccination breaks the immune tolerance against HBV in AAV-HBV mice

The results obtained from the experiments in wild-type mice demonstrate that immunization with VSV-GP-HBs/c vaccines, especially protein prime – VSV-GP-HBs/c boost regimen, could induce potent HBV-specific immune responses. Thereafter, the question of whether the VSV-GP-HBs/c vaccinations could overcome HBV-specific immune tolerance in persistently infected AAV-HBV mice was addressed.

Previous studies have shown that immunization with the protein prime – MVA boost *TherVacB* regimen could stimulate strong HBV-specific antibody and T-cell responses, thereby achieved the immune control against HBV in AAV-HBV mice (Kosinska, 2019). The results of this study also confirmed the efficacy of *TherVacB* immunization employing MVA boost (Fig.2.55 – Fig.2.57). Furthermore, immunization with protein prime – VSV-GP boost regimen induced comparably strong HBV-specific humoral and cellular immune responses as classical *TherVacB* immunization (Fig.2.55 – Fig.2.57). In addition, the levels of serum HBsAg and HBeAg decreased remarkably after immunization with both protein/MVA and protein/VSV-GP regimens, but not in the non-vaccinated group (Fig.2.55). These findings imply that VSV-GP-HBs/c could be a suitable alternative boost vector to improve the antiviral efficacy of *TherVacB*.

To explore whether it is possible to replace protein with the new VSV-GP vector for

priming, one group of mice was primed twice with VSV-GP-HBs/c and boosted with MVA-HBs/c. The results of the present study show that immunization of mice with 2* VSV-GP/MVA regimen resulted in very low HBV-specific antibody responses and undetectable T-cell responses (Fig.2.55 – Fig.2.57). These results confirm the previous observation that priming with potent adjuvanted antigens is crucial for *TherVacB* to induce strong HBV-specific antibody and T-cell responses.

3.4.3 General remarks and potential applications of VSV-GP-HBs/c vector

The results of this study demonstrate that VSV-GP-HBs/c vaccinations could break the immune tolerance against HBV and induce robust HBV-specific immune responses in the preclinical mouse models. Despite their excellent efficacy, viral vectors also present several issues during clinical applications.

First and foremost, safety concerns remain a significant challenge in the development of viral vector vaccines (Humphreys and Sebastian, 2018; Choi and Chang, 2013). The application of retroviral and lentiviral vectors carries the risk of integration into the host genome and may trigger tumorigenesis (Modlich and Baum, 2009). By contrast, that would not be a consideration for VSV, an RNA virus, which does not generate DNA intermediates during the viral replication (Humphreys and Sebastian, 2018). However, as wild-type VSV has been reported to be neurovirulent upon intracranial inoculation (Johnson, 2007), attenuation or abrogation of the VSV's natural neurotoxicity is a main concern of VSV application. The VSV-GP vector investigated in this study is a non-neurotoxic chimeric variant, in which the G protein of VSV is replaced by the LCMV-derived glycoprotein (Muik, 2014). In addition, this genetic modification did not diminish its efficacy in a variety of studies (Muik, 2014; Tober, 2014; Schreiber, 2019). The VSV-GP-HBs/c vaccine investigated in this study also proved safe and well-tolerated in the used preclinical mouse models (Fig.2.53). Nevertheless, further safety evaluations of the VSV-GP-HBs/c vaccine would be necessary during the clinical development.

Another challenge to the clinical application of viral vectors is the presence of pre-existing immunity against the vector (Choi and Chang, 2013). This is caused by

previous exposure to the virus, which resulted in the production of neutralizing antibodies (Ura, 2014). These neutralizing antibodies directed against the viral vector can significantly decrease the immunization efficacy. However, this problem could be circumvented by employing the viruses that do not circulate in humans or choosing different viral serotypes for prime and boost immunizations (Choi and Chang, 2013). Since VSV primarily infects rodents and hoofed livestock, but not humans, the seroprevalence of VSV in human population is extremely low (Lichty, 2004). More excitingly, it was formerly observed that VSV-GP vector did not induce vector-specific neutralizing antibodies *in vivo* (Tober, 2014). These characteristics of VSV-GP vector may facilitate VSV-GP-HBs/c vaccines to avoid the problems associated with pre-existing immunity against the vector during the clinical application.

Collectively, VSV-GP demonstrates potent efficacy as well as good safety profiles, and rarely displays vector-specific immunity in humans. Therefore, VSV-GP-HBs/c represents a promising vector candidate to improve the *TherVacB* regimen. There are several potential applications of VSV-GP-HBs/c vector during the clinical development of *TherVacB*. VSV-GP-HBs/c may serve as a substitute boost vector of MVA for the *TherVacB* regimen in the patients that harbor the pre-existing immunity against MVA vector. Furthermore, as MVA-specific immunity may become dominant upon repetitive application (Kastenmuller, 2007), it is not possible to employ MVA vector repetitively to boost the immune responses induced by *TherVacB*. Thus, VSV-GP-HBs/c could also be used as an additional vector to further boost the immune responses after the immunization with MVA-based *TherVacB* regimen. Last but not least, as the VSV-GP vector can be repetitively applied without losing vaccine efficacy (Tober, 2014), it would be interesting to investigate the efficacy of *TherVacB* immunization in combination with multiple VSV-GP-HBs/c administrations.

3.5 Conclusion

To summarize the studies presented in this thesis, the improvement of the therapeutic chronic hepatitis B vaccine (*TherVacB*) regimen has been achieved by determining the optimal immunization protocol, by employing the novel adjuvants for protein priming, and by developing the novel boost viral vector VSV-GP-HBs/c. First of all, the results of this study demonstrate that the improved *TherVacB* immunization could stimulate strong HBV-specific immune responses and lead to long-term immune control of HBV in persistent HBV replication mouse models. Furthermore, the data presented herein highlight the critical role of CD4 T cells in mediating immune responses against HBV. Last but not least, this work reveals that efficient protein priming with a Th1/Th2-balanced adjuvant is the key to *TherVacB* success. Without potent protein priming, the vaccine-induced immune responses proved very weak, even when multiple viral vectors were employed for immunization.

The improvements of *TherVacB* outlined in this thesis would be beneficial for the successful translation of *TherVacB* into clinical use and may have some implications for the development of other vaccines. Moreover, by detecting the factors critical to *TherVacB* success, this study might provide a basis for further rationally designing or improving the therapeutic vaccines against chronic hepatitis B and other

4. Materials and methods

4.1 Materials

4.1.1 Vaccine components

4.1.1.1 Antigens

Recombinant HBsAg (genotype A, adw) is a particulate HBV protein produced in yeast, which was purchased from Biovac (Cape Town, South Africa). Recombinant HBcAg (genotype D, ayw) is a particulate HBV protein produced in *E. coli*, which was kindly provided by Dr. Andris Dišlers, APP Latvijas Biomedicinas (Riga, Latvia).

Both HBsAg and HBcAg were used in priming immunization of therapeutic hepatitis B vaccine (*TherVacB*).

4.1.1.2 Adjuvants

Cyclic di-AMP (c-di-AMP) adjuvant was kindly provided by Prof. C. Guzmán (Helmholtz center for infection research) or purchased from InvivoGen company (San Diego, USA). Poly-ICLC adjuvant was kindly provided by LEUKOCARE biotechnology company (Martinsried, Germany). The RIG-I Ligand adjuvant was kindly provided by Prof. G. Hartmann, University of Bonn (Bonn, Germany). Aluminum hydroxide adjuvant was purchased from InvivoGen company (San Diego, USA).

Liposome (Lipo)- and squalene-in-water emulsion (SWE)-based combination adjuvants were formulated by combining various doses of immunostimulants TLR4 ligand monophosphoryl lipid A (MPL) and QS21 saponin with the Lipo and SWE delivery systems. These combination adjuvants and water-in-oil emulsion adjuvant Montanide ISA720 were kindly provided by Vaccine Formulation Institute (Lausanne, Switzerland).

These listed adjuvants were formulated with recombinant HBsAg/HBcAg for the priming immunization of *TherVacB*.

4.1.1.3 Viral vectors

Recombinant MVA-S and MVA-core are MVA vectors encoding HBsAg and HBcAg (HBV genotype D, ayw), respectively. Recombinant MVA-HBs/c is an MVA vector encoding HBsAg and HBcAg simultaneously with a P2A linker in between. These MVA vectors were generated in Prof. Protzer's lab, and were further amplified on DF-1 cells. VSV-GP vector is a non-toxic VSV chimeric variant with its G protein replaced by LCMV-derived glycoprotein, kindly provided by Prof. D. von Laer and Dr. J. Kimpel, Innsbruck Medical University (Innsbruck, Austria). Recombinant VSV-GP-HBs/c is a VSV-GP vector encoding both HBsAg and HBcAg with a P2A linker in between, which was constructed in this study. Both VSV-GP vectors were amplified on BHK-21 cells. These MVA vectors were used for the boost immunization of *TherVacB*. The VSV-GP-HBs/c vector was employed in different regimens to improve *TherVacB*.

4.1.2 Mouse models

4.1.2.1 Wild-type C57BL/6 mice

Eight to ten weeks old C57BL/6 mice (haplotype H-2^b) were purchased from Envigo RMS GmbH (Düsseldorf, Germany) or Janvier Labs (Le Genest-Saint-Isle, France). The mice were kept under specific pathogen-free (SPF) conditions at the animal facility of Technical University of Munich (TUM), following institutional guidelines.

4.1.2.2 HBV transgenic mice, strain HBV1.3.32

HBV transgenic (HBVtg) mouse lineage 1.3.32 was established on a C57BL/6 background (haplotype H-2^b). This mouse model encodes a 1.3-fold overlength HBV genome (genotype D, ayw), replicates HBV within the liver, and expresses all HBV antigens (Guidotti, 1995). The used HBVtg mice in this study were matched for sex, age (10 – 15 weeks old), and serum HBV antigen levels. The mice were bred and kept under SPF conditions at the biosafety level 2 animal facility of Helmholtz Center Munich (HMGU), following the institutional guidelines.

4.1.2.3 AAV-HBV mice

Persistent HBV replication in wild-type C57BL/6 mice was established by intravenous injection of a recombinant adeno-associated viral vector (AAV) carrying a 1.2-fold HBV genome (genotype D, ayw) (AAV-HBV1.2) as described in section 4.2.6.3. AAV-HBV1.2 virus stocks were produced by the Plateforme de Thérapie Génique in Nantes, France (INSERM U1089). The AAV-HBV mouse model shows persistence of HBV transcription and antigen expression, and HBV-specific immune tolerance can be observed (Dion, 2013; Lan, 2017), thereby, it is a suitable model to mimic chronic HBV infection. The mice were maintained under SPF conditions at the biosafety level 2 animal facilities of TUM or HMGU, following the institutional guidelines.

4.1.3 Cell lines

The used cell lines belong to the laboratory stocks of AG Protzer, TUM/HMGU.

Cell line	Description	Application
DF-1	Chicken embryo fibroblast cell line	MVA amplification
BHK-21	Baby hamster kidney fibroblast cell line	MVA titration and VSV-GP-HBs/c amplification and titration
HEK 293T	Human embryonic kidney cell line; Expressing a mutant version of SV40 large T antigen	VSV-GP-HBs/c rescue (plasmid transfection)

4.1.4 Cell culture media

Medium	Ingredients
DF-1 cell culture medium (DMEM GlutaMAX™ full medium)	DMEM GlutaMAX™ medium 10% FCS 50 U/ml penicillin/streptomycin
BHK-21 cell culture medium (RPMI full medium)	RPMI 1640 medium 10% FCS 50 U/ml penicillin/streptomycin
HEK 293T cell culture medium	DMEM medium 10% FCS 50 U/ml penicillin/streptomycin

Materials and methods

Murine primary lymphocyte culture medium	RPMI full medium
Murine hepatocyte digestion medium	RPMI full medium 200µg/ml collagenase type IV
Human monocytes differentiation medium	RPMI full medium 2 mM L-glutamine 20 ng/ml GM-CSF 20 ng/ml IL-4
Human dendritic cell culture medium	RPMI full medium 2 mM L-glutamine

4.1.5 Antibodies

4.1.5.1 Antibodies and dyes used for flow cytometric analysis of murine primary lymphocytes

Antibody/Dye	Dilution	Article number	Supplier
anti-mCD3 FITC	1:100	100203	Biologend
anti-mCD4 APC	1:100	553051	BD Biosciences
anti-mCD4 APC	1:100	17-0041-83	eBioscience
anti-mCD4 PE-Cy7	1:200	25-0042-82	eBioscience
anti-mCD8a Pacific Blue	1:90	558106	BD Biosciences
anti-mCD8a V500	1:150	560776	BD Biosciences
anti-mCD44 FITC	1:150	11-0441-85	eBioscience
anti-mCD45.2 PE	1:200	12-0454-83	eBioscience
anti-mCD49a PerCp-Cy5.5	1:200	142611	Biologend
anti-mCD69 AlexFluor 700	1:150	561238	BD Biosciences
anti-mIFN γ FITC	1:300	554411	BD Biosciences
anti-mTNF α PE-Cy7	1:200	557644	BD Biosciences
anti-hGzmB PE (cross-reactivity)	1:100	GRB04	Invitrogen
anti-mPD1 PerCp-eFluor 710	1:200	46-9985-82	eBioscience
anti-mTim-3 PE-Cy7	1:200	134010	Biologend
anti-mTIGIT APC	1:150	142105	Biologend
anti-mLag3 eFluor450	1:200	48-2231-80	eBioscience
anti-mCX3CR1 PE-Cy7	1:150	149016	Biologend
anti-mCXCR6 FITC	1:100	151108	Biologend
anti-mKLRG1 eFluor450	1:150	48-5893-80	eBioscience
Strep Tactin-APC	1:50	6-5010-001	IBA lifesciences
Strep Tactin-PE	1:50	6-5000-001	IBA lifesciences
Fixable Viability Dye eFluor780	1:5000	65-0865-18	eBioscience

4.1.5.2 Antibodies used for flow cytometric analysis of human primary cells

Antibody	Dilution	Article number	Supplier
anti-hCD1a PE	1:100	300106	Biologend
anti-hCD11c PerCp	1:100	337234	Biologend
anti-hCD14 BV510	1:100	301841	Biologend
anti-hCD80 PE	1:100	560925	BD Pharmigen
anti-hCD83 BV421	1:100	305324	Biologend
anti-hCD86 APC	1:200	305412	Biologend
anti-hCCR7 PE-Cy7	1:100	353226	Biologend
anti-hHLA-DR FITC	1:400	307632	Biologend
Human Fc Block	1:20	564220	BD Pharmigen

4.1.5.3 Other antibodies and conjugates

Antibody	Dilution	Application	Supplier
Mouse anti-HBs serum	1:2700	ELISA	A. Kosinska
Mouse anti-HBc serum	1:5000	ELISA	J. Su
Mouse naïve serum	1:2500	ELISA	J. Su
Goat anti-mouse IgG ₁	1:1000	ELISA	Sigma-Aldrich
Goat anti-mouse IgG _{2b}	1:1000	ELISA	Sigma-Aldrich
Rabbit anti-goat IgG, HRP conjugated	1:1000	ELISA	Sigma-Aldrich
Goat anti-mouse IgG, HRP conjugated	1:1000 or 1:10000	ELISA or WB	Sigma-Aldrich
Mouse Anti-Tubulin	1:5000	WB	Sigma-Aldrich
Mouse Anti-HBc (8C9)	1:1	WB	E. Kremmer
Mouse Anti-HBs (HB1)	1:1000 or 1:250	WB or IF	A. Zvirbliene
Polyclonal rabbit Abs (DAKO)	1:400	IF	DAKO
Anti-mouse IgG, Alex Fluor 647 conjugated	1:500	IF	Invitrogen
Anti-rabbit IgG, Alex Fluor 594 conjugated	1:1000	IF	Invitrogen
Anti-mCD4 (GK1.5)	-	<i>In vivo</i> depletion	AG Feederle, HMGU
Anti-mCD8 (RmCD8.2)	-	<i>In vivo</i> depletion	AG Feederle, HMGU
Anti-mouse IgG2b (isotype)	-	<i>In vivo</i> depletion	AG Feederle, HMGU

ELISA: Enzyme-linked immunosorbent assay; WB: Western blot; IF: Immunofluorescence.

Materials and methods

4.1.6 Peptides

Peptides used for *ex vivo* stimulation of murine lymphocytes are H-2K^b-restricted, which were synthesized by peptides&elephants GmbH, Germany.

4.1.6.1 HBsAg-derived peptide pool

Numbering	Amino acid position	Amino acid Sequence
Sp3-37	145-159	GNCTCIPIPSSWAF
Sp3-38	149-163	CIPIPSSWAFKYLW
Sp3-39	153-167	PSSWAFKYLWEWAS
Sp3-40	157-171	AFKYLWEWASARFS
Sp3-41	161-175	YLWEWASARFSWLSL
Sp3-42	165-179	WASARFSWLSLLVPF
Sp3-43	169-183	RFSWLSLLVPFVQWF
Sp3-44	173-187	LSELLVPFVQWFVGLS
Sp3-45	177-191	VPFVQWFVGLSPTVW
Sp3-46	181-195	QWFVGLSPTVWLSAI
Sp3-47	185-199	GLSPTVWLSAIWMMW
Sp3-48	189-203	TVWLSAIWMMWYWGP
Sp3-49	193-207	SAIWMMWYWGPSLYS
Sp3-50	197-211	MMWYWGPSLYSIVSP
Sp3-51	201-215	WGPSLYSIVSPFIPL
Sp3-52	205-219	LYSIVSPFIPLPIF
Sp3-53	209-223	VSPFIPLPIFFCLW
Sp3-54	213-226	IPLPIFFCLWVYI

4.1.6.2 HBcAg-derived peptide pool

Numbering	Amino acid position	Amino acid Sequence
Cp2-188	70-87	TWVGGNLEDPISRDLVVS
Cp2-189	77-94	EDPISRDLVVS YVNTNMG
Cp2-190	84-101	LVVSYVNTNMGLKFRQLL
Cp2-191	91-108	TNMGLKFRQLLWFHISCL
Cp2-192	98-115	RQLLWFHISCLTFGRET
Cp2-193	105-122	ISCLTFGRET VIEYLVSF
Cp2-194	112-129	RET VIEYLV SFGVWIRTP
Cp2-195	119-136	LVSFGVWIRTPPAYRPPN
Cp2-196	126-143	IRTPPAYRPPNAPILSTL
Cp2-197	133-150	RPPNAPILSTLPETT VVR
Cp2-198	140-157	LSTLPETT VVRRRGRSPR

4.1.6.3 Cytotoxic T lymphocytes epitopes

The following cytotoxic T lymphocytes (CTL) epitope peptides were used for *ex vivo* stimulation of murine lymphocytes. Moreover, B8R, C₉₃, S₁₉₀, OVA_{S8L} peptides were also used for MHC class I multimer conjugation.

CTL Epitope	Specificity	Amino acid Sequence
B8R	MVA	TSYKFESV
NP ₅₂	VSV	RGYVYQGL
C ₉₃	HBcAg	MGLKFRQL
S ₁₉₀	HBsAg (adw)	VWLSAIWM
S ₂₀₈	HBsAg (adw)	IVSPFIPL
OVA _{S8L}	Ovalbumin	SIINFEKL

4.1.7 Plasmids

Plasmid	Transgene product	Source
pVAX1-HBs/c	HBsAg-P2A-HBcAg	AG Protzer
pVSV-GP-HBs/c	VSV-GP-HBs/c	generated in this study
T436	VSV-GP-luciferase	J. Kimpel

4.1.8 Oligonucleotides

All used oligonucleotides were synthesized by Microsynth AG (Balgach, Switzerland).

Primer	Sequence (5'–3')	Application
HBs-P2A-HBc_fw	GATGCACTCGAGTGCCACCATGGAGAA CATC	Cloning pVSV-GP-HBs/c
HBs-P2A-HBc_rev	ACCCGGGCTAGCCTAACATTGAGAT TCCCG	Cloning pVSV-GP-HBs/c
HBV 1745	GGAGGGATACATAGAGGTTTCCTTGA	qPCR, HBV DNA
HBV 1844	GTTGCCCGTTTGTCTCTAATTC	qPCR, HBV DNA
mPrp_fw	GCGGTACATGTTTTACGGTAGTA	qPCR, normalization
mPrp_rev	GAGCAGGCCCATGATCCA	qPCR, normalization

Materials and methods

4.1.9 Enzymes

Product	Supplier
Accutase	Gibco
Collagenase type 4	Worthington
FastDigest restriction enzymes	Thermo Fisher Scientific
Phusion® Hot Start Flex 2x Master Mix	New England Biolabs
RNase A	Macherey-Nagel
T4 DNA Ligase	Thermo Fisher Scientific
Trypsin	Thermo Fisher Scientific

4.1.10 Commercial kits

Product	Supplier
ARCHITECT anti-HBe Reagent Kit	Abbott
ARCHITECT anti-HBs Reagent Kit	Abbott
ARCHITECT HBeAg Reagent Kit	Abbott
ARCHITECT HBsAg Reagent Kit	Abbott
ECL Western Blotting Detection Kit	GE Healthcare
EndoFree Plasmid Maxi Kit	Qiagen
Enzygnost® Anti-HBc monoclonal kit	Siemens Healthcare Diagnostics
Enzygnost® HBe monoclonal kit	Siemens Healthcare Diagnostics
Fixation/Permeabilization Solution Kit	BD Pharmingen
GeneJET Plasmid Miniprep Kit	Thermo Fisher Scientific
Human IL-6 uncoated ELISA	Invitrogen
Human Pan Monocyte Isolation Kit	Miltenyi Biotech
Human TNF ELISA Set (BD OptEIA)	BD Biosciences
LightCycler 480 SYBR green master mix	Roche
Mouse IFN γ uncoated ELISA	Invitrogen
Mouse IL-5 uncoated ELISA	Invitrogen
Mouse Monoclonal Antibody Isotyping Reagents	Sigma-Aldrich
NucleoSpin Tissue DNA	Macherey-Nagel
Plasmid PlusMidi Kit	Qiagen
QIAquick Gel Extraction Kit	Qiagen
QIAquick PCR Purification Kit	Qiagen

4.1.11 Buffers and solutions

Buffer/Solution	Ingredients
50× TAE buffer, pH8.0	2M Tris 2M Acetic acid 50mM EDTA H ₂ O
ELISA coating Carbonate buffer, pH9.6	0.05 M Carbonate-Bicarbonate H ₂ O
ELISA blocking buffer	5% (v/v) FCS PBS
ELISA washing buffer PBST	0.05% Tween 20 PBS
RIPA lysis buffer	50 mM Tris, pH 8.0 100 mM NaCl 1mM EDTA 0.5% sodium deoxycholate 0.1% SDS 1% NP-40 H ₂ O
6× SDS Protein Loading Buffer	375 mM Tris-HCl, pH 6.8 6% (w/v) SDS 4.8% (w/v) Glycerol 9% (v/v) 2-Mercaptoethanol 0.03% (w/v) Bromophenol blue H ₂ O
SDS-PAGE running buffer (10×)	25 mM Tris 192 mM glycine 0.1% (w/v) SDS H ₂ O
SDS-PAGE stacking gel, 5%, 2 ml	0.24 ml 40 % PAA/BISAA 0.5 ml 1M Tris pH 8.8 20 µl 10% SDS 2 µl TEMED 15 µl APS 1.25 ml H ₂ O

Materials and methods

SDS-PAGE separating gel, 12.5%, 8 ml	2.5 ml 40 % PAA/BISAA 3 ml 1M Tris pH 8.8 80 µl 10% SDS 7 µl TEMED 40 µl APS 2.5 ml H ₂ O
Western Blot blocking solution	5% (m/v) skim milk powder PBS
Western Blot washing buffer TBST pH7.4, 10×	200 mM Tris 1.4 M NaCl 0.1% (w/v) Tween 20 H ₂ O
Western blot transfer buffer, pH8.3	25 mM Tris 190 mM glycine 20% (v/v) methanol H ₂ O
Coomassie staining solution	0.1% (w/v) Coomassie brilliant blue-R250 40% (v/v) MetOH 10% (v/v) Acetic acid 50% (v/v) H ₂ O
Coomassie de-staining solution	40% (v/v) MetOH 10% (v/v) Acetic acid 50% (v/v) H ₂ O
10 mM Tris buffer, pH 9.0	10 mM Tris H ₂ O
36 % Sucrose, pH9.0	36% sucrose (w/v) 10 mM Tris buffer
80% Percoll solution, 100ml	72 ml pure Percoll 8 ml 10x PBS 20 ml 1x PBS
40% Percoll solution, 100ml	50 ml 80% Percoll solution 50 ml 1x PBS 100 IU/ml Heparin
ACK lysis buffer, pH7.2	150 mM NH ₄ Cl 10 mM KHCO ₃ 0.1 mM Na ₂ EDTA H ₂ O

FACS buffer	1% (v/v) FCS PBS
MACS buffer, pH7.2	2 mM EDTA 0.5% (w/v) BSA PBS

4.1.12 Chemicals and reagents

Product	Supplier
2-Mercaptoethanol	Roth
2-Phenoxyethanol	Roth
Acetic acid	Roth
Agarose	PeqLab
Ammonium persulfate (APS)	Roth
Ampicillin	Roth
Biocoll separating solution (density 1.077 g/ml)	Biochrom
Bovine serum albumin (BSA)	Roth
Brefeldin A (BFA)	Sigma-Aldrich
Coomassie brilliant blue-R250	Roth
D(+)-Saccharose	Roth
DAPI Fluoromount-G mounting solution	Southern Biotech
Dimethyl sulfoxide (DMSO)	Sigma-Aldrich
DNA ladder 1kb/100bp	Eurogentec
Ethanol	Roth
Ethylenediaminetetraacetic acid (EDTA)	Roth
Fetal calf serum (FCS)	Thermo Fisher scientific
Glycerol	Roth
Glycine	Roth
Heparin-Natrium 25000	Ratiopharm
Hydrochloric acid (HCl)	Roth
Isoflurane	Henry Schein
Isopropanol	Roth
Kanamycin	Roth
L-Glutamine, 200 mM	Gibco
Mercaptoethanol, 50 mM	Gibco
Methanol (MeOH)	Roth
Milk powder	Roth
NP-40	Serva

Materials and methods

Page RulerPlus Protein standard (SDS-PAGE)	Thermo Fisher scientific
Paraformaldehyde (PFA), 4 %	ChemCruz
Penicillin/streptomycin, 10000 U/ml	Gibco
Percoll density gradient media	GE Healthcare
Phosphate Buffered Saline (PBS), pH 7.4	Gibco
Phosphate-buffered saline (PBS), 10×	Gibco
Recombinant human GM-CSF	Peprtech
Recombinant human IL-4	Peprtech
RNAlater RNA Stabilization Reagent	Qiagen
Roti [®] -Safe GelStain	Roth
Sodium bicarbonate (NaHCO ₃)	Roth
Sodium carbonate (Na ₂ CO ₃)	Roth
Sodium chloride (NaCl)	Roth
Sodium hydroxide (NaOH)	Roth
Sulfuric acid (2 N)	Roth
Tetramethylethylenediamine (TEMED)	Roth
TMB, stabilized chromogen	Invitrogen
Tris(hydroxymethyl)-aminomethane (TRIS)	Roth
Triton X-100	Roth
Trypan blue	Gibco
Tween 20	Roth
Yeast extract	Roth

4.1.13 Laboratory devices and equipment

Product	Supplier
'Accu-jet pro' pipette	Brand
Agarose Gel electrophoresis device	PeqLab
Aperio AT2 slide scanner	Leica Biosystems
Architect [™] platform	Abbott Laboratories
BEP III platform	Siemens Healthcare
Cell culture incubator	Heraeus
Centrifuge 5920R	Eppendorf
CytoFLEX S	Beckman Coulter
ECL imaging system	Intas Science Imaging
ELISA-Reader Infinite F200	Tecan
Epson Perfection V200 Photo	Epson
Flow cytometer FACS Canto II	BD Biosciences

Fluoview FV10i confocal microscope	Olympus
Freezing device	Nalgene
Fusion Fx7 Imaging System	PeqLab
Leica Bond MAX system	Leica Biosystems
Libra 120 transmission electron microscope	Zeiss
LightCycler® 480 II	Roche
MACS separator MultiStand	Miltenyi Biotech
Multichannel Pipette	ABiMED
NanoDrop One	Thermo Fisher Scientific
Neubauer improved hemocytometer	Brand
Ohmeda Tec4 Anesthetic Vaporizer	Datex-Ohmeda
Optima L-90K Ultracentrifuge	Beckman Coulter
PCR Thermal Cycler	Thermo Fisher Scientific
pH meter	Mettler Toledo
Pipettes	Eppendorf
Reflotron® Reflovet Plus	Roche Diagnostics
Rotary microtome	Thermo Fisher Scientific
SCN 400 slide scanner	Leica Biosystems
SDS-PAGE device	Bio-Rad
Shaker and incubator for bacteria	INFORS AG; Heraeus
Sterile hood HERA safe	Thermo Fisher Scientific
Table-top centrifuge 5417R	Eppendorf
Thermo Mixer F1.5	Eppendorf
Ultracentrifuge SW 32 Ti Rotor	Beckman Coulter
Ultracentrifuge SW 41 Ti Rotor	Beckman Coulter
Ultrasonic homogenizer	Bandelin
Vi-CELL™ XR Cell Viability Analyzer	Beckman Coulter
Western Blotting Mini Trans-Blot® Cell device	Bio-Rad
Zeiss Axiovert 40C Inverted Microscope	Zeiss
Zetasizer Nano ZS instrument	Malvern

Materials and methods

4.1.14 Consumables

Product	Supplier
Amersham Hybond-P	GE healthcare
Blood lancets	Paul Marienfeld
Cell culture flasks, dishes, plates	TPP
Cell strainers 70 µm / 100 µm	Falcon
Centrifuge tubes, SW32 / SW41	Beckman Coulter
Disposable Capillary Zeta Cells	Malvern
Falcon tubes, 15 ml / 50 ml	Greiner Bio-One
Filter tips	Greiner Bio-One
Filters, 0.22 µm / 0.45 µm	Sarstedt
FrameStar® 96 Well plates for qPCR	4titude
Greiner Bio-One Cryotubes	Merck
HistoBond® adhesive microscope slides	Paul Marienfeld
Insulin syringes	B. Braun
MACS separation columns (MS, LS)	Miltenyi Biotech
Microvette 1.1 ml Serum-Gel tubes	Sarstedt
Microvette 500 LH-Gel tubes	Sarstedt
Needles 20, 23, 27 gauge	B. Braun
Nunc MaxiSorp flat-bottom 96 well plates	Thermo Fisher scientific
PCR tubes	Thermo Fisher scientific
Pipette tips 10 µl – 1 ml	Greiner Bio-One
Pipettes (disposable) 2, 5, 10, 25, 50 ml	Greiner Bio-One
Reaction tubes 1.5 ml, 2 ml	Eppendorf
Reagent reservoirs, sterile	Corning
Reflotron ALT (GPT) stripes	Roche Diagnostics
Round coverslips	VWR international
Surgical Disposable Scalpels	B. Braun
Syringes 1, 2, 5, 20 ml	B. Braun
UV cuvettes micro	Merck
V-bottom 96-well plates	Roth

4.1.15 Software

Software	Application	Supplier
Aperio eSlide Manager	Immunohistochemistry data analysis	Leica Biosystems
FlowJo 10.4	Flow cytometry data analysis	BD Biosciences
FV10-ASW 4.2 viewer	Immunofluorescence image analysis	Olympus
Graph Pad Prism 5.01	Graph design, statistical calculation	Graph Pad Software Inc
LightCycler 480 Software 1.5.1.62	qPCR data analysis	Roche
Serial Cloner 2.6.1	DNA sequence analysis	Serial Basics
Zetasizer software v7.13	Physicochemical data analysis	Malvern

4.2 Methods

4.2.1 General cell culture

4.2.1.1 Maintenance of cells

All primary cells or cell lines were cultured under standard cell culture conditions (37 °C, 5% CO₂, 95% humidity), and cell culture experiments were carried out under sterile conditions.

Adherent DF-1 cells were cultured in DMEM GlutaMAX™ medium supplemented with 10% FCS, 50 U/ml penicillin/streptomycin (referred to as DMEM GlutaMAX™ full medium) using T175 cell culture flasks. Cells were passaged 1:10 twice a week.

Adherent BHK-21 cells were cultured in RPMI 1640 medium supplemented with 10% FCS, 50 U/ml penicillin/streptomycin. Depending on confluency, cells were passaged 1:6 to 1:10 every three to four days.

Adherent 293T cells were cultured in DMEM medium supplemented with 10% FCS, 50 U/ml penicillin/streptomycin. Cells were passaged every three to four days based on the confluency.

For passaging, cells were washed once with 1x PBS and detached from the cell culture flasks by incubation with trypsin at 37 °C for two to three minutes. Afterwards, fresh cell culture medium was added to stop trypsin digestion. Cells were placed to new T175 flasks in 25 ml of fresh cell culture medium with the given concentration for further culture.

4.2.1.2 Counting of cells

To determine the cell numbers, first, cells (primary cells or cell lines) were resuspended thoroughly to obtain a single-cell suspension. For manual cell counting, 10 µl of the cell suspension was 1:1 diluted with trypan blue to stain dead cells, then counted employing a Neubauer improve hemocytometer under a light microscope (Zeiss). For automated counting, 25 µl of cell suspension was diluted 1:20 with PBS in a Vi-CELL sample vial and counted on a Vi-CELL™ XR Cell Viability Analyzer (Beckman Coulter).

4.2.1.3 Freezing and thawing of cells

For freezing, cells (primary cells or cell lines) were centrifuged at 560 x g for five minutes and resuspended with 500 µl of FCS containing 10% dimethyl sulfoxide (DMSO) in a cryovial. Then, the cryovial was placed at a cryo-freezer and stored at -80 °C. At least 24 hours later, frozen cells were transferred to -80 °C or liquid nitrogen for long-term storage.

For the thawing of cells, cell vials were quickly transferred from -80 °C or liquid nitrogen to a 37 °C water bath. Thawed cells were resuspended carefully and transferred to a new 50 ml falcon tube containing prewarmed culture medium. After centrifugation (560 x g, 5 min), cells were resuspended in the respective culture medium and either rested overnight (primary cells) or seeded in cell culture flasks (cell lines).

4.2.2 Recombinant MVA amplification

4.2.2.1 Amplification of recombinant MVA

To amplify recombinant MVAs (MVA-S, MVA-core, MVA-HBs/c) on a large scale, first, a pre-amplification MVA stock was generated. One T175 flask of confluent DF1 cells were incubated with 5 ml of DMEM GlutaMAX™ full medium containing 5 µl of previously purified MVA stock for one hour at 37 °C to facilitate the virus adsorption. Then, cells were supplemented with another 20 ml of DMEM GlutaMAX™ full medium and cultured for two to three days at 37 °C until a cytopathic effect was visible. Afterwards, the infected cells were removed from the flasks using a cell scraper and transferred together with the medium to a new 50 ml falcon tube to store at -80 °C (referred to as pre-amplification MVA stock).

In the next step, recombinant MVAs were produced on a large scale by the infection of 25 to 30 T175 flasks of DF1 cells. For this purpose, the pre-amplification MVA stock was diluted with DMEM GlutaMAX™ full medium and applied to these confluent DF1 cells (5 ml per flask), following by 20 ml of fresh full medium adding one hour after incubation. When the cytopathic effects were observed after two to three days of culture, the cells containing recombinant MVA were detached with cell scrapers and

Materials and methods

harvested by centrifugation (4000 x g, 5 min). Cell pellets were finally resuspended in 30 ml of 10 mM Tris buffer (pH 9.0) and stored at -80 °C for further MVA purification.

4.2.2.2 Purification of recombinant MVA

In the first step, to disrupt the cell membranes and release the MVA particles, the harvested cells were exposed to three freezing-thawing cycles (-80 °C / 37 °C), and three subsequent sonication steps. Briefly, cells were sonicated for 30 seconds three times on ice using an ultrasonic homogenizer (Bandelin) and then centrifuged (4000 x g, 5 min). The supernatant was collected in a new 50 ml falcon tube and the remaining cell debris was resuspended in 25 ml of 10 mM Tris buffer for the second sonication step. The procedure was repeated in total three times and resulted in 78 ml of virus supernatant.

In the next step, the MVA particles were concentrated by two-step sucrose cushion ultracentrifugation. For the first sucrose cushion, 25 ml of 36% sucrose in 10 mM Tris buffer was placed into each of six sterile SW32 centrifuge tubes. Subsequently, 13 ml of the MVA supernatant was carefully overlaid on the sucrose cushion of each tube. After centrifugation at 13,500 rpm and 4 °C for 90 minutes (Beckman Coulter, SW32 Ti rotor), the supernatant was discarded and the air-dried virus pellets were resuspended and pooled in 12 ml of 10 mM Tris buffer. For the second sucrose cushion, 2 ml of 12 ml MVA suspension, obtained from the first sucrose cushion, was carefully overlaid on 10 ml of 36% sucrose solution in each of six sterile SW41 centrifuge tubes and centrifuged (13,500 rpm, 4 °C, 90 min, SW41 Ti rotor). The purified MVA was finally resuspended in 200 – 300 µl of 10 mM Tris buffer and stored at -80 °C.

4.2.2.3 Determination of recombinant MVA titer

To determine the titer of newly purified MVA stock, BHK-21 monolayers were cultured till 90% confluency in 100 µl of RPMI medium containing 10% FCS in a flat-bottom 96-well plate at 37 °C. Then, the purified MVA stock was 10-fold serially diluted in RPMI medium containing 2% FCS to result in dilutions from 10^{-7} to 10^{-12} . 100µl of each virus dilution was added per well to a total of 16 replicates. After seven-day incubation, the

cytopathic effect of infection was analyzed by light microscopy (Zeiss) and the viral titer in infectious units (IFU)/ml was calculated with the following equation:

$$y = \{10^{a-0.5 + (Xa/16) + (Xb/16) + (Xc/16)}\} \times 10$$

a represents the highest dilution with 100 % of infected wells (e.g. 10^{-8} ; $a = 8$);

Xa, **Xb**, and **Xc** represent the numbers of infected wells in further dilutions.

The titers of MVA vectors were determined in cooperation with Julia Sacherl.

4.2.3 Characterization of the stability and integrity of novel adjuvant formulations *in vitro*

4.2.3.1 Physicochemical characterizations of the antigen/adjuvant formulations

The investigated antigen/adjuvant formulations (further referred to as adjuvant formulations) were kindly manufactured by the Vaccine Formulation Institute (VFI). Afterwards, the physicochemical characterizations of Lipo- and SWE-based formulations were performed by VFI at week 0, and after the incubation at 4 °C for one week and two weeks.

The average particle size and polydispersity index (PDI) of Lipo- and SWE-based formulations were characterized by dynamic light scattering (DLS) on a Zetasizer Nano ZS instrument (Malvern). Briefly, 10 µl of the formulation was diluted with 90 µl of PBS, subsequently 70 µl of the diluted formulation was placed in a UV cuvette for the measurement.

Zeta potential was measured by electrophoretic mobility on the same Zetasizer Nano ZS instrument. To this purpose, 10 µl of the formulation was diluted with 990 µl of 1 mM NaCl. Then, 1 ml of the diluted formulation was placed in a capillary zeta cell for the measurement.

The pH of formulation was measured by voltammetry on a pH meter (Mettler Toledo) equipped with a microelectrode. The measurement was performed 3 times with a sample aliquot of 50 µl. The room temperature was defined at 22 °C.

4.2.3.2 Enzyme-linked immunosorbent assay of adjuvanted HBsAg and HBcAg

The 96-well Nunc MaxiSorp plates were coated with 0.25 µg/ml and 0.625 µg/ml adjuvant formulations in 100 µl of carbonate buffer for HBsAg and HBcAg enzyme-linked immunosorbent assay (ELISA), respectively. The original HBsAg and HBcAg were included as positive controls. After overnight coating at 4 °C, plates were washed four times with PBS containing 0.05% tween (PBST) and blocked with 200 µl of blocking buffer (PBS containing 5% FCS) for one hour at room temperature (RT). The murine sera containing anti-HBs (1:2700 in PBS) and anti-HBc (1:5000 in PBS) were employed as primary antibodies for HBsAg and HBcAg ELISA, respectively. After four washing steps with PBST, 100 µl of the diluted sera were added to each well of respective plates, followed by two-hour incubation at RT. Then, 100 µl of secondary horseradish peroxidase (HRP)-conjugated goat anti-mouse IgG (1:1000 in PBS) was added to the PBST-washed plates and incubated for one hour at RT. After five washing steps, 100 µl of stabilized chromogen TMB solution was added to each well. The plates were incubated in the dark for two to three minutes and the reaction was stopped by adding 100 µl of 2N sulfuric acid per well. The optical density (OD) was determined at the wavelength of 450 nm (measurement) and 560 nm (background subtraction) employing an ELISA-Reader Infinite F200 (Tecan).

4.2.3.3 Native agarose gel electrophoresis of adjuvanted HBcAg

Native agarose gel electrophoresis (NAGE) was performed by using 1% w/v agarose gel containing Roti®-GelStain, with a thickness of 0.5 – 0.7 cm. The samples of 10 µg of formulated or original HBcAg were mixed with the DNA Gel loading dye and loaded into the wells of the agarose gel. Then, the electrophoresis was performed in 1 x TAE buffer at 150 V for 90 minutes (Bio-Rad). The nucleic acid in the HBcAg particle was visualized employed a Fusion Fx7 Imaging System (PeqLab). Hereafter, for the capsid protein detection, the gel was stained with Coomassie blue staining solution for 20 – 30 minutes and de-stained with the destaining solution for approximately 24 hours to remove excess dye from the background gel matrix. During the destaining procedure, the destaining solution needs to be changed every four to six hours. On the next day,

the gel with clearly visible protein bands was scanned with an Epson scanner (Epson).

4.2.3.4 Western blot analysis of adjuvanted HBsAg and HBcAg

For the Western blot analysis, 50 ng of the adjuvant formulations and original HBsAg or HBcAg were mixed with the SDS protein loading dye and denatured at 95 °C for 10 minutes. Then, these proteins were separated using Sodium Dodecyl Sulfate-polyacrylamide gel electrophoresis (SDS-PAGE) for approximately 90 minutes at 30 mA (Bio-Rad). Next, the proteins on the gel were blotted to a methanol-activated polyvinylidene difluoride (PVDF) membrane. The transfer was conducted using a Mini Trans-Blot® Cell device for two hours at 300mA (Bio-Rad). Afterwards, membranes were blocked with 5% milk powder in Tris-buffered saline (TBS) containing 1% Tween-20 (TBST) for one hour on a shaker at RT. For the immunoblotting, membranes were incubated with HBsAg-specific mouse monoclonal antibody (mAb) HB1 (1:1000 in TBST) or HBcAg-specific mouse mAb 8C9 in-house hybridoma supernatant (1:1 in 3% milk-TBST solution) overnight at 4 °C. Following three washing steps with TBST for 10 minutes each, membranes were incubated with secondary HRP-conjugated goat anti-mouse IgG (1:10,000 dilution in TBST) for two hours at 4 °C. After three washing steps, the blots were developed using Amersham ECL Prime Western Blotting Detection Reagent and protein bands were visualized by an ECL Chemocam Detection System (Intas).

4.2.3.5 Transmission electron microscopy

The Lipo-3 adjuvanted HBsAg/HBcAg or Lipo-3 adjuvant-only were absorbed for five minutes onto formvar/carbon film-coated copper grids. The grids were then negatively stained with 1% [w/v] phosphotungstic acid (PTA) for 20 seconds. Images were acquired using a Libra 120 transmission electron microscope with a magnification of 40,000x (Zeiss). The transmission electron microscopy analysis was kindly performed by Julia Sacherl.

4.2.4 Generation and stimulation of human monocyte-derived dendritic cells *in vitro*

4.2.4.1 Isolation of human peripheral blood mononuclear cells

Human peripheral blood mononuclear cells (PBMCs) were isolated by density gradient centrifugation using Biocoll solution. Fresh blood from healthy donors was mixed with heparin to avoid coagulation and 1:1 diluted with pre-warmed RPMI 1640 medium. 25 ml of the diluted blood was carefully overlaid on 12.5 ml of Biocoll solution in a 50 ml falcon tube. After centrifugation at 1200 x g, RT for 20 minutes without brake, PBMCs located in the middle ring were transferred to a new 50 ml falcon tube. The harvested PBMCs were washed twice and subsequently counted with the Vi-CELL™ XR Cell Viability Analyzer as described in section 4.2.1.2.

4.2.4.2 Generation of human monocyte-derived dendritic cells

Untouched monocytes were isolated from freshly prepared PBMCs by a negative selection magnetic-activated cell sorting (MACS) with human Pan Monocyte Isolation Kit. The isolation was performed following the manufacturer's instructions.

The isolated monocytes were cultivated in a 10 cm cell culture dish with RPMI 1640 medium supplemented with 10% FCS, 50 U/ml penicillin/streptomycin, 2 mM L-glutamine, 20 ng/ml recombinant GM-CSF and 20 ng/ml recombinant IL-4. On the next day, cells were supplemented with another 20 ng/ml GM-CSF and 20 ng/ml IL-4. 5 ml of fresh culture medium including the same amount of GM-CSF and IL-4 was added after three days of culture. At day 6, the floating cells were harvested as immature human monocyte-derived dendritic cells (hMoDCs) for further studies.

4.2.4.3 Stimulation of hMoDCs with adjuvants

Approximately 1×10^5 immature hMoDCs were incubated in 200µl of cell culture medium containing 1/40 immunization dose of Lipo- or SWE-based combination adjuvants (listed in table 2.2), or delivery systems only, or 1µg/ml LPS or without adjuvant (no adj) in a 96-well flat-bottom plate. Two sets of stimulated cells were incubated for 6 and 48 hours, respectively. Upon incubation, supernatants were

harvested to determine the cytokine secretion by ELISA. Adherent hMoDCs were detached by incubation with Accutase for seven minutes. Subsequently, the expression of co-stimulatory molecules and activation markers on the cell surface was analyzed by flow cytometry.

4.2.4.4 Characterization of hMoDCs activation

To study the cytokine secretion profile of activated hMoDCs, the concentrations of proinflammatory cytokine IL-6 and TNF α in supernatants were determined by commercial ELISA kits, according to the manufacturer's instructions. ELISAs were performed on Nunc MaxiSorp plates and absorbance was measured with an ELISA-Reader Infinite F200 (Tecan).

For the analyses of cell surface markers by flow cytometry, cells were pre-incubated with 20 μ l of human BD Fc Block™ for 10 minutes. Afterwards, 30 μ l of fluorescence-labeled antibody cocktail recognizing human CD14, CD11c, CD86, CD80, CD83, HLA-DR molecules was directly added to each well for the cell surface staining. In addition, to exclude the dead cells from the analysis, the fixable viability dye eF780 was added to the antibody cocktail. After 25 minutes of incubation on ice in the dark, cells were washed twice and analyzed on a CytoFlexS flow cytometer (Beckmann Coulter).

4.2.5 Generation and characterization of VSV-GP-HBs/c vector

4.2.5.1 Cloning of plasmid VSV-GP-HBs/c

To generate VSV-GP virus encoding HBsAg and HBcAg (VSV-GP-HBs/c), first, the gene of interest was cloned into the VSV-GP genomic plasmid (pVSV-GP). Plasmid T436 was a pVSV-GP variant that contains the viral genes for VSV (N, P, M, L, the glycoprotein of LCMV) and the luciferase gene on position 5 under a T7 promoter. The position 5 in the plasmid is flanked by the restriction sites XhoI and NheI. The pVAX1 plasmid containing the sequences of HBsAg and HBcAg with a P2A linker (HBs/c) were constructed previously in AG Protzer, TUM. The cloning strategy of pVSV-GP-HBs/c was to exchange the luciferase gene in T436 plasmid with HBs/c insert from the pVAX1 plasmid. Therefore, the luciferase gene on position 5 of T436 was removed by

Materials and methods

the XhoI and NheI restriction enzyme digestion. Subsequently, the HBs/c insert was cleaved out of the pVAX1 plasmid using the same restriction enzymes and then ligated into the XhoI/NheI site of pVSV-GP to obtain pVSV-GP-HBs/c.

4.2.5.2 Rescue and production of VSV-GP-HBs/c virus

The recombinant VSV-GP-HBs/c was rescued by the reverse genetics system, as described previously (Marzi, 2011). Briefly, using the calcium-phosphate precipitation method, 293T cells were simultaneously transfected with the following DNA mix: genomic plasmid pVSV-GP-HBs/c; plasmids expressing VSV proteins: N, P, M, L, and original G protein of VSV; and the plasmid expressing the bacteriophage T7 polymerase. After 48 – 72 hours incubation at 37 °C, visible cytopathic effects were observed and the transfected cells were harvested as crude cell suspension of newly rescued virus. To promote the newly rescued virus growth, the crude cell suspension was co-cultivated with BHK-21 cells for two to three passages. Afterwards, the newly rescued virus was purified by two-round plaque purification.

To amplify the new VSV-GP-HBs/c vector, 1.1×10^7 BHK-21 cells were seeded in a 15 cm cell culture dish and incubated overnight at 37 °C. On the next day, the ~80 % confluent cells were infected with 0.01 multiplicity of infection (MOI) of the virus and incubated at 37 °C for 24 – 36 hours until massive cytopathic effect could be observed. Then, the supernatant containing virus particles was collected and filtrated with a 0.45 µm filter. Next, the virus was concentrated by 20% sucrose cushion centrifugation at 4000 x g overnight. Afterwards, the supernatant was discarded and the virus pellet was resuspended in PBS and aliquoted for storage at -80 °C. Thereafter, the titer of the virus stock was determined by TCID₅₀ (median tissue culture infective dose) assay.

The rescue and production of VSV-GP-HBs/c vector were performed together with Dr. Janine Kimpel in the Division of Virology, Innsbruck Medical University.

4.2.5.3 Validation of antigen expression in BHK-21 cells after VSV-GP-HBs/c infection by Western blot analysis

For the Western blot analysis, ~90 % confluent BHK-21 cells in a 6-well plate were

infected with 0.1 MOI of 'empty' VSV-GP or VSV-GP-HBs/c for 40 hours. Then, the cell culture medium was removed and the cell lysates were prepared. To this purpose, 250 μ l of RIPA buffer containing 1 x protease inhibitor was applied to each well of the 6-well plate. After incubation on ice for five minutes, cell debris was pelleted by centrifugation (12,000 x g, 10 min, 4 °C) and the supernatant (protein lysate) was collected. Protein lysate was mixed with SDS protein loading dye and denatured at 95 °C for 10 minutes. Afterwards, the protein lysates were stored at -20 °C for the further western blot analysis. The detailed procedures of Western blot were presented previously in section 4.2.3.4.

4.2.5.4 Validation of antigen expression in BHK-21 cells after VSV-GP-HBs/c infection by immunofluorescence staining

For the immunofluorescence staining, 2×10^5 BHK-21 cells per well were seeded into a 24-well plate containing one sterile coverslip in each well. After 24 hours of culture, cells reached a confluency of ~90%. Then, cells were infected with 0.1 MOI VSV-GP or VSV-GP-HBs/c and incubated for 40 hours. Afterwards, the infected cells were fixed with 4% paraformaldehyde (PFA) (pH 7.4) for 20 minutes at RT and permeabilized with PBS containing 0.1% Triton X-100 for 10 minutes at RT. Blocking was performed for two hours at RT using PBS containing 10% goat serum. Next, cells were incubated with 300 μ l of primary HBsAg-specific mouse mAb HB1 (1:250) or HBcAg-specific rabbit polyclonal antibodies DAKO (1:400) in PBS containing 1% goat serum overnight at 4 °C. After three washing steps with PBS, cells were incubated with 300 μ l of respective secondary Alex Fluor 647-conjugated anti-mouse IgG (1:500) or Alex Fluor 594-conjugated anti-rabbit IgG (1:1000) antibodies in PBS containing 1% goat serum for two hours at RT in the dark. After another three washing steps with PBS, the coverslips with the stained cells were transferred to microscope slides and mounted with DAPI Fluoromount-G (SouthernBiotech). Following overnight storage in the dark at 4 °C, the slides were analyzed employing a Fluoview FV10i confocal microscope (Olympus).

4.2.6 Mouse experiments

Animal experiments were conducted in strict accordance with the German regulations of the Society for Laboratory Animal Science (GV-SOLAS) and the European Health Law of the Federation of Laboratory Animal Science Associations (FELASA). Experiments were approved by the District Government of Upper Bavaria (permission numbers: 55.2-1-54-2532-103-12 and ROB-55.2-2532.Vet_02-18-24). Mice were kept under specific-pathogen-free (SPF) conditions at the biosafety level 2 animal facilities of TUM or HMGU, following institutional guidelines.

4.2.6.1 Weight monitoring

The weight of mice was monitored weekly throughout the experiments to determine the potential side effects of treatments.

4.2.6.2 Blood withdrawal

Mice were bled from the submandibular vein (cheek pouch) using bleeding lancets. Blood was collected in Microvette 500 Lithium Heparin (LH)-Gel tubes when both flow cytometric analysis of leukocytes and HBV serological analyses were needed. Blood was collected in Microvette 1.1 ml Serum-Gel tubes when only HBV serological analyses were required. Plasma or serum samples were obtained by centrifugation of blood (10,000 x g, 10 min). Afterwards, the isolated plasma or sera were transferred into new tubes and stored at -20 °C for further analyses.

4.2.6.3 AAV-HBV transduction

Eight to ten weeks old C57BL/6 male mice were transduced with $4-6 \times 10^9$ genome equivalents (GE) of AAV-HBV1.2 vector (diluted with PBS in 100 μ l) through tail vein injection. Persistent HBV replication was established six weeks after the AAV-HBV transduction. Mice were bled shortly before the first immunization and allocated into groups with comparable HBeAg and HBsAg levels. The intravenous injection of AAV-HBV1.2 vector was kindly performed by Dr. Anna Kosinska.

4.2.6.4 Vaccine administration

Intramuscular injection (i.m.) of mice was administered in the quadriceps muscles of both hind limbs using a 27-gauge needle. The tip of the needle was directed away from the femur and sciatic nerve. Adjuvanted antigens and recombinant viral vectors for immunization were diluted to the given concentration in 100 µl of sterile PBS and 50 µl per leg was injected.

Subcutaneous (s.c.) vaccine administration was performed into the loose skin over the interscapular with an insulin syringe. The s.c. injection was used for the adjuvanted antigen administration during the study of delivery route comparison. The adjuvanted antigen was diluted in a volume of 100 µl and injected into each mouse.

For the intraperitoneal (i.p.) injection, the conscious mouse was held in a supine position with its posterior end slightly elevated. The administration was performed with an insulin syringe almost parallel to its vertebral column to avoid accidental penetration of the viscera. The i.p. injection was used for recombinant MVA administration during the study of delivery route comparison. The volume for recombinant MVA immunization was 200 µl per mouse.

In the present study, mice were immunized with a heterologous protein prime – MVA boost therapeutic hepatitis B vaccine (*TherVacB*) regimen as describes previously (Backes and Jäger, 2016). Briefly, mice were immunized twice with 10 µg of each particulate HBsAg and HBcAg formulated with different adjuvants at a 2-week interval. Two weeks after the second protein immunization, mice received 3×10^7 infectious units of each recombinant MVA vectors expressing HBV S or HBV core proteins. The detailed immunization schemes for individual experiments are stated in the respective result parts.

4.2.6.5 T-cell subset depletion

For depletion of CD4 T cells during the priming phase of *TherVacB*, mice were injected intraperitoneally (i.p.) with 300 µg of anti-mouse CD4 GK1.5 mAb one day before and 150 µg on the day of first protein immunization. On the day of second protein immunization, the mice received 150 µg of GK1.5 mAb to maintain the depletion. As

Materials and methods

an isotype control, rat IgG_{2b} mAb was injected with the same dose and schedule as anti-mouse CD4 GK1.5 mAb.

For depletion of CD8 T cells during the priming phase of *TherVacB*, mice received 50 µg and 25 µg of anti-mouse CD8 RmCD8.2 mAb i.p. on the day of first and second immunization, respectively.

To monitor the recovery rate after depletion, the levels of CD4 and CD8 T cells in the blood of the depleted mice were examined during the experiment by flow cytometry using the cell surface staining method described in section 4.2.4.3.

4.2.6.6 Organ removal

At the endpoint of experiments, mice were euthanized by cervical dislocation. After skin incision, the axillary and inguinal lymph nodes were removed by curved forceps and stored in the RPMI 1640 medium (referred to as wash medium) on ice. Then, the abdominal cavity was open via one midline incision. Blood was collected from the inferior vena cava with a 1 ml syringe. Afterwards, liver perfusion was performed to flush out the non-liver associated lymphocytes from the hepatic vasculature. For this purpose, liver was perfused with PBS through the portal vein until the liver was drained off blood and appeared pale. Subsequently, the liver and spleen were excised from the mice and kept in the wash medium on ice until further procedures.

4.2.7 Isolation of lymphocytes from different murine organs

4.2.7.1 Isolation of splenocytes

For splenocyte isolation, spleen was mashed through a 100 µm cell strainer with the plunger of a 2 ml syringe. After centrifugation at 560 x g, 4 °C for five minutes, erythrocytes were lysed by incubating the cells with ammonium-chloride-potassium (ACK) lysis buffer for one minute at RT. The lysis reaction was terminated by adding 45 ml of wash medium and cells were centrifuged as described above. Subsequently, cell pellet was resuspended in 4 ml of RPMI 1640 medium supplemented with 10% FCS and 50 IU/ml penicillin-streptomycin (referred to as RPMI full medium). Last, the

single-cell suspension was obtained by filtrating the resuspended cells through a 100 µm cell strainer.

4.2.7.2 Isolation of liver-associated lymphocytes

Liver-associated lymphocytes (LALs) were isolated by density gradient centrifugation. Murine liver was mashed through a 100 µm cell strainer with the plunger of a 2 ml syringe. After washing, cells were resuspended in 10 ml of freshly prepared enzyme solution (200 µg/ml of collagenase type IV in RPMI full medium) and digested for 30 minutes at 37 °C. Digestion was stopped by adding 40 ml of wash medium. After centrifugation, cells were resuspended in 3 ml of 40% Percoll solution containing 100 IU/ml Heparin and carefully overlaid on 3ml of 80% Percoll solution in a 15 ml falcon tube. Then, the cells were centrifuged at 1700 x g, RT, for 20 minutes, without brake. Thereafter, the lymphocyte layer between 40% and 80% Percoll solution was collected to a new 50 ml falcon tube. After one more washing step, the cells were resuspended in a minimal volume of RPMI full medium needed for further analyses.

The isolation of splenocytes and LALs was performed with the kind support from Dr. Anna Kosinska.

4.2.7.3 Isolation of lymphocytes from blood

To isolate the lymphocytes from murine blood, first, 20 µl of heparinized whole blood was transferred from the Microvette 500 LH-Gel tubes to the wells of a V-bottom 96-well plate. Then, the cells were incubated with 250 µl of ACK lysis buffer for seven minutes at RT to lyse the erythrocytes. Another round of lysis with two-minute incubation was performed if the erythrocytes were not completely lysed during the first round. After washing, the lymphocytes were used for further analyses.

4.2.7.4 Isolation of lymphocytes from lymph nodes

To generate a single-cell lymphocyte suspension from lymph nodes, the collected lymph nodes were homogenized thoroughly with the plunger of a 2 ml syringe on a 70 µm cell strainer. Subsequently, cells were washed once with 45 ml of wash medium and resuspended in the desired amount of RPMI full medium.

4.2.8 Detection of T-cell responses in murine primary lymphocytes

In the present study, HBV-specific T-cell responses were characterized by major histocompatibility complex (MHC) class I multimer staining, intracellular cytokine staining, and cytokine secretion in the supernatants of cultured primary lymphocytes.

4.2.8.1 Multimer staining

MHC class I multimer staining was used to detect the presence of antigen-specific CD8 T cells. MHC class I multimers conjugated with H-2K^b-restricted HBV derived peptides S₁₉₀, C₉₃, or ovalbumin-derived peptide (OVA_{S8L}) were kindly produced by Prof. Dirk Busch's lab (Institute of Microbiology, TUM). Hereafter, all the staining steps for flow cytometry analyses were incubated on ice in the dark. Per sample, 0.4 µg of multimer was labeled with 0.4 µl of Strep-Tactin-APC in 30 µl of FACS buffer (PBS containing 1% FCS) and incubated for 30 minutes. Afterwards, the APC-labelled multimers were incubated with splenocytes or LALs in a V-bottom 96-well plate for 20 minutes. Subsequently, 20 µl of fluorescence-labeled antibody cocktail recognizing CD8 and other immunophenotyping cell surface molecules were directly added to each well and incubated for another 30 minutes. Dead cells were excluded from analysis by staining with Fixable Viability Dye e780. After incubation, cells were washed twice with FACS buffer and analyzed on the CytoFlexS flow cytometer. Data analysis was performed using FlowJo software. Data are presented as relative values after background subtraction determined by OVA_{S8L} multimer. The multimer staining was performed together with Dr. Anna Kosinska.

4.2.8.2 Intracellular cytokine staining

For estimation of intracellular production of the cytokines, first, primary lymphocytes were stimulated with indicated peptides or peptide pools overnight in the presence of brefeldin A (BFA) *ex vivo*. Up to 2×10^6 of freshly isolated splenocytes, LALs, or lymphocytes from blood per well were plated in flat-bottom 96-well plates in 200 µl of RPMI full medium. For stimulation, HBsAg- and HBcAg-derived overlapping peptide pools or individual peptides were added to the cells in a final concentration of 2 µg/ml.

While cells stimulated with ovalbumin-derived peptide (OVA_{S8L}) served as a negative control, cells stimulated with MVA- or VSV-derived peptides B8R or NP52 were set up as positive controls. The amino acid sequences of the peptides used for stimulation were listed at 4.1.6. After one-hour stimulation at 37 °C, BFA was added to the cells with a final concentration of 1 µg/ml. Subsequently, cells were cultured for 14 – 16 hours at 37 °C and the intracellular cytokine staining (ICS) was performed on the following day.

After the incubation time, cells were transferred to V-bottom 96-well plates for the staining. All the following incubation steps were performed on ice in the dark. First, cells were stained with the cocktail containing anti-CD4, anti-CD8 antibodies, and fixable viability dye eF780 in 50 µl of FACS buffer for 30 minutes. After one washing step with 200 µl of FACS buffer, cells were fixed and permeabilized with 80 µl of Cytofix/Cytoperm for 17 minutes. Next, cells were washed once with 200 µl of 1 x Perm/Wash buffer, and stained with anti-IFN γ , anti-TNF α , and anti-Granzyme B antibodies in 50 µl of 1 x Perm/Wash buffer for 25 minutes. Afterwards, cells were washed once with 1 x Perm/Wash buffer and once with FACS buffer, and then resuspended in 200 µl of FACS buffer for the measurements on the CytoFlexS flow cytometer. Analysis was performed with the FlowJo software. Data are presented as relative values after background subtraction determined by OVA_{S8L} peptide.

4.2.8.3 Cytokine secretion by stimulated splenocytes

Up to 2×10^6 freshly isolated splenocytes per well were seeded into flat-bottom 96-well plates. For the stimulation, 20 µg/ml HBsAg or HBcAg were added to the cells in a final volume of 300 µl per well. After 48-hour incubation at 37 °C, the supernatants of the cells were harvested and stored at -20 °C.

The concentration of IFN γ and IL-5 in the supernatants were determined by commercial ELISA kits, according to the manufacturer's instructions. ELISAs were performed on Nunc MaxiSorp plates and absorbance was measured with an ELISA-Reader Infinite F200.

4.2.9 Analyses of HBV parameters in murine serum and liver tissue

4.2.9.1 Quantification of serum HBsAg and HBeAg

HBsAg, HBeAg titers were quantified in serum samples diluted 1:20 or 1:100 with PBS on an Architect™ platform (Abbott Laboratories) using the quantitative HBsAg test (6C36-44; cut-off, 0.25 IU/mL), the HBeAg Reagent Kit (6C32-27) with HBeAg Quantitative Calibrators (7P24-01; cut-off, 0.20 PEI U/mL).

4.2.9.2 Detection of anti-HBs and anti-HBc in murine serum

The level of anti-HBs was quantified in serum samples 1:100 diluted in PBS on the Architect™ platform using the anti-HBs test (7C18-27; cut-off, 12.5 mIU/mL). The level of anti-HBc was determined after 1:50 or 1:100 dilution in PBS using the Enzygnost® Anti-HBc monoclonal test on a BEP III platform (Siemens Healthcare).

The IgG subclasses of anti-HBs and anti-HBc were detected by ELISA. The detailed procedures of ELISA were described previously in section 4.2.3.2. The main steps of IgG subclasses ELISA are presented in the following. First, the 96-well Nunc MaxiSorp plates were coated with 0.25 µg/ml of HBsAg or 0.625 µg/ml of HBcAg at 4 °C overnight. After blocking, the investigated murine sera were added to both HBsAg and HBcAg coated plates with a dilution of 1:10,000 for two-hour incubation at RT. Next, 100 µl of goat anti-mouse IgG₁ (1:1000) or IgG_{2b} (1:1000) was applied to each well and incubated for one hour at RT. For detection, plates were incubated with HRP-conjugated rabbit anti-goat IgG (1:1000) for 30 minutes at RT. Optical density was read on the ELISA-Reader Infinite F200.

4.2.9.3 Evaluation of serum ALT level

Alanine aminotransferase (ALT) level was measured in serum samples diluted 1:4 with PBS using Reflotron® ALT tests (Roche Diagnostics), according to the manufacturer's instructions.

4.2.9.4 Analysis of intrahepatic HBV DNA

For the intrahepatic HBV DNA analysis, approximately 20 mg of liver tissue was cut from the murine liver and stored at -20 °C in 180 µl of T1 buffer of NucleoSpin Tissue Kit (Macherey-Nagel). On the day of DNA isolation, the sample was thawed and DNA was extracted according to the manufacturer’s instructions.

Total intrahepatic HBV DNA (primers: HBV 1745, HBV 1844) and mouse single copy prion protein (mPrp), as a reference gene (primers: mPrp_fw, mPrp_rev), were determined by quantitative PCR (qPCR) on a LightCycler 480 real-time PCR system (Roche). One reaction of qPCR contained 5 µl of LightCycler 480 SYBR Green Master Mix, 0.5 µl of forward and reverse primers (20 µM), 4 µl of extracted DNA (≤ 50 ng total DNA). Detailed information about primer sequences are listed in section 4.1.8 and the conditions of the PCR reaction are presented below. Data was analyzed by advanced relative quantification considering primer efficiency and normalization to mPrp gene using the LightCycler 480 software (Roche).

The qPCR program for HBV DNA copies normalized to mPrp:

	Temperature [°C]	Time [sec]	Ramp [°C/sec]	Acquisition mode	Cycles
Denaturation	95	300	4.4		1
Amplification	95	25	4.4	Single	45
	60	10	2.2		
	72	30	4.4		
Melting	95	1	4.4	continuous: 5°C	1
	65	60	2.2		
	95		0.11		
Cooling	40	30	2.2		1

4.2.9.5 Immunohistochemistry

For histological analysis, liver tissue samples were fixed in 4% PFA for 48 hours and then stored in PBS until paraffin-embedding. The paraffin sections were subjected to hematoxylin/eosin (HE) and core-specific immunohistochemistry staining as previously described (Kosinska, 2019). Briefly, 2-µm-thin liver sections were prepared with

Materials and methods

a rotary microtome (Thermo Fisher Scientific). Immunohistochemistry was performed using a Bond Max system (Leica) with core-specific primary rabbit polyclonal antibodies (1:50) and HRP-coupled secondary anti-rabbit IgG antibody. Slides were scanned using an SCN 400 slide scanner (Leica Biosystems). Afterwards, the numbers of core-positive hepatocytes were determined based on localization, intensity, and distribution of the signal in random 10 view fields (40x magnification). The mean numbers of core-positive hepatocytes were quantified per mm². The procedures of immunohistochemistry were kindly performed by the core facility Comparative experimental Pathology (CeP) in University hospital Rechts der Isar, TUM.

4.2.10 Statistical analysis

Statistical analyses were performed using GraphPad Prism version 5.0 for Windows (GraphPad Software Inc.). Results are presented as individual or mean values with standard error of the mean (SEM). Statistical difference was analyzed using Student's unpaired two-tailed t-test, Wilcoxon test, Mann-Whitney test, Kruskal-Wallis test with Dunn's multiple comparison correction, 2-way ANOVA with Tukey's multiple comparison correction. Significance levels were defined as: * $p < 0.05$, ** $p < 0.01$, *** $p < 0.001$.

5. List of figures

Fig.1.1 The structure of HBV virions and subviral particles.....	18
Fig.1.2 The genome organization of HBV.....	19
Fig.1.3 The mechanisms involved in T-cell exhaustion during chronic HBV infection.	21
Fig.1.4 Antiviral functions of HBV-specific CD8 T cells.....	26
Fig.1.5 Antiviral functions of B cells and antibodies in HBV infection.	27
Fig.1.6 The potential mechanisms of action of adjuvants.....	34
Fig.2.1 Immunization scheme of adjuvant selection.	42
Fig.2.2 Antibody responses and HBV serological analyses of adjuvant selection. ...	43
Fig.2.3 T-cell response analysis of adjuvant selection.	44
Fig.2.4 Immunization scheme of MVA dose titration.	45
Fig.2.5 Antibody responses and HBV serological analyses of MVA dose titration. ..	46
Fig.2.6 T-cell response analysis of MVA dose titration.	47
Fig.2.7 Immunization scheme of protein dose titration.....	48
Fig.2.8 Antibody responses and HBV serological analyses of protein dose titration. 49	
Fig.2.9 T-cell response analysis of protein dose titration.	50
Fig.2.10 Immunization scheme of different delivery routes for various adjuvants.....	51
Fig.2.11 Antibody response and antigen level analyses of different delivery routes for various adjuvants.	53
Fig.2.12 T-cell response analysis of different delivery routes for various adjuvants. 56	
Fig.2.13 Weight monitoring of different delivery routes for various adjuvants.....	57
Fig.2.14 Physicochemical characterization of the Lipo- and SWE-based formulations.	62
Fig.2.15 Antigen integrity analysis of the adjuvant formulations at week 0 <i>in vitro</i> . ..	64
Fig.2.16 Antigen integrity analyses of the adjuvant formulations after 12 weeks of storage <i>in vitro</i>	65
Fig.2.17 The scheme of human-derived dendritic cell generation and stimulation. ..	67
Fig.2.18 Activation of hMoDCs by Lipo- and SWE-based combinations adjuvants. .	68

List of figures

Fig.2.19 Immunization scheme of novel adjuvant formulations in wild-type C57BL/6 mice.	69
Fig.2.20 Humoral responses induced by immunization with novel adjuvant formulations in wild-type C57BL/6 mice.	71
Fig.2.21 CD4 T-cell responses induced by the immunization with novel adjuvant formulations in wild-type C57BL/6 mice.	72
Fig.2.22 CD8 T-cell responses induced by immunization with novel adjuvant formulations in wild-type C57BL/6 mice.	74
Fig.2.23 Immunization scheme of novel adjuvant formulations in short-term analysis of AAV-HBV mice.	76
Fig.2.24 Antibody response and antigen decrease induced by immunization with novel adjuvant formulations in short-term analysis of AAV-HBV mice.	77
Fig.2.25 Validation of T-cell response analysis in murine blood.	78
Fig.2.26 T-cell responses in blood induced by immunization with novel adjuvant formulations in the short-term analysis of AAV-HBV mice.	80
Fig.2.27 Experimental scheme and weight monitoring of AAV-HBV mice immunized with novel adjuvant formulations in long-term analysis.	81
Fig.2.28 Antibody responses induced by immunization with novel adjuvant formulations in long-term analysis of AAV-HBV mice.	83
Fig.2.29 Helper T-cell responses induced by immunization with novel adjuvant formulations in long-term analysis of AAV-HBV mice.	85
Fig.2.30 Antigen-specific CD8 T cells induced by immunization with novel adjuvant formulations in the liver and spleen of AAV-HBV mice in long-term analysis.	86
Fig.2.31 The functionality of S-specific CD8 T cells induced by immunization with novel adjuvant formulations in the liver and spleen of AAV-HBV mice in long-term analysis.	87
Fig.2.32 The functionality of core-specific CD8 T cells induced by immunization with novel adjuvant formulations in the liver and spleen of AAV-HBV mice in long-term analysis.	89

Fig.2.33 Long-term antiviral effects induced by immunization with novel adjuvant formulations in AAV-HBV mice.....	91
Fig.2.34 Experimental scheme of adjuvant only for priming in AAV-HBV mice.....	94
Fig.2.35 Antibody responses induced by priming with adjuvant only in AAV-HBV mice.	94
Fig.2.36 T-cell responses induced by priming with adjuvant only in AAV-HBV mice.	95
Fig.2.37 Antigen decreases induced by priming with adjuvant only in AAV-HBV mice.	96
Fig.2.38 Experimental scheme of different types of adjuvants for priming in AAV-HBV mice.	97
Fig.2.39 The humoral immune responses of different types of adjuvants for priming in AAV-HBV mice.	98
Fig.2.40 Helper T-cell responses of different types of adjuvants for priming in AAV-HBV mice.	100
Fig.2.41 The CD4 and CD8 T-cell responses of different types of adjuvants for priming in AAV-HBV mice.....	101
Fig.2.42 CD4 and CD8 T-cell depletion in different organs of naïve mice.	104
Fig.2.43 Experimental scheme and monitoring of CD4 and CD8 T-cell counts after depletion during <i>TherVacB</i> in AAV-HBV mice.	106
Fig.2.44 Antigen kinetics and antibody responses after depletion of CD4 or CD8 T cells during the priming phase of <i>TherVacB</i> in AAV-HBV mice.....	107
Fig.2.45 T-cell responses after CD4 and CD8 T-cell depletion during the priming of <i>TherVacB</i> in AAV-HBV mice.	109
Fig.2.46 Cloning strategy and control digestion of pVSV-GP encoding HBsAg and HBcAg.....	112
Fig.2.47 Scheme of recombinant VSV-GP virus generation.	113
Fig.2.48 HBsAg and HBcAg expression in BHK-21 cells after VSV-GP-HBs/c infection.	115
Fig.2.49 First immunogenicity trial of VSV-GP-HBs/c in wild-type C57BL/6 mice....	117

List of figures

Fig.2.50 Immunization schemes of different heterologous prime-boost strategies with VSV-GP-HBs/c in wild-type C57BL/6 mice.	118
Fig.2.51 Antibody and CD4 T-cell responses induced by immunization with different heterologous prime-boost strategies with VSV-GP-HBs/c in wild-type C57BL/6 mice.	120
Fig.2.52 CD8 T-cell responses induced by immunization with different heterologous prime-boost strategies with VSV-GP-HBs/c in wild-type C57BL/6 mice.	122
Fig.2.53 Weight monitoring of the wild-type C57BL/6 mice immunized with different heterologous prime-boost strategies.	123
Fig.2.54 Immunization schemes of heterologous prime-boost strategies with VSV-GP-HBs/c in AAV-HBV mice.	124
Fig.2.55 Antigen level alteration and antibody responses induced by heterologous prime-boost strategies with VSV-GP-HBs/c in AAV-HBV mice.	125
Fig.2.56 CD4 T-cell responses induced by heterologous prime-boost strategies with VSV-GP-HBs/c in AAV-HBV mice.	126
Fig.2.57 CD8 T-cell response analysis after heterologous prime-boost immunization with VSV-GP-HBs/c in AAV-HBV mice.	128

6. References

- Acres B & Bonnefoy J-Y. (2008). Clinical development of MVA-based therapeutic cancer vaccines. *Expert review of vaccines*, 7(7), 889-893.
- Afolabi M O, Ndure J, Drammeh A, Darboe F, et al. (2013). A phase I randomized clinical trial of candidate human immunodeficiency virus type 1 vaccine MVA. HIVA administered to Gambian infants. *PloS one*, 8(10), e78289.
- Aguilar J, Lobaina Y, Muzio V, Garcia D, et al. (2004). Development of a nasal vaccine for chronic hepatitis B infection that uses the ability of hepatitis B core antigen to stimulate a strong Th1 response against hepatitis B surface antigen. *Immunology and cell biology*, 82(5), 539-546.
- Aguilar J & Rodriguez E. (2007). Vaccine adjuvants revisited. *Vaccine*, 25(19), 3752-3762.
- Aguilar J C & Lobaina Y. (2014). Immunotherapy for Chronic Hepatitis B using HBsAg-based Vaccine Formulations: From Preventive Commercial Vaccines to Therapeutic Approach Julio Cesar Aguilar. *Euroasian Journal of Hepato-Gastroenterology*, 4(2), 92.
- Al-Sadeq D W, Taleb S A, Zaied R E, Fahad S M, et al. (2019). Hepatitis B Virus Molecular Epidemiology, Host-Virus Interaction, Coinfection, and Laboratory Diagnosis in the MENA Region: An Update. *Pathogens*, 8(2).
- Al Mahtab M, Akbar S M F, Aguilar J C, Guillen G, et al. (2018). Treatment of chronic hepatitis B naïve patients with a therapeutic vaccine containing HBs and HBe antigens (a randomized, open and treatment controlled phase III clinical trial). *PloS one*, 13(8), e0201236.
- Allweiss L & Dandri M. (2016). Experimental in vitro and in vivo models for the study of human hepatitis B virus infection. *Journal of hepatology*, 64(1), S17-S31.
- Alter M J, Hadler S C, Margolis H S, Alexander W J, et al. (1990). The changing epidemiology of hepatitis B in the United States. Need for alternative vaccination strategies. *JAMA*, 263(9), 1218-1222. Retrieved from <https://www.ncbi.nlm.nih.gov/pubmed/2304237>.
- Ando K, Guidotti L G, Wirth S, Ishikawa T, et al. (1994). Class I-restricted cytotoxic T lymphocytes are directly cytopathic for their target cells in vivo. *The Journal of Immunology*, 152(7), 3245-3253.
- Arevalo J A & Washington A E. (1988). Cost-effectiveness of prenatal screening and immunization for hepatitis B virus. *JAMA*, 259(3), 365-369. Retrieved from <https://www.ncbi.nlm.nih.gov/pubmed/2961895>.
- Arora S, McDonald R A, Toews G B & Huffnagle G B. (2006). Effect of a CD4-depleting antibody on the development of *Cryptococcus neoformans*-induced allergic bronchopulmonary mycosis in mice. *Infection and immunity*, 74(7), 4339-4348.
- Asabe S, Wieland S F, Chattopadhyay P K, Roederer M, et al. (2009). The size of the viral inoculum contributes to the outcome of hepatitis B virus infection. *Journal of virology*, 83(19), 9652-9662.

References

- Ascarated S. (2009). Safety Data of Montanide ISA 51VG and Montanide ISA 720VG in Human Therapeutic Vaccines. Paper presented at the journal of immunotherapy.
- Aucouturier J, Dupuis L, Deville S, Ascarateil S & Ganne V. (2002). Montanide ISA 720 and 51: a new generation of water in oil emulsions as adjuvants for human vaccines. *Expert review of vaccines*, 1(1), 111-118.
- Awate S, Babiuk L A B & Mutwiri G. (2013). Mechanisms of action of adjuvants. *Frontiers in immunology*, 4, 114.
- Backes S, Jager C, Dembek C J, Kosinska A D, et al. (2016). Protein-prime/modified vaccinia virus Ankara vector-boost vaccination overcomes tolerance in high-antigenemic HBV-transgenic mice. *Vaccine*, 34(7), 923-932.
- Baschieri S. (2012). *Innovation in Vaccinology: from design, through to delivery and testing*: Springer Science & Business Media.
- Bauer S, Kirschning C J, Häcker H, Redecke V, et al. (2001). Human TLR9 confers responsiveness to bacterial DNA via species-specific CpG motif recognition. *Proceedings of the national academy of sciences*, 98(16), 9237-9242.
- Bertoletti A & Ferrari C. (2016). Adaptive immunity in HBV infection. *J Hepatol*, 64(1 Suppl), S71-S83.
- Billaud J N, Peterson D, Schodel F, Chen A, et al. (2005). Comparative antigenicity and immunogenicity of hepadnavirus core proteins. *J Virol*, 79(21), 13641-13655.
- Biswas S, Spencer A J, Forbes E K, Gilbert S C, et al. (2012). Recombinant viral-vectored vaccines expressing Plasmodium chabaudi AS apical membrane antigen 1: mechanisms of vaccine-induced blood-stage protection. *J Immunol*, 188(10), 5041-5053.
- Bourguine M, Crabe S, Lobaina Y, Guillen G, Aguilar J C & Michel M-L. (2018). Nasal route favors the induction of CD4+ T cell responses in the liver of HBV-carrier mice immunized with a recombinant hepatitis B surface-and core-based therapeutic vaccine. *Antiviral Research*, 153, 23-32.
- Bournazos S & Ravetch J V. (2017). Fcγ receptor function and the design of vaccination strategies. *Immunity*, 47(2), 224-233.
- Brewer J M, Conacher M, Hunter C A, Mohrs M, Brombacher F & Alexander J. (1999). Aluminium hydroxide adjuvant initiates strong antigen-specific Th2 responses in the absence of IL-4-or IL-13-mediated signaling. *The Journal of Immunology*, 163(12), 6448-6454.
- Buchbinder S P, Mehrotra D V, Duerr A, Fitzgerald D W, et al. (2008). Efficacy assessment of a cell-mediated immunity HIV-1 vaccine (the Step Study): a double-blind, randomised, placebo-controlled, test-of-concept trial. *The Lancet*, 372(9653), 1881-1893.
- Burton A R, Pallett L J, McCoy L E, Suveizdyte K, et al. (2018). Circulating and intrahepatic antiviral B cells are defective in hepatitis B. *J Clin Invest*, 128(10), 4588-4603.

- Cavanaugh J S, Awi D, Mendy M, Hill A V, Whittle H & McConkey S J. (2011). Partially randomized, non-blinded trial of DNA and MVA therapeutic vaccines based on hepatitis B virus surface protein for chronic HBV infection. *PloS one*, 6(2), e14626.
- Cerino A, Bremer C M, Glebe D & Mondelli M U. (2015). A human monoclonal antibody against hepatitis B surface antigen with potent neutralizing activity. *Plos one*, 10(4), e0125704.
- Chai N, Chang H E, Nicolas E, Han Z, Jarnik M & Taylor J. (2008). Properties of subviral particles of hepatitis B virus. *J Virol*, 82(16), 7812-7817.
- Chen D S. (2009). Hepatitis B vaccination: The key towards elimination and eradication of hepatitis B. *J Hepatol*, 50(4), 805-816.
- Chisari F V & Ferrari C. (1995). Hepatitis B Virus Immunopathogenesis. *Annual Review of Immunology*, 13(1), 29-60.
- Chisari F V, Isogawa M & Wieland S F. (2010). Pathogenesis of hepatitis B virus infection. *Pathol Biol (Paris)*, 58(4), 258-266.
- Choi Y & Chang J. (2013). Viral vectors for vaccine applications. *Clinical and experimental vaccine research*, 2(2), 97-105.
- Coffman R L, Sher A & Seder R A. (2010). Vaccine adjuvants: putting innate immunity to work. *Immunity*, 33(4), 492-503.
- Coller B-A G, Blue J, Das R, Dubey S, et al. (2017). Clinical development of a recombinant Ebola vaccine in the midst of an unprecedented epidemic. *Vaccine*, 35(35), 4465-4469.
- Colloca S, Barnes E, Folgori A, Ammendola V, et al. (2012). Vaccine vectors derived from a large collection of simian adenoviruses induce potent cellular immunity across multiple species. *Science translational medicine*, 4(115), 115ra112-115ra112.
- Cooper D, Wright K J, Calderon P C, Guo M, et al. (2008). Attenuation of recombinant vesicular stomatitis virus-human immunodeficiency virus type 1 vaccine vectors by gene translocations and g gene truncation reduces neurovirulence and enhances immunogenicity in mice. *Journal of virology*, 82(1), 207-219.
- Cooper L J, Mittendorf E A, Moyes J & Prabhakaran S. (2018). *Immunotherapy in Translational Cancer Research*: John Wiley & Sons.
- Corti D & Lanzavecchia A. (2013). Broadly neutralizing antiviral antibodies. *Annual review of immunology*, 31, 705-742.
- Cross E W, Blain T J, Mathew D & Kedl R M. (2019). Anti-CD8 monoclonal antibody-mediated depletion alters the phenotype and behavior of surviving CD8+ T cells. *PloS one*, 14(2), e0211446.
- Dandri M, Burda M R, Török E, Pollok J M, et al. (2001). Repopulation of mouse liver with human hepatocytes and in vivo infection with hepatitis B virus. *Hepatology*, 33(4), 981-988.
- Dane D S, Cameron C H & Briggs M. (1970). Virus-like particles in serum of patients with Australia-antigen-associated hepatitis. *Lancet*, 1(7649), 695-698.
- Davis H L. (2008). Novel vaccines and adjuvant systems: the utility of animal models for predicting immunogenicity in humans. *Human vaccines*, 4(3), 246-250.

References

- Dembek C & Protzer U. (2015). Mouse models for therapeutic vaccination against hepatitis B virus. *Medical microbiology and immunology*, 204(1), 95-102.
- Den Haan J M & Bevan M J. (2000). A novel helper role for CD4 T cells. *Proceedings of the National Academy of Sciences*, 97(24), 12950-12952.
- Dikici B, Bosnak M, Ucmak H, Dagli A, Ece A & Haspolat K. (2003). Failure of therapeutic vaccination using hepatitis B surface antigen vaccine in the immunotolerant phase of children with chronic hepatitis B infection. *Journal of gastroenterology and hepatology*, 18(2), 218-222.
- Dion S, Bourguine M, Godon O, Levillayer F & Michel M L. (2013). Adeno-associated virus-mediated gene transfer leads to persistent hepatitis B virus replication in mice expressing HLA-A2 and HLA-DR1 molecules. *J Virol*, 87(10), 5554-5563.
- Dooms H & Abbas A K. (2002). Life and death in effector T cells. *Nature immunology*, 3(9), 797-798.
- Draper S J, Angov E, Horii T, Miller L H, et al. (2015). Recent advances in recombinant protein-based malaria vaccines. *Vaccine*, 33(52), 7433-7443.
- Dupinay T, Gheit T, Roques P, Cova L, et al. (2013). Discovery of naturally occurring transmissible chronic hepatitis B virus infection among *Macaca fascicularis* from Mauritius Island. *Hepatology*, 58(5), 1610-1620.
- EASL guideline. (2017). EASL 2017 Clinical Practice Guidelines on the management of hepatitis B virus infection. *Journal of hepatology*, 67(2), 370-398.
- Ebensen T, Debarry J, Pedersen G K, Blazejewska P, et al. (2017). Mucosal administration of cycle-di-nucleotide-adjuvanted virosomes efficiently induces protection against influenza H5N1 in mice. *Frontiers in immunology*, 8, 1223.
- Einstein M H, Baron M, Levin M J, Chatterjee A, et al. (2009). Comparison of the immunogenicity and safety of Cervarix™ and Gardasil® human papillomavirus (HPV) cervical cancer vaccines in healthy women aged 18–45 years. *Human vaccines*, 5(10), 705-719.
- EMA adjuvant guideline. (2005). Guideline on adjuvants in vaccines for human use.
- Eng N F, Bhardwaj N, Mulligan R & Diaz-Mitoma F. (2013). The potential of 1018 ISS adjuvant in hepatitis B vaccines: HEPLISAV™ review. *Human vaccines & immunotherapeutics*, 9(8), 1661-1672.
- Ferrari C, Bertolotti A, Penna A, Cavalli A, et al. (1991). Identification of immunodominant T cell epitopes of the hepatitis B virus nucleocapsid antigen. *The Journal of clinical investigation*, 88(1), 214-222.
- Fontaine H, Kahi S, Chazallon C, Bourguine M, et al. (2015). Anti-HBV DNA vaccination does not prevent relapse after discontinuation of analogues in the treatment of chronic hepatitis B: a randomised trial—ANRS HB02 VAC-ADN. *Gut*, 64(1), 139-147.
- Fox C B, Kramer R M, Barnes V L, Dowling Q M & Vedvick T S. (2013). Working together: interactions between vaccine antigens and adjuvants. *Therapeutic advances in vaccines*, 1(1), 7-20.
- Ganem D & Prince A M. (2004). Hepatitis B virus infection—natural history and clinical consequences. *New England Journal of Medicine*, 350(11), 1118-1129.

- Garcon N & Di Pasquale A. (2017). From discovery to licensure, the Adjuvant System story. *Hum Vaccin Immunother*, 13(1), 19-33.
- Gehring A J & Protzer U. (2019). Targeting Innate and Adaptive Immune Responses to Cure Chronic HBV Infection. *Gastroenterology*, 156(2), 325-337.
- Geng M, Xin X, Bi L Q, Zhou L T & Liu X H. (2015). Molecular mechanism of hepatitis B virus X protein function in hepatocarcinogenesis. *World J Gastroenterol*, 21(38), 10732-10738.
- Gerdts V. (2015). Adjuvants for veterinary vaccines--types and modes of action. *Berliner und Munchener tierarztliche Wochenschrift*, 128(11-12), 456-463.
- Gerlich W H. (2007). The enigma of concurrent hepatitis B surface antigen (HBsAg) and antibodies to HBsAg. *Clinical Infectious Diseases*, 44(9), 1170-1172.
- Gerlich W H. (2013). Medical virology of hepatitis B: how it began and where we are now. *Virology*, 10, 239.
- Guidotti L G, Matzke B, Schaller H & Chisari F V. (1995). High-level hepatitis B virus replication in transgenic mice. *Journal of virology*, 69(10), 6158-6169.
- Guidotti L G, Rochford R, Chung J, Shapiro M, Purcell R & Chisari F V. (1999). Viral clearance without destruction of infected cells during acute HBV infection. *Science*, 284(5415), 825-829.
- Guo W-N, Zhu B, Ai L, Yang D-L & Wang B-J. (2018). Animal models for the study of hepatitis B virus infection. *Zoological research*, 39(1), 25.
- Gupta R K, Rost B E, Relyveld E & Siber G R. (1995). Adjuvant properties of aluminum and calcium compounds. *Pharm Biotechnol*, 6, 229-248.
- Halperin S A, Ward B J, Dionne M S, Langley J M, et al. (2013). Immunogenicity of an investigational hepatitis B vaccine (hepatitis B surface antigen co-administered with an immunostimulatory phosphorothioate oligodeoxyribonucleotide) in nonresponders to licensed hepatitis B vaccine. *Human vaccines & immunotherapeutics*, 9(7), 1438-1444.
- Hoebe C J, Vermeiren A P & Dukers-Muijers N H. (2012). Revaccination with Fendrix(R) or HBVaxPro(R) results in better response rates than does revaccination with three doses of Engerix-B(R) in previous non-responders. *Vaccine*, 30(48), 6734-6737.
- Honorati M, Borzi R, Dolzani P, Toneguzzi S & Facchini A. (1997). Distribution of IgG subclasses after anti-hepatitis B virus immunization with a recombinant vaccine. *International Journal of Clinical and Laboratory Research*, 27(2-4), 202-206.
- Hösel M, Quasdorff M, Wiegmann K, Webb D, et al. (2009). Not interferon, but interleukin - 6 controls early gene expression in hepatitis B virus infection. *Hepatology*, 50(6), 1773-1782.
- Hu J & Liu K. (2017). Complete and Incomplete Hepatitis B Virus Particles: Formation, Function, and Application. *Viruses*, 9(3).
- Huang L-R, Wu H-L, Chen P-J & Chen D-S. (2006). An immunocompetent mouse model for the tolerance of human chronic hepatitis B virus infection. *Proceedings of the National Academy of Sciences*, 103(47), 17862-17867.

References

- Huang L R, Gäbel Y A, Graf S, Arzberger S, et al. (2012). Transfer of HBV genomes using low doses of adenovirus vectors leads to persistent infection in immune competent mice. *Gastroenterology*, 142(7), 1447-1450. e1443.
- Humphreys I R & Sebastian S. (2018). Novel viral vectors in infectious diseases. *Immunology*, 153(1), 1-9.
- Hwang J-R & Park S-G. (2018). Mouse models for hepatitis B virus research. *Laboratory animal research*, 34(3), 85-91.
- Ilan Y, Nagler A, Adler R, Tur-Kaspa R, Slavin S & Shouval D. (1993). Ablation of persistent hepatitis B by bone marrow transplantation from a hepatitis B-immune donor. *Gastroenterology*, 104(6), 1818-1821.
- John von Freyend M, Untergasser A, Arzberger S, Oberwinkler H, et al. (2011). Sequential control of hepatitis B virus in a mouse model of acute, self-resolving hepatitis B. *Journal of viral hepatitis*, 18(3), 216-226.
- Johnson J E, Nasar F, Coleman J W, Price R E, et al. (2007). Neurovirulence properties of recombinant vesicular stomatitis virus vectors in non-human primates. *Virology*, 360(1), 36-49.
- Julander J G, Colonna R J, Sidwell R W & Morrey J D. (2003). Characterization of antiviral activity of entecavir in transgenic mice expressing hepatitis B virus. *Antiviral research*, 59(3), 155-161.
- Kalvodova L. (2010). Squalene-based oil-in-water emulsion adjuvants perturb metabolism of neutral lipids and enhance lipid droplet formation. *Biochemical and biophysical research communications*, 393(3), 350-355.
- Karnowski A, Chevrier S, Belz G T, Mount A, et al. (2012). B and T cells collaborate in antiviral responses via IL-6, IL-21, and transcriptional activator and coactivator, Oct2 and OBF-1. *Journal of Experimental Medicine*, 209(11), 2049-2064.
- Kastenmuller W, Gasteiger G, Gronau J H, Baier R, et al. (2007). Cross-competition of CD8+ T cells shapes the immunodominance hierarchy during boost vaccination. *The Journal of experimental medicine*, 204(9), 2187-2198.
- Kennedy R C, Shearer M H, Watts A M & Bright R K. (2003). CD4+ T lymphocytes play a critical role in antibody production and tumor immunity against simian virus 40 large tumor antigen. *Cancer Res*, 63(5), 1040-1045. Retrieved from <https://www.ncbi.nlm.nih.gov/pubmed/12615720>.
- Kensil C, Wu J, Anderson C, Wheeler D & Amsden J. (1998). QS-21 and QS-7: purified saponin adjuvants. *Developments in biological standardization*, 92, 41-47.
- Kim J H, Ghosh A, Ayithan N, Romani S, et al. (2020). Circulating serum HBsAg level is a biomarker for HBV-specific T and B cell responses in chronic hepatitis B patients. *Scientific reports*, 10(1), 1-12.
- Klinman D M, Currie D, Gursel I & Verthelyi D. (2004). Use of CpG oligodeoxynucleotides as immune adjuvants. *Immunological reviews*, 199(1), 201-216.
- Knipe D & Howley P. (2007). *Fields Virology*, ed Fifth. In: Philadelphia, USA, Lippincott Williams & Wilkins, a Wolters Kluwer business.
- Ko C, Michler T & Protzer U. (2017). Novel viral and host targets to cure hepatitis B. *Curr Opin Virol*, 24, 38-45.

- Kool M, Fierens K & Lambrecht B N. (2012). Alum adjuvant: some of the tricks of the oldest adjuvant. *Journal of medical microbiology*, 61(7), 927-934.
- Kosinska A D, Bauer T & Protzer U. (2017). Therapeutic vaccination for chronic hepatitis B. *Curr Opin Virol*, 23, 75-81.
- Kosinska A D, Pishraft-Sabet L, Wu W, Fang Z, et al. (2017b). Low hepatitis B virus-specific T-cell response in males correlates with high regulatory T-cell numbers in murine models. *Hepatology*, 66(1), 69-83.
- Kosinska A D, Moeed A, Kallin N, Festag J, et al. (2019). Synergy of therapeutic heterologous prime-boost hepatitis B vaccination with CpG-application to improve immune control of persistent HBV infection. *Sci Rep*, 9(1), 10808.
- Kumru O S, Joshi S B, Smith D E, Middaugh C R, Prusik T & Volkin D B. (2014). Vaccine instability in the cold chain: mechanisms, analysis and formulation strategies. *Biologicals*, 42(5), 237-259.
- Kundi M. (2007). New hepatitis B vaccine formulated with an improved adjuvant system. *Expert Rev Vaccines*, 6(2), 133-140.
- Kutscher S, Bauer T, Dembek C, Sprinzl M & Protzer U. (2012). Design of therapeutic vaccines: hepatitis B as an example. *Microbial biotechnology*, 5(2), 270-282.
- Laky K & Kruisbeek A M. (2016). In vivo depletion of T lymphocytes. *Current Protocols in Immunology*, 113(1), 4.1. 1-4.1. 9.
- Lamontagne R J, Bagga S & Bouchard M J. (2016). Hepatitis B virus molecular biology and pathogenesis. *Hepatoma Res*, 2, 163-186.
- Lan Y H, Lo Y-C, Wu P-Y & Tao M-H. (2017). Induction of Virus-specific Immune Tolerance in A Chronic Hepatitis B Virus Mouse Model. *The Journal of Immunology*, 198(1 Supplement), 158.116-158.116.
- Ledgerwood J E, DeZure A D, Stanley D A, Coates E E, et al. (2017). Chimpanzee adenovirus vector Ebola vaccine. *New England Journal of Medicine*, 376(10), 928-938.
- Leroux-Roels G. (2010). Unmet needs in modern vaccinology: adjuvants to improve the immune response. *Vaccine*, 28, C25-C36.
- Lichty B D, Power A T, Stojdl D F & Bell J C. (2004). Vesicular stomatitis virus: re-inventing the bullet. *Trends in molecular medicine*, 10(5), 210-216.
- Liu H, Geng S, Wang B, Wu B, et al. (2016). Immuno-potentiating pathway of HBsAg-HBIG immunogenic complex visualized. *Human vaccines & immunotherapeutics*, 12(1), 77-84.
- Lobaina Y & Michel M-L. (2017). Chronic hepatitis B: Immunological profile and current therapeutic vaccines in clinical trials. *Vaccine*, 35(18), 2308-2314.
- Locarnini S, Littlejohn M, Aziz M N & Yuen L. (2013). Possible origins and evolution of the hepatitis B virus (HBV). *Semin Cancer Biol*, 23(6 Pt B), 561-575.
- Locarnini S, Hatzakis A, Chen D S & Lok A. (2015). Strategies to control hepatitis B: Public policy, epidemiology, vaccine and drugs. *J Hepatol*, 62(1 Suppl), S76-86.
- Lok A S-F. (2005). The maze of treatments for hepatitis B. *New England Journal of Medicine*, 352(26), 2743-2745.
- Lok A S, Zoulim F, Dusheiko G & Ghany M G. (2017). Hepatitis B cure: From discovery to regulatory approval. *Hepatology*, 66(4), 1296-1313.

References

- Lu L L, Suscovich T J, Fortune S M & Alter G. (2018). Beyond binding: antibody effector functions in infectious diseases. *Nature Reviews Immunology*, 18(1), 46.
- Lucifora J, Xia Y, Reisinger F, Zhang K, et al. (2014). Specific and nonhepatotoxic degradation of nuclear hepatitis B virus cccDNA. *Science*, 343(6176), 1221-1228.
- Lucifora J, Salvetti A, Marniquet X, Maily L, et al. (2017). Detection of the hepatitis B virus (HBV) covalently-closed-circular DNA (cccDNA) in mice transduced with a recombinant AAV-HBV vector. *Antiviral Research*, 145, 14-19.
- Luckheeram R V, Zhou R, Verma A D & Xia B. (2012). CD4(+) T cells: differentiation and functions. *Clin Dev Immunol*, 2012, 925135.
- Maini M K, Boni C, Ogg G S, King A S, et al. (1999). Direct ex vivo analysis of hepatitis B virus-specific CD8(+) T cells associated with the control of infection. *Gastroenterology*, 117(6), 1386-1396.
- Maini M K & Gehring A J. (2016). The role of innate immunity in the immunopathology and treatment of HBV infection. *Journal of hepatology*, 64(1), S60-S70.
- Maini M K & Pallett L J. (2018). Defective T-cell immunity in hepatitis B virus infection: why therapeutic vaccination needs a helping hand. *Lancet Gastroenterol Hepatol*, 3(3), 192-202.
- Maini M K & Burton A R. (2019). Restoring, releasing or replacing adaptive immunity in chronic hepatitis B. *Nat Rev Gastroenterol Hepatol*, 16(11), 662-675.
- Mancini - Bourguine M, Fontaine H, Scott - Algara D, Pol S, Br  chot C & Michel M L. (2004). Induction or expansion of T - cell responses by a hepatitis B DNA vaccine administered to chronic HBV carriers. *Hepatology*, 40(4), 874-882.
- Marshall J D, Gresner M L, Heeke D S, Buchmann P, et al. (2007). A novel therapeutic HBV vaccine induces potent surface-and core-specific immunogenicity in mice, rhesus macaques and HBV transgenic mice. Paper presented at the Hepatology.
- Martin P, Dubois C, Jacquier E, Dion S, et al. (2015). TG1050, an immunotherapeutic to treat chronic hepatitis B, induces robust T cells and exerts an antiviral effect in HBV-persistent mice. *Gut*, 64(12), 1961-1971.
- Marzi A, Feldmann H, Geisbert T W & Falzarano D. (2011). Vesicular stomatitis virus-based vaccines for prophylaxis and treatment of filovirus infections. *Journal of bioterrorism & biodefense* (4).
- Mbawuike I N, Acuna C, Caballero D, Pham-Nguyen K, et al. (1996). Reversal of age-related deficient influenza virus-specific CTL responses and IFN-  production by monophosphoryl lipid A. *Cellular immunology*, 173(1), 64-78.
- Meraz I M, Hearnden C H, Liu X, Yang M, et al. (2014). Multivalent presentation of MPL by porous silicon microparticles favors T helper 1 polarization enhancing the anti-tumor efficacy of doxorubicin nanoliposomes. *PLoS one*, 9(4), e94703.
- Mescher M F, Curtsinger J M & Jenkins M. (2006). Adjuvants and the initiation of T-cell responses. In *Vaccine Adjuvants* (pp. 49-67): Springer.
- Michler T, Kosinska A D, Festag J, Bunse T, et al. (2020). Knockdown of Virus Antigen Expression Increases Therapeutic Vaccine Efficacy in High-Titer Hepatitis B Virus Carrier Mice. *Gastroenterology*, 158(6), 1762-1775 e1769.

- Miletic H, Fischer Y H, Neumann H, Hans V, et al. (2004). Selective transduction of malignant glioma by lentiviral vectors pseudotyped with lymphocytic choriomeningitis virus glycoproteins. *Human gene therapy*, 15(11), 1091-1100.
- Milich D R & McLachlan A. (1986). The nucleocapsid of hepatitis B virus is both a T-cell-independent and a T-cell-dependent antigen. *Science*, 234(4782), 1398-1401.
- Milich D R, McLachlan A, Thornton G B & Hughes J L. (1987). Antibody production to the nucleocapsid and envelope of the hepatitis B virus primed by a single synthetic T cell site. *Nature*, 329(6139), 547-549.
- Modlich U & Baum C. (2009). Preventing and exploiting the oncogenic potential of integrating gene vectors. *The Journal of clinical investigation*, 119(4), 755-758.
- Morrow W J W, Sheikh N A, Schmidt C S & Davies D H. (2012). *Vaccinology: principles and practice*: John Wiley & Sons.
- Mueller S N & Ahmed R. (2009). High antigen levels are the cause of T cell exhaustion during chronic viral infection. *Proceedings of the National Academy of Sciences*, 106(21), 8623-8628.
- Muik A, Stubbert L J, Jahedi R Z, Geiß Y, et al. (2014). Re-engineering vesicular stomatitis virus to abrogate neurotoxicity, circumvent humoral immunity, and enhance oncolytic potency. *Cancer research*, 74(13), 3567-3578.
- Murphy K & Weaver C. (2016). *Janeway's immunobiology*: Garland science.
- Nanishi E, Dowling D J & Levy O. (2020). Toward precision adjuvants: optimizing science and safety. *Curr Opin Pediatr*, 32(1), 125-138.
- Nash K. (2009). Telbivudine in the treatment of chronic hepatitis B. *Advances in therapy*, 26(2), 155-169.
- Nassal M. (2015). HBV cccDNA: viral persistence reservoir and key obstacle for a cure of chronic hepatitis B. *Gut*, 64(12), 1972-1984.
- Newman M, Wu J-Y, Gardner B, Anderson C, et al. (1997). Induction of cross-reactive cytotoxic T-lymphocyte responses specific for HIV-1 gp120 using saponin adjuvant (QS-21) supplemented subunit vaccine formulations. *Vaccine*, 15(9), 1001-1007.
- Nguyen M H, Wong G, Gane E, Kao J-H & Dusheiko G. (2020). Hepatitis B virus: advances in prevention, diagnosis, and therapy. *Clinical Microbiology Reviews*, 33(2).
- Obeng-Adjei N, Choo D K, Saini J, Yan J, et al. (2012). Synthetic DNA immunogen encoding hepatitis B core antigen drives immune response in liver. *Cancer gene therapy*, 19(11), 779-787.
- Palumbo G A, Scisciani C, Pediconi N, Lupacchini L, et al. (2015). IL6 inhibits HBV transcription by targeting the epigenetic control of the nuclear cccDNA minichromosome. *PLoS One*, 10(11), e0142599.
- Pardoll D M. (2012). The blockade of immune checkpoints in cancer immunotherapy. *Nat Rev Cancer*, 12(4), 252-264.
- Penna A, Artini M, Cavalli A, Levrero M, et al. (1996). Long-lasting memory T cell responses following self-limited acute hepatitis B. *The Journal of clinical investigation*, 98(5), 1185-1194.

References

- Phillips S, Chokshi S, Riva A, Evans A, Williams R & Naoumov N V. (2010). CD8+ T cell control of hepatitis B virus replication: direct comparison between cytolytic and noncytolytic functions. *The journal of immunology*, 184(1), 287-295.
- Pol S & Michel M-L. (2006). Therapeutic vaccination in chronic hepatitis B virus carriers. *Expert review of vaccines*, 5(5), 707-716.
- Pondé R A. (2013). Atypical serological profiles in hepatitis B virus infection. *European journal of clinical microbiology & infectious diseases*, 32(4), 461-476.
- Protzer U, Maini M K & Knolle P A. (2012). Living in the liver: hepatic infections. *Nat Rev Immunol*, 12(3), 201-213.
- Ramlau R, Quoix E, Rolski J, Pless M, et al. (2008). A phase II study of Tg4010 (Mva-Muc1-II2) in association with chemotherapy in patients with stage III/IV Non-small cell lung cancer. *Journal of Thoracic Oncology*, 3(7), 735-744.
- Raziorrouh B, Heeg M, Kurktschiev P, Schraut W, et al. (2014). Inhibitory phenotype of HBV-specific CD4+ T-cells is characterized by high PD-1 expression but absent coregulation of multiple inhibitory molecules. *PLoS One*, 9(8), e105703.
- Reed S G, Orr M T & Fox C B. (2013). Key roles of adjuvants in modern vaccines. *Nature medicine*, 19(12), 1597-1608.
- Revill P, Testoni B, Locarnini S & Zoulim F. (2016). Global strategies are required to cure and eliminate HBV infection. *Nature reviews Gastroenterology & hepatology*, 13(4), 239-248.
- Revill P A, Chisari F V, Block J M, Dandri M, et al. (2019). A global scientific strategy to cure hepatitis B. *The Lancet Gastroenterology & Hepatology*, 4(7), 545-558.
- Riedl P, Stober D, Oehninger C, Melber K, Reimann J & Schirmbeck R. (2002). Priming Th1 immunity to viral core particles is facilitated by trace amounts of RNA bound to its arginine-rich domain. *The Journal of Immunology*, 168(10), 4951-4959.
- Rijckborst V, Sonneveld M J & Janssen H. (2011). chronic hepatitis B - anti - viral or immunomodulatory therapy? *Alimentary pharmacology & therapeutics*, 33(5), 501-513.
- Saeidi A, Zandi K, Cheok Y Y, Saeidi H, et al. (2018). T-cell exhaustion in chronic infections: reversing the state of exhaustion and reinvigorating optimal protective immune responses. *Frontiers in immunology*, 9, 2569.
- Sakaguchi S, Wing K, Onishi Y, Prieto-Martin P & Yamaguchi T. (2009). Regulatory T cells: how do they suppress immune responses? *International immunology*, 21(10), 1105-1111.
- Schillie S, Harris A, Link-Gelles R, Romero J, Ward J & Nelson N. (2018). Recommendations of the Advisory Committee on Immunization Practices for Use of a Hepatitis B Vaccine with a Novel Adjuvant. *MMWR Morb Mortal Wkly Rep*, 67(15), 455-458.
- Schreiber L-M, Urbiola C, Das K, Spiesschaert B, et al. (2019). The lytic activity of VSV-GP treatment dominates the therapeutic effects in a syngeneic model of lung cancer. *British journal of cancer*, 121(8), 647-658.
- Schunk M K & Macallum G E. (2005). Applications and optimization of immunization procedures. *ILAR journal*, 46(3), 241-257.

- Sebastian S & Gilbert S C. (2015). Recombinant modified vaccinia virus Ankara-based malaria vaccines. *Expert Rev Vaccines*, 15(1), 91-103.
- Seeger C & Mason W S. (2015). Molecular biology of hepatitis B virus infection. *Virology*, 479-480, 672-686.
- Shah R R, Dodd S, Schaefer M, Ugozzoli M, et al. (2015). The development of self-emulsifying oil-in-water emulsion adjuvant and an evaluation of the impact of droplet size on performance. *Journal of Pharmaceutical Sciences*, 104(4), 1352-1361.
- Shimizu Y, Guidotti L G, Fowler P & Chisari F V. (1998). Dendritic cell immunization breaks cytotoxic T lymphocyte tolerance in hepatitis B virus transgenic mice. *The Journal of Immunology*, 161(9), 4520-4529.
- Shiver J W, Fu T-M, Chen L, Casimiro D R, et al. (2002). Replication-incompetent adenoviral vaccine vector elicits effective anti-immunodeficiency-virus immunity. *Nature*, 415(6869), 331-335.
- Snook A E, Magee M S, Schulz S & Waldman S A. (2014). Self-tolerance eliminates CD4+ T, but not CD8+ T or B, cells corrupting cancer immunotherapy. *European journal of immunology*, 44(7), 1956.
- Snow E C. (2012). *Handbook of B and T Lymphocytes*: Academic Press.
- Spellman M & Martin J. (2011). 751 TREATMENT OF CHRONIC HEPATITIS B INFECTION WITH DV-601, A THERAPEUTIC VACCINE. *Journal of Hepatology*, 54, S302.
- Stevens T L, Bossie A, Sanders V M, Fernandez-Botran R, et al. (1988). Regulation of antibody isotype secretion by subsets of antigen-specific helper T cells. *Nature*, 334(6179), 255-258.
- Stoop J N, van der Molen R G, Baan C C, van der Laan L J, et al. (2005). Regulatory T cells contribute to the impaired immune response in patients with chronic hepatitis B virus infection. *Hepatology*, 41(4), 771-778.
- Suder E, Furuyama W, Feldmann H, Marzi A & de Wit E. (2018). The vesicular stomatitis virus-based Ebola virus vaccine: From concept to clinical trials. *Human Vaccines & Immunotherapeutics*, 14(9), 2107-2113.
- Sunbul M. (2014). Hepatitis B virus genotypes: global distribution and clinical importance. *World J Gastroenterol*, 20(18), 5427-5434.
- Swain S L, McKinstry K K & Strutt T M. (2012). Expanding roles for CD4+ T cells in immunity to viruses. *Nature Reviews Immunology*, 12(2), 136-148.
- Tang H. (2019). *Hepatitis B Virus Infection: Molecular Virology to Antiviral Drugs* (Vol. 1179): Springer.
- Tatsis N & Ertl H C. (2004). Adenoviruses as vaccine vectors. *Molecular Therapy*, 10(4), 616-629.
- Thimme R, Wieland S, Steiger C, Ghayeb J, et al. (2003). CD8(+) T cells mediate viral clearance and disease pathogenesis during acute hepatitis B virus infection. *J Virol*, 77(1), 68-76.
- Tober R, Banki Z, Egerer L, Muik A, et al. (2014). VSV-GP: a potent viral vaccine vector that boosts the immune response upon repeated applications. *Journal of virology*, 88(9), 4897-4907.

References

- Toledo H, Baly A, Castro O, Resik S, et al. (2001). A phase I clinical trial of a multi-epitope polypeptide TAB9 combined with Montanide ISA 720 adjuvant in non-HIV-1 infected human volunteers. *Vaccine*, 19(30), 4328-4336.
- Trautmann T, Kozik J-H, Carambia A, Richter K, et al. (2014). CD4+ T-cell help is required for effective CD8+ T cell-mediated resolution of acute viral hepatitis in mice. *PLoS One*, 9(1), e86348.
- Truckenmiller M E & Norbury C C. (2004). Viral vectors for inducing CD8+ T cell responses. *Expert opinion on biological therapy*, 4(6), 861-868.
- Trujillo H, Blanco A, García D, Freyre F, et al. (2014). Optimization of a Therapeutic Vaccine Candidate by Studying Routes, Immunization Schedules and Antigen Doses in HBsAg-positive Transgenic Mice. *Euroasian journal of hepatogastroenterology*, 4(2), 70-78.
- Tsai S, Chen P-J, Lai M, Yang P, et al. (1992). Acute exacerbations of chronic type B hepatitis are accompanied by increased T cell responses to hepatitis B core and e antigens. Implications for hepatitis B e antigen seroconversion. *The Journal of clinical investigation*, 89(1), 87-96.
- Ura T, Okuda K & Shimada M. (2014). Developments in viral vector-based vaccines. *Vaccines*, 2(3), 624-641.
- Van Damme P & Van Herck K. (2007). A review of the long-term protection after hepatitis A and B vaccination. *Travel medicine and infectious disease*, 5(2), 79-84.
- Vandepapelière P, Lau G K, Leroux-Roels G, Horsmans Y, et al. (2007). Therapeutic vaccination of chronic hepatitis B patients with virus suppression by antiviral therapy: a randomized, controlled study of co-administration of HBsAg/AS02 candidate vaccine and lamivudine. *Vaccine*, 25(51), 8585-8597.
- Velkov S, Ott J J, Protzer U & Michler T. (2018). The Global Hepatitis B Virus Genotype Distribution Approximated from Available Genotyping Data. *Genes (Basel)*, 9(10). doi:10.3390/genes9100495
- Velu V, Nandakumar S, Shanmugam S, Jadhav S S, Kulkarni P S & Thyagarajan S P. (2007). Comparison of three different recombinant hepatitis B vaccines: GeneVac-B, Engerix B and Shanvac B in high risk infants born to HBsAg positive mothers in India. *World J Gastroenterol*, 13(22), 3084-3089.
- Volckmar J, Knop L, Stegemann-Koniszewski S, Schulze K, et al. (2019). The STING activator c-di-AMP exerts superior adjuvant properties than the formulation poly (I: C)/CpG after subcutaneous vaccination with soluble protein antigen or DEC-205-mediated antigen targeting to dendritic cells. *Vaccine*, 37(35), 4963-4974.
- Volz A & Sutter G. (2017). Modified vaccinia virus Ankara: history, value in basic research, and current perspectives for vaccine development. In *Advances in virus research (Vol. 97, pp. 187-243)*: Elsevier.
- Weber O, Schlemmer K-H, Hartmann E, Hagelschuer I, et al. (2002). Inhibition of human hepatitis B virus (HBV) by a novel non-nucleosidic compound in a transgenic mouse model. *Antiviral research*, 54(2), 69-78.

- Wen Y-M, Wu X-H, Hu D-C, Zhang Q-P & Guo S-Q. (1995). Hepatitis B vaccine and anti-HBs complex as approach for vaccine therapy. *The Lancet*, 345(8964), 1575-1576.
- Wheeler A W, Marshall J S & Ulrich J T. (2001). A Th1-inducing adjuvant, MPL, enhances antibody profiles in experimental animals suggesting it has the potential to improve the efficacy of allergy vaccines. *Int Arch Allergy Immunol*, 126(2), 135-139.
- Wherry E J, Blattman J N, Murali-Krishna K, van der Most R & Ahmed R. (2003). Viral persistence alters CD8 T-cell immunodominance and tissue distribution and results in distinct stages of functional impairment. *J Virol*, 77(8), 4911-4927.
- WHO guideline. (2006). Guidelines of stability evaluation of vaccines: World Health Organization.
- WHO guideline (2015). Guidelines for the prevention care and treatment of persons with chronic hepatitis B infection: Mar-15: World Health Organization.
- WHO report (2017). Global hepatitis report 2017: World Health Organization.
- WHO (2020). Route of administration, World Health Organization. Retrieved from <https://vaccine-safety-training.org/route-of-administration.html>
- Woo A S J, Kwok R & Ahmed T. (2017). Alpha-interferon treatment in hepatitis B. *Annals of translational medicine*, 5(7).
- Wu C-y, Kirman J R, Rotte M J, Davey D F, et al. (2002). Distinct lineages of Th 1 cells have differential capacities for memory cell generation in vivo. *Nature immunology*, 3(9), 852-858.
- Xia Y, Stadler D, Lucifora J, Reisinger F, et al. (2016). Interferon- γ and tumor necrosis factor- α produced by T cells reduce the HBV persistence form, cccDNA, without cytolysis. *Gastroenterology*, 150(1), 194-205.
- Xu D-Z, Huang K-L, Zhao K, Xu L-f, et al. (2005). Vaccination with recombinant HBsAg-HBIG complex in healthy adults. *Vaccine*, 23(20), 2658-2664.
- Xu D-Z, Zhao K, Guo L-M, Chen X-Y, et al. (2008). A randomized controlled phase IIb trial of antigen-antibody immunogenic complex therapeutic vaccine in chronic hepatitis B patients. *PloS one*, 3(7), e2565.
- Xu D-Z, Wang X-Y, Shen X-L, Gong G-Z, et al. (2013). Results of a phase III clinical trial with an HBsAg-HBIG immunogenic complex therapeutic vaccine for chronic hepatitis B patients: experiences and findings. *Journal of hepatology*, 59(3), 450-456.
- Yahia E. (2009). Cold chain development and challenges in the developing world. Paper presented at the VI International Postharvest Symposium 877.
- Yan H, Zhong G, Xu G, He W, et al. (2012). Sodium taurocholate cotransporting polypeptide is a functional receptor for human hepatitis B and D virus. *Elife*, 1, e00049.
- Yang P L, Althage A, Chung J & Chisari F V. (2002). Hydrodynamic injection of viral DNA: a mouse model of acute hepatitis B virus infection. *Proceedings of the National Academy of Sciences*, 99(21), 13825-13830.

References

- Yang P L, Althage A, Chung J, Maier H, et al. (2010). Immune effectors required for hepatitis B virus clearance. *Proceedings of the National Academy of Sciences*, 107(2), 798-802.
- Yang S, Lee C, Park S-H, Im S, et al. (2006). Correlation of antiviral T-cell responses with suppression of viral rebound in chronic hepatitis B carriers: a proof-of-concept study. *Gene therapy*, 13(14), 1110-1117.
- Ye B, Liu X, Li X, Kong H, Tian L & Chen Y. (2015). T-cell exhaustion in chronic hepatitis B infection: current knowledge and clinical significance. *Cell death & disease*, 6(3), e1694-e1694.
- Younis S Y, Barrier-Quer C, Heuking S, Sommandas V, et al. (2018). Down selecting adjuvanted vaccine formulations: a comparative method for harmonized evaluation. *BMC immunology*, 19(1), 1-11.
- Zhang L, Wang W & Wang S. (2015). Effect of vaccine administration modality on immunogenicity and efficacy. *Expert review of vaccines*, 14(11), 1509-1523.
- Zhou L, Chong M M & Littman D R. (2009). Plasticity of CD4+ T cell lineage differentiation. *Immunity*, 30(5), 646-655.
- Zhu J & Paul W E. (2008). CD4 T cells: fates, functions, and faults. *Blood, The Journal of the American Society of Hematology*, 112(5), 1557-1569.
- Zimmermann P & Curtis N. (2019). Factors that influence the immune response to vaccination. *Clinical microbiology reviews*, 32(2).
- Zoulim F, Fournier C, Habersetzer F, Sprinzl M, et al. (2020). Safety and immunogenicity of the therapeutic vaccine TG1050 in chronic hepatitis B patients: a phase 1b placebo-controlled trial. *Human Vaccines & Immunotherapeutics*, 16(2), 388-399.

Publications and meetings

a) Articles in peer-reviewed journals

Kosinska AD, Moeed A, Kallin N, Festag J, **Su J**, Steiger K, et al. Synergy of therapeutic heterologous prime-boost hepatitis B vaccination with CpG-application to improve immune control of persistent HBV infection. **Scientific Reports** 2019; 9:10808.

Michler T*, Kosinska AD*, Festag J, Bunse T, **Su J**, Ringelhan M, et al. Knockdown of Virus Antigen Expression Increases Therapeutic Vaccine Efficacy in High-Titer Hepatitis B Virus Carrier Mice. **Gastroenterology** 2020; 158:1762-1775 e1769. (* *co-first authorship*)

Ko C, **Su J**, Festag J, Bester R, Kosinska AD, Protzer U. Hepatitis B virus (HBV) cccDNA is formed by intramolecular recombination in mice transduced with a recombinant AAV vector carrying an overlength HBV genome (*Submitted to **Antiviral Research***).

Su J, Brunner L, Sacherl J, Frank G, Thiele F, Ates-Öz E, et al. Protein prime with novel adjuvant activates CD4 T cells to initiate therapeutic vaccine-mediated efficacy against chronic hepatitis B (*In preparation*).

b) Conference proceedings

Su J, Kosinska AD, Brunner L, Sacherl J, Frank G, Singethan K, et al. Exploring TH1/TH2 adjuvants to improve the efficacy of the therapeutic vaccination against chronic hepatitis B. **J Hepatol** 2019; vol. 70 | e383–e624.

c) International conferences

2018 international HBV meeting, October 3-6, 2018, Taormina, Italy.

Poster presentation; Preclinical evaluation of novel adjuvants to improve the efficacy of the therapeutic vaccination against chronic hepatitis B.

The International Liver Congress 2019, April 10-14, 2019, Vienna, Austria.

Poster presentation: Exploring Th1/Th2 adjuvants to improve the efficacy of the therapeutic vaccination against chronic hepatitis B.

d) Scientific workshops

HAI-IDR Summer School, October 14-17, 2015, Munich, Germany.

5th Translational DZIF school, November 20-22, 2017, Lübeck, Germany.

TRANSVAC Workshop: Clinical development and biomanufacturing, October 15-18, 2018, Oxford, UK.

TRANSVAC Workshop: Adjuvants and Vaccine Formulation, March 25-28, 2019, Geneva, Switzerland.

3rd ENOVA Adjuvant Workshop, September 23-24, 2019, Belgrade, Serbia.

Oral presentation: Novel adjuvant evaluation to improve the efficacy of the therapeutic vaccination against chronic hepatitis B.

Acknowledgments

Studying abroad, especially for a Ph.D. in Germany, is definitely not easy. Here, I would like to express my sincere gratitude to all the colleagues, friends, and families who helped me to walk through this long journey.

First of all, I would like to thank my supervisor, Prof. Ulrike Protzer, for providing me the opportunity to pursue my Ph.D. study at the Institute of Virology, and guiding me throughout. Thank you also for the invaluable input and continuous support for my projects during these years. As a beginner of scientific researches, I learned a lot from you to be an excellent scientist and leader, and also really appreciate the learning opportunities you offered me for my personal development in the academic field.

I would like to thank the members of my thesis committee, Prof. Percy Knolle and Prof. Markus Gerhard, for giving me very useful scientific advice and kind encouragement during every meeting.

Especial thanks go to my mentor Dr. Anna Kosinska. At the beginning, thank you for warmly helping me settle down at a new institute in a foreign country, and patiently teaching me all the skills of methods of *in vivo* studies. During the project process, your constructive discussions and suggestions about the experiments, and strong support during the tough mouse experiment days, helped me a lot. Moreover, I am deeply grateful for your considerable patience in correcting every single piece of my writing for this thesis. Without you, I wouldn't manage the Ph.D. study smoothly.

I would like to acknowledge our cooperation partners of adjuvant project: Livia Brunner, Géraldine Frank, Maria Lawrenz, Patrice Dubois from vaccine formulation institute (VFI). Thank you for the pleasant collaboration and consistent adjuvant formulation preparation, even when I needed the formulations urgently. I also would like to thank our collaborators of viral vector project: Janine Kimpel, Prof. Dorothee von Laer from Medical University of Innsbruck. Thank you for hosting me to do the short laboratory rotation in your lab and showing me how to construct the VSV-GP viral vector.

Acknowledgments

I want to thank Katrin Singethan and Julia Sacherl for teaching me the methods of *in vitro* antigen integrity analyses. Julia also offered many kind helps in organizing the reagents for long-term vaccine stability experiment. I thank Frank Thiele for writing the adjuvant service application and animal experiment approvals for my projects. I thank Martin Mück-Häusl for his useful suggestions about the cloning of novel viral vector. I acknowledge Susanne Miko, Theresa Asen, Philipp Hagen, Romina Bester for their great technical assistance during my work, especially for the mouse experiments. I am grateful to Oliver Quitt, Edanur Ates-Öz, Martin Feuerherd, Chunkyu Ko, Zhe Xie, Fuwang Chen for their kind proofreading or editorial help for this thesis.

I also would like to thank Hélène Kerth, Julia Festag, Florian Wilsch, Martin Kächele, Tanja Bauer, Nina Körber, Thomas Michler, Shanshan Luo, Marvin Festag, Lili Zhao, Lisa Wolff, Sophia Schreiber, Wen-Min Chou, Fenna Kolbe, Karin Wisskirchen, Andreas Oswald, Stoyan Velkov, Christoph Blossey, Daniela Stadler, Jochen Wettengel, Shubhankar Ambike, Cho-Chin Cheng, Till Bunse, Antje Malo, Hassan Moeini, Daniela Rizzi, Andrea Schmidbauer and all other colleagues in Virology. You all offered direct and indirect support for my work and daily life as a foreigner in Germany, as well as created a very pleasant working atmosphere.

I highly appreciate the financial support provided by Chinese Scholarship Council (CSC) for my Ph.D. study.

In the daily life, thank all my friends in Germany, in Shanghai, in my hometown. It is your warm support that helped me adjust to the new environment in Germany and get through those difficult times in work and life.

I would like to thank my beloved husband Libin Li, who accompanies me to come to Germany. I cannot imagine how I can manage everything and walk through the difficulties without you. I feel so lucky that I have you in my life!

Last but not least, I want to express the deepest gratitude to my dear parents and families. Your unconditional love is the strength that always motivates me to walk forward.